

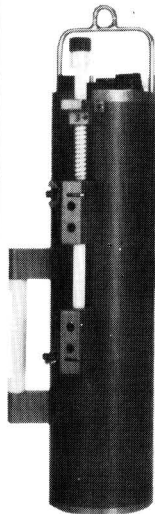


FEBRUARY 1985

ENVIRONMENTAL SCIENCE & TECHNOLOGY

ES&T

**Acid
deposition
control**
Page 112



INTRODUCING

NEW STATE-OF-THE-ART INSTRUMENTATION:

The SEASTAR IN SITU WATER SAMPLER

Uses microprocessor control and extraction columns to make the most significant advance in water sampling technology since the Nansen bottle.

FEATURES:

- Capable of large volume ultra-trace water sampling
- Equally useful for organic and inorganic applications
- Utilizes a variety of types of extraction columns, each with guaranteed blank levels
- Microprocessor-controlled for unprecedented flexibility of sampling, and precise control of flow rate and sample volume
- Can be moored (for days or weeks) or triggered with a messenger from a hydrowire
- Totally self-contained, powered by D-cell batteries

BUILT WITH PRIDE BY

 **SEASTAR INSTRUMENTS LTD**

2045 MILLS ROAD, SIDNEY, B.C. CANADA V8L 3S1 (604) 656-0891 TELEX 049-7526

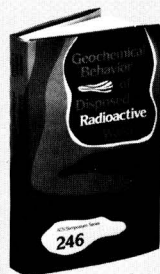
Geochemical Behavior of Disposed Radioactive Waste

G.S. Barney and W.W. Schulz, Editors
Rockwell Hanford Operations
J.D. Navratil, Editor
Rockwell International Rocky Flats Plant

Examines the complex issue of radioactive waste disposal and the health hazards at underground waste sites. Assesses the chemical and physical behavior of wastes from the nuclear fuel cycle, from nuclear weapons testing, and from medical and research activities.

CONTENTS

Sorption and Desorption Reactions with Interbedded Materials • Reactions Between Tc and Fe-Containing Minerals • Radionuclide Sorption Mechanisms and Rates on Granitic Rock • Actinide and Technetium Sorption on Fe-Silicate and Dispersed Clay Colloids • Adsorption of Nuclides on Hydrous Oxides • High-Level Waste Components on Solubility and Sorption of Co, Sr, Np, Pu, Am • Hydrolysis of Am(III) and Pu(V) • Aging Effect on Solubility and Crystallinity of Np(V) Hydrous Oxide • Geochemical Controls on Radionuclide Releases from Waste Repository in Basalt • Radionuclide-Humic Acid Interactions • Oxygen Consumption and Redox Conditions in Basalt • Monitoring and Control of Eh-pH Conditions in Hydrothermal Experiments • Cs - Feldspars Interaction • Interaction of Groundwater and Basalt Fissure Surfaces and Effect on Actinide Migration • Organics and Radionuclides Subsurfaces Migration • Uranium Mining Releases • Uranium Mobility and Roll-Front Deposits • Crystal Chemistry of ABO₄ Compounds • Transformation Characteristics of LaV_xNb_{1-x}O₄ Compounds • Stability of Tetravalent Actinides in Perovskites • α and β Decay in the Solid State • Effects of Water Flow Rates on Leaching • Borosilicate Glass-Containing Waste • Leach Resistance of Iodine Compounds • Nuclear Waste - View from Washington, D.C.



New!

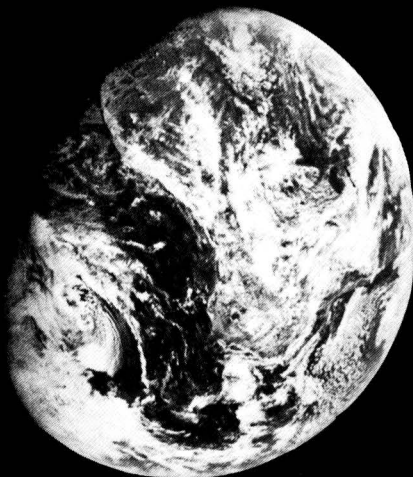
Order from:
American Chemical Society
Distribution Office Dept. 70
1155 Sixteenth St., N.W.
Washington, DC 20036
or CALL TOLL FREE
800-424-6747 and use your
VISA, MasterCard, or
American Express credit
card.

ACS Symposium Series No. 246
424 pages (1984) Clothbound
LC 84-3106

ISBN 0-6412-0827-1
Expert \$95.95

ENVIRONMENTAL SCIENCE & TECHNOLOGY

ES&T



The premiere research publication in the environmental field.

Environmental science continues to be one of the fastest growing fields. And ES&T has grown right along with it!

ES&T continues to give you the practical, hard facts you need on this science . . . covering research, techniques, feasibility, products and services.

Essential reading for environmental scientists both in the business and academic world . . . ES&T has increased its emphasis on peer-reviewed research dealing with water, air, and waste chemistry in addition to adding critical reviews of important environmental science issues—all relevant to understanding the management of our natural environment.

Also included are discussions on environmental analyses, governmental regulations, current environmental lab activities, and much more!

For rate information, and to subscribe, call toll free:

(800) 424-6747

Environmental Science & Technology

© Copyright 1985 by the American Chemical Society

Editor: Russell F. Christman
Associate Editor: John H. Seinfeld
Associate Editor: Philip C. Singer

ADVISORY BOARD

Julian B. Anđelman, Marcia C. Dodge, Steven Eisenreich, William H. Glaze, Michael R. Hoffmann, Lawrence H. Keith, Donald Mackay, Jarvis Moyers, Kathleen C. Taylor, Eugene B. Welch

WASHINGTON EDITORIAL STAFF

Managing Editor: Stanton S. Miller
Associate Editor: Julian Josephson

MANUSCRIPT REVIEWING

Manager: Janice L. Fleming
Associate Editor: Monica Creamer
Assistant Editor: Yvonne D. Curry
Assistant Editor: Mary Ellen Provencher

MANUSCRIPT EDITING

Assistant Manager: Mary E. Scanlan
Assistant Editor: Ruth A. Linville

GRAPHICS AND PRODUCTION

Production Manager: Leroy L. Corcoran
Art Director: Alan Kahan
Staff Artist: Julie Katz
Production Editor: Kate Kelly

BOOKS AND JOURNALS DIVISION

Director: D. H. Michael Bowen
Head, Journals Department: Charles R. Bertsch
Head, Production Department: Elmer M. Pusey
Head, Research and Development Department:
Lorin R. Garson

ADVERTISING MANAGEMENT

Centcom, Ltd.

For officers and advertisers, see page 119.

Please send *research* manuscripts to Manuscript Reviewing, *feature* manuscripts to Managing Editor. For editorial policy and author's guide, see the January 1985 issue, page 22, or write Janice L. Fleming, Manuscript Reviewing Office, *ES&T*. A sample copyright transfer form, which may be copied, appears on the inside back cover of the January 1985 issue.

Environmental Science & Technology, *ES&T* (ISSN 0013-936X), is published monthly by the American Chemical Society at 1155 16th Street, N.W., Washington, D.C. 20036; 202-872-4600, TDD 202-872-8733. Second-class postage paid at Washington, D.C., and at additional mailing offices. POSTMASTER: Send address changes to Membership & Subscription Services, P.O. Box 3337, Columbus, Ohio 43210.

SUBSCRIPTION PRICES 1985: Members, \$26 per year; nonmembers (for personal use), \$35 per year; institutions, \$149 per year. Foreign postage, \$8 additional for Canada and Mexico, \$14 additional for Europe including air service, and \$23 additional for all other countries including air service. Single issues, \$13 for current year; \$13.75 for prior years. Back volumes, \$161 each. For foreign rates add \$1.50 for single issues and \$10.00 for back volumes. Rates above do not apply to nonmember subscribers in Japan, who must enter subscription orders with Maruzen Company Ltd., 3-10 Nihon bashi 2 chome, Chuo-ku, Tokyo 103, Japan. Tel: (03) 272-7211.

COPYRIGHT PERMISSION: An individual may make a single reprographic copy of an article in this publication for personal use. Reprographic copying beyond that permitted by Section 107 or 108 of the U.S. Copyright Law is allowed, provided that the appropriate per-copy fee is paid through the Copyright Clearance Center, Inc., 21 Congress St., Salem, Mass. 01970. For reprint permission, write Copyright Administrator, Books & Journals Division, ACS, 1155 16th St., N.W., Washington, D.C. 20036.

REGISTERED NAMES AND TRADEMARKS, etc., used in this publication, even without specific indication thereof, are not to be considered unprotected by law.

SUBSCRIPTION SERVICE: Orders for new subscriptions, single issues, back volumes, and microfiche and microform editions should be sent with payment to Office of the Treasurer, Financial Operations, ACS, 1155 16th St., N.W., Washington, D.C. 20036. Phone orders may be placed, using Visa, Master Card, or American Express, by calling toll free (800) 424-6747 from anywhere in the continental U.S. Changes of address, subscription renewals, claims for missing issues, and inquiries concerning records and accounts should be directed to Manager, Membership and Subscription Services, ACS, P.O. Box 3337, Columbus, Ohio 43210. Changes of address should allow six weeks and be accompanied by old and new addresses and a recent mailing label. Claims for missing issues will not be allowed if loss was due to insufficient notice of change of address, if claim is dated more than 90 days after the issue date for North American subscribers or more than one year for foreign subscribers, or if the reason given is "missing from files."

The American Chemical Society assumes no responsibility for statements and opinions advanced by contributors to the publication. Views expressed in editorials are those of the author and do not necessarily represent an official position of the society.

ES&T

CONTENTS

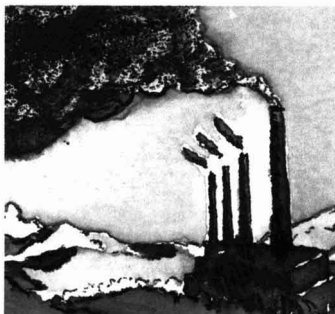
Volume 19, Number 2, February 1985

FEATURES



106

Biodegradation of organic chemicals. A comparison of test results found in the laboratory with those found in nature. Martin Alexander, Cornell University, Ithaca, N. Y.



112

Acid deposition control. A discussion of the prospects and limits of benefit-cost analysis. Thomas D. Crocker, University of Wyoming, Laramie, Wyo., and James L. Regens, University of Georgia, Athens, Ga.

REGULATORY FOCUS

117

Chemicals advisory programs. Richard Dowd discusses international programs and U.S. involvement in regulating world trade in chemicals.

DEPARTMENTS

- 99 Editorial
- 103 Currents
- 118 Classified
- 119 Consulting services

RESEARCH

121

Condition numbers as criteria for evaluation of atmospheric aerosol measurement techniques. Fariba F. Farzanah, Carolyn R. Kaplan, Po Y. Yu, Juan Hong, and James W. Gentry*

A brief discussion of condition number theory and calculation is presented, and three specific applications are discussed.

127

Effects of dissolved organic carbon on the adsorption properties of plutonium in natural waters. Donald M. Nelson*, William R. Penrose, John O. Karttunen, and Paige Mehlhoff

It is shown that colloidal organic carbon in natural surface waters is a major factor controlling the distribution of reduced plutonium between solid and dissolved phases.

132

Light scattering studies of the relationship between cation binding and aggregation of a fulvic acid. Alan W. Underdown, Cooper H. Langford*, and Donald S. Gamble

Pseudochelation, a cooperative effect between aggregation and binding of strongly complexed cations that is independent of electrostatics, is identified.

137

Differential pulse anodic stripping voltammetry of cadmium(II) at a membrane-covered electrode: Measurement in the presence of model organic compounds. Ronald B. Smart* and Edward E. Stewart

The effects of eight surfactants on the differential pulse anodic stripping voltammetry of Cd(II) at both the mercury film electrode and the membrane-covered mercury film electrode are presented.

ESTHAG 19(2) 97-200 (1985)
ISSN 0013-936X

Credit: p. 105, *ES&T's* Julian Josephson
Cover: Bette Hileman

141

Voltammetric methods for distinguishing between dissolved and particulate metal ion concentrations in the presence of hydrous oxides. A case study on lead(II). Maria de Lurdes Simões Gonçalves, Laura Sigg, and Werner Stumm*

Results indicate that voltammetric methods can be used to measure the distribution of metal ions between the soluble and particulate phases without separation of the solid phase.

146

Environmental neutralization of polonium-218. Scott D. Goldstein and Philip K. Hopke*

Ionization potential of the polonium dioxide ion is determined, neutralization of ²¹⁸Po by nitrogen dioxide gas in dry nitrogen is explored, and the existence of a scavenging mechanism is studied.

151

Hydroxyl radical oxidation of isoprene. Chee-liang Gu, Carolyn M. Rynard, Dale G. Hendry, and Theodore Mill*

The products of the oxidation of isoprene with OH radicals and the mechanism of their formation are reported.

155

Fluorescence characteristics of polychlorinated biphenyl isomers in cyclodextrin media. Robert A. Femia, Stephen Scypinski, and L. J. Cline Love*

The feasibility of employing cyclodextrin to separate various PCB isomers in aqueous solution with subsequent identification by fluorescence emission spectroscopy is discussed.

159

Kinetics and atmospheric implications of the gas-phase reactions of NO₃ radicals with a series of monoterpenes and related organics at 294 ± 2 K. Roger Atkinson,* Sara M. Aschmann, Arthur M. Winer, and James N. Pitts, Jr.

Rate constants for the reactions of NO₃ radicals with a series of monoterpenes are determined by use of a relative rate constant technique.

164

Evaluating two-resistance models for air stripping of volatile organic contaminants in a countercurrent, packed column. Paul V. Roberts,* Gary D. Hopkins, Christoph Munz, and Arturo H. Riojas

Results indicate that the two-resistance approach incorporating the Onda relations represents a significant improvement over the assumption of liquid-phase control.

173

Lake Ontario oxygen model. 1. Model development and application. William J. Snodgrass* and Robert J. Dalrymple

Model predictions for seasonal and annual variations of oxygen in the epilimnion and hypolimnion of Lake Ontario show reasonable agreement with observations for a 9-year period.

180

Lake Ontario oxygen model. 2. Errors associated with estimating transport across the thermocline. William J. Snodgrass*

Errors associated with ignoring the flux of mass and heat into the epilimnion due to entrainment are assessed for a dissolved oxygen model.

186

Comparison of organic combustion products in fly ash collected by a Venturi wet scrubber and an electrostatic precipitator at a coal-fired power station. Florence L. Harrison,* Dorothy J. Bishop, and Barbara J. Mallon

The ESP extracts contain more compounds in greater quantities than the WS extracts, but the amount of solvent-extractable organic compounds present in either fly ash is small.

NOTES

193

Influence of pH and ionic strength on the aqueous-nonaqueous distribution of chlorinated phenols. John C. Westall,* Christian Leuenberger, and René P. Schwarzenbach

The influence of inorganic counterions on the distribution of ionizable organic compounds in the octanol-water system is examined.

CORRESPONDENCE

198

Comment on "Fish/sediment concentration ratios for organic compounds." James E. Breck

Michael Stewart Connor

CORRECTION

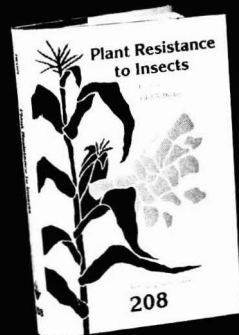
200

Pollutant emissions from portable kerosene-fired space heaters. Gregory W. Traynor,* James R. Allen, Michael G. Apte, John R. Girman, and Craig D. Hollowell

*To whom correspondence should be addressed.

This issue contains no papers for which there is supplementary material available in microform.

Plant Resistance to Insects



Paul A. Hedin, Editor
U.S. Department of Agriculture

Explores different biochemical mechanisms of plant resistance to insects. Includes effect of plant resistance on attacking insects, insect feeding mechanisms, and roles of individual plant constituents. Covers ecological, histochemical, biochemical, and physiological aspects.

CONTENTS

Patterns in Defensive Natural Product Chemistry • Physiological Constraints on Plant Chemical Defenses • Impact of Variable Plant Defensive Chemistry on Susceptibility of Insects to Natural Enemies • Responses to Attack by Tent Caterpillars and Webworms • Plant Trichomes and Glands in Insect Resistance • Regulation of Synthesis and Accumulation of Proteinase Inhibitors • Plant Polyphenols and Their Association with Proteins • Natural Photosensitizers in Plant Resistance to Insects • Natural Inducers of Plant Resistance to Insects • Cytochrome P-450 Involvement in Interactions Between Plant Terpenes and Insect Herbivores • Plant Characteristics Influencing Insect Behavior • Differential Sensory Perceptions of Plant Compounds by Insects • Nutrient-Allelochemical Interactions in Host Plant Resistance • Chemical Basis for Host Plant Selection • Detoxication, Deactivation, and Utilization of Plant Compounds by Insects • Protective Allelochemicals of Certain Leguminous Plants • Cytotoxic and Insecticidal Chemicals of Desert Plants • Role of Lipids in Plant Resistance to Insects • Insect Ecdysis Inhibitors and Feeding Deterrents • Factors in Cotton Contributing to Resistance to Tobacco Budworm

Based on a symposium sponsored by the Division of Pesticide Chemistry of the American Chemical Society.

ACS Symposium Series No. 208
376 pages (1983) Clothbound
LC 82-22622 ISBN 0-8412-0756-9
US & Canada \$46.95 Export \$56.95

Order from:
American Chemical Society
Distribution Office — 03
1155 Sixteenth St., N.W.
Washington, DC 20036
or CALL TOLL FREE 800-424-6747
and use your credit card.

Uncertainty and environmental risk assessment

Environmental risk assessment can be characterized as the use of scientific data to define the probability of some harm affecting a portion of the environment under stated circumstances. This differs from risk management, which can apply the risk assessment in conjunction with economic and social considerations.

Environmental scientists from many disciplines provide scientific data for the process of risk assessment and generally are well aware of the uncertainty of their data. How researchers estimate scientifically the uncertainty of their data and transmit these determinations to those charged with environmental decision making was emphasized at a recent workshop that examined the effect of dioxins on human health and the environment. A colleague involved in making regulatory decisions placed a high priority on the need for scientists to express the uncertainty of data applied in risk assessments. Further clarification revealed that he was requesting both technical and judgmental interpretation of uncertainty of the data.

Although his comments were directed toward environmental risk assessments of dioxin, they also have a generic application. We define statistically the uncertainty of our data by various methods, but rarely do we express an opinion on the judgmental component of our research. For example, convention requires that expressions of LC50s (the concentration of test material that kills 50% of the test organisms in a designated time) include fiducial (confidence) limits established at a given level of significance, which indicates the certainty, and thus the uncertainty, of the data. This also is true for dose-effect data in other testing. Sensitivity and error analyses are applied to some ecological data for the same purpose.

In this regard, much research effort is being devoted to "validate" models that are constructed to predict the effects and environmental concentrations of the pollutants evaluated in risk assessments. Often these models are constructed from laboratory-derived data that cannot actually be validated because laboratory conditions from which the models were developed cannot be duplicated in the environment. Rather than validate, we subjectively estimate the limits of applicability of labo-

ratory data to field situations. Knowledge of these limits reduces the uncertainty of the extrapolations and predictions and strengthens assessments of risk. It is prudent to point out here that some variables, such as climatic conditions, used in long-range predictive models will always carry a high degree of uncertainty.

Scientists are often reluctant to provide judgmental opinions on the uncertainty of data where the opinion goes beyond the statistical or technical aspects of the data. Nevertheless, several techniques have been developed to elicit such judgments from scientists. Modifications of the Delphi technique have been used to combine opinions in development of water quality measures and in military science applications. The Adaptive Environmental Assessment (AEA) process successfully develops dynamic models and submodels that estimate the effect of a pollutant or other stress on the environment. This process is based in part on judgmental decisions by the participants. Such techniques are truly methods of "objectifying" the subjective.

My workshop colleague suggested that scientists are best equipped to make technical and judgmental analyses of the uncertainty of a given data base and should provide such analyses to those making environmental decisions. I agree with the suggestion, but believe strongly that scientists must clearly separate expressions of uncertainty based on statistics from those based on judgment in order to retain credibility and contribute to risk assessment in a positive manner.

Thomas W. Duke



Thomas W. Duke is the Senior Research Scientist at the EPA's Environmental Research Laboratory in Gulf Breeze, Fla.

The Countmaster alpha/beta counting

A compact, convenient low-level alpha/beta counting system, the Countmaster™ from EG&G ORTEC has introduced a new era in enhanced counting capabilities. Less than half the size and weight of conventional counters, the Countmaster represents an innovative concept in detector design. Developed by the pioneer in nuclear instrumentation, it provides new dimensions in performance, convenience, flexibility and value.

240 sample capacity

Countmaster from EG&G ORTEC features a standard counting capacity at least twice that of any other low-level alpha/beta counter. For larger sample volume requirements, the Countmaster system can be conveniently and economically expanded to handle 480, 720 or 960 samples. Modular design allows up to four counters to be operated through one master controller (an IBM-PC).



Powerful IBM-PC

Computer control with the IBM-PC combines dramatic power, flexibility and ease of use. Countmaster offers unprecedented analytical power, information handling/storage capacity and flexibility. Software is menu-driven and adapts easily to your specialized requirements. Total alpha/beta counting and analytical functions are standard including multichannel analysis.

The display monitor prompts and guides users through each task. Special function keys enhance convenience. BASIC allows simple programming for special requirements. It all adds up to easy, user-friendly operation.

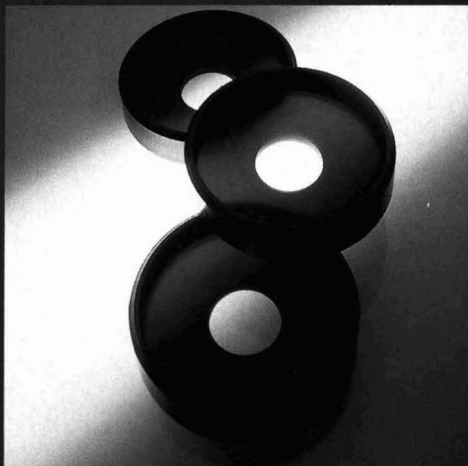
**TWICE THE
CAPACITY
IN HALF
THE SPACE.**

low-level automatic system from EG&G ORTEC

In addition, the Countmaster can be networked with a central mainframe via IEEE-488 or RS-232-C port.

Countmaster is available separately to use with any in-place IBM computer.

Optional HP-85 computer and/or software is available.



Jam-free sample changer

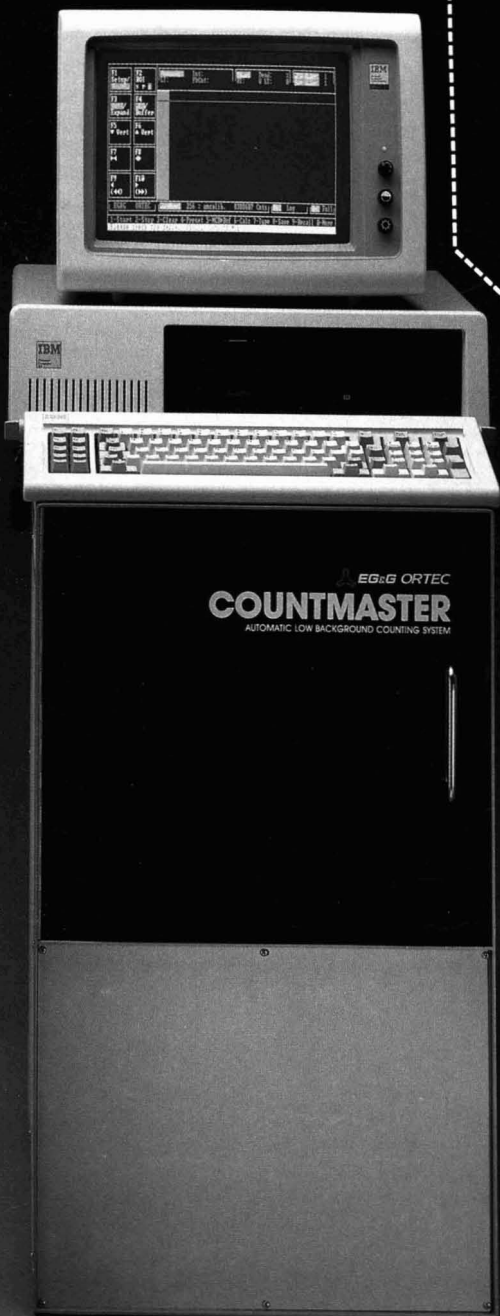
Reliability is inherent by design in the Countmaster. A special automatic sample changer assures reliable performance. The robotic manipulator has no square edges to catch or jam. Round sample holders facilitate smooth changing. Any misaligned sample is readjusted automatically by an exclusive anti-jamming feature to insure trouble-free operation.

Exclusive sample tracking system

Keeping track of all samples—from receipt to storage—is easy with the Countmaster. Each sample holder has an exclusive magnetic recording system. Special read and record heads allow 16 bits of information in any format. A message-repeat feature insures coding is always read accurately.

Find out how the Countmaster can enhance your low-level alpha/beta counting capabilities. Contact your EG&G ORTEC Regional Sales Manager or write/call:

 **EG&G ORTEC**
100 Midland Road, Oak Ridge, TN 37830
Phone: 1-800-251-9750 or 615-483-2157/Telex: 55-7450



For Over Six Decades...



The Leader in the Field.

Few endeavors depend more on a constant flow of new advances and breakthroughs than does the field of analytical chemistry. Keeping pace with these changes has continued to make Analytical Chemistry the pinnacle of publications in the field . . . for over 6 decades.

Call now for your own personal subscription to a publication you don't want to be without—Analytical Chemistry.

Call Toll Free (800) 424-6747



American Chemical Society
1155 16th St., NW
Washington, DC 20036

ES&T CURRENTS

INTERNATIONAL

There is a lot of exaggeration about the cost of controlling acid rain through the retrofitting of power plants, according to Ian Torrens, director of the Resources and Energy Division, Environmental Directorate of the Organization for Economic Cooperation and Development. Torrens spoke at a press conference sponsored by the Center for Environmental Information (Rochester, N.Y.). For instance, in West Germany, capital costs would be \$60-\$100/kW for 95% flue gas desulfurization (FGD). That, with operating costs, could raise consumer rates there by 6-10%, rather than by the 30-50% originally forecast. FGD with 60% reduction could increase rates by 3-4%. By comparison, Torrens estimates a 5-12% rate increase for U.S. consumers if acid rain controls are mandated.

FEDERAL

EPA has presented Congress with a study on Superfund implementation, as mandated by Section 301 of the Superfund law. The agency projected an increase in its National Priorities List to between 1500 and 2500 sites with an assumed baseline of 1800 sites. The average cleanup cost would be \$8.1 million per site. Cleanup by parties responsible for creating the sites should account for 50% of the effort. EPA also made a worst-case cost estimate of \$22.7 billion to clean up 2500 Superfund sites, based on recovery of 40% of these costs from disposers and a cleanup cost of \$12 million per site. The study, which listed EPA's accomplishments through fiscal year 1984, noted that Superfund reauthorization is a top priority for 1985.

EPA has received a proposed national policy document on nonpoint source water pollution from a special task force led by Jack Ravan, EPA's assistant administrator for water. The plan is to have EPA act as the lead agency in coordinating inter-agency and state actions. States would be required to develop and carry out nonpoint source strategies on state and private lands. The plan's

success will depend on the cooperation of the private sector and on identifying appropriate roles for government and business.



DeConcini: Water is becoming unusable

"Do we have a water crisis on our hands? Absolutely," says Sen. Dennis DeConcini (D-Ariz.). "It's not that we are running out of water, but rather that the water America has is steadily, and too quickly, becoming unusable." DeConcini spoke recently at a National Press Club luncheon organized by the National Water Alliance (Washington, D.C.). The culprit is contamination, DeConcini observes; it is found nationwide in surface and groundwater, and arises far more from day-to-day human activities than from sudden disasters. Meanwhile, "we stand almost frozen by indecision as to what action to take." DeConcini sees the 99th Congress as the forum whose decisions "may greatly affect [national] water policy over the next 20 years."

Will the Council on Environmental Quality (CEQ) fall to the budget axe? The Reagan administration is reported to be considering abolition of the CEQ as one move to help ease the federal deficit. However, officials at the Office of Management and Budget say that they know of no such proposal; neither does CEQ chairman A. Alan Hill. Still, the CEQ has been shrinking steadily since 1981 when its staff was reduced from 46 to 12. As of the end of fiscal year 1984, only 10 were left on the CEQ staff.

Final guidelines for a geologic repository system for disposing of

spent nuclear fuel and high-level radioactive waste from commercial power plants have been issued by the Department of Energy. These guidelines establish the performance requirements for the system and define the technical and environmental qualifications that potential sites must meet. They were published in the *Federal Register* Dec. 6, 1984, and became effective 30 days thereafter. Copies of the guidelines are available from the Department of Energy, Public Inquiries.

Is it appropriate to start control actions against acid rain now, or to await better scientific understanding of its causes and effects? According to a General Accounting Office report highlighting the debate, there is uncertainty about the extent and timing of anticipated effects of acid rain. Thus, policy makers must weigh the risks of potentially avoidable environmental damage against the economic effect of actions that may prove unwarranted.

EPA is expected to spend \$280 million on groundwater protection by the time fiscal year 1985 ends, according to Marian Mlay, director of the agency's Office of Groundwater Protection. Activities will focus on determining what contaminant levels will be too low to affect health, what are affordable costs for monitoring and cleaning up contamination, who should pay these costs, and the implications of deliberately abandoning selected aquifers by using them as hazardous waste injection sites. Most of the funds are to be spent under the provisions of Superfund and the Resource Conservation and Recovery Act.

STATES

EPA has asked state and local governments to increase their budgets to meet new requirements of the Resource Conservation and Recovery Act Amendments of 1984 (RCRA). To help the states, EPA has allocated \$30 million of \$100 million in funds requested beyond its original fiscal year 1986 budget to carry out new RCRA provisions. It is uncertain, however, whether EPA will receive

these additional funds. Rather, the agency will be expected to obtain funds from existing programs. Former EPA Administrator William Ruckelshaus said that EPA will observe the new law to the best of its ability, but for its provisions to be successful, much would depend upon state efforts.

The effort to clean up the Chesapeake Bay will be joined by the Department of Agriculture's Soil Conservation Service (SCS). Gerald Calhoun, former Maryland state conservationist, will be SCS's liaison with EPA's Chesapeake Bay Program in Annapolis, Md., as well as with other federal agencies on the cleanup team. Calhoun will coordinate SCS programs in Delaware, Maryland, New York, Pennsylvania, Virginia, and West Virginia to help reduce agricultural sources of nonpoint pollution to the bay. Calhoun says that the best management practices to reduce erosion can reduce nonpoint pollution and will improve soil productivity by keeping nutrients in place.

During last year's warm summer, California's Bay Area experienced 22 days during which air became unhealthy. This term denotes the exceedance of a federal air quality standard at any one of the 21 monitoring stations the Bay Area Air Quality Management District (San Francisco) maintains. The chief culprits are ozone and its precursors. Nevertheless, last year's levels were an improvement. In 1969, the dirtiest year on record, there were 65 days on which the air was classified as unhealthy. Through a hydrocarbon reduction plan—hydrocarbons are suspected of being ozone precursors—the district hopes to attain zero unhealthy days by 1987.

Minnesota plans to present industrial companies with a Governor's Award for Outstanding Achievements in Hazardous Waste Management. This award program is seen as an incentive to reduce the volume of hazardous wastes in the state and as an encouragement for the development of new management methods. The awards, which will be presented by Gov. Rudy Perpich, could be given for substituting nonhazardous materials in a manufacturing process, cutting waste generation through process changes, or reducing waste generation by installing new equipment. Methods of energy production also may be recognized with awards that will be given based on the rec-

ommendations of judges from scientific, environmental, industrial, and academic organizations.

EPA has denied petitions by Maine, New York, and Pennsylvania that the agency invoke Section 126 of the Clean Air Act to force several Midwestern states to reduce particulate and SO_x emissions. The petitions, which were filed in 1980 and 1981, name Kentucky, Illinois, Indiana, Michigan, Ohio, Tennessee, and West Virginia as offenders. EPA's decision was delayed until an order for a ruling by a federal district court was issued. In response to the denial, seven Northeastern states said that they intend to sue EPA.

SCIENCE

A new study to evaluate the toxicity of complex mixtures is being launched by the Commission on Life Sciences, an arm of the National Research Council. Previously, toxicity studies emphasized single chemicals. The first phase will focus on sample preparation and modification required for tests using a single administration of a specified mixture. The second phase will entail multiple administrations. Among questions to be studied are when mixtures and their fractions should be tested, how to collect and standardize samples, how to assay potential interactions of mixtures, how thoroughly component chemicals should be identified, and how the chemical analysis should be coordinated with the mixture's biological assay.

An aid in monitoring human exposure to certain toxic substances has been announced by the National Bureau of Standards (NBS). The method will measure materials such as arsenic, mercury, lead, and sulfates in human urine to assess short-term exposure. Blood tests are currently the main choice for long-term exposure. For this purpose, NBS has developed a standard reference material (SRM 2670) in a powdered, freeze-dried form. This SRM provides a standard for both low and elevated levels of several toxic anions and cations.

Solar ultraviolet (UV) radiation might affect the stratospheric ozone layer substantially, say scientists from the National Center for Atmospheric Research and NASA. Data from the *Nimbus* satellite showed variations on the order of 0.5%, with a peak every 13.5 days.

The sun's UV radiation followed an identical cycle. Measurements were taken of particular wavelengths of infrared light that indicate the abundance of ozone. The scientists estimate that over an 11-year sunspot cycle, with its greater variations in UV radiation, stratospheric ozone concentrations could vary by as much as 12%.

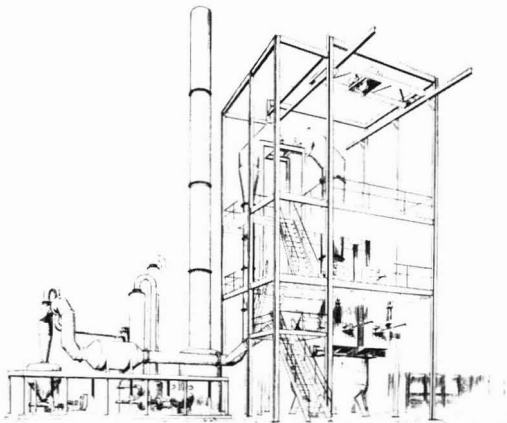
TECHNOLOGY

Ground was broken late last year to build a facility that will produce 82% cellulose fiber from waste. The plant will be a 300-t/d addition to the Somerville, Mass., trash transfer station. The proprietary waste-to-fiber system is being marketed in the U.S. and Canada by Orfa AG, a subsidiary of the 165-year-old Swiss chemical company Chemische Fabrik Uetikon. Orfa spokesmen say that the process is a closed system that releases no effluents, pollutants, or odors to the environment and can serve as an alternative to landfills. They also say that the fiber product is clean and sterile.

"Reduce hazardous waste generation by means of new technology and procedures," suggests the U.S. Naval Civil Engineering Laboratory (NCEL, Port Huene, Calif.). Accordingly, through its Naval Facilities Engineering Command, NCEL is carrying out 10 such projects. One entails developing a new chrome plating process to eliminate millions of gallons of hazardous wastewater each year. Savings of \$85 million over 10 years are anticipated. Another project involves substituting other chemicals for cyanide in cadmium plating. Still others aim at safeguarding indoor air quality in workplaces and family housing.

Simultaneous removal of sulfur and nitrogen oxides from flue gas by high-speed electron bombardment may soon be possible through a system developed by Ebara Company (Japan). A \$6.2-million pilot system will be tested by Indianapolis Power and Light Company. SO_x and NO_x are put through an electrostatic precipitator and then bombarded with high-speed electrons in the presence of ammonia. This produces ammonium sulfate and nitrate, two important commercial fertilizer feedstocks. Although costs are now estimated to be about the same as for limestone scrubbing, Ebara predicts decreases will be brought about by advances in electron acceleration technology.

PCB destroyer prototype



A unit to destroy more than 99.9999% of polychlorinated biphenyls (PCBs) in capacitors is under development by Arc Technologies Co., a joint venture of Electro-Pyrolysis, Inc. (Wayne, Pa.) and Chemical Waste Management, Inc. (Oak Brook, Ill.). A prototype of the unit is expected by mid-year and will be tested at Lake Charles, La. The system uses a sealed electric arc furnace working at 1600 °C. The furnace contains a pool of molten metal into which the PCB capacitors are loaded without being opened or shredded. The process leaves an inert residue. Off-gases are then passed through a plasma surrounding the arc at 6000 °C, which, with flaring, completes destruction. The only residuals would be a harmless slag and dilute hydrochloric acid.

Three nuclear safety monitoring systems recently passed factory acceptance tests. Known as Inadequate Core Cooling Monitors, the systems were developed by Energy Inc. (Idaho Falls, Idaho). They are to be installed at the Connecticut Yankee and Millstone Units II and III nuclear power plants owned by Northeast Utilities Service Company (Berlin, Conn.). The monitors receive signals from plant instrumentation and display information to plant operators concerning reactor coolant level, coolant temperatures at the core exit, and subcooling-superheating margins in the reactor vessel. This type of monitoring became required by the Nuclear Regulatory Commission as a result of the Three Mile Island mishap.

BUSINESS

EPA's groundwater monitoring rules are faulty, according to the National Solid Wastes Management Association (NSWMA, Washington, D.C.). For instance, the controversial "student's t-statistical test" can produce false positive indications of contamination through erroneous pH and conductance readings. Also, false negatives, especially for total organic carbon and total organic halogens, can be a problem. NSWMA urged EPA to "adjust testing requirements for monitoring under RCRA interim rules now in effect. Because of slow-paced permitting, these rules are likely to be the operative policy for a long time."

The Department of Energy is seeking proposals from small, innovative firms in 26 "soft energy" fields for development of new sources of energy. The fields to be represented include solar, botanical, and plasma technology. Proposals are due by March 15 from firms with 500 or fewer employees. About 100 successful proposals will be funded up to \$50,000, with possible funding of up to \$500,000 for a second phase for the most successful ideas. The Small Business Innovation Development Act of 1982 authorizes the program and funding through the department's Small Business Innovation Research program. Information is available from the SBIR Program Manager (301-353-5707).

Hazardous waste generators will turn increasingly to outside special-

ists in treatment, storage, and disposal, possibly creating a \$2.5-billion market by 1988, according to a forecast by Frost & Sullivan (New York, N.Y.). This market was worth about \$1 billion in 1982. The key to market opportunities will be the ability to supply treatment processes that reduce the potential for hazard or result in reusable materials from the wastes, according to company spokesmen. The principal market will continue to be the chemical industry, with the second-place machinery industry constituting about 7% of the total market.

Although much is said about leaking underground storage tanks, little is ever said about why a tank fails, according to the Steel Tank Institute (STI, Northbrook, Ill.). Once such failures are thoroughly analyzed, tanks of proper materials and design could be made. This will sharply reduce chances of failure, STI representatives believe. Principal causes of failure include external and internal corrosion of metal or fiberglass tanks, as well as outdoor freezing, thawing, and flooding. For metal tanks, especially those made of steel, one preventive measure could be improved cathodic protection.

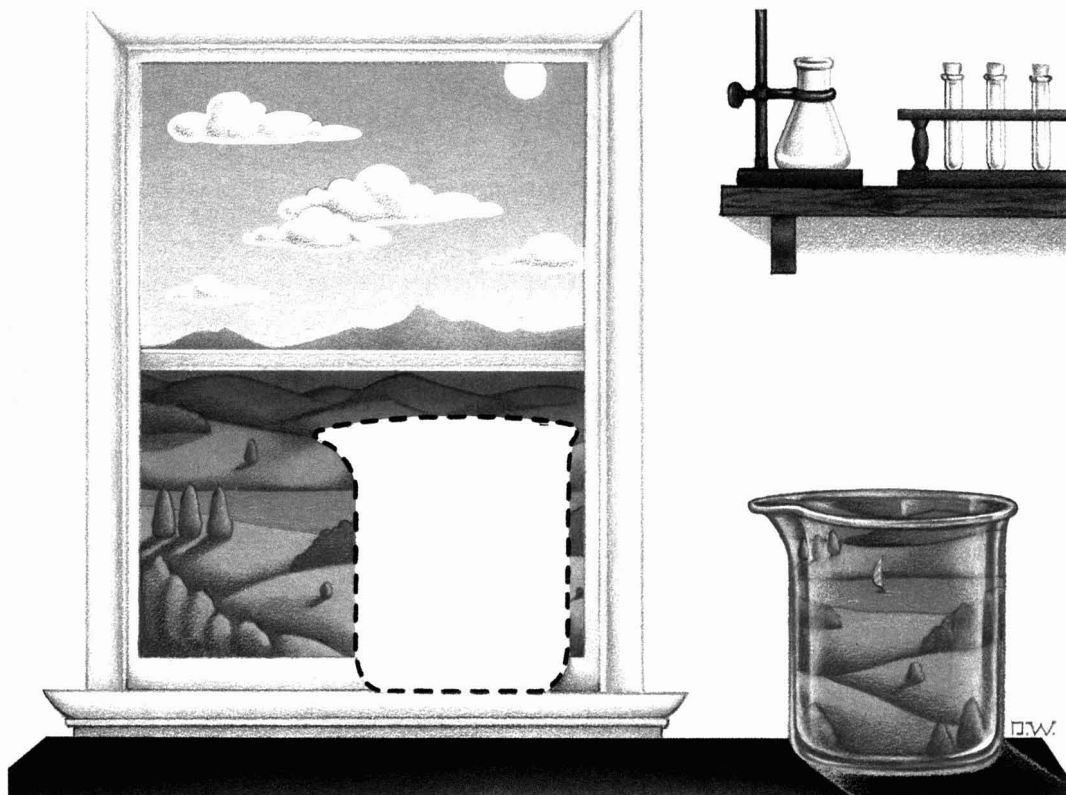


Mahoney: More environmental specialists now in private sector

The private sector now employs the largest number of environmental specialists, according to Jim Mahoney of Bechtel Corporation (San Francisco, Calif.). Most of these specialists were in the government and at universities 10 to 15 years ago. Mahoney observed that with this added environmental staff, industries can develop new approaches to environmental problems that take into account trade-offs between environmental goals and economic growth. Mahoney also noted that there is now a more cooperative atmosphere among industry, government, and environmental groups. This is in contrast with the strong adversary relationships of the 1970s.

Biodegradation of organic chemicals

Laboratory tests using chemical concentrations greater than those found in nature may lead to erroneous conclusions about microbial transformation in nature



Martin Alexander
*College of Agriculture
and Life Sciences
Cornell University
Ithaca, N.Y. 14853*

There have been extensive studies on the occurrence, kinetics, and products

of microbial transformation of organic compounds. Many of these investigations were designed to serve as models to predict what will occur in natural water, soil, sewage, and other ecosystems. Researchers assumed that if a compound was mineralized, cometabolized, or resistant to microbial conver-

sion at the levels normally used for biodegradation tests, it would be similarly mineralized, cometabolized, or resistant at the parts-per-billion level, or even lower levels, in nature. It also was assumed that the products would be the same regardless of substrate concentration and that the kinetics would

be unchanged except that rates would decline in direct proportion to substrate concentration.

The purpose of this article is to show that erroneous conclusions may be reached from studies or routine tests done with organic chemicals at the levels often employed for predicting chemical fate in nature. These errors in extrapolation from high to low concentration may occur in routine evaluations of biodegradation, careful assessments of kinetics, or the establishment of products formed in water, soil, or sediments.

For the present purpose, high concentrations are not considered to be those toxic to common heterotrophic bacteria and fungi (that is, those species requiring organic compounds). Rather, the concentrations are in ranges not usually deemed to be inhibitory; for example, they are in the range of 1–100 $\mu\text{g/mL}$ of water or 1–100 $\mu\text{g/g}$ of soil or sediment, on a dry-weight basis. Low concentrations, in contrast, are considered to be below the ranges cited; that is, in the parts-per-billion (ng/mL or ng/g) or parts-per-trillion (pg/mL or pg/g) range. The anomalies that occur at toxic chemical concentrations that we consider to be high lie outside the scope of this review because such levels are rarely encountered in nature.

Concern about the microbial metabolism of synthetic molecules at these low levels is of practical importance for several reasons. First, criteria and standards for water quality refer to maximum acceptable levels of many organic pollutants that are below 100 ng/mL . Second, numerous toxicants are harmful at levels in the parts-per-billion range (1, 2), and risk assessments suggest that many others are probably injurious even in such trace amounts. Third, a substance may be nontoxic in the amounts that exist free in the water or outside the microbial cell in soil, but if the chemical is subject to bioconcentration, species at higher trophic levels may be harmed. Although the toxic chemical affecting the species at the higher trophic level is now at a high concentration within the organism, the chemical is not subject to microbial decomposition because it is within the tissues of the animal or plant and not free in water, soil, or sediments. The final reason for concern is that undesirable tastes and odors in fresh waters may result from the presence of certain compounds at the nanograms-per-milliliter level (3).

Rate proportional to concentration

The rate of mineralization of a number of organic compounds in samples

of fresh water is directly proportional to their concentration over a wide range of concentrations. The maximum rate of mineralization of diethylamine in stream water, for example, is a linear function of its initial concentration from values below 10 pg/mL to greater than 10 $\mu\text{g/mL}$ (4). The rate of mineralization of aniline in lake water is a linear function of its initial concentration at levels from 5.7 pg/mL to 50 ng/mL (5). The rate of conversion of phenol and *p*-nitrophenol to CO_2 similarly is a direct function of their initial levels over a range from less than 1.0 pg/mL to more than 100 ng/mL . The rates of microbial destruction of benzoate, benzylamine, and di(2-ethylhexyl) phthalate are affected over several orders of magnitude at concentrations below 1.0 $\mu\text{g/mL}$ (6). These observations are not unexpected based on studies of pure cultures of microorganisms (7).

Thresholds

It is often assumed that microorganisms are able to metabolize and presumably are able to grow on all low concentrations of organic compounds that they do mineralize at higher concentrations. The finding that some organic compounds are mineralized even at levels below 1.0 pg/mL suggests that at least some chemicals can be transformed at trace levels. Nevertheless, it is important to distinguish between compounds that can be transformed at low concentrations by large populations of nongrowing cells and substrates that must support growth for significant degradation to occur. Therefore, it is worth considering whether multiplication is possible at very low levels of organic nutrients.

Considerable research has been conducted in recent years on oligotrophic microorganisms (8, 9). The oligotroph is able to grow at low nutrient levels, whereas the eutrophic species multiplies at high concentrations. For example, some oligotrophs will grow in media that have organic substrates added at 1 $\mu\text{g C/ml}$ but not at 5 mg C/ml (10). These organisms appear to have high affinities for the organic molecules they use as carbon sources for growth (11–13).

It is to the oligotroph that one must turn to assess whether extremely low concentrations of organic substrates will allow for reproduction. Consider that a single organism must use up a certain amount of organic nutrients to provide enough energy to maintain the cell. Therefore, when the nutrient concentration is quite high, diffusion will provide molecules to the cell surface at a rate that is rapid enough to meet the energy needs for maintenance and

growth alike.

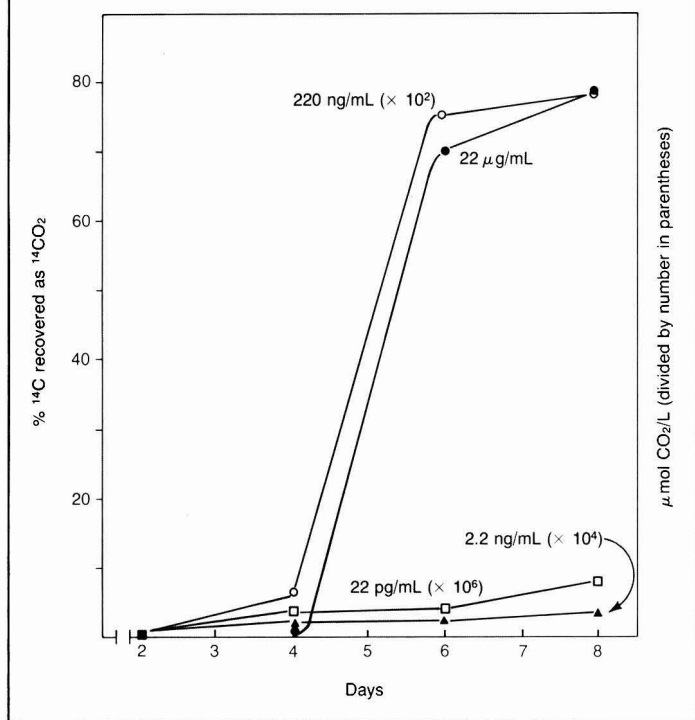
At lower concentrations, in contrast, the needs for maintenance, but not for growth, are satisfied by diffusion of the molecules. At still lower levels, neither need is met. A threshold concentration would then exist, the threshold being the lowest concentration that will support growth. These considerations of diffusivity and concentration of chemical can be used to formulate a theoretical mathematical model to define the level of an organic compound below which an organism is unable to grow (14).

Attempts to demonstrate a threshold are confounded by the presence of dissolved organic compounds in natural environments at levels higher than the calculated thresholds. Even in media made from high-purity water and other purified ingredients, populations may reach 10^4 to 10^5 cells/mL following additions of a small inoculum. Nevertheless, if a chemical is degraded by species unable to use the organic compounds present in that natural environment or the contaminating carbon in a culture medium, a threshold should be evident in the environment or in the medium when the chemical is present at some low concentration.

Thresholds have indeed been found in natural water. In stream water, for example, less than 10% of 2,4-dichlorophenoxyacetate (2,4-D) was mineralized in eight days at initial levels of 2.2 ng/mL and 22 pg/mL , but almost 80% of the herbicide at initial concentrations of 0.22 $\mu\text{g/mL}$ and 22 $\mu\text{g/mL}$ was mineralized in the same period (Figure 1). Similarly, unexpectedly slow mineralization of 1-naphthyl-*N*-methylcarbamate occurred at 3.0 ng/mL and 30 pg/mL , but the insecticide was readily mineralized at higher levels. With time, 2,4-D was extensively mineralized, but the process was quite slow (15). Conversely, no threshold was observed in lake water that initially received 10 pg/mL or less of 2,4-D, *p*-nitrophenol, or phenol (6). The slow loss probably indicates the presence of populations with low activity on natural nutrients of the stream water that are also active on 2,4-D.

Thresholds may also exist in soil. In a laboratory study, it was found that some compounds disappeared from the water phase during passage of such effluents through 107-cm-long columns of soil; but phthalate esters, which are mineralizable at high concentrations, did not disappear from the effluents as a result of passage through the columns. These data may explain why a number of presumably biodegradable compounds are present in groundwater adjacent to sites where trace organics are

FIGURE 1
Formation of CO₂ from 2,4-D added to stream water at four initial concentrations



being applied to the soil (16). In addition, the rate of destruction of *o*-sec-butylphenyl *N*-methylcarbamate (BPMC) in soil at 0.2 $\mu\text{g/g}$ and 1.0 $\mu\text{g/g}$ was far slower than would be predicted, assuming that the rate was a linear function of the chemical concentration over the range of 0.2–10 μg of the pesticide per gram of soil (17).

Thresholds have also been noted in culture. Thus, Jannasch reported the absence of detectable growth of marine bacteria at low concentrations of normally biodegradable substrates (18). Similarly, a threshold concentration was found for the metabolism of glucose by a marine bacterium, but the threshold concentration was reduced by the threshold of amino acids (19). *Pseudomonas* sp. grew readily and mineralized glucose provided at 18 ng/mL, but the bacterium mineralized almost none of the sugar when supplied at 18 pg/mL to an inoculum of 10^3 cells/mL (4). Shehata and Marr reported that they could not maintain a culture of *Escherichia coli* by continuous transfer of the bacterium in a medium containing less than 18 ng glucose/mL (7); Koch and Wang observed no growth of the same species in continuous culture at 18 ng glucose/mL (20). *Aeromonas* hy-

drophila also fails to multiply at low levels of starch (21).

One might expect that the threshold concentration will vary with the organism. If the populations are all eutrophs, the critical concentration will be high. If the active species include one or more oligotrophs, the values will be low. Furthermore, as pointed out above, if the organisms obtain energy and carbon for growth by using natural organic constituents of the environment, the threshold for a particular chemical may be below the level of detection possible using current analytical procedures.

The existence of thresholds may be the reason for the persistence of low levels of biodegradable organic substances in natural environments. Because the identities of most of the organic constituents are unknown, it is not clear whether many of the compounds are intrinsically resistant or persist because of their low concentrations. A portion of the dissolved organic matter in natural waters may be innately resistant to microbial attack (22). However, many synthetic organic molecules at low levels are found in natural water (23, 24). Although the presence of many of these may be at-

tributable to their intrinsic resistance to microbial metabolism, some are mineralizable at high concentrations in culture. Their presence may be a result of the inability of microorganisms to destroy substrates readily at very low levels.

Good examples of the durability of trace amounts of synthetic organic compounds that are usually destroyed at higher levels are 2,4-D and dichlorophenol; these aromatics sometimes persist for years in minute amounts (3). The existence of a threshold is also suggested by the presence of several organic compounds in wastewater following land infiltration. Toluene, xylenes, naphthalene, and phthalate esters—all are good substrates for microorganisms when they are at high concentrations—were found at levels of 0.01–2.4 ng/mL (16). Even natural products, such as individual amino acids, may be present in coastal waters at levels below 0.05–3 ng/mL (25), although these levels may represent not a threshold but a steady-state concentration resulting from their simultaneous formation and destruction.

Because the effects of low substrate levels on growth, enzyme induction, and enzyme activity and the use of mixtures of substrates have not been clarified, it is not now certain which phenomena account for thresholds in natural environments.

Apparent inhibition

Many synthetic organic compounds are toxic to indigenous species when they are introduced at moderate concentrations into water, soil, sediment, or sewage. These chemicals are known to be inhibitory, as a rule, only at moderately high levels; that is, above about 10 $\mu\text{g/mL}$. However, toxicity is sometimes evident even at lower levels. For example, 2,4-D is mineralized by the microflora of certain waters at concentrations below 10 ng/mL but not at 200 ng/mL (6). However, this herbicide does not usually retard the growth of the common test heterotrophs even at 100-fold-higher levels.

Similarly, the mineralization of a linear alcohol ethoxylate added to bay water at 0.42–31.2 ng/mL was much less at the higher concentrations than would be predicted based on tests of the lower concentrations (26). It is therefore possible that the activity in such waters results from the metabolism of oligotrophs that are uniquely sensitive even to such trace amounts of their substrates.

A previously unobserved phenomenon may explain the lack of mineralization of nanogram-per-milliliter levels of chemicals that are converted to CO₂ at

lower concentrations: The responsible populations shift from metabolic sequences yielding CO_2 to pathways that yield solely organic products. The shift is thus from mineralization at a lower concentration to cometabolism at the higher. For example, isopropyl *N*-phenylcarbamate (IPC) is mineralized in samples of some fresh waters when it is added at 400 $\mu\text{g/mL}$, but it is cometabolized at 1.0 $\mu\text{g/mL}$ (27).

Similar observations have been made with 3-(4-chlorophenyl)-1,1-dimethylurea (monuron) added to sewage (Wang and Alexander, unpublished data). Therefore, the absence of mineralization at higher concentrations of chemicals that are mineralized at lower concentrations may sometimes be a result of an inhibition of all microorganisms capable of metabolizing that compound. It may also be due to the inhibition of the mineralizing but not the cometabolizing populations.

Carbon assimilation

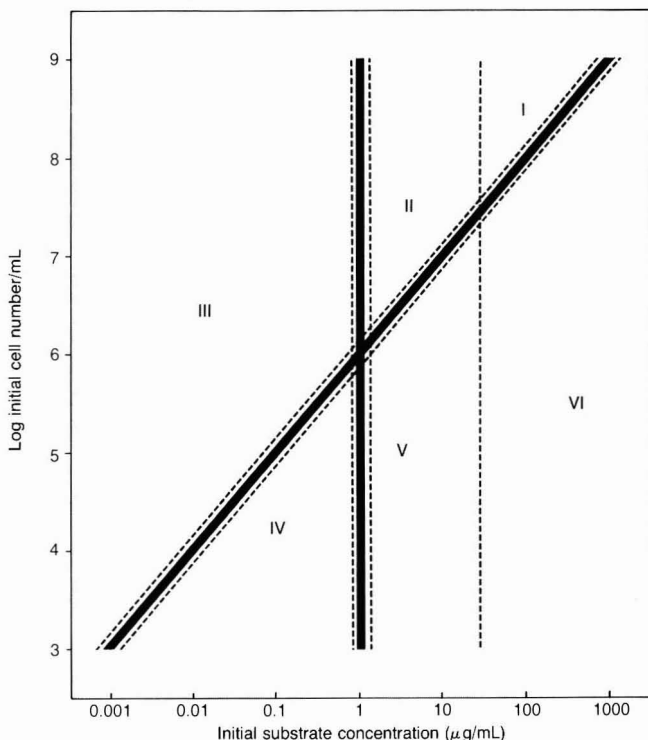
Substrates that are cometabolized do not serve as nutrients, and hence carbon from these organic molecules should not be assimilated by the microflora bringing about the transformation. This lack of incorporation has been verified for the decomposition of several herbicides in sewage (28). In contrast, mineralization by microorganisms is often assumed to be performed by species that assimilate part of the carbon from the molecules they metabolize.

This is apparently not necessarily the case at low chemical concentrations. For example, in the metabolism of ^{14}C -labeled 2,4-D added to stream water at 2.2 ng/mL , only 1.2% of the ^{14}C was found in the particulate fraction of the water, which should contain the microbial cells (15). During the mineralization of aniline added to lake water at 24 $\mu\text{g/mL}$ to 250 ng/L , no incorporation into the cells was detected after a period of eight days (5).

Additional support for the apparent lack of assimilation comes from findings that the carbon of certain compounds is nearly quantitatively converted to CO_2 in sewage or fresh water that contains oxygen (5, 6). Such observations suggest that few microbial cells if any are formed from the carbon of the substrate, or that the cells themselves are decomposed and their constituents converted to CO_2 in a few days. The absence of incorporation or low values for assimilation is not universal, however. Thus, when marine bacteria are provided with 10–50 nM amino acids, they assimilate 74–86% of the compounds (29).

Mineralization without incorporation is of practical interest. The occurrence

FIGURE 2
Kinetic models as a function of initial substrate concentration and bacterial cell density^a



^a I, II, III, IV, V, and VI designate regions in which zero-order, Monod (without growth), first-order, logistic, Monod (with growth), and logarithmic kinetics are expected (31)

of mineralization without assimilation suggests that microorganisms are not multiplying at the expense of the compound and that where acclimation is sought to enhance biodegradation, as in waste treatment procedures, no such acclimation will occur. In view of the importance of obtaining the growth of microbial populations to achieve rapid biodegradation in waste treatment, it is critical to evaluate the possible absence of acclimation in treatment systems designed to destroy chemicals at low concentrations in waste streams.

Kinetics

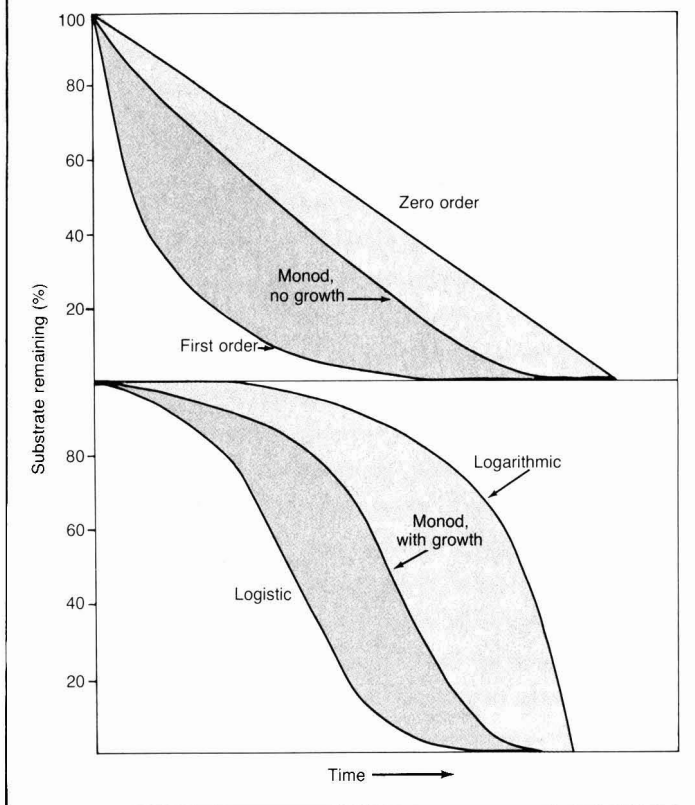
Considerable attention has been given to the kinetics of bacterial growth in pure culture. The most common growth pattern studied by bacteriologists is logarithmic or exponential kinetics. Such a pattern of increase in bacterial numbers is regularly observed when small numbers of cells of individual species are introduced into solutions with high concentrations of organic and inorganic nutrients. The concentration of the organic substrate is considerably in excess of the bacterium's K_s value

(that is, the substrate concentration at which the biodegradation proceeds at half the maximum rate).

If the cell density is so great that the quantity of substrate is insufficient to support a significant increase in cells, the kinetics of the disappearance of organic chemicals present at high levels (appreciably above K_s) is zero order (linear with time) for pure cultures and probably also for processes in nature catalyzed at individual sites by single populations. Zero-order kinetics under these circumstances results from levels of substrate that are saturating for the initial enzymatic reactions and from the absence of a significant increase in active biomass. Often, when samples of natural environments are challenged with a chemical to increase the population size of mineralizing organisms, the rate of decomposition of a second increment of the same chemical is zero order (30), presumably because of the absence of significant increases in biomass as the second increment is degraded.

Two patterns of kinetics can be envisioned when a single bacterial species is

FIGURE 3
Disappearance curves for chemicals that are mineralized as related to individual kinetic models



provided with a mineralizable substrate at concentrations below the K_s value (31). In the first pattern, there is no appreciable increase in cell numbers either because there is a threshold or because the initial cell number is too large, relative to the quantity of organic compound, to permit an appreciable increase in abundance of bacteria. At constant biomass and severely limiting substrate levels, the rate is proportional to the concentration of residual substrate, which falls continually. This is typical of first-order kinetics, which has been reported for the decomposition of EDTA (32), 2,4-D (33), and many other compounds in soil and for glucose, linear alcohol ethoxylate (26), and various other chemicals in water. Some investigators have extended first-order kinetics to consider that the rate in different waters is proportional not only to substrate concentration but also to bacterial numbers when the former is below K_s (34).

In the second pattern, few cells of the active species are present initially, and the chemical concentration, although

low, is above any threshold that might exist. Under these conditions, the bacteria will grow, but at a rate that falls constantly with the diminishing and always limiting substrate concentration. A growth pattern in which there is an ever-increasing population encountering an ever-decreasing nutrient resource resembles the classical logistic growth curve well known in population ecology. The logistic curve is symmetrical about the point of inflection in the curve and has an S-shape (35).

A generalized approach to the kinetics of growth was formulated by J. Monod and often is described as Monod kinetics. This model describes rates as a function of substrate level over a range of concentrations, and it is particularly useful when the initial concentration is in the mixed-order region. Many measurements of Monod growth kinetics parameters have been made (36). Often, the disappearance of low levels of organic compounds is assumed to follow first-order kinetics, although the precision of the data are not great enough to distinguish between

first-order and logistic kinetics.

The kinetics expected at different chemical concentrations and different initial numbers of bacterial cells are shown in Figure 2. The shapes of the curves for chemical disappearance that coincide with these kinetics are given in Figure 3.

An anomaly in the kinetics at low concentration was noted in the mineralization of diethanolamine in stream water. Thus, evolution of CO_2 from diethanolamine was constant with time at 21 $\mu\text{g}/\text{mL}$; the process was linear (4). The cometabolism of *N*-nitrosodiethanolamine in samples of lake water was also linear with time (37). Linear rates of mineralization also were observed for aniline at 5.7 $\mu\text{g}/\text{mL}$ to 500 ng/mL ; phenol at 102 $\mu\text{g}/\text{mL}$ to 20 mg/mL ; di(2-ethylhexyl) phthalate at 21 $\mu\text{g}/\text{mL}$ to 200 ng/mL ; 2,4-D at 1.5 $\mu\text{g}/\text{mL}$; and benzylamine at 310 ng/mL (5) in fresh waters; and for toluene at 0.38 ng/mL and 3.8 ng/mL in seawater (38).

Conclusion

The rates of mineralization of some organic compounds are directly proportional to their concentration, so predictions of biodegradation rates can be made using laboratory tests of high levels of chemicals. With these compounds, however, the kinetics of the process and therefore the shapes of the curves of chemical disappearance will be a function of concentration. Other chemicals are mineralized at trace levels but may be cometabolized only at higher concentrations. There is a threshold below which certain, usually mineralizable molecules are not converted to CO_2 . Microorganisms may not assimilate carbon from chemicals present in trace amounts in natural environments; they will not grow or produce the large, acclimated populations needed for enhanced biodegradation. It is possible to predict the minimum concentration of a chemical necessary to support microbial growth. Based on these findings, tests of biodegradation, mineralization, or cometabolism that are performed using chemical concentrations greater than those that prevail in nature may lead to erroneous conclusions about the occurrence, rates, and products of microbial transformation in nature.

Acknowledgment

The research of the author was supported by funds provided by the Environmental Protection Agency, the U.S. Army Research Office, and the U.S. Department of Agriculture.

Before publication this article was reviewed for suitability as an *ES&T* feature by Dennis Focht, University of California,

Riverside, Calif. 92502; H. H. Cheng, Washington State University, Pullman, Wash. 99164; and James Martin, University of California, Riverside, Calif. 92502.

References

- (1) Batterton, J.; Winters, K.; van Baalen, C. *Science* **1978**, *199*, 1068-70.
- (2) Powers, C. D. et al. *Appl. Environ. Microbiol.* **1977**, *34*, 760-64.
- (3) Faust, S. D.; Aly, O. M. *J. Am. Water Works Assoc.* **1964**, *56*, 267-79.
- (4) Boethling, R. S.; Alexander, M. *Environ. Sci. Technol.* **1979**, *13*, 989-91.
- (5) Subba-Rao, R. V.; Rubin, H. E.; Alexander, M. *Appl. Environ. Microbiol.* **1982**, *43*, 1139-50.
- (6) Rubin, H. V.; Subba-Rao, R. V.; Alexander, M. *Appl. Environ. Microbiol.* **1982**, *43*, 1133-38.
- (7) Shehata, T. E.; Marr, A. G. *J. Bacteriol.* **1971**, *107*, 210-16.
- (8) Poindexter, J. S. *Adv. Microb. Ecol.* **1981**, *5*, 63-89.
- (9) Kuznetsov, S. I.; Dubinina, G. A.; Lapteva, N. A. *Annu. Rev. Microbiol.* **1979**, *33*, 377-87.
- (10) Ishida, Y.; Kadota, H. *Microb. Ecol.* **1981**, *7*, 123-30.
- (11) Ishida, Y. et al. *Microb. Ecol.* **1982**, *8*, 23-32.
- (12) van der Kooij, D.; Hijnen, W.A.M. *Appl. Environ. Microbiol.* **1981**, *41*, 216-21.
- (13) Bartholomew, G.; Pfander, F. K. *Appl. Environ. Microbiol.* **1983**, *45*, 103-9.
- (14) Schmidt, S. K.; Shuler, M. L.; Alexander, M. *J. Theor. Biol.*, in press.
- (15) Boethling, R. S.; Alexander, M. *Appl. Environ. Microbiol.* **1979**, *37*, 1211-16.
- (16) Hutchins, S. R.; Tomson, S. B.; Ward, C. H. *Environ. Toxicol. Chem.* **1983**, *2*, 195-216.
- (17) Ueji, J.; Kanazawa, J. *Bull. Environ. Contam. Toxicol.* **1979**, *21*, 29-36.
- (18) Jannasch, H. W. *Limnol. Oceanogr.* **1967**, *12*, 264-71.
- (19) Law, A. T.; Button, D. K. *J. Bacteriol.* **1977**, *128*, 115-23.
- (20) Koch, A. L.; Wang, C. H. *Arch. Microbiol.* **1982**, *131*, 36-42.
- (21) van der Kooij, D.; Visser, A.; Hijnen, W.A.M. *Appl. Environ. Microbiol.* **1980**, *39*, 1198-204.
- (22) Barber, R. T. *Nature* **1968**, *220*, 274-75.
- (23) Jungclaus, G. A.; Lopez-Avila, V.; Hites, R. A. *Environ. Sci. Technol.* **1978**, *12*, 88-96.
- (24) Meijers, A. P.; van der Leer, R. C. *Water Res.* **1976**, *10*, 597-604.
- (25) Williams P.J.LeB.; Berman, T.; Holm-Hansen, O. *Mar. Biol.* **1976**, *35*, 41-47.
- (26) Yashon, R. D.; Schwab, B. S. *Environ. Sci. Technol.* **1982**, *16*, 433-36.
- (27) Wang, Y. S.; Subba-Rao, R. V.; Alexander, M. *Appl. Environ. Microbiol.* **1984**, *47*, 1195-200.
- (28) Jacobson, S. N.; O'Mara, N. L.; Alexander, M. *Appl. Environ. Microbiol.* **1980**, *40*, 917-21.
- (29) Palumbo, A. V.; Ferguson, R. L. *J. Exp. Mar. Biol. Ecol.* **1983**, *69*, 257-66.
- (30) Suflija, J. M.; Robinson, J. A.; Tiedje, J. M. *Appl. Environ. Microbiol.* **1983**, *45*, 1466-73.
- (31) Simkins, S.; Alexander, M. *Appl. Environ. Microbiol.* **1984**, *47*, 1299-306.
- (32) Tiedje, J. M. *J. Environ. Qual.* **1977**, *6*, 21-26.
- (33) Parker, L. W.; Doxtader, K. G. *J. Environ. Qual.* **1982**, *11*, 679-84.

- (34) Paris, D. F. et al. *Appl. Environ. Microbiol.* **1981**, *41*, 603-9.
- (35) Odum, E. P. "Fundamentals of Ecology"; W. B. Saunders: Philadelphia, Pa., 1971.
- (36) Robinson, J. A.; Tiedje, J. M. *Appl. Environ. Microbiol.* **1983**, *45*, 1453-58.
- (37) Yordy, J. R.; Alexander, M. *Appl. Environ. Microbiol.* **1980**, *39*, 559-65.
- (38) Button, D. K.; School, D. M.; Robertson, B. R. *Appl. Environ. Microbiol.* **1981**, *41*, 936-41.



Martin Alexander is Liberty Hyde Bailey Professor in the College of Agriculture and Life Sciences at Cornell University. He received a Ph.D. from the University of Wisconsin in 1955. Alexander has served as a member or chairman of committees of EPA, the National Academy of Sciences, and other national and international agencies and has consulted with a variety of companies in the area of biodegradation. His research is on biodegradation, the fate of genetically engineered microorganisms, and biological nitrogen fixation.

I Have Designer Genes



T-SHIRTS

\$8.50 Your DNA has its way with this ingenious T-shirt. Blue pocket and red print on beige 50% cotton/50% poly machine washable blend. Small (34), Medium (36-38), Large (40-42), Extra Large (44). Write for quantity discounts.

American Chemical Society, Education Div.
1155 Sixteenth Street, NW
Washington, DC 20036, USA (202) 872-4588

Please send "I have Designer Genes" T-Shirts as follows:

_____ S _____ M _____ L _____ XL

I understand the price is \$8.50 each plus \$1.95 per order, U.S.A. (\$3.70 foreign) for shipping and handling.

Check enclosed

Visa No. _____ Exp. Date _____

MasterCard No. _____ Interbank Code _____ Exp. Date _____

Name _____

Address _____

City _____ State _____ ZIP _____

The developers of the NIEH/EPA CIS FEIN-MARQUART ASSOCIATES

are pleased to announce that the world's largest collection of useful online chemical information

The CIS

is now available to the public through
Fein-Marquart's wholly owned subsidiary
CIS, Inc.

The CIS now includes The Merck Index Online

and databases and programs relating to
*Chemical Structures, Environment, Toxicology, Regulations,
Spectroscopy, Nucleotide Sequences, Chemical and Physical Properties,
and Analysis and Modeling.*

For information, call or write
CIS, Inc.

7215 York Road
Baltimore, MD 21212
301-321-8440

or
800-CIS-USER

Acid deposition control

A benefit-cost analysis: Its prospects and limits

Thomas D. Crocker

*Department of Economics
University of Wyoming
Laramie, Wyo. 82071*

James L. Regens

*Institute of Natural Resources
University of Georgia
Athens, Ga. 30602*

Because of its ability to deal with aggregate efficiency, benefit-cost analysis is a potentially useful component of policy evaluation. Its utility, however, is constrained by the availability of reliable data. Even economic feasibility can be difficult to establish empirically, particularly if control benefits appear to be highly subtle and intangible while compliance costs appear to be concrete. As a result, a requirement that decisions about each significant environmental regulation, unless prohibited by statute, be made on the basis of such formal analyses creates a major analytical challenge. The objective of generating estimates of net control benefits, the gross benefits less costs, may be impossible without reliance on limited scientific data and allowance for large margins of error.

The policy issue

The acid rain controversy provides an excellent example of the assets and liabilities of using benefit-cost analyses to guide policy choice. Unfortunately, as Olson points out (1), the large temporal and spatial scales for acid deposition make experimentation and observation extremely difficult. Nevertheless, based on existing information, strong qualitative justification can be offered for some willingness to override strict scientific canons against speculation about the harmful effects of acid deposition.

Precipitation chemistry data indicate that the geographic scope of acid deposition covers most of eastern North America. More limited data suggest that high-elevation (>2900 m), rural areas in the western U.S. are also experiencing low pH bulk precipitation (2).



Although the effects hypothesized to be associated with acid deposition include those on soils, forests, crops, and materials, conclusive evidence exists only for injury to aquatic ecosystems. A large body of evidence indicates that chemical and biological alterations can take place in lakes and streams. The most visible of these alterations is in the loss of fish populations. Studies of mature forests also indicate reduced growth patterns as well as increased mortality in recent decades for primarily coniferous species in localized areas of the northeastern U.S. (3).

However, because responses tend to be subtle and causal linkages complex, terrestrial ecosystem findings on materials, forests, crops, and soil are equivocal. Finally, although the direct risk to human health from acid deposition (as opposed to respirable sulfates) is presumed to be relatively low, it has been postulated that certain health risks may be associated with acid fog, including the leaching of metals into drinking-water supplies and those events documented in the Los Angeles Basin. (See *ES&T*, Vol. 17, No. 3, 1983, p. 117A.)

Given current scientific knowledge about the phenomenon of acid deposition, it is clear that policy makers confront a dilemma. Reasons exist to take mitigative actions. First, although its extent as well as the rate at which damage is induced remains uncertain, the mere existence of the perception of a problem compels a response. Second, manmade sources generally are the overwhelming contributors to acid deposition in eastern North America. Although expensive, control technology to significantly reduce in emissions from those sources is available. Thus, it is reasonable to assume that reducing SO₂ emissions over a broad area for several years will produce an essentially proportionate reduction in sulfate deposition (4).

Moreover, other aspects of air quality in eastern North America—regional visibility, particulate matter loadings, and ambient SO₂ levels—are affected strongly by the precursors to acid deposition, and they are likely to be improved if atmospheric loadings of precursor emissions are reduced. But unlike the proportionality between long-term average emissions and deposition, the site-specific changes in deposition patterns and pH that would occur within sensitive receptor areas are not clear.

Benefit-cost perspectives

Because the choices of emitters and receptors differ according to whether or not a market exists in property rights to emit precursors and because of the lack

TABLE 1
Estimates of 1978 maximum economic losses caused by acid deposition in the eastern third of the U.S.^a

Effects category	Maximum losses ^b (in billions)
Materials	\$2.00
Forest ecosystems	1.75
Direct agricultural	1.00
Aquatic ecosystems	0.25
Others ^c	0.10

^aEstimates are for the potential total benefits due to the complete elimination of acid deposition effects.
^bIn 1978 dollars
^cIncludes health, water supply systems, etc.
Source: Reference 5

of proxy markets, it may be impossible to trace economically efficient outcomes (those that would occur if all potential voluntary exchanges were to be realized) for the acid deposition problem. The economic criterion is then reduced to whether those who gain from a change in precursor control could, in principle, compensate the losers and still have some residual gain. This simply restates the fact that efforts to assess the benefits and costs of acid deposition control must necessarily presume that acceptable resolutions have already been found for a variety of natural science, social, and ethical problems, such as who "owns" the waste assimilative capacity of the atmosphere.

A benefit-cost analysis of acid deposition thus requires three kinds of information:

- the differential changes across space and time that acid deposition control causes in people's alternative opportunities to produce and consume,
- the responses of prices to these changes, and
- the adaptations emitters and receptors can make to these changes in opportunities and prices.

Accounting for the results of the last two facets is the economic analysis portion of benefit-cost analysis. If accurate information on economic consequences is desired, some formal analysis of the last two issues is inescapable. For example, the effects of acid deposition in a given region may not be great enough to affect the relative prices of different crops. However, unless the effects on crop yield are equal across the spectrum of crops grown in the region, the relative rewards of growing one crop rather than another will change, and producers will substitute the relatively less affected crop. Similarly, if differential yield effects are small, the price responses across crops are likely to differ, provid-

ing another source of changes in relative rewards across alternative crops.

The benefits of control

Crocker reported estimates by impact category of the maximum economic values for eliminating all acid deposition effects on current annual yields for existing economic activities in the eastern third of the U.S. (5) (Table 1). No other comprehensive value estimates or rank-orderings at the national level have appeared since, and we believe that no new information justifies changing the original ordering. However, because the calculations were based on assumptions about effects the magnitudes of which are still being defined, they should be treated as highly tentative.

The effects on materials were assigned the highest monetary value, even though only Haagenrude's and Atteraa's study of zinc and steel corrosion rates provides a separate measure of acid deposition effects (6). Many economic studies of the effects of SO₂ and total suspended particulates on materials are available, but without exception they neglect price responses and adaptations. Most even fail to consider the technology or activity of which the affected material is a part.

Numerous inexpensive adaptation opportunities are generally available for production and consumption involving metals, ceramics, textiles, paint, and paper. But for buildings already in place, fewer opportunities exist. Moreover, the unit value of buildings is high, and the fraction of the nation's wealth that they constitute is large.

The heterogeneity of these buildings and structures is equally important. For example, there is rather strong indirect evidence that acid deposition is linked to severe economic damage to public and private structures that fall into the category of cultural heritage. One ex-

trème example is the Statue of Liberty.

Of all the effects of acid deposition, those on forest ecosystems seem the least understood, although there is increasing evidence that substantial effects exist. Qualitative statements, without probability statements attached, abound. Acid deposition may

- increase the fertility of sulfur-poor or nitrogen-poor soils,
- leach plant nutrients from soils in which these elements are plentiful,
- remove soil-binding agents,
- increase heavy metals in soils to toxic levels, or
- harm forest plant foliage.

Given this array of possibilities, one might adopt Johnsson's position that sufficient reason exists to attribute some fraction of the observed reductions in forest growth rates to acid deposition (7). For example, the National Academy of Sciences Panel on Nitrates ascribed a 5% reduction in the annual growth rates of eastern U.S. forests to acid deposition (8). A simple multiplication of this reduction by a weighted average of 1977 standing timber prices (9) provides an estimate of nearly \$600 million annually in lost timber production alone. Losses in forest outdoor recreation, water storage, wildlife habitats, and other forest services must be added to this.

Agricultural damage has been demonstrated at lower than current ambient pH levels (between 2.0 and 3.0). Most crops studied, however, have demonstrated no consistent sensitivity to acid deposition.

From an economic perspective, it is difficult to rationalize the large amount of research and the attention from the news media caused by acid deposition's effects on aquatic ecosystems. The current economic consequences of these effects are small relative both to the economic value of all freshwater sport fishing in North America, and estimates (even with order-of-magnitude errors) of the value of current effects on other categories. Too many substitute lakes and too many alternative outdoor recreational opportunities exist. In fact, in a study that does account for the substitutions that fishermen make, Menz and Mullen estimate that the 1982 value of the Adirondack lake and pond sport fishery losses to currently licensed fishermen was between \$1.7 and \$3.2 million (10).

Acid deposition also has caused concern about increased corrosion of household, commercial, and industrial water supply systems and about the indirect effects of this corrosion on human health. Most drinking water supply systems nevertheless already have treatment facilities for liming. The eco-

nomical damage caused by corrosion is thus offset by the relatively small costs of acquiring and applying the additional lime necessary to overcome it.

The costs of control

There are a number of policy options available for achieving emissions reductions in the major precursors of acid deposition—SO₂, NO_x, and volatile organic carbons (VOCs)—all of which are anthropogenic in origin. Absolute SO₂ and VOC emissions and the rate of growth in NO_x emissions have declined markedly since 1970. Future declines, however, will depend on the strictness of environmental regulations and on economic activity, energy prices, and technology.

Although uncertainty surrounds each of those factors, trends must be estimated to project the costs of control. Over the long term, perhaps 40 years or more, a significant reduction in emissions may result as existing sources are displaced by facilities subject to new source performance standards (NSPS). It is debatable, however, whether the replacement of existing sources with new ones will result in emissions levels low enough to reduce acid deposition loadings to environmentally acceptable targets.

Such an assertion rests on several fundamental assumptions. First, growth rates in utilities and other major industries must remain relatively low compared with historical rates. Second, technological advances must permit more stringent NSPS, or innovative incentives for control must be developed, thereby reducing aggregate emissions. Finally, no irreversible damage must be allowed to occur within the next three to four decades. If these assumptions are valid, then the opportunity costs of achieving additional reductions now are substantial, relative to known as opposed to plausible damage (11).

Proposals for imposing controls on acid deposition now focus on reducing SO₂ emissions because of the greater difficulty in achieving significant reductions in NO_x emissions and the uncertainty about whether nitrate acidity is as harmful as sulfate acidity. As a result, it is important to consider the costs of such an abatement program. As Table 2 indicates, it is generally more cost effective to switch to lower sulfur coals or residual oil than it is to employ flue gas desulfurization (FGD). However, such switching poses potential equity and adjustment problems relating to the regional losses of miners' jobs that would result from shifts in the coal market. Although the economics of the limestone injection multistage burner (LIMB) seem promising, LIMB

commercialization does not appear likely prior to the mid-1990s, even if its expenses are substantially underwritten by the federal government. Moreover, because of economies of scale for pollution control efforts differ between the utility sector and the industrial sector—including fuel purchase, control technology, and transportation—capturing SO₂ reductions from utilities instead of industrial sources appears to be relatively more cost effective.

Any attempt to quantify the actual costs of an emissions reduction program in terms of control costs, coal market shifts, or electricity rates, however, requires the analyst to specify a number of prior conditions. Both the size of the rollback—for example, four, eight, or 12 million tons per year—and the geographical area in which the emissions reductions are required must be specified. The timing of additional controls is also a major determinant of costs. The imposition of further controls now, for example, implies the use of currently available technology, such as FGD, whereas a delay will allow consideration of possible new technologies, such as LIMB. The advantages of delay must be weighed against interim damage to the environment.

There are numerous reviews available that detail the amount of money emitters will be required to spend for controlling acid deposition precursors (12). Empirical results for reductions in SO₂ by utilities generally have been uniform across studies. Annual cost estimates range from \$1 billion to \$2 billion for a 40% reduction, and from \$2 billion to \$4 billion for a 50% reduction. A cost of \$5 billion to \$6 billion is estimated for a 66–75% reduction. Predicted average increases in electricity rates have ranged from 1.4% for a four-million-ton rollback, to 8% for a rollback of twelve million tons.

It is surprising, at least to the community of economists, that this recent work suggests the costs of alternative strategies for SO₂ control have only minor differences. For example, systems based on state implementation plans for controlling at least one acid deposition precursor tend to be as cost effective as economic incentive systems (13–15).

Atkinson attributes this mainly to the greater aggregate quantity of emissions that localized economic incentive strategies allow in order to meet local ambient standards (15). Emissions are distributed spatially such that the dispersal properties of the local atmosphere are used more effectively. These greater emissions provide more material for long-range transport, and when the material is removed to meet ambient standards that account for long-range

TABLE 2
Incremental costs of SO₂ emissions reduction strategies

Control strategies	Costs	
	(in dollars per ton SO ₂)	
Coal cleaning		
North Appalachia and east Midwest coal	\$50-600	
South Appalachia coal	700-1000	
Utility strategies^a		
Fuel Switching		
Shift from high- to low-sulfur coal	250-350	
Shift from high- to medium-sulfur coal	350-400	
Shift from medium- to low-sulfur coal	400-500	
Shift from high- to low-sulfur residual oil	300-400	
Flue gas desulfurization		
Shift from unscrubbed to scrubbed high-sulfur coal	400-600	
Shift from unscrubbed to scrubbed medium-sulfur coal	600-1500	
Shift from unscrubbed to scrubbed low-sulfur coal	1800-3000	
Limestone injection multistaged burners ^b		
High-sulfur coal	250-500	200-350
Medium-sulfur coal	300-1100	250-700
Low-sulfur coal	600-2000	500-1200
Industrial strategies^c		
Fuel Switching		
Shift from high- to low-sulfur coal	250-350	
Shift from high- to medium-sulfur coal	350-400	
Shift from medium- to low-sulfur coal	400-500	
Shift from high- to low-sulfur residual oil	300-400	
Flue gas desulfurization		
Shift from unscrubbed to scrubbed high-sulfur coal	400-600	
Shift from unscrubbed to scrubbed medium-sulfur coal	600-1500	
Shift from unscrubbed to scrubbed low-sulfur coal	1800-3000	

^aRepresentative costs for a 500-MW power plant. Costs will vary for each region and year.

^bRemoval of SO₂ for retrofits expected to be between 50% (first column) and 60% (second column).

^cRepresentative costs for a 170-million-Btu/hour industrial boiler. Costs will vary for each region and year.

Source: Reference 18

transport, the advantage of the economic incentive strategies is drastically reduced.

Conclusion

Partly because of the fuzzy state of existing scientific information and partly because of their intrinsic failings, benefit-cost measurements of acid deposition control may well involve major errors of commission and omission. Indeed, the methods used to assess price responses and people's adaptations are valid only when a projected change is so small that an evaluation of states proximate to the status quo is sufficient, and when a projected change does not significantly alter the sets of technical and economic options available in other markets, locations, and times.

The literature on acid deposition is replete with conjecture about the mining of ecosystem nutrients and the ac-

cumulation of ecosystem toxins. These speculations imply long-term damage. The irreversibility of many of these effects, should they occur, means that efforts to attach values to them must account for the possible loss of future opportunities to enjoy ecosystem amenities and life support services. Although the relevant abstract principles are well understood (16), economic practice is much weaker in empirically establishing the quantitative impact of option foreclosures upon future price structures.

The value of benefit-cost analysis of acid deposition control resides more in its potential contributions to clearer statements of the problem than in its provision of accounts for social and ecological bookkeeping. Benefit-cost analysis as an accounting exercise will emphasize those aspects that can be readily quantified and priced, such as the decay of materials. Rather than en-

couraging the exploration of ways to live with scientific and economic ambiguities, benefit-cost analyses will tend to avoid them. Because most ambiguities arise from long-term depletion of ecosystem nutrients and the effects of toxin accumulation, a myopic perspective is encouraged.

The long-term effects suggest that the conditions and value of future natural ecosystems might depend on current management choices, implying that the management problem has dynamic and sequential features.

Tesfatsion has shown that if the workings of the natural system are well understood, and if the net gains of any particular action are highly correlated over the long term, the outcomes of myopic decision rules closely approximate those that embody sequential features (17). Yet few currently characterize the scientific or economic aspects of acid deposition transport and control as being well understood on less than a broad spatial and temporal scale (4). In addition, differing damage thresholds across materials and ecosystem components imply that net gains are not highly correlated over time.

The dominant dynamic and stochastic features of acid deposition control advise caution in using the valuation numbers a conventional benefit-cost analysis provides. The methods are better viewed as a set of tools that illustrate the natural system consequences of market responses and people's adaptations to variations in acid deposition levels.

Whatever the policy objectives and criteria, benefit-cost studies force policy makers to face the inherent tradeoffs of the acid deposition problem and the influences that individuals and institutions choose to exercise on the structure of these tradeoffs.

Acknowledgment

Before publication, this article was reviewed for suitability as an *ES&T* feature by Lester Lave, Carnegie-Mellon University, Pittsburgh, Pa. 15213; Richard N. L. Andrews, Institute for Environmental Studies, University of North Carolina, Chapel Hill, N.C. 27514; and Richard Liroff, Conservation Foundation, Washington, D.C. 20036.

References

- (1) Olson, M. *American Economic Review* 1982, 72, 262-66.
- (2) Lewis, W. M., Jr.; Grant, M. C. *Science* 1980, 207, 176-77.
- (3) Vogelmann, H. M. *Natural History*, November 1982.
- (4) "Acid Deposition Atmospheric Processes in Eastern North America: A Review of Current Scientific Understanding"; National Research Council; National Academy Press: Washington, D.C. 1983.
- (5) Crocker, T. D. Statement before the Select Committee on Small Business and Commit-

- tee on Environmental and Public Works, "Economic Impact of Acid Rain," U.S. Senate Report, 96th Congress, 2nd Session, Sept. 23, 1980; pp. 100-111.
- (6) Haagenrude, S. E.; Atteraaas, L. Presented at the 158th Meeting of the Electrochemical Society, Hollywood, Fla., Oct. 5-10, 1980.
- (7) Jonsson, B. In "Proceedings of the First International Symposium on Acid Precipitation and the Forest Ecosystem," Technical Report NE-23; Northeastern Forest Experimental Station: Upper Darby, Pa., 1976.
- (8) "Nitrates: An Environmental Assessment"; Panel on Nitrates; National Academy of Sciences, National Research Council: Washington, D.C., 1978; p. 577.
- (9) "Forest Statistics of the U.S., 1977—Review Draft"; U.S. Forest Service; U.S. Government Printing Office: Washington, D.C., 1978.
- (10) Menz, F. C.; Mullen, J. K. In "Economic Perspectives on Acid Deposition Control"; Crocker, T. D., Ed.; Butterworth Publishers: Boston, Mass., 1984; pp. 135-56.
- (11) Regens, J. L. In "Economic Perspectives on Acid Deposition Control"; Crocker, T. D., Ed.; Butterworth Publishers: Boston, Mass., 1984; pp. 5-20.
- (12) Rubin, E. S. *Environ. Sci. Technol.* **1983**, *17*, 366-77A.
- (13) "The Regional Implications of Transported Air Pollutants: An Assessment of Acidic Deposition and Ozone," Interim Draft, Office of Technology Assessment, U.S. Congress: Washington, D.C., July 1982.
- (14) Silverman, B. G. *J. Air Pollut. Control Assoc.* **1982**, *32*, 1031-42.
- (15) Atkinson, S. E. *Canadian Journal of Economics* **1983**, *16*, 704-22.
- (16) Dasgupta, P. S.; Heal, G. M. "Economic Theory and Exhaustible Resources"; Cambridge University Press: New York, N.Y., 1979.
- (17) Tesfatsion, L. *Journal of Economic Dynamics and Control* **1981**, *3*, 31-38.
- (18) "Acid Deposition," unpublished briefing document; U.S. EPA: Washington, D.C., 1983.



Thomas D. Crocker (l.) is a professor of economics at the University of Wyoming. He has served on the faculties of the Universities of California and Wisconsin and was a member of the EPA Science Advisory Board. The development of means to value environmental goods and the properties of alternative allocation systems for these goods have dominated his research.



James L. Regens (r.) is an associate professor of political science and a research fellow in the Institute of Natural Resources at the University of Georgia. He received his B.S. and M.A. from the University of Arizona and a Ph.D. from the University of Oklahoma. From 1980 to 1983, Regens served with the EPA; he was joint chair of the federal Interagency Task Force on Acid Precipitation (1981-1982) and chairman of the Energy and Environment Group of the Organization for Economic Cooperation and Development (1981-1983).

MANAGEMENT CONSULTANT 67¢



You couldn't sign on a more valuable ally than **Chemical & Engineering News.**

For \$35 a year (just 67¢ per weekly issue), we'll help you spot trends that are going to impact your company's sales, production, construction, and prices.

We'll give you advance information on where to concentrate R&D efforts, how the import/export market's shaping up, what employment prospects look like industry-wide.

We'll take you to Capitol Hill for the inside scoop on policy makers, legislation, and regulatory affairs... around the world for an overview of the chemical industry... and across the country for an in-depth look at what your competition's up to.

With **Chemical & Engineering News**, you'll know which way the wind's blowing in time to take decisive action. You'll get special issues with the facts and figures you need to make intelligent choices. And you'll enjoy crisp, accurate reporting by the only chemical publication with a fully staffed Washington bureau.

So call the toll-free number below, and hire us today. Your very first issue will show you why the best managers wouldn't manage without us.

To subscribe call:

(800) 424-6747 (U.S. only)

**CHEMICAL &
ENGINEERING**

NEWS

International chemicals advisory programs



Richard M. Dowd

For several years, the U.S. has been engaged in the international dialogue on the safety and environmental aspects of world trade in chemicals. In addition to monitoring the regulatory activities of the European Economic Community, the U.S. participates in the Organization for Economic Cooperation and Development's Chemicals Programme (OECD-CP) and the International Programme on Chemical Safety (IPCS). Both groups develop methodologies and testing guidelines for chemicals, promote plans to protect public health and the environment, and exchange information on chemicals' properties.

OECD's chemicals program

Founded in 1971, the OECD-CP, which is composed of the U.S. and 24 other countries, seeks to harmonize national policies among member countries in order to reduce the distortions in trade that may result from disparate national controls. Another goal is to lessen the administrative burden of managing the risks associated with the production, distribution, and use of chemicals. Once an OECD decision or recommendation has been made, it must then be put into effect by each member country.

The program first considered problems associated with the use of polychlorinated biphenyls, mercury, and cadmium. In 1973, restrictions on mercury emissions and PCB use were adopted. Numerous other substances, such as chlorofluorocarbons, also have been studied.

As the U.S. Toxic Substances Control Act of 1976 (TSCA) was enacted, and as similar laws or agreements (such as the Sixth Amendment of the European Economic Community) came into effect elsewhere, the OECD-CP focused on procedures to assess the potential hazard of chemicals before their entry into the marketplace. Expert groups were established to examine testing methods and the sequence in which tests should be performed.

In 1979 a hazard assessment group, charged with harmonizing assessment methods, was also established. Other groups have given guidance on good laboratory practice and confidentiality of data, written an international glossary of key terms, and developed information exchange procedures.

Testing guidelines adopted

By the end of 1984, 70 test guidelines (for determining the physical and chemical properties of a substance, its effects on biotic systems, rates of degradation and accumulation, and potential health effects) had been adopted. If implemented by member countries, the guidelines could lower testing and assessment costs and reduce the use of animals in chemical testing. Data generated following the test guidelines and principles of good laboratory practice in one country need not be regenerated for notification or other uses in another member country.

Within the past two years, the OECD also has recommended minimum pre-market data requirements and guidelines for reviewing existing chemicals. These guidelines are more stringent than those required by TSCA, and EPA estimates they could cost \$50,000 per chemical, on average. In April 1984, the OECD recommended that member countries exchange information related to the export of banned or severely restricted chemicals. This action would provide information to importing countries on an estimated 150-200 substances that are banned or restricted in

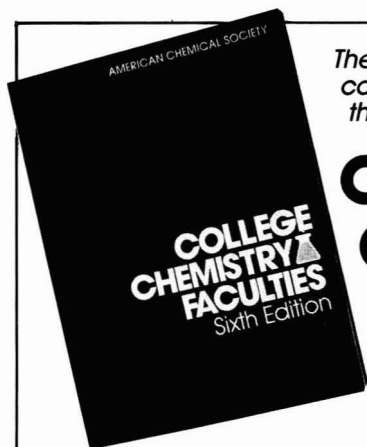
exporting countries. This will enable importers to make informed decisions about the use of these chemicals. EPA sources say that such notifications are already provided annually with the first shipment of some substances defined under Section 12 of TSCA.

A similar United Nations resolution was recently opposed by the U.S. because it encourages the preparation of virtually "random" lists of banned or restricted substances, even though there are no common definitions of these terms among the 158 member countries of the United Nations. The Chemical Manufacturers Association, for instance, would prefer an arrangement whereby notification of any regulation of a substance by an exporting country would have to be distributed annually by the federal government to all importing countries.

The OECD also has agreed to coordinate its efforts with the IPCS, which is sponsored by the United Nations Environment Programme, the World Health Organization, and the International Labor Organization. The IPCS seeks cooperation among the OECD countries and others, such as China, the Soviet Union, India, Saudi Arabia, and Mexico, on protocols for testing chemicals, methodologies for health risk assessments, and guidelines for managing chemical emergencies, workplace standards, and manpower development.

Participants in these international advisory programs generally agree that the world chemicals trade will benefit from the coordination of individual countries' regulatory programs. In developing countries, however, they believe that an infrastructure of expertise and experience in environmental and safety management must be developed.

Richard M. Dowd, Ph.D., is a Washington, D.C., consultant to Environmental Research & Technology, Inc.



The most complete listing of college chemistry faculties in the U.S. and Canada

COLLEGE CHEMISTRY FACULTIES

SIXTH EDITION



multi-purpose reference, COLLEGE CHEMISTRY FACULTIES is an important tool for researchers, recruiters, industrial chemistry labs, students and teachers as well as college and high school counselors and libraries.

For convenient researching, the directory provides:

1. State-by-state listings of institutions showing degrees offered, staff members and their major fields, department address and phone number.
2. Index of faculty members' names.
3. Index of institutions.

Covering 2,400 two-year and four-year colleges and universities in the U.S. and Canada, COLLEGE CHEMISTRY FACULTIES lists the current affiliations and major teaching fields of over 18,000 faculty members.

State-by-state listings make it easy for students and faculty to find chemistry departments in any area they choose, and for marketers to use the state listings for planning sales and service territories.

Just published, the Sixth Edition of COLLEGE CHEMISTRY FACULTIES is available in time for the fall semester. Order now and keep your information up-to-date. Soft cover, 8 1/2" x 11", 204 pages. . . \$34.00

CALL TOLL FREE 1-800-424-6747

(for credit card orders),
write, or mail coupon below.

American Chemical Society Distribution Office 1155 Sixteenth Street, NW, Washington, DC 20036

Please send _____ copies of **COLLEGE CHEMISTRY FACULTIES** @ \$34.00. On prepaid orders, ACS pays shipping and handling charges.

- Payment enclosed (payable to American Chemical Society)
 Bill me Bill company

Charge my MasterCard VISA Barclay Card ACCESS

Card # _____ Interbank # _____ (MasterCard only)

Expiration Date _____ Signature _____

Name _____

Company/Organization _____

Address _____ Telephone Number _____

Billing Address _____

City _____ State _____ ZIP _____

56170/2504/E710

CLASSIFIED SECTION

POSITIONS OPEN

Dames & Moore, an International Consulting, Engineering and Geoscience firm, has immediate openings in its California offices for entry-level and experienced professionals in the following disciplines:

**CIVIL ENGINEERS
GEOLOGISTS
HYDROGEOLOGISTS
ENVIRONMENTAL ENGINEERS**

We are particularly interested in applicants that are highly motivated, aggressive and possess excellent communication skills. Applicants with 1-6 years experience and a Masters degree in the conduct of hazardous waste remedial projects are invited to submit their resume to:

Rita Armstrong

Dames & Moore

500 Sansome Street
San Francisco, CA 94111

Equal Opportunity Employer M/F/H/V

POSITION ANNOUNCEMENT ASSISTANT/ASSOCIATE PROFESSOR TENURE TRACK

Department of Environmental Health
College of Public Health
University of Oklahoma at Oklahoma City
Health Sciences Center

Application Deadline April 15, 1985, or Until the Position is Filled
Position Available July 1, 1985

Minimum qualifications include an earned doctorate in Environmental Health or a closely related discipline, primary expertise in the area of environmental planning/policy-making and resource management, demonstrated competence or evidence of outstanding promise in research, and proficiency in computer applications to environmental health. Additional consideration will be given to candidates having a general sanitation or environmental biology background, post-doctoral training, teaching, and/or field experience. Applicants should submit a resume and the names of four references to:

Robert Y. Nelson, Ph.D.,
Chair, Environmental Health Search Committee
College of Public Health
Department of Environmental Health
P. O. Box 26901
Oklahoma City, Oklahoma 73190
(405) 271-2070

THE UNIVERSITY OF OKLAHOMA IS AN EQUAL OPPORTUNITY/
AFFIRMATIVE ACTION EMPLOYER.

**USE THE
CLASSIFIED
SECTION**

INDEX TO THE ADVERTISERS IN THIS ISSUE

ADVERTISERS

PAGE NO.

EG&G Ortec 100-101
Charles Tombras Advertising

Fein-Marquart Associates, Inc. 111

Seastar Instruments Ltd. IFC

Advertising Management for the American
Chemical Society Publications

CENTCOM, LTD

President

Thomas N. J. Koerwer

Executive Vice President Senior Vice President
James A. Byrne Benjamin W. Jones

Alfred L. Gregory, Vice President
Clay S. Holden, Vice President
Robert L. Voepel, Vice President
Joseph P. Stenza, Production Director

25 Sylvan Road South
P.O. Box 231
Westport, Connecticut 06881
(Area Code 203) 226-7131.
Telex No. 643310

ADVERTISING SALES MANAGER
James A. Byrne, VP

ADVERTISING PRODUCTION MANAGER
Geri Anastasia

SALES REPRESENTATIVES

Philadelphia, Pa. . . . Patricia O'Donnell, CENTCOM, LTD., GSB Building, Suite 425, 1 Belmont Ave., Bala Cynwyd, Pa 19004 (Area Code 215) 667-9666

New York, N.Y. . . . Dean A. Baldwin, CENTCOM, LTD., 60 E. 42nd Street, New York 10165 (Area Code 212) 972-9660

Westport, Ct. . . . Edward M. Black, CENTCOM, LTD., 25 Sylvan Road South, P.O. Box 231, Westport, Ct. 06881 (Area Code 203) 226-7131

Cleveland, Oh. . . . Bruce Poorman, CENTCOM, LTD., 325 Front St., Suite 2, Berea, OH 44017 (Area Code 216) 234-1333

Chicago, Ill. . . . Michael J. Pak, CENTCOM, LTD., 540 Frontage Rd., Northfield, Ill 60093 (Area Code 312) 441-6383

Houston, Tx. . . . Dean A. Baldwin, CENTCOM, LTD., (Area Code 215) 667-9666

San Francisco, Ca. . . . Paul M. Butts, CENTCOM, LTD., Suite 1070, 2672 Bayshore Frontage Road, Mountainview, CA 94043. (Area Code 415) 969-4604

Los Angeles, Ca. . . . Clay S. Holden, CENTCOM, LTD., 3142 Pacific Coast Highway, Suite 200, Torrance, CA 90505 (Area Code 213) 325-1903

Boston, Ma. . . . Edward M. Black, CENTCOM, LTD. (Area Code 203) 226-7131

Atlanta, Ga. . . . Edward M. Black, CENTCOM, LTD., Phone (Area Code 203) 226-7131

Denver, Co. . . . Paul M. Butts, CENTCOM, LTD. (Area Code 415) 969-4604

professional consulting services directory

ENVIRONMENTAL
SCIENCE, TECHNOLOGY,
AND ENGINEERING.

EA
ECOLOGICAL ANALYSTS
Huntington Beach, Calif. • Lubbock, Texas • Sparks, Md. 21157 • 301-771-4958
Baltimore • Chicago • Cincinnati • Lincoln • New York • San Francisco

CONSULTING GROUND-WATER GEOLOGISTS
ROUX ASSOCIATES INC

ROUX

- RCRA Monitoring
- Superfund Response
- Site Evaluation
- Aquifer Clean-Up
- Resource Development

50 NORTH NEW YORK AVENUE
HALESITE, NEW YORK 11743 516 673-4921
500 PURDY HILL ROAD
MONROE, CONNECTICUT 06468 203 268-2846

Dunn Geoscience

ALBANY, NY 518/783-4182
BUFFALO, NY 716/894-1500
NEW YORK CITY 212/712-2851
LACONIA, NH 603/528-4025
HARRISBURG, PA 717/761-8710

Geologic and Hydrologic Consultants
• Ground Water Assessment & Supply
• Solid & Hazardous Waste Site Design

GERAGHTY & MILLER, INC.
Groundwater Consultants

The North Shore Atrium
6800 Jericho Tpke., Syosset, NY 11791
(516) 921-6060

ADDITIONAL LOCATIONS
AIKEN, SC • NEWTOWN, PA • OAK RIDGE, TN

ANNAPOLIS
BATON ROUGE
DENVER
HACKENSACK, NJ
PALM BEACH GARDENS
TAMPA

THE CONSULTANTS' DIRECTORY

UNIT	Six Issues	Twelve Issues
1" x 1 col.	\$55	\$50
1" x 2 col.	110	100
1" x 3 col.	160	140
2" x 1 col.	110	100
2" x 2 col.	200	180
4" x 1 col.	200	180

Geri Anastasia
ENVIRONMENTAL
SCIENCE & TECHNOLOGY
25 Sylvan Road South
P.O. Box 231
Westport, CT 06881
Or call her at (203) 226-7131

COMPLETE ANALYTICAL SERVICES

BML

- Gas Chromatography/ Mass Spectroscopy
- Trace Metal Analyses - ICAP, AA, GFAA
- Drinking Water Analyses
- Industrial Hygiene Services
- Research and Development
- Environmental Field Sampling
- EPA Priority Pollutant Analyses

Brochure and/or fee schedule available on request

BARRINGER MAGENTA LTD.
304 Carlingview Drive Rexdale Ont Canada (416) 675-3870
US Office Denver CO 80401 (303) 232-8811

Clayton Environmental Consultants

- Industrial Hygiene Surveys
- AIHA - Accredited and CDC - Licensed Laboratories
- GC/MS, HPLC, X-Ray Diffraction, AA, and Electron Microscopy (SEM/EDS)
- Hazardous Waste Management
- Emission and Ambient Air Surveys
- Engineering Design
- Environmental Audits
- Materials and Material Safety Data Sheets
- Expert Testimony

25711 Southfield Rd • Southfield, MI • 48075 • 313 424 8860

Atlanta, GA • Edison, NJ • Windsor, Ont.
(404) 952-3064 • (201) 225-6040 • (519) 255-9797

A Technical Service of Marsh & McLennan

ENVIRODYNE ENGINEERS

a consulting engineering and sciences firm

- environmental engineering analytical chemistry
- priority pollutant analyses
- environmental monitoring and assessment
- hazardous waste monitoring
- hazardous waste management
- transportation engineering
- energy engineering
- construction management

12161 Lackland Road
St. Louis, Missouri 63141
(314) 434-6960

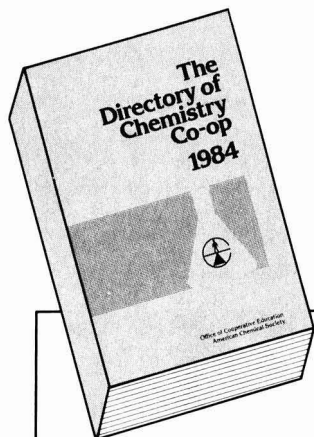
Baltimore / Chicago / New York

Complete Analytical Services
SINCE 1919

- Screening of Industrial Waste for EPA Priority Pollutants using Finnigan OWA-30 GC/MS.
- NPDES & SPDES Organic & Inorganic Testing.
- Drinking Water Analysis to EPA Standards.
- Bioassay, Bioaccumulation & Toxicity Studies of Industrial Waste, Municipal Sludge & Dredge Spoils.
- Leachate Potential Studies & Analysis.
- Total Instrumental Analysis: A.A., GC/MS, G.C., I.R., TOC & TOD
- RCRA Hazardous Waste Testing.

NEW YORK TESTING LABORATORIES
81 Urban Avenue, Westbury, N.Y. 11590
(516) 334-7770

RECRUITERS ... EDUCATORS ... CHEMISTS ...



NOW AVAILABLE FROM ACS

THE DIRECTORY OF CHEMISTRY CO-OP

The indispensable guide to cooperative education programs in the U.S. and Canada.

If you are interested in co-op programs as participant, sponsor, or advisor, take advantage of this unique, authoritative reference! Get practical, accurate information on 265 chemistry, chemical engineering, and chemistry-related cooperative education programs in the U.S. and Canada.

In-depth coverage includes contact names and addresses, program size, typical work schedules, academic requirements, geographical and program indices, and a great deal more.

As a reference, this timely resource is essential for:

- Schools interested in starting co-op
- Employers seeking sources of co-op students
- High school students and advisors wishing to locate co-op schools
- Co-op professionals requiring a convenient source of information

SAVE 25%!

This informative, 280-page paperbound volume is available for just \$15.00 a copy (After April 1, 1985, the price will be \$20.00) Order now to take advantage of these special introductory savings.

PHONE TOLL FREE!

Call 1-800-424-6747 (credit card orders only) to order your copy at this special price or mail coupon today!

Please send _____ copies of the *ACS Directory of Chemistry Co-op* @ \$15.00 per copy to:

Name _____

Address _____

Check the method of payment: Check or money order enclosed Credit card: Visa MasterCard Barclay Access American Express

Cardholder Name _____

Card No. _____

Exp. Date _____ Interbank No. _____

(MasterCard and Access only)

Signature _____

Amount Enclosed \$ _____
Make checks payable to **ACS Co-op Directory**.
Orders must be prepaid. California residents,
add 6% sales tax.

Return to: **Office of Cooperative Education**
American Chemical Society
1155 Sixteenth St., N.W.
Washington, DC 20036

Condition Numbers as Criteria for Evaluation of Atmospheric Aerosol Measurement Techniques

Fariba F. Farzanah, Carolyn R. Kaplan, Po Y. Yu, Juan Hong, and James W. Gentry*

Department of Chemical and Nuclear Engineering, University of Maryland, College Park, Maryland 20742

■ In this paper the use of condition numbers as a criterion for evaluating experimental designs in measurements of airborne particulates is examined. The steps required to compute the condition numbers and a description of appropriate scaling are discussed. The method is illustrated with three examples: the selection of indicator elements in source-receptor models, the relevance of condition number to classifier type and inversion algorithms, and in the location of experiments in size distribution measurements. From the magnitude of the condition number it is possible to choose a priori likely candidates for indicator elements and to discriminate among algorithms used to invert penetration measurements for the size distribution.

Introduction

The objective of this paper is to show that mathematical parameters designated as condition numbers $C(N;\alpha)$ provide a guide for experiment design and provide explanations for observed phenomena such as the comparative insensitivity of particle size distribution measurements with inertial impactors relative to diffusion batteries. The approach discussed here is applicable for any set of linear algebraic equations where the number of equations or relations I is greater than the number of variables N . The parameters α refers to the particular definition of norm used to define the condition number. The condition numbers depend only on the matrix coefficients. As a result the condition numbers do not depend on the precision of experimental measurements nor do they weigh unusual experimental difficulties that might preclude certain measurements.

In this paper we first present a brief discussion of the theory of condition numbers describing the method of their calculation for two norms. Next we discuss their application to three specific cases: (1) the selection of indicator elements which are used in determining the relative importance of source strengths (1-3); (2) the use of condition numbers to provide a means of comparison of different classifiers and for the evaluation of inversion algorithms in determining the size distribution of aerosols; (3) the selection of experimental conditions or number of terms which can be used in determining size distributions. For example, we show that if one attempts to express the size distribution as measured with a diffusion battery as a sum of m size classes, the value of m must be less than 5. Otherwise, the condition number is too large.

Condition Numbers

An objective of our analysis is to develop a quantitative criterion to provide a basis for selection between inversion algorithms and which provides an a priori estimate of the effect of random experimental scatter on the reliability of the inversion. Such a criterion should be independent of the error associated with the measurements depending only on the particular inversion algorithm and the location of the experimental measurements. During the mid-forties several mathematical criteria were developed to determine the effect of round off error in the solution of large sets of linear algebraic equations with digital computers (4, 5).

Subsequent development led to the use of condition numbers, which for a set of N algebraic equations written as

$$[A][X] = [B] \quad (1)$$

may be expressed by

$$C(N;\alpha) = \|A\|_{\alpha} \|A^{-1}\|_{\alpha} \quad (2)$$

where $\|A\|_{\alpha}$ is the α norm for the matrix of coefficients A . First, it is clear from the definition of $C(N;\alpha)$ that $C(N;\alpha)$ depends only on A and is independent of measurements which would correspond to the B vector. Second, the condition number depends both on the matrix and the inverse. For sets of equations that are nearly singular the coefficients of the inverse matrix are large so that one would expect the condition number to be large.

The condition numbers defined as above have two important properties: First, the perturbation in the norm of the solution is bounded by the product of the condition number and the relative perturbation of the forcing vector (i.e., measurements). That is (6)

$$\frac{\|\Delta X\|_{\alpha}}{\|X\|_{\alpha}} \leq C(N;\alpha) \frac{\|\Delta B\|_{\alpha}}{\|B\|_{\alpha}} \quad (3)$$

Physically this implies that the relative error in the retrieved function is bounded by the condition number times the relative experimental error. Consequently one cannot compensate for a badly designed experiment, with increased experimental precision. Second, one has the relationship between condition numbers defined for any two norms α and β where $a_2 > a_1 \geq 0$ (2).

$$a_1 C(N;\beta) \leq C(N;\alpha) \leq a_2 C(N;\beta) \quad (4)$$

Typical values are $a_1 \sim 1/2$ and $a_2 \sim 2$. This inequality implies that if a set of equations is badly conditioned, the

condition numbers for any norm will be large. Consequently to test the system of equations, it is necessary to calculate only one norm, preferably the one requiring the least computation.

In our opinion the condition numbers that are the simplest to use are $C(N;1)$ or $C(N;\infty)$, where for a vector X the norm $\|X\|_1$ is defined as

$$\|X\|_1 = \sum_j |X_j| \quad (5)$$

and the norm $\|X\|_\infty$ is the component with the largest absolute value. For these norms the matrix norms are given by

$$\|A\|_2 = \text{maximum } (J) \text{ for } \sum_{i=1}^N |a_{ij}| \quad (6)$$

and

$$\|A\|_\infty = \text{maximum } (I) \text{ for } \sum_{j=1}^N |a_{ij}|$$

The first norm $\|A\|_1$ is the maximum of the sum of the elements for each column in the matrix while the second norm is the maximum of the sum of the elements in each row. The computation of the condition number requires only the determination of the inverse matrix A^{-1} and several summations.

For matrices determined from linear least-squares regression, the condition number $C(N;2)$ is equal to the ratio of the maximum to minimum eigenvalues. To some extent the condition numbers can be affected by normalization of the matrix of coefficients A . If the rows are normalized so that the sum of their elements is one, then the value of $C(N;\infty)$ is a minimum. This does not imply that $C(N;\infty)$ is less than $C(N;2)$ or that for some other normalization an even lower condition number can be obtained for $C(N;\alpha)$ where α does not approach ∞ (8).

Usually as the number of elements in the matrix increases, then the condition numbers increase; however, there are exceptions. In summary we recommend that either $C(N;1)$ or $C(N;\infty)$ be calculated with the matrix of coefficients normalized so that the sum of the coefficients along a row is one.

Indicator Elements

Recently considerable effort has been spent in identifying pollutant sources by identifying trace compounds or elements in ambient samples and relating their composition to the composition of possible sources. A widely used method is neutron activation where the composition of 20-30 elements can be inferred by measuring the energy and magnitudes of the decay products of irradiated samples. For a well-defined system the mathematical problem is to solve the matrix equation

$$[A][S] = [M] \quad (7)$$

where $[M]$ is the elemental compositions found in the measured sample, $[S]$ is the strength of various sources, and the elements A_{ij} of the matrix $[A]$ are the composition of element i in the j th source. Normally the number of elements measured will be larger than the number of sources, so that the source strengths are found by linear least-squares regression; that is

$$[A]^T[A][S] = [A]^T[M] \quad (8)$$

During the past 15 years researchers have found that better results could be obtained if not all elements were used in the least-squares regression but rather a group of six to eight "indicator" elements which could then be used

Table I. Condition Numbers as Criteria for Indicator Element Selection

case	elements	missing element	$C(N;\infty)$	$C(N;1)$
1	27		10.5	17.9
2	24		13.7	30.0
3	8		5.4	7.4
4	16		38.0	67.0
5	23	Na	33.0	59.0
		As	19.0	40.0
		Se	19.0	40.0
		Pb	14.0	35.0
		V	14.0	33.0
		Mn	15.0	33.0
		Zn	14.0	32.0
		Al	13.0	28.0
		Fe	13.0	29.0

to estimate the sources of five or six generic sources: marine, soil, oil- and coal-fired power plants, refuse incineration, and motor vehicle transportation (1-3). On the basis of their experience they found that Al, Fe, Na, V, Zn, Pb, Mn, and As made a good set of indicator elements.

The question we examine here is could one arrive at a similar set of elements a priori using the criterion that the best set of "indicator elements" would be the set which has the minimum condition number. If the set of elements obtained from condition number analysis were the same as that obtained from experience, it would provide a mathematical justification after the fact for their choice and suggest a procedure for screening elements or compounds as potential markers in the absence of prior experience. It should be stressed that the condition numbers do not depend on the reliability of measurements, and should certain elements or compounds be unsuitable because of their volatility or uncertainty in measurements, they must be eliminated from the group of potential marker compounds before the condition numbers are calculated.

In this section we hope to show that condition number analysis and current practice using neutron activation analysis coincide and that the condition numbers provide a quantifiable basis for evaluating the relative importance of specific elements.

The computational model we used was as follows: The source strengths of 27 elements for six generic sources (marine, oil- and coal-powered power plants, soil, incineration, and transportation) were taken from the data of Kowalczyk et al. (1). Condition numbers were computed for five cases: (1) least squares regression with 27 elements; (2) least-squares regression with 24 nonvolatile elements (I, Cl, and Br were eliminated from the original set of 27); (3) least-squares regression with the eight indicator elements proposed by Kowalczyk; (4) least-squares regression with the 16 nonvolatile elements which were *not* selected by Kowalczyk as indicator elements; (5) least-squares regression with 23 nonvolatile elements (these were obtained by removing one element from the set of 24 elements). The results of the condition number analysis are presented in Table I.

We expect to observe that the condition number for 27 elements is less than for the set of 24. Since one would normally expect a larger matrix to yield a larger condition number, the explanation must lie in that from condition number analysis the three elements were more suitable for indicator elements than a number of others in the group of 24 nonvolatile elements. The explanation for this discrepancy between condition number analysis and practice is that these elements are found in volatile compounds so

that there is unacceptable experimental scatter in the ambient measurements. This emphasizes the first key point in the condition number analysis that uncertainty in measurements is not considered.

Comparing the three cases of the 24 nonvolatile elements with those of the 8 indicator elements and the remaining 16, we find that the best results are obtained for the 8 indicator elements as indicated by the smaller condition numbers. More significant is that when these elements are removed, the condition number for 16 elements is much larger than for the complete set of 24. This suggests a criterion for indicator elements that when the removal of an element from a class of suitable candidate elements results in a larger condition number (i.e., more uncertainty in the source strengths), it should be considered as a prospective indicator element.

By use of this test each of the elements was removed in turn from the set of 24. It was found that the greatest increase occurred for six elements Na, As, Se, Pb, V, and Mn, with the greatest change shown when sodium was removed. These results were in agreement with the selection of elements used by Kowalczyk except for two minor differences. Condition number analysis provided no basis for choosing Fe and Al. Also, it suggests that Se would be a suitable indicator element although the shifts in condition numbers for any of these three elements are relatively small. The most significant shift occurs for sodium, which occurs at high concentration in marine aerosol while no other nonvolatile element shows a similar trend.

In summary, condition numbers provide a quantitative basis for choosing indicator elements. When properly used (i.e., preselecting the compounds to eliminate those unsuitable because of uncertainty in measurement), they should prove a useful criterion in selecting suitable compounds. Simulations show agreement with current practice.

In practice, one frequently uses a weighted least-squares regression. A danger in this method, however, is that it can lead to negative source strengths. Can the condition numbers provide an a priori test as to whether a particular weighting or solution method will lead to negative strengths? The answer is no and yes. Condition numbers provide no test as to the value or sign of the solution. However, negative solutions for physically based solutions almost always have the property that small shifts in the measurements mean large shifts in the solution. Choosing a weighting mode or solution method which gives a minimum condition number dampens the oscillation in the solutions caused by small perturbations in the measurements, making negative solutions more unlikely.

The choice of using an overspecified system has the advantage of minimizing the relative error in the measurement. Usually the condition number will be larger, so that, in order to minimize the error in the solutions, there is a trade-off between reduced measurement error and larger condition number. We have found that for additional measurements the condition number increases slowly so that one obtains better results with more measurements. Our studies suggest that it is unlikely that the condition number can be used to optimize the number of experiments. However, they do provide the best criteria for choosing the number of terms in a correlation.

Relations between Condition Numbers and Classifier Mode

In most measurements of the size distribution for atmospheric aerosols, the fraction of particles passing through the stage is measured. In some cases, the mass

or surface area is measured instead of the particle number. For one classifier, inertial impactors, the field instrument nearly always consists of several stages in sequence. For other classifiers (i.e., diffusion batteries and elutriators) the size distribution is determined from measurements of the fractional penetration at different operating conditions (i.e., flow rate). Researchers soon discovered that measurements with inertial impactors could be inverted relatively more easily than diffusion battery measurements. This fact was manifest in that the retrieved size distributions were more nearly reproducible in replicate measurements and that the retrieved size distributions were less ambiguous. Moreover, Maigne (9) found that, for measurements with diffusion batteries, a more reliable distribution was obtained when the difference in fractional penetrations between two flow rates was used instead of the fractional penetration (the directly measured variable). The latter is a curious result for the raw data as the measurements are the same and one would intuitively expect the reliability of the inversion to be unchanged.

The objective of this section is to compute the condition numbers for different modes of inversion and for different classifiers. In order to determine the effect of the condition number on the accuracy of inversion, it is necessary to use a specific algorithm. We chose the linear inversion algorithm with cross validation (10). In this algorithm the matrix of coefficients are not normalized, so that one does not have a condition number directly comparable to that described above. Instead one has a ratio of the maximum to minimum eigenvalues, which is for symmetrical matrices, the condition number $C(N;2)$.

The procedure used in this section was to first assume a trial distribution (a log-normal distribution with a known mean and standard deviation). The simulated aerosol then passed through a classifier operating at six different conditions. These conditions would correspond to different sizes for cyclones and inertial impactors or to a different flow rate for diffusion batteries and elutriators. The fraction particle loss of the aerosol stream leaving the impactor was computed for the six stages individually and grouped sequentially. This simulated fractional penetration was perturbed with a small random error. The inversion algorithm was then used to retrieve the initial distribution for the two cases where the simulated measurement was with and without error.

First, we calculated the condition number for a sequence of six classifiers. In this case, the Nyström algorithm was applied. In this method the size distribution function is a mixture of six sizes, with the frequencies in size class obtained from the solution of the algebraic equations:

$$\text{Ef}(D_j, Q_k) F_j = \bar{\text{Ef}}(Q_k) \quad (9)$$

where Q_k is the flow rate, $\text{Ef}(D_j, Q_k)$ is the theoretical efficiency for particles of size D_j and flow rate Q_k , and $\bar{\text{Ef}}$ is the experimental efficiency. For this set of equations the condition number can be calculated from the matrix of coefficients $\text{Ef}(D_j, Q_k)$. The matrix elements were normalized so that the sum of the elements in each row was one. This gives the minimum value for $C(6; \infty)$. The results for the four types of classifiers are given in Table II.

The efficiencies for the inertial impactors were from the correlation of Marple and Liu (11). The inertial impactors are nearly ideal as is apparent from the condition numbers of 1.2. For the cyclone and the elutriator the expressions of Stern (12) and Pich (13) were used, respectively. The condition numbers were $\sim 2 \times 10^2$, about 2 orders of magnitude larger. The condition numbers for the diffusion battery were based on the expression for efficiency from

Table II. Normalized Conditions Numbers for Six Particle Size Classifiers in Sequence

classifier (type)	condition no.			
	$C(6,1)$	$C(6,2)$	$C(6,\infty)$	$\lambda_{\max}/\lambda_{\min}$
inertial impactor	1.2	1.2	1.2	6.0
elutriator	2.3×10^2	1.5×10^2	1.9×10^2	2.9×10^3
diffusion battery	3.4×10^4	2.0×10^4	2.8×10^4	5.4×10^4
cyclone	2.3×10^2	1.6×10^2	2.0×10^2	5.9×10^4

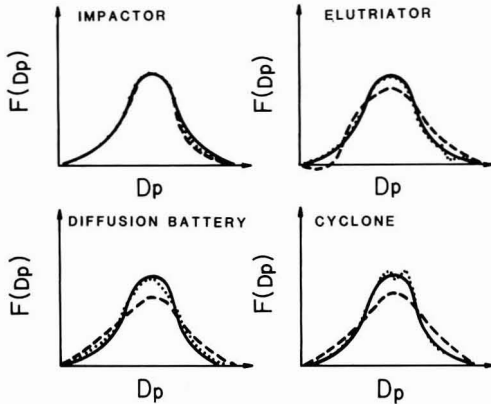


Figure 1. Comparison of retrieved functions for four classifiers by linear inversion algorithm. (—) Given; (---) retrieved (exact); (···) retrieved (error).

Gormley and Kennedy (14). The condition numbers were again 2 orders of magnitude higher. On the basis of the condition number, one would expect more difficulty in analyzing measurements with the diffusion battery than with the elutriator or cyclone. Data reduction of measurements with the inertial impactor should be relatively simple. This is in accord with experience.

The effect of the condition number on the inversion can be seen in Figure 1 where the retrieved distribution with and without error are compared for the four classifiers. The difference in the dotted curve (measurements without error) and the test distribution is small even for the diffusion battery where the difference is the greatest. However, for the measurements with error, the initial distribution is retrieved only for the inertial impactor. This result is a direct consequence of the condition number relation (eq 3) where the relative error in the solution is proportional to the product of the condition number and the relative error in the measurement. Only for the low condition numbers of the inertial impactor does the retrieved distribution agree with the initial distribution when there is experimental error. Generally the effect of random error is to broaden the retrieved function and obscure the fine structure. This suggests that only limited information can be obtained from measurements with diffusion batteries, and one would be unlikely to discriminate between unimodal and bimodal distributions.

A somewhat similar result is obtained when a comparison is made between analyses of cumulative and discrete measurements. These results are shown in Figure 2 where the two modes of analysis are made for an elutriator. The ratio $\lambda_{\max}/\lambda_{\min}$ for the two cases is 3×10^3 and 2×10^5 , respectively. This parameter is related to $C(N,2)$ for the unnormalized matrix. Consequently, the 2 orders of magnitude difference is comparable to a similar shift in the normalized condition numbers. The conclusion that one draws is that analysis in the discrete mode has a much lower condition number than analysis in the cumulative

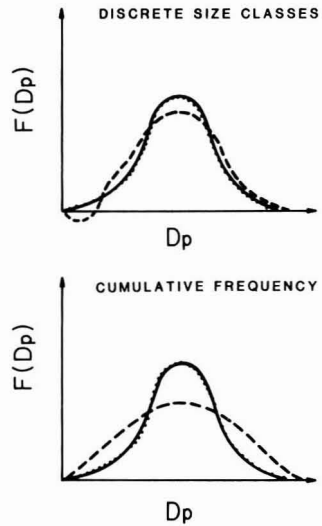


Figure 2. Comparison of retrieved functions for elutriator by different measurement modes, given a unimodal distribution. (—) Given; (---) retrieved (exact); (···) retrieved (error).

mode. This explains the results obtained by Maigne et al. (9).

It is important to note that analysis with a discrete mode does not depend on the measurements but only their analysis. When the cumulative frequencies are measured, a discrete distribution is constructed by taking the difference of two adjacent cumulative frequencies. The basis for analysis is to choose the mode that has a minimum condition number.

Most procedures currently used for determining the size distribution constrain the function to positive values and/or smooth the function. Effectively these procedures constrain the oscillation of the eigenvalues resulting in lower condition numbers. These procedures work effectively when the problem is overspecified, with there being more experiments than variables to be determined.

Characterization of Particle Size Distributions

In determining the particle size distribution for atmospheric or laboratory aerosols, it is necessary to invert Fredholm integral equations of the form

$$\int_a^b K(x,y) F(y) dy = G(x) \quad (10)$$

where the value of $G(x)$ is known at least at a finite number of points, $K(x,y)$ is a known kernel either based on theory or empirical correlations, and $F(y)$ is the unknown size distribution. For example, if one considers aerosol measurements, the fractional penetration $\overline{\text{Pt}}(Q)$ is a measured function of flow rate Q while $\text{Pt}(Q,D)$ is the theoretical penetration (a function of size D and flow rate Q). Consequently the size distribution function $F(D)$ is given by the integral equation

$$\int_0^\infty \text{Pt}(Q,D) F(D) dD = \overline{\text{Pt}}(Q) \quad (11)$$

The simplest algorithm is to measure the penetration for I flow rates solving the set of algebraic equations

$$A_{ij}X_j = B_i \quad (12)$$

where X_j are the values of the size distribution function at J different sizes (collocation points) and B_i are the

experimental penetration values at the I flow rates. It is convenient to choose the number of flow rates equal to the number of points of collocation. The values A_{ij} are the theoretical penetrations for a size D_j at a flow rate Q_i times the weight appropriate for approximating the integral with numerical quadrature.

A number of solution algorithms for the solution of eq 12 have been suggested (10, 18, 16). Our purpose is not to compare these algorithms but to suggest criteria for experiment selection and to develop tests that would indicate a priori the suitability of specific inversion algorithms. As discussed below condition numbers were used to determine criteria (1) for determining the number of collocation points and (2) for estimating optimal operation condition of experiments such as flow rates.

For examining the condition number criteria, the following model was adopted:

(1) The collocation sizes were symmetrically located about $D = 1.0$ on a logarithmic scale with the minimum size of $D = 0.1$ and a maximum size of $D = 10.0$.

(2) The fractional penetration was given by the relations

$$\text{Pt}(Q_i, D_j) = 1 - \left(\frac{D_j}{D_i^*} \right)^n \quad D_j \leq D_i^* \quad (13)$$

$$\text{Pt}(Q_i, D_j) = 0 \quad D_j > D_i^* \quad (14)$$

where D_i^* is a characteristic size dependent on the flow rate Q_i and n is an exponent peculiar to the type of classifier. Representative values for n are $n = 2/3$ for diffusion batteries (12), $n \approx 2$ for elutriators or settling chambers (18), $n \approx 2-2.5$ for cyclones and centrifuges, and $n \approx 4-6$ for inertial impactors. For an ideal classifier, one has perfect separation and a sharp cutoff point with $n \rightarrow \infty$.

(3) The effect of varying the flow rate was simulated by choosing different values of D_i^* . Condition numbers were calculated for four numbers (3, 5, 7, and 13) of collocation points. The flow rates were chosen such that

$$\ln D_i^* = \ln D_j + \theta \ln \frac{D_{j+1}}{D_j} \quad (15)$$

where θ was between 0 and 1. defined in this way there are $j - 1$ different values of D_i^* . The N th equation is the normalization relation

$$\sum_{j=1}^N X_j = \sum_{j=1}^N F_j = 1 \quad (16)$$

If the value of θ was 0.5, the points D_i^* would fall midway between the collocation sizes.

(4) For the four numbers of collocation sizes, two condition numbers $C(N;1)$ and $C(N;\infty)$ were computed for a wide range of power law exponents n between 0.35 and 4.0. Four different values (0.25, 0.4, 0.5, and 0.6) of the location parameter, θ , were used. The matrices were normalized so that the maximum element in each row was 1.0 prior to calculating $C(N;1)$ and so that the sum of the elements in each row was 1.0 prior to calculating $C(N;\infty)$.

In Figures 3 and 4 the condition numbers $C(N;\infty)$ are plotted as a function of the exponent n with the number of collocation points, N , as a parameter. The location parameter θ takes the values 0.5 in Figure 3 and 0.6 in Figure 4. Although there is some difference in detail, the principal conclusions are the same for both values of θ and incidentally for $C(N;1)$ as well as $C(N;\infty)$. These conclusions were the following: (1) The condition number $C(\tilde{N};\infty) > C(N;\infty)$ if $\tilde{N} > N$. (2) The condition numbers are usually a decreasing function of n . They tend to be relatively constant when $n > 3.0$ (inertial impactors). (3) For some

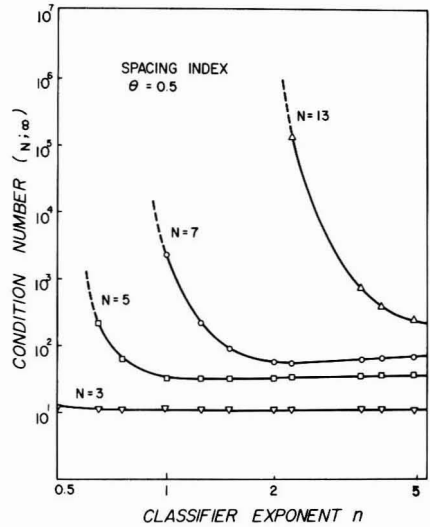


Figure 3. Condition number $C(N,\infty)$ as a function of n ($\theta = 0.5$).

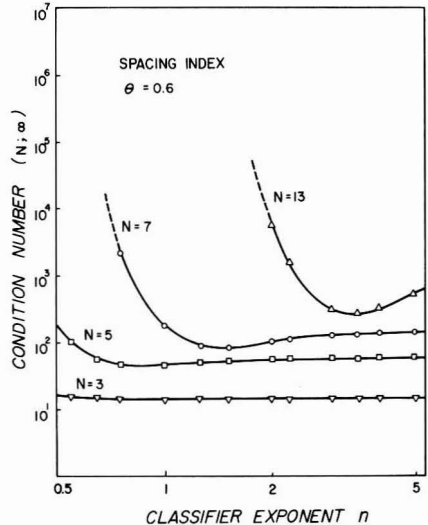


Figure 4. Condition number $C(N,\infty)$ as a function of n ($\theta = 0.6$).

smaller value of n the condition number shows a substantial increase of several orders of magnitude. The critical value, n_c , where this jump occurs increases with N . (4) There were small numerical differences when θ was varied, but the trends remained substantially the same.

The value of n where the condition number exceeded 10^3 was approximately 0.55 for 5 collocation points, 1.05 for 7 points, and 2.1 for 13 points. When the number of collocation points was three or less, the condition numbers remained small for values of $n > 0.35$. The upshot of the analysis was that for the diffusion batteries, $n \sim 0.67$, no more than 5 collocation points could be used suitably and for inertial impactors one might expect to use in excess of 13 collocation points.

The effect of spacing can be dramatic as shown in Table III where the condition numbers $C(7;\infty)$ and $C(13;\infty)$ are expressed as functions of θ . For values of $n > n_c$, there is almost no effect of spacing as indicated by the column of $C(7;\infty)$ corresponding to $n = 2.1$. However, for the values

Table III. Effect of Spacing (θ) on Condition Numbers

spacing parameter θ	exponent n	condition no.	
		$C(7, \infty)$	$C(13, \infty)$
0.25	1.05	32	1.8×10^9
0.4	1.05	58	$>10^{10}$
0.5	1.05	114	$>10^{10}$
0.6	1.05	709	$>10^{10}$
0.25	2.1	21	74
0.4	2.1	17	141
0.5	2.1	19	1.4×10^5
0.6	2.1	17	4.8×10^4

Table IV. Values of Condition Number $C(N; \infty)$ as a Function of Number of Collocation Points (N) and Spacing Index (θ)^a

no. of collocation points (N)	condition no. ($N; \infty$)		spacing index θ	
	0.6	0.5	0.4	0.25
3	5	5	5	5
5	9	9	10	11
7	14	20	15	19
13	57	40	40	49

^aPower law exponent n is 3.5.

of n near the transition, as for example $C(13; \infty)$ with $n = 2.1$ and $C(7; \infty)$ with $n = 1.05$, the effect of θ can be critical. From these simulations one can conclude that the location of experiments can appreciably affect the accuracy of the size distribution measurement.

For large values of n ($n > 3.5$) which would correspond to inertial impactors, the trend of the condition number $C(N; \infty)$ with N and θ is shown in Table IV. It is evident that there is no consistent trend with regard to θ . Moreover, the condition numbers do not vary greatly. On the other hand, there is a consistent increase with the number of collocation points, with the condition number approximated by

$$C(N; \infty) \approx 0.9N^{1.5} \quad (17)$$

This is a relatively weak dependence. To summarize, the condition numbers are very sensitive to the characteristic exponent of the classifier. Below a critical value, n_c , the intensity of the distribution function (histogram) can be evaluated at only a limited number of collocation points. For diffusion batteries ($n = 0.67$) the value of N is approximately 5 while for elutriators ($n = 2.0$) between 7 and 13 points can be founded. For inertial impactors ($n > 4$) one does not seem restricted by the number of collocation points.

Conclusions

In this paper the use of condition numbers as criteria for experiment selection and design in atmospheric measurements are described and illustrated. The paper presents a brief description of the steps in calculating the condition numbers with suggestions for appropriate normalization. Next the use of condition numbers is demonstrated for the examples: (1) the selection of indicator elements for source identification and (2) the determination of particle size distributions in experiment selection.

The best choice of condition number was found to be $C(N; \infty)$ normalized so that the sum of the elements in each

row are equal to one. The algorithm for calculating $C(N; \infty)$ requires only the determination of the inverse from the matrix consisting of the coefficients. Typically the values were about 20% less than $C(N; 1)$.

Criteria for indicator elements based on condition numbers were the same as those found by more extensive simulations and sensitivity analysis. They do not reflect a priori constraints based on inaccuracies in the measurement.

The condition number criteria proved to be useful in indicating the limitations of information obtainable from penetration measurements. Simulations suggest that the location of experiments may prove to be decisive in classifiers with moderately sharp separations as, for example, elutriators or centrifuges. In general, the condition number proves to be an unambiguous, easy-to-calculate procedure for estimating the information obtainable from experiments and a criterion that can readily be adopted to preliminary experimental designs.

Acknowledgments

We express our gratitude to the Computer Science Center of the University of Maryland.

Literature Cited

- (1) Kowalczyk, G. S.; Choquette, C. E.; Gordon, G. E. *Atmos. Environ.* **1978**, *12*, 1143.
- (2) Gordon, G. E. *Environ. Sci. Technol.* **1980**, *14*, 792.
- (3) Gordon, G. E.; Zoller, W. H.; Kowalczyk, G. S.; Rheingrover, S. W. In "Composition of Source Components Needed for Aerosol Receptor Models"; Marcies, E. S., Ed.; American Chemical Society: Washington, DC, 1981; ACS Symp. Ser. No. 167, pp 51-74.
- (4) Turing, A. M. *J. Mech. Appl. Math.* **1948**, *1*, 287.
- (5) von Neumann, J.; Goldstine, H. *Bull. Am. Math. Soc.* **1947**, *53*, 1021.
- (6) Westlake, J. R. "The Handbook of Numerical Matrix Inversion and Solution of Linear Equations"; Wiley: New York, 1968, Chapter 4.
- (7) Ortega, J. M.; Rheinboldt, W. C. "Iterative Solution of Nonlinear Equations in Several Variables"; Academic Press: New York, 1970.
- (8) Noble, B. "Applied Linear Algebra"; Prentice-Hall: Englewood Cliffs, NJ, 1969; Chapter 8, p 234.
- (9) Maigne, J. P.; Turpin, P. Y.; Madelaine, G.; Bricard, J. *J. Aerosol Sci.* **1974**, *5*, 339-355.
- (10) Crump, J. G.; Seinfeld, J. H. *Aerosol Sci. Technol.* **1982**, *1*, 15.
- (11) Marple, V.; Liu, B. Y. H. *Environ. Sci. Technol.* **1974**, *8*, 648.
- (12) Stern, A. C.; Caplan, K. J.; Bush, P. D. "Cyclone Dust Collectors"; American Petroleum Institute: New York, 1956.
- (13) Gormley, P.; Kennedy, M. *Proc. R. Ir. Acad., Sect. A* **1949**, *52A*, 163-169.
- (14) Pich, J. *J. Aerosol Sci.* **1972**, *3*, 351.
- (15) Twomey, S. *J. Comput. Phys.* **1975**, *18*, 188-200.
- (16) Cooper, D. W.; Spielman, L. *Atmos. Environ.* **1976**, *10*, 723.
- (17) Cheng, Y. S.; Keating, J. A.; Kanapilly, G. M. *J. Aerosol Sci.* **1980**, *11*, 549.
- (18) Jess, W. T. *J. Aerosol Sci.* **1974**, *5*, 583.

Received for review February 14, 1984. Revised manuscript received July 10, 1984. Accepted September 14, 1984. This work was supported by the State of Maryland Department of Natural Resources (P678004) and the National Science Foundation (CPE 83 14700) (J.W.G., F.F.F., P.Y.Y., and C.R.K.). This work was also supported by the DuPont Co. (DuPont Young Faculty Grant) (J.H.).

Effects of Dissolved Organic Carbon on the Adsorption Properties of Plutonium in Natural Waters

Donald M. Nelson,* William R. Penrose, John O. Karttunen, and Paige Mehlhaff

Environmental Research Division, Argonne National Laboratory, Argonne, Illinois 60439

■ The colloidal organic carbon (COC) found in natural aquatic systems is shown to profoundly inhibit the adsorption of reduced plutonium (oxidation states III or IV) to suspended sediment particles. This effect can be described by a system of equilibria in which COC competes with the solid particles for Pu(III,IV). Pu(III,IV) forms both 1:1 and 1:2 complexes with COC. Low pH conditions suppress the formation of 1:2 complexes but not 1:1 complexes. When corrected for the influence of COC, the intrinsic adsorption coefficient (K_D) for plutonium(III,IV) falls in the range $(0.5-3) \times 10^6$ for all the surface waters examined. On a weight basis, the COC and natural sediments have approximately equal affinities for plutonium.

Introduction

The hazard associated with the entry of plutonium into aquatic systems is largely determined by the extent to which it remains in solution. As such, it is directly available for uptake by man from drinking water, particularly since it is only partially removed by ordinary water treatment processes (1). Its movement from areas of confinement or known contamination into uncontaminated areas is similarly controlled by the proportion existing in the dissolved phase. Before reliable assessments of hazard can be made, therefore, the factors controlling the adsorptive behavior of plutonium must be understood.

Low concentrations of plutonium are now ubiquitous in aquatic and terrestrial ecosystems. Typically, dissolved concentrations vary from 10^{-17} M in areas contaminated only with global fallout (2) up to about 10^{-14} M near certain industrial sources (3). Studies at these ambient concentrations have yielded useful information about the behavior of plutonium in natural aquatic systems which may be used as a first approximation to its behavior at the higher levels considered dangerous to health. These measurements have shown that, in most natural aquatic systems, plutonium is largely associated with the solid phase, which may be either sediments or suspended particles. This association is generally expressed as a distribution coefficient, or K_D , which is the ratio of the activity per unit weight of sediment or solids to the activity per unit weight of water. Only in the deep ocean, where the amount of available solid phase is limited, does the majority of plutonium remain in solution (4).

One factor responsible for limiting the distribution coefficient in certain waters is the presence of part of the plutonium as the poorly sorbed oxidized form, oxidation states V and/or VI. This is the major dissolved form in some oligotrophic waters. Lake Michigan and Clear Lake, Manitoba, for example, carried 87% and 86% of their dissolved plutonium, respectively, in the oxidized form (5). Coastal seawater contained a similar proportion of oxidized element, ranging from 70% to 92% (6).

In other waters, Pu(V,VI) is only a minor component or is absent; the dissolved Pu consists of one or both of the reduced forms, oxidation states III and/or IV. But even in those waters where Pu(V,VI) predominates, a significant proportion of dissolved plutonium is in the reduced state, and the particle-bound plutonium is essentially all in the reduced form. The distribution coefficient of this reduced form has been shown to be corre-

lated with the concentration of dissolved organic carbon (DOC) in the water (5).

The involvement of DOC in the mobility of plutonium in soil and natural waters has been suggested by some workers (7, 8), questioned by others (9, 10), and ignored by most. No attempts have been made to apply a mechanistic explanation or model to the data describing the action of DOC.

Much of the dissolved organic carbon in natural waters consists of "humic substances", which originate from the decay of organic matter in soils and water. The resulting product is very stable to further decay and is of indeterminate structure, with carboxyl, methoxy, phenolic, quinone, and other functional groups, and molecular weights of <1000 to over 200 000 (11). Moreover, it has substantial chelation properties for metals, especially iron, and may moderate the toxicity of copper, zinc, and other transition metals (12). Dissolved organic carbon is traditionally defined (17) as that proportion of total organic carbon which passes a 0.45- μ m filter, even though it is generally recognized that it consists of a continuum of molecular sizes ranging from small, fully hydrated (i.e., dissolved) species to large, colloidal ones. In this report, the traditional definition of DOC is retained. In addition that component of DOC that does not pass a M_r 1000 cutoff ultrafiltration membrane is referred to as "colloidal organic carbon" (COC).

Here we propose to confirm the conjecture of Wahlgren and Orlandini (5) that organic carbon (specifically the COC) plays a significant, and probably primary, role in regulating the binding of reduced plutonium to sediments. We further propose that this behavior can be described by simple equilibrium equations.

Materials and Methods

Distribution Coefficients (K_D) of Ambient Plutonium. The concentrations of three forms of ambient plutonium were measured in 20-50-L water samples by the method of Lovett and Nelson (14). The three forms were (a) total plutonium in suspended particulates, (b) dissolved Pu(III,IV), and (c) dissolved Pu(V,VI). Immediately after collection, the sample was filtered through a tared 0.45- μ m nitrocellulose filter (Millipore type HAWP, up to 293 mm in diameter). Internal standards of $^{236}\text{Pu(VI)}$ and $^{242}\text{Pu(IV)}$, at about 10 times the expected activity of $^{239+240}\text{Pu}$, were added to the filtrate which was then made 0.8 M in nitric acid. Samples preserved in this way were stable for several months with no significant loss or interconversion of the internal standards. Equilibrium between the added and analyte isotopes (within the oxidized and reduced groups) was promoted by the strong acid conditions and by the fluoride and dichromate used in the subsequent separation step. Pu(III,IV) was later coprecipitated with lanthanum or neodymium fluoride, separated by anion-exchange chromatography, and electrodeposited for α -spectrometric assay. The original Pu(V,VI) was then reduced by the addition of ferrous ion, collected by a second coprecipitation step, and assayed in the same way.

No oxidation state separation was carried out on the particulate fraction. Dried filters were weighed to determine mass of sediment recovered. Afterward, internal

standards were added to the filters, which were then digested in acid. The filter plutonium was recovered by anion-exchange chromatography and electrodeposition (5).

Distribution coefficients were calculated according to the definition $K_D = (\text{activity per kilogram of filterable solids}) / (\text{activity per liter of water})$. In this work, as in that of Wahlgren and Orlandini (5), only "reduced" plutonium was used in the calculation, since only the lower states bind to particles to any significant degree (6). This refinement permitted Wahlgren and Orlandini (5) to detect the correlation between DOC concentration and the K_D of reduced plutonium in ambient waters; if total plutonium had been used in the calculation, the variable proportion in the higher oxidation states would have caused the resulting K_D 's to be substantially lower in some waters and would have obscured the relationship.

Laboratory Measurements of K_D . A consistent procedure was established for the measurement of K_D under controlled conditions. Samples of fine-grained sediment were collected from the Miami-Erie Canal near Miamisburg, OH, and from deep Lake Michigan. These were stored as slurries in the dark near 0 °C; aliquots of slurry were dried and weighed from time to time to determine the sediment concentration. Measured amounts of these slurries were then added to 100 or 200 mL of the water under examination. Water samples were always filtered (0.45 μm) before experiments were begun. ^{237}Pu tracer, previously adjusted to the desired oxidation state (14), was added to a concentration of about 10^{-14} M. (The absolute plutonium concentrations were determined by the amounts of ^{236}Pu , ^{238}Pu , and ^{239}Pu which were formed during the manufacture of ^{237}Pu , but total Pu concentrations never exceeded 10^{-12} M.) The mixture was then stirred for 7 days in a glass flask. At the end of this time, it was filtered through a Millipore 0.45- μm filter. Pu(II,III,IV) and Pu(V,VI) were separated sequentially from the filtrate as described above. The particulate matter and the two rare earth fluoride precipitates were counted by using a NaI(Tl) gamma spectrometer to determine the ^{237}Pu in each fraction. Material balances indicated little or no adsorption of Pu to the walls of the equilibration flasks.

Dissolved Organic Carbon. Colloidal organic carbon was separated from water samples by ultrafiltration. Samples of lake or seawater (usually about 10 L) were filtered through a 0.45- μm Millipore filter and then charged into an Amicon Model 2000 ultrafiltration apparatus, assembled with a UM-2 filter (cutoff M_w 1000). The ultrafiltration was carried out under nitrogen pressure until about 1 L of liquid, containing the colloidal material, remained. This purely physical procedure separates on the basis of molecular size and places minimum physical or chemical stress on the molecules retained. Because there is little discrimination toward small molecules or ions, these remain at the same concentration in both ultrafiltrate and retained fluid (retentate). Therefore, when filtrate and retentate were later recombined, any intermediate concentration of COC could be obtained without varying other solutes.

Organic carbon concentrations in sample water, ultrafiltrate, and retentate were measured with a Sybron-Barnstead PhotoChem organic carbon analyzer. Depending on the water source, from 10 to 70% of the original dissolved organic carbon passed through the ultrafilter. The material balance indicated no significant losses of organic carbon in the separation process.

Results

Ambient K_D Measurements. Including the work of

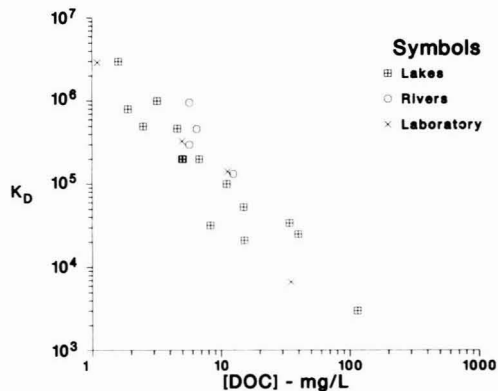


Figure 1. Relationship of the K_D of ambient reduced plutonium to dissolved organic carbon concentration for 15 lakes and four rivers. The results of four laboratory measurements of K_D using added ^{237}Pu tracer are shown for comparison.

Wahlgren and Orlandini (5), the concentration of organic carbon and the K_D for ambient Pu(III,IV) have been measured in water samples from 19 different bodies of water of widely varying chemistry. When these ambient K_D 's were plotted vs. organic carbon, a strong inverse relationship was revealed which held over about 3 orders of magnitude in K_D (Figure 1). In addition, water from four lakes was equilibrated with sediment from the Miami-Erie Canal by using added ^{237}Pu tracer. These laboratory K_D measurements agreed well with the ambient values. As a result, we were convinced that the laboratory determinations of K_D were satisfactory approximations to the natural adsorption properties of plutonium and that the K_D was relatively independent of the source of the sediment used.

Time Course of Equilibration. Under ordinary conditions, natural waters are in contact with sediments or suspended particles for extended periods of time. It was therefore necessary to determine whether plutonium adsorption (or desorption) would reach equilibrium within an experimentally reasonable time. In addition to the adsorption-desorption processes, the interconversion of Pu(III,IV) and Pu(V,VI) must also occur, since only the Pu(III,IV) form adsorbs to particles to any significant degree.

By use of Lake Michigan sediment and water from Lake Michigan and a pond on the Argonne National Laboratory site, the rates of equilibration were measured by using both added Pu(IV) and added Pu(VI). The results, shown in Figure 2, clearly demonstrated that equilibrium was reached in about 7 days, regardless of the source of the water or the initial oxidation state of plutonium. A 7-day time period was subsequently used in all laboratory determinations of K_D .

Independence of K_D from Sediment Concentration. Experiments were conducted in which the concentration of sediment was varied over a wide range. The K_D of reduced Pu was found not to be systematically affected by sediment concentration; this was true both for 0.45- μm filtered water and for water from which the COC of $M_w > 1000$ had been removed by ultrafiltration (Table I). The systematic difference in K_D between the filtered and ultrafiltered waters reflects the effect of COC on K_D .

Reversibility of Binding to Sediment. Measurements of K_D assume that the system is in true equilibrium. To demonstrate this, an experiment was designed to measure the K_D when equilibrium was approached from the di-

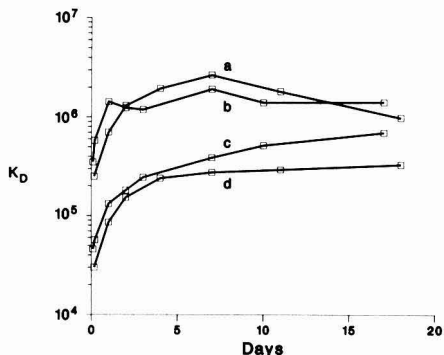


Figure 2. Approach to equilibrium of binding of ^{237}Pu to Lake Michigan sediment (75 mg/L) in laboratory measurements. Curves a and b were generated by using Lake Michigan water (DOC about 1–2 mg/L) and curves c and d by using higher DOC water (10–12 mg/L) from a pond on the Argonne site. Pu(IV) was added to (a) and (d); Pu(VI) in (b) and (c). The K_D 's shown were for reduced Pu only.

Table I. Effect of Sediment Concentration on the K_D of Reduced Pu in Laboratory Equilibrations Using Water from the ANL Pond and Sediment from the Miami-Erie Canal

sediment concn, mg/L	$K_D \times 10^{-6}$, L/kg	
	ultrafiltered water	filtered water
1000	4.9	1.5
300	10.1	1.7
100	8.9	1.6
30	11.2	1.3
10	5.5	0.61
3	4.9	0.48
1	3.1	1.1

rections of both adsorption and desorption.

A mixture of Argonne pond water (300 mL), Lake Michigan sediment (55 mg), and tracer ^{237}Pu was equilibrated for 7 days. A 100-mL aliquot was removed for determination of the K_D . The remaining sediment and water were separated by centrifugation and mixed with fresh water (1000 mL) and sediment (11 mg), respectively. The desorption and continued adsorption were measured again during the approach to equilibrium. The resulting K_D 's were in fact similar, indicating that, at least over the time scale of this experiment, the plutonium remains easily exchangeable and in equilibrium between dissolved and adsorbed forms (Table II).

Variation of COC Concentration. To explore the correlation between the observed K_D for Pu(III,IV) and the organic carbon concentration, we manipulated the COC concentrations in groups of waters by recombining ultrafiltered water in differing proportions with retentate from the same ultrafiltration. The concentration of COC were increased in steps of about threefold. The K_D was determined according to the standard procedure using sediment concentrations of 40–60 mg/L.

Such experiments were conducted with nine different water sources. In each experiment, there was a clear, systematic relationship between COC concentration and the K_D for Pu(III,IV) (Figures 3 and 4). Above specific concentrations of COC, the K_D 's decreased dramatically (i.e., $1/K_D$ increased). In Lake Michigan water (Figure 3A), this only occurred at COC concentrations considerably higher than ambient, but in other samples such as that from the Argonne pond, the ambient level of COC was sufficient to substantially reduce the K_D (Figure 3B). The

Table II. Demonstration of the Reversibility of Plutonium Binding to Sediments

experimental step	$K_D \times 10^{-6}$, L/kg	
	replicate 1	replicate 2
initial adsorption	2.4	0.74
second adsorption (7 days)	1.05	0.52
desorption	day 1, 4.1 day 2, 3.0 day 3, 2.7 day 8, 2.7 day 10, 2.9	day 1, 2.1 day 2, 1.5 day 6, 1.4 day 9, 1.6 day 14, 2.0

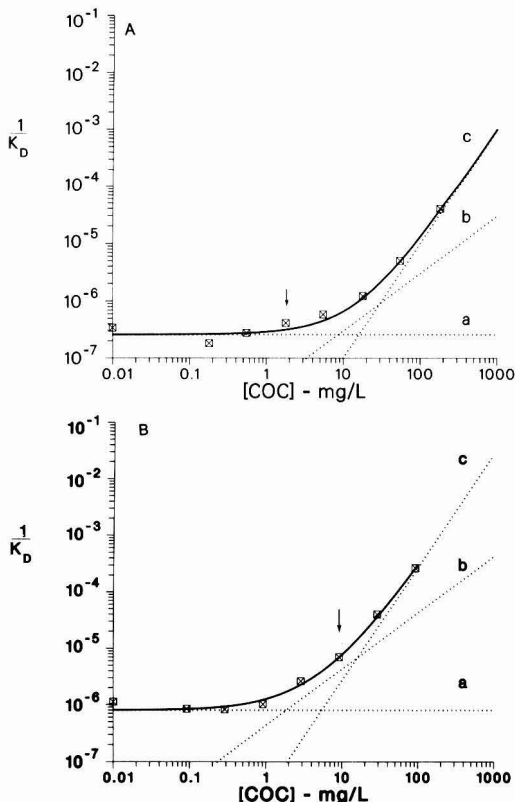


Figure 3. Adsorption of ^{237}Pu in the presence of sediment and varying concentrations of homologous COC. The binding constant (K_D) is displayed here in an inverse form, which represents the concentrations of species in equilibrium with a unit concentration of Pu bound to the sediment phase. The solid curve was generated by a least-squares fit to the data points. This curve is the sum of individual components (dotted) representing the following: Pu not complexed with COC (curve a, slope = 0), the 1:1 complex of Pu with COC (curve b, slope = 1), and the 1:2 complex (curve c, slope = 2). Panel A was derived by using Lake Michigan water and panel B with water from a pond on the Argonne site. The arrows indicate the concentration of COC in the original water.

slopes of these logarithmic plots often approached, but never exceeded, two at high COC concentrations. This implied the existence of complexes containing two molecules of COC per Pu atom; in some samples the slope was near one, implying only 1:1 complexes were important. The most remarkable observation was that, at low concentrations of COC, K_D 's fell into the range $(0.5\text{--}3.0) \times 10^6$ for all water samples examined. Variations in COC concentration, therefore, accounted for nearly all of the ob-

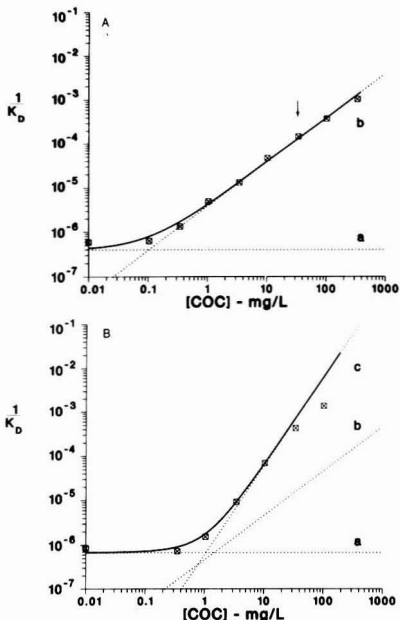
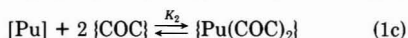
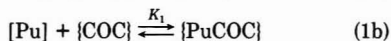
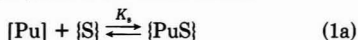


Figure 4. Speciation of Pu at low and high pH. (A) Okeefenokee Swamp water at ambient pH of 4. (B) Okeefenokee Swamp water raised to pH 8. Arrows indicate the concentration of DOC in the original water sample. Dotted lines are defined as in Figure 3.

served natural variation in adsorption of reduced plutonium.

A model describing the effect of COC on K_D was developed that views the data in terms of competing equilibria, between Pu(III,IV) and sediment particles on one hand and Pu(III,IV) and COC on the other:



where $[Pu]$ is the sum of all dissolved Pu(III,IV) species, except the complexes with COC, in moles per liter, $\{S\}$ is solid concentration in kilograms per liter, $\{COC\}$ is COC concentration in kilograms per liter, and K_s , K_1 , and K_2 are the corresponding formation constants. By use of a derivation similar to that of Schubert (15), the following equation, valid when the plutonium concentration was very small, was derived:

$$\frac{1}{K_D} = \frac{1}{K_D^0} + \frac{K_1}{K_S} \{COC\} + \frac{K_2}{K_S} \{COC\}^2 \quad (2)$$

where K_D^0 was the limiting distribution coefficient (at $\{COC\} = 0$). The solid curves displayed in Figures 3 and 4 were obtained when our data were fitted to this model by using a least-squares procedure. The constants derived from the fits are displayed in Table III, along with data for water bodies not shown in the figures. Substantial variations in K_1/K_S and K_2/K_S are observed among the waters. These variations presumably are related to differences in composition of the COC from various sources. No matter what causes these among-source variations, in each water the response of K_D to varying COC concentration could be fit to eq 2, suggesting that in all waters the K_D of reduced Pu is controlled by simple mass action laws.

Table III. Constants Derived from Least-Squares Fit of K_D Measurements at Varying COC Concentrations to eq 2^a

source of water	$1/K_D^0 \times 10^6$, kg/L	K_1/K_S	K_2/K_S , L/kg
Okeefenokee Swamp	0.035 (40)	3.85 (9)	-0.002 (90)
Volo Bog	0.23 (14)	2.94 (13)	0.003 (50)
Banks Lake	0.098 (16)	0.56 (15)	0.001 (40)
Argonne Pond	0.080 (12)	0.43 (30)	0.027 (5)
Saganashkee Slough	0.072 (12)	0.42 (30)	0.023 (24)
Bay of Fundy	0.085 (15)	0.35 (30)	0.012 (60)
ELA Lake 239	0.081 (11)	0.20 (60)	0.048 (20)
Gulf of Mexico	0.038 (13)	0.16 (30)	-0.002 (110)
Lake Michigan	0.026 (10)	0.03 (40)	0.001 (24)

^aPercentage errors (estimated in the fit) are shown in parentheses.

Effect of pH. The natural waters investigated in this work fall into two classes. In most samples, 1:2 complexes played an important role at high COC concentrations. Others showed little involvement of 1:2 complexes at any COC concentration tested. The waters showing exclusively 1:1 complexes are characterized by pH values as low as 4. Because pH is known to affect the structure of metal-organic complexes, experiments were devised to study the effect of pH on binding.

One set of experiments used Okeefenokee Swamp water (ambient pH ~4) that had been adjusted to pH 8 with sodium hydroxide. Simultaneously, water from ELA-239, a near-neutral lake, was adjusted to pH 4 with hydrochloric acid and used to determine K_D .

Only monovalent complexes were important in Okeefenokee Swamp water at the ambient pH of 4, and the 1:2 complexes were very weak; i.e., the line (c) representing 1:2 complexes in Figure 4A is below the limit of the graph. When the pH was raised to 8, however, the situation was reversed (Figure 4B), with K_1/K_S decreasing from 3.85 to 0.46 and K_2/K_S increasing from <0.002 to 0.59.

In the complementary experiment, when the pH of ELA-239 water was lowered, the 1:1 complexes became dominant, i.e., K_1/K_S increased from 0.20 to 3.63, and the 1:2 complex, K_2/K_S , diminished, i.e., decreased from 0.048 to <0.001. It was apparent, therefore, that qualitative differences in plutonium binding were related to pH and that these differences involved the type of complex formed.

Discussion

We have determined that colloidal organic carbon in natural surface waters is a major factor controlling the distribution of reduced plutonium between solid and dissolved phases. Wahlgren and Orlandini (5) noted a strong negative correlation between "dissolved" organic carbon concentration and K_D in natural surface waters but could not say conclusively whether DOC or some other correlated variable was responsible. The work reported here establishes a causal relationship, since the use of ultrafiltration and reconstitution allowed the COC concentration to be manipulated independently of other constituents. The relationship with K_D was shown to follow a simple mass-action mechanism involving competition between solids and COC for the available plutonium. The mechanism postulates a single type of binding site on the surface of the solid phase and two soluble complexes containing one and two molecules of COC per Pu atom, respectively.

In the absence of COC, binding to solids was maximal, and limiting distribution coefficients (K_D^0) were in the range $(0.5-3.0) \times 10^6$. This was a narrow range, compared to the variations over 3 orders of magnitude observed when

K_D is measured directly in the ambient water (Figure 1) (5), and represents not only experimental error but also contributions due to the varying concentrations of other potential ligands such as carbonate. The narrowness of the range of K_D^0 , compared to the range of K_D even though alkalinity, pH, and other characteristics of the waters varied greatly among the water bodies sampled, suggests the effects of COC dominated those of other potential ligands.

Although the competitive binding model successfully explained the observed equilibrium data, it was helpful to demonstrate that some of the fundamental assumptions of the model were satisfied. The independence of K_D from the weight of sediment used, for example, assured that there was an excess of binding sites on the solids and that there was no interaction among binding sites over the concentration ranges used in these experiments. In most experimental systems, K_D has been found to decrease with increasing sediment concentration, a phenomenon that has been thoroughly described but not yet explained (16-18). The experiments reported in Table I, as well as other, unpublished observations, have established that this phenomenon is not observed for Pu(III,IV) when our methods are used and that the simple equilibrium assumptions are satisfied. That plutonium being desorbed from sediments approached the same K_D as that being adsorbed confirmed that binding was truly reversible, that no occlusion of bound plutonium was occurring, and that the relationship $[Pu]\{S\}K_s = \{PuS\}$ was followed by the system.

It is worthwhile pointing out that the ratio K_1/K_S represents the relative affinities of COC and solids for reduced Pu, on a weight basis. This ratio was close to one for most waters, indicating approximately equal affinities of Pu(III,IV) for either phase. This generalization broke down in Lake Michigan, where the COC had substantially less affinity for plutonium. It was observed during these experiments that COC from Lake Michigan, when concentrated, was lighter in color than that from other sources and that a larger fraction of the total carbon was not retained by the ultrafilter. This may be related to the very long residence time of water in Lake Michigan, about 100 years, which may result in more highly degraded organic matter, with fewer functional groups appropriately juxtaposed to chelate metals (19). Conversely, the higher affinities of DOC from such sources as the Okefenokee Swamp and Volo Bog imply complex structures with more effective binding sites.

Acknowledgments

We are grateful to R. P. Larsen for fruitful discussions during the progress of this research and for a critical

reading of the manuscript, to R. L. Watters for his unstinting encouragement, and to K. A. Orlandini and D. N. Metta for helpful discussions and assistance with experimental work. P.M. was a Summer Research Participant with the Argonne Department of Educational Programs.

Registry No. Pu, 7440-07-5.

Literature Cited

- (1) Alberts, J. J.; Wahlgren, M. A. *Health Phys.* **1977**, *32*, 295-297.
- (2) Wahlgren, M. A.; Nelson, D. M. *Verh. Int. Ver. Limnol.* **1975**, *19*, 317-332.
- (3) Heatherington, J. A.; Jefferies, D. F.; Lovett, M. B. In "Impacts of Nuclear Releases into the Aquatic Environment"; IAEA: Vienna, 1975; pp 193-212.
- (4) Wong, K. M.; Jokela, T. A.; Noshkin, V. E. In "Radioelement Analysis: Progress and Problems"; Lyon, W. S., Ed.; Ann Arbor Science Publishers: Ann Arbor, MI, 1980; pp 207-214.
- (5) Wahlgren, M. A.; Orlandini, K. A. In "Environmental Migration of Long-Lived Radionuclides"; IAEA: Vienna, 1982; pp 757-774.
- (6) Nelson, D. M.; Lovett, M. B. *Nature (London)* **1978**, *276*, 599-601.
- (7) Bondietti, E. A.; Reynolds, S. A.; Shanks, M. H. In "Transuranium Elements in the Environment"; IAEA: Vienna, 1976; pp 273-287.
- (8) Nishita, H.; Haug, R. M. *Soil Sci.* **1979**, *128*, 291-296.
- (9) Cleveland, J. M.; Rees, T. F. *Environ. Sci. Technol.* **1976**, *10*, 802-806.
- (10) Rees, T. F.; Cleveland, J. M.; Gottschall, W. C. *Environ. Sci. Technol.* **1978**, *12*, 1085-1087.
- (11) Schnitzer, M.; Khan, S. U. "Humic Substances in the Environment"; Marcel Dekker: New York, 1972; pp 1-372.
- (12) Neubecker, T. A.; Allen, H. E. *Water Res.* **1983**, *17*, 1-14.
- (13) Sharp, J. H. *Limnol. Oceanogr.* **1973**, *18*, 441-447.
- (14) Lovett, M. B.; Nelson, D. M. In "Techniques for Identifying Transuranic Speciation in Aquatic Environments"; IAEA: Vienna, 1981; pp 27-35.
- (15) Schubert, J. *Anal. Chem.* **1950**, *22*, 1359-1368.
- (16) Aston, S. R.; Duursma, E. K. *Neth. J. Sea Res.* **1973**, *6*, 225-240.
- (17) Di Toro, D. M.; Horzempa, L. M.; Casey, M. M.; Richardson, W. J. *Great Lakes Res.* **1982**, *8*, 336-349.
- (18) Voice, T. C.; Rice, C. P.; Weber, W. J., Jr. *Environ. Sci. Technol.* **1983**, *17*, 513-518.
- (19) Wetzel, R. G. "Limnology", 2nd ed.; W. B. Saunders: New York, 1983; p 680.

Received for review May 17, 1983. Revised manuscript received January 11, 1984. Accepted September 10, 1984. This work was funded by the U.S. Department of Energy, Office of Health and Environmental Research.

Light Scattering Studies of the Relationship between Cation Binding and Aggregation of a Fulvic Acid

Alan W. Underdown

Chemistry Department, Carleton University, Ottawa, Ontario, K1S-5B6 Canada

Cooper H. Langford*

Chemistry Department, Concordia University, Montreal, Quebec, H3G-1M8 Canada

Donald S. Gamble

Chemistry and Biology Research Institute, Agriculture Canada, Ottawa, Ontario, K1A-0C6 Canada

■ The cation binding properties of fulvic acids which serve as a laboratory model for organic ligand complexation in natural systems (lakes, streams, and soil solution) are now known to vary with degree of occupation of binding sites by a cation. One important factor in interpretation is the state of aggregation of the ligand. This study has shown that Rayleigh light scattering, which monitors molecular or aggregate size, can be a useful complementary tool in complexation studies to those methods which monitor the free metal ion and permit calculation of free and bound metal ion or to those that are functional group specific. Measurements at a limited number of scattering angles have shown that the "polydispersity" (defined by scattering at angles 45° and 135°) can decrease while overall complexation increases, pointing to selective aggregation among the smaller, more oxygenated fraction of the fulvic acid mixture. A cooperative effect between aggregation and binding of strongly complexed cations (e.g., Cu²⁺) has been identified. The effect is independent of electrostatics since it is not produced by ions like Mg²⁺ and it depends on coverage in a way suggestive of cooperative interactions. The effect is termed pseudochelation. Aggregation of the fulvic acid can also be induced by the combination of protonation and high ionic strength. Neither of these variables alone induces aggregation in the same range.

Introduction

A series of recent papers (1-3) has emphasized that soil organic ligands such as fulvic acids are polyelectrolyte mixtures whose cation binding properties vary with the degree of coverage of cation sites by the cation. This is a consequence of at least two distant factors: (1) the complexity of the natural mixture and (2) polyelectrolyte structural and electrostatic effects. A major remaining issue which has not been extensively addressed before is the role of aggregation.

Metal ion speciation and its environmental consequences can be influenced by the interrelations between cation binding and aggregate particle size distribution. The light scattering technique allows investigation of this distribution with minimum disturbance to the sample. In spite of this, there have been few reported studies. Wershaw and Pinckney (4, 5) have investigated the effects of pH, concentration, and concentration in humic acid solutions by low-angle X-ray scattering. Studies using visible light include one by Orlov (6) on pH effects and studies of "turbidity" by Saar and Weber (1) and Pagenkorp and Whitworth (7). (Ultracentrifugation studies of the larger humate samples which reach some of the conclusions presented here for fulvates have been reported by Sipos et al. (8).) The present study differs from its predecessors in several respects: (1) the use of long wavelength light

to avoid fluorescence, (2) examination of the contribution of "extraneous" scattering material by successive filtration experiments, and (3) examination of the particle size distribution in relation to angular variation of light scattering.

The study involves measurement of light scattering using our previously established degree of cation site coverage functions (2, 9, 10) for the cations H⁺, Cu²⁺, and Mg²⁺. These cation site occupancies were estimated from ion selective electrode potentiometric titrations.

Light Scattering

Light scattering from solutions may be described by the ratio R_θ (11) which is the ratio of scattered to incident light intensity normalized to unit scattering volume and distance from the detector. This ratio is related to the properties of each of the various different scattering particles in a fulvic acid by eq (1). The scattering ratio is proportional

$$R_\theta = \frac{2\pi^2 n_0 (dn/dc)^2}{N_{av} \lambda^4} P(\theta) MC \quad (1)$$

to the solution concentration, C , the molecular weight, M , and the polarizability difference between the solute and the solvent dn/dc . Here, n_0 and n are the refractive indexes of the solvent and the solution, respectively. N_{av} is Avogadro's number, and λ is the wavelength of the incident light. The particle scattering factor, $0 < P(\theta) < 1$, describes the reduction in scattering intensity due to the interference of light scattered from different parts of the same particle. (These will be particles of sizes greater than $\lambda/20$ of the wavelength of light.) For monodisperse systems $P(\theta)$ can provide information on particle size or shape if either one is known. For polydisperse systems, $P(\theta)$ can provide information about size distribution. $D(45/135)$, given by eq 2, provides a qualitative measure of the degree

$$D(45/135) = \frac{\langle R_{45} \rangle}{\langle R_{135} \rangle} \quad (2)$$

of polydispersity in a distribution of spherical scatterers (12). In this equation, brackets denote the observed averages. The subscripts refer to the angle at which scattering is observed. Two points should be noted. The first of these is that $P(\theta)$ is usually a decreasing function of θ . (That is, the derivative is negative.) The second is the consideration that $dP(\theta)/d\theta$ increases with increasing particle size. For particles smaller than about 5% of the wavelength of light, $P(\theta)$ becomes essentially independent of θ . The net result is that the larger particles scatter light more effectively at 45° than they do at 135°. Consequently, $D(45/135)$ is an increasing function of polydispersity for a fixed average particle size. This will prove

to be a key point in the qualitative interpretation of changes in scattering induced by cation binding.

Experimental Section

Materials. The fulvic acid was extracted from a sample of a Bh horizon podzol from Prince Edward Island which is the source of an extensively characterized fulvic acid (13-15). The extraction procedure was as described. The present sample was compared to the earlier batch, "FA1", both prepared by the same method (9), for acidimetric titration end points using Gran's functions. The values of 4.98 and 7.74 mmol/g of FA were reproduced within 2%. Other materials were reagent grade used without further purification. Purified water was prepared by passing "tap" distilled water from the building system through a Millipore ion-exchange and filtration system followed by distillation from alkaline permanganate in an all glass still. Fulvic acid (FA) stock solutions were prepared by dissolving 0.1000 g of solid FA in 100 mL of purified water. They were then equilibrated overnight before use or filtration. Despite preliminary observations that stock solutions were stable over several weeks, stock solutions older than 1 week were discarded.

Light Scattering Measurements. Measurements were carried out on a Brice-Phoenix universal light scattering photometer which has the essential feature for colored solutions such as these of permitting detection at 0°. The instrument was modified to replace the lamp with a 5-mW He-Ne laser from Coherent Radiation.

Data were acquired by measuring the output of an IP 1 photomultiplier tube (PMT) for 3 min. The dark current was recorded between each measurement. Signals at different angles, which differed greatly in intensity, were kept on scale with neutral density filters whose absorbance was determined with the PMT at 0°. The apparatus was calibrated for absolute intensity by measuring the scattering from doubly distilled benzene for which R_{90} is known to be $8.765 \times 10^6 \text{ cm}^{-1}$ at 633 nm (18). A measured dissymmetry ratio of 1.00 indicated the absence of extraneous scattering. The Rayleigh scattering ratio, R_{θ} , was calculated as explained by Underdown et al. (16).

Under certain conditions, scattering by FA solutions varies somewhat with time. This is due to slow processes of varying degrees of reversibility which follow a sudden change in the solution composition. Such processes involve the chemical and physical state of these colloids. To provide a basis for comparison over the whole range of solution composition with a maximum of reproducibility, a 20-min "aging" period was used at the start of all experiments. The sample preparation protocol included the following steps: (1) solutions were made from filtered stock solutions with FA stock added last before dilution with purified water to the final volume; (2) samples were purged with nitrogen which had been filtered through a 0.05- μm filter, water scrubber, and cellulose filter; (3) the sample was transferred to scattering cell and covered with a tightly fitting Teflon cap; (4) after alignment, the cell was allowed to stand in the dark for 5 min. When cations were to be titrated into a sample, it proved to be best to add stock solution through ports in the Teflon cap. A pH electrode and nitrogen purge could also be inserted. The minor corrections of scattering for dilution during a titration were easily made. Temperature in the scattering cell was maintained constant at $25 \pm 1 \text{ }^\circ\text{C}$ by circulating water through a stage and a coil surrounding the upper part of the cell holder.

Absorbance and Fluorescence Measurements. UV-vis spectra were recorded on a Cary 14 spectrophotometer in 1.00-cm quartz cells. Fluorescence measurements were

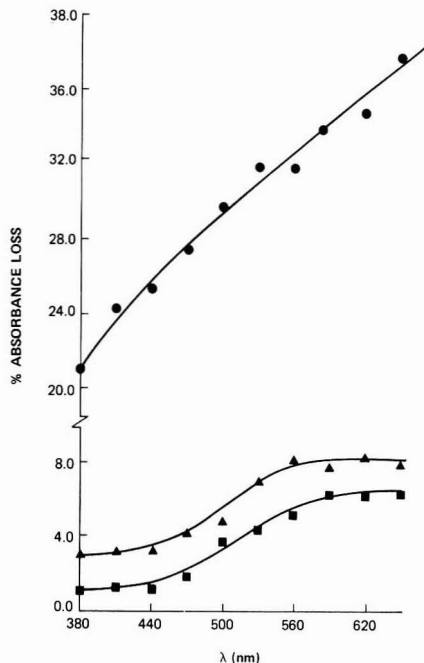


Figure 1. Wavelength dependence of the decrease in the visible absorbance of the FA on filtration through variable pore size filters: (●) 0.05, (▲) 0.2, and (■) 0.4 μm . Solution pH 3.5; concentration 0.1 g/mL. Note that total A and R_{90} are both linearly dependent on concentration in this range of concentration.

made on a Perkin-Elmer 2104-S spectrometer using 1.00-cm cells and right-angle detection. The band-pass of the monochromators was nominally 10 nm. Fluorescence intensities were corrected for sample absorbance by using the relation in eq 3 where A_{ex} and A_{em} are absorbances

$$F_{\text{cor}} = F \frac{e^{1.151(A_{\text{ex}} + A_{\text{em}})}}{1 + 1.02d^2} \quad (3)$$

measured at excitation and emission wavelengths on separate sets of samples, F is fluorescence intensity, and d is the width of the fluorescing volume. This equation is discussed in ref 12.

Filtration Experiments. Filtration experiments were conducted to examine the distribution of particle sizes and types. Two techniques were employed: micropore filtration with polycarbonate filters (which are essentially free of ion-exchange properties) and gel filtration. The fractionation achieved was monitored by both light scattering and absorbance at 465 nm. This second parameter was used because a good argument has been made (16) that absorbance monitors the total quantity of fulvic acid nearly independent of particle size. This argument was confirmed by drying and weighing several used 0.4- μm filters. Gel filtration experiments were also monitored by fluorescence spectroscopy.

The gel filtration column was prepared from 20 g of decanted Sephadex G-75 and conditioned by passing purified water through for 24 h. Fulvic acid samples were applied as 0.3 g in 15 mL and eluted with a 1-m hydrostatic head with a flow rate of 0.02 mL/s.

Results

Filtration Fractionation. The micropore filter results, monitored by R_{90} and A_{464} , are listed in Table I and Figure

Table I. Comparative Effects of Filtration with Micropore Filters on Light Scattering and Photometric Absorbance (FA at 1 mg/mL)

filter (μm)	pH	% loss in absorbance ^a (=465 nm)	% loss in scattering ^a (R_{90})
0.4	3.6	3	58
0.2	3.6	5	90
0.05	3.6	30	96
0.4	7.0	0	12
0.2	7.0	0	34
0.05	7.0	15	70

^aThese values are to be interpreted in the context of the result that both A and R_{90} are linear functions of concentration in this concentration range. Percent loss of absorbance has been calibrated gravimetrically as a measure of mass loss only for 0.4- μm filters.

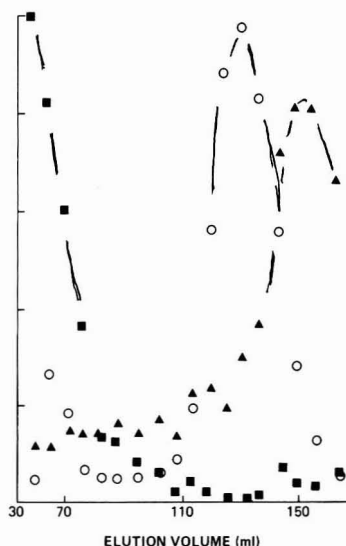


Figure 2. Three approximate "peaks" in the gel filtration curve for the FA as monitored by the three experimental probes: (■) light scattering at 90° , (○) visible absorbance at 465 nm, and (▲) fluorescence at 480 nm with 370-nm excitation. FA 0.3 g in 15 mL; pH 3.5. Hydrostatic head 1 m; flow 0.02 mL/s. The purpose of this figure is to show that the fractionation of the sample monitored by different probes is different. The wide poorly defined peaks are *not* to be interpreted.

1. Since R_{90} and A_{465} are both linear functions of fulvic acid concentration in the range 0.0–0.3 g/L, apparently about half of those particles that are effective for "extinction" in each of the two experiment types are removed by a 0.4- μm filter and about 90% by a 0.2- μm filter when the solution is acidic. In neutral solution, a similar result is obtained with a shift to smaller filter pore size. In contrast, only the smallest pore size filter (0.05 μm) causes large decreases of A . (The most absorbing particles appear to be smaller.)

Figure 2 shows a gel filtration experiment monitored by R_{90} , A_{465} , and fluorescence. The result is consistent with the filtration result in that a "large particle" fraction is identified by R_{90} , where the term large particle is adopted following the conventional interpretation of gel filtration. A fraction having a "smaller" particle size is detected by A_{465} . Finally, fluorescence seems to be associated with particles of still different, perhaps smaller, size. It should be emphasized that the gel filtration does not yield clean results and is significant only for its qualitative support

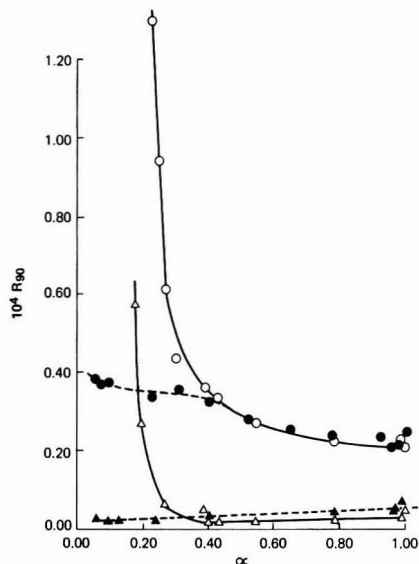


Figure 3. Dependence of aggregation of the FA on degree of dissociation of the carboxylic acid groups before and after filtration through a 0.2- μm pore size filter and with and without addition of 0.100 M KCl to raise ionic strength. Filtered samples are represented by triangles, open (Δ) for 0.1 M KCl and closed (\blacktriangle) for low ionic strength. Data for unfiltered samples of the total FA are represented by circles, open (○) for 0.1 M KCl and closed (●) for low ionic strength. pH range for these two values is 3.5–6.5. FA concentration 0.7 mg/mL.

for the simplest interpretation of the filtration experiments.

Protonation and Ionic Strength Effects. In Figure 3, the degree of protonation of the type A carboxyl groups (those titrated up to the first equivalence point in the Gran's plots of Gamble) is seen to relate to an aggregation process monitored by R_{90} . However, it is quite interesting that this process is related to a "salting out" type of effect since aggregation is pronounced only in solutions of high ionic strength. The relatively high degree of aggregation that occurs when the protonated sample is exposed to 0.10 M KCl is seen for both the total sample and the "smaller particle" (less scattering) fraction of the sample which passes a 0.2- μm filter. Similar effects are observed with NaCl. When the curves in the absence of added electrolyte are compared, a subtle but interesting result is evident.

At low ionic strength (Figure 3, no KCl), an opposite trend of R_{90} with dissociation of protons is seen for the total sample and the smaller particle fraction which passes a 0.2- μm filter. The fraction including larger particles appears to "disaggregate" with deprotonation as one might expect from H-bonded aggregates as protons are lost. The smaller fraction, however, slightly increases scattering power with deprotonation as one might expect for a polymer expansion associated with accumulating negative charge on carboxylates. (These two contradictory mechanisms have both been suggested in the past. The two may be complementary, aggregation being broken up by pH while components "unfold" to function as more efficient scatterers.)

The aggregation process induced by the combination of protonation and ionic strength is elucidated more fully in Figure 4 which shows R_{90} and $D(45/135)$ as functions of FA concentration in the medium at 0.1 M ionic strength. The upward curvature of the R_{90} vs. FA plot implies overall increase of scattering (by implication, aggregation). In

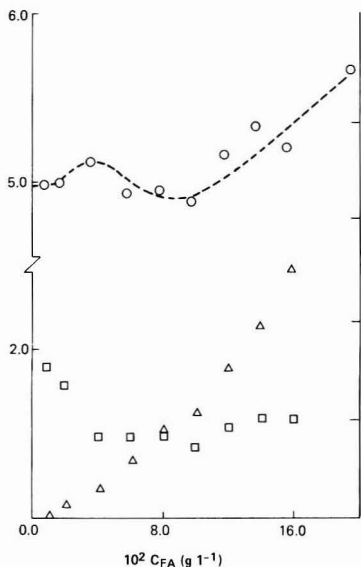


Figure 4. Dependence of light scattering on concentration of FA under circumstances where aggregation is favored by pH and ionic strength (pH 2.0, 0.1 M KCl). (Δ) R_{90} ; (O) $D(45/135)$; (\square) $D(90/135)$. Note that light scattering depends linearly on concentration of FA at higher pH where aggregation is not favored by acid and KCl. Abscissa is arbitrary and relative.

contrast, the D ratios initially decrease. This puzzling result can be understood if it is recognized that the aggregation process in a polydisperse mixture can favor the aggregation of the smaller particles so that the initial effect is to narrow the polydispersity. Although this intimate picture of the aggregation induced by the combination of low pH and high ionic strength may not be important to natural solutions because of the present high acidity and salt concentration, the unusual relationship between R_{90} and D will be seen below for aggregation processes produced by strongly binding cations.

Copper Ion Effects. Titrimetric results (2, 10) indicate that at pH 6 this FA sample binds approximately 6.0 mmol of Cu(II)/g, with this value taken as the total capacity. Figure 5 shows the 90° scattering of an unfractionated FA sample as a function of Cu(II) ion bound. Data are given for both pH 6.0 and pH 3.6. At the latter pH, the titration data (2, 10) showed that protons compete to a significant degree with Cu for the weaker binding sites and that the apparent Cu binding capacity decreases.

The results in Figure 5 indicate that aggregation is important. This is not a "precipitation" effect such as that reported by Saar and Weber. The light scattering is time independent, and no settling is observed in over 50 h. (It is also immediately worth looking forward to results with Mg(II) mentioned below and K(I) effects mentioned above to indicate that it is not an ionic strength or electrostatic effect.)

It is of interest to compare the aggregation curve in Figure 5 to some details of the 6.0 mmol of Cu(II) binding sites identified at pH 6. According to functional group analyses of Schnitzer and Skinner (13) supported by the detailed interpretation of the acidimetric titration curves of Gamble (9) and recent ^{13}C NMR data (17), a maximum of 3.0 mmol of these sites may be phenol chelate types. Schnitzer showed that methylation of the phenolic groups greatly reduced the Cu(II) binding of the FA. Thus, it seems very probable that the strong Cu(II) sites occupied

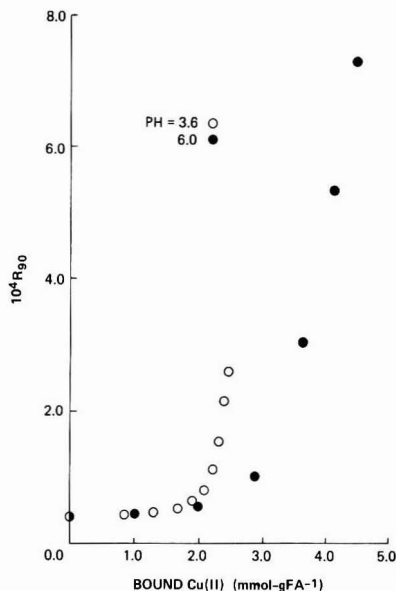


Figure 5. Cu(II) titration of FA monitored by Rayleigh scattering. The degree of Cu(II) binding indicated is calculated from ISE titration. 0.1 mg/mL FA. No added background electrolyte. (O) pH 3.6; (●) pH 6.0.

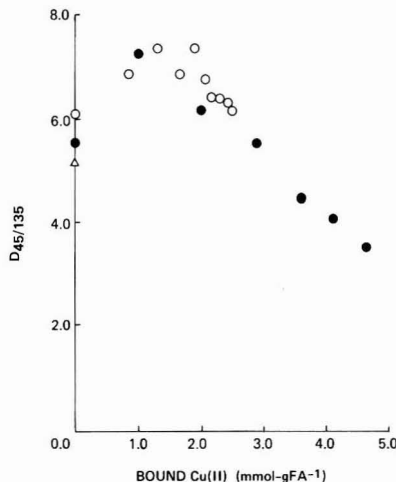


Figure 6. Dissymmetry ratio observed during the Cu(II) titration of FA. Conditions are as in Figure 5.

first as the sample is titrated with Cu(II) include phenolic ones constituting as much as 3 mmol/g. The blocking experiments label them as Cu(II) chelating sites.

The shape of the curve in Figure 5 could be interpreted as a crude titration curve where R_{90} is the monitor. An approximate end point near 3.0 mmol of Cu(II)/g of FA at pH 6 is indicated by the break in the R_{90} curve. This could be easily interpreted in terms of binding of Cu(II) to chelation sites which fail to contribute to aggregation because they are localized strong binding sites whereas Cu(II) can function as a bridging ligand at monodentate sites. One further remark is necessary. It must be explained why the slope of the aggregation curve is so steep past the break. This can only be explained by a cooperative type of equilibrium. The algebra of 1:1 binding does not permit this shape. This point will be important to the final discussion.

The effect of Cu(II) on the dissymmetry ratio, $D(45/135)$ is shown in Figure 6. Again, the interesting result of a relationship between increasing R_{90} and decreasing $D(45/135)$ is seen. The aggregation process induced by Cu(II) also appears to be specific for the smaller particles in the FA mixture.

The results presented in the figures refer to unfractionated samples. Similar results were obtained with the fraction of the sample that passed through a 0.2- μm filter.

Magnesium Ion Effects. Experiments have been conducted with the effect of Mg(II) ion on R_{90} in the concentration range where results of Lee et al. (10) indicate titration of the FA with Mg(II). These experiments are important in distinguishing aggregation effects related to electrostatic charge neutralization from those related to specific complexation processes. Although small increases of R_{90} are associated with titration with Mg(II), R_{90} increasing $\sim 10\%$ in the concentration range from 0 to 0.5 g/L FA, the effects are at least an order of magnitude smaller than Cu(II) effects and do not show either the break or the steep slope past the break seen in Figure 5. It seems safe to conclude that Cu(II) effects must be explained by specific binding processes and not electrostatic effects since corresponding aggregation cannot be produced by Mg(II) or, indeed, larger amounts of K^+ (unless the sample is fully protonated first). The contrast between effects of Cu^{2+} and Mg^{2+} has also been reported for effects on ultracentrifugation of humics by Sipos et al. (8).

Discussion

Sample. A few comments are appropriate about the choice of the fulvic acid used in this study. It is a natural mixture but not a raw natural material. Ion-exchange procedures have been applied to produce a metal-free sample in a fully protonated form. This is necessary for analysis of cation binding. The initial state must be defined. The fractionation results described above indicate that the mixture could be further simplified chemically. On balance, this seems unwise. At the level of complexity used here, the sample is close enough to the natural state to offer properties that may be directly extrapolated to natural systems. However, it has been simplified enough to allow strict accounting of cation binding. It is intended to be a compromise material, neither strictly "geological" nor strictly "chemical".

Copper Ion Induced Aggregation: Pseudochelation. In the early phases of the "titration" of the FA with Cu(II), there is little aggregation as the Cu(II) ions occupy mainly the chelating sites on one FA unit. As Gamble pointed out, another type of binding site is one in which donor groups (carboxylates) come from two units. Bridged complexing of this type is quite conventional. It corresponds to the formula CuL_2 . It can produce aggregation (as is seen in the case of Cu(II)) which will not occur (as the present facts demand) with weakly coordinating metals like K or Mg. However, there is one more feature to be explained. The slope of the increase of aggregation with excess of Cu(II) over chelating sites is very steep and implies a "cooperative" effect where dependence on (Cu^{2+}) concentration is more than linear as conventional CuL_2 formation would imply. This cooperative effect is exactly what might be expected in the case of the FA. The polymer has H-bonding sites and hydrophobic regions. These groups and/or regions should interact and stabilize the bridged complex additionally. The phenomenon can be viewed as one in which the organic molecule associates and then complexes Cu(II). This has been called "pseudochelation" (3). The probable importance of H bonding is indicated

by the selective aggregation of smaller (possibly more oxygenated) particles.

General Conclusions. Light scattering work clearly reinforces the impression that has been growing from compleximetric titrations. The important soil and water organic ligands that are represented by our fulvic acid are complex mixtures of aggregating units with a variety of acidic and/or complexation sites. To the extent that our material is typical, FA's appear to be composed of small units that readily aggregate by bridging interactions using strongly complexing metal ions or protons at high ionic strength and, in addition, some larger particles that can aggregate without other ions. Our data suggest that optical absorbance, ion selective electrode measurements, and fluorescence read this mixture differently. Thus, the complexing capacity and metal ion binding strength observed for a soil organic material may well be a function of pH, ionic strength, previous metal ion loading, and method of monitoring. All of these contribute to the difficulty of the subject of environmental complexing studies.

Acknowledgments

We thank Stephen Lee for access to results prior to publication on Mg(II)-induced aggregations.

Registry No. Cu, 7440-50-8.

Literature Cited

- (1) Saar, R. A.; Weber, J. H. *Geochem. Cosmochim. Acta* **1979**, *44*, 1381.
- (2) Gamble, D. S.; Underdown, A. W.; Langford, C. H. *Anal. Chem.* **1980**, *52*, 1901.
- (3) Langford, C. H.; Gamble, D. S.; Underdown, A. W.; Lee, S. In "Aquatic and Terrestrial Humic Substances"; Christman, R. F.; Gjessing, E. T., Eds.; Ann Arbor Science: Ann Arbor, MI, 1983; Chapter 11.
- (4) Wershaw, R. L.; Pinckney, J. H. *J. Res. U.S. Geol. Surv.* **1973**, *1*, 701.
- (5) Wershaw, R. L.; Pinckney, J. H. *J. Res. U.S. Geol. Surv.* **1977**, *5*, 565.
- (6) Orlov, D. S.; Gorshkova, E. I. *Dokl. Vyssh. Skl. Biol. Nauk.* **1965**, *1*, 207.
- (7) Pagenkopf, G. K.; Whitworth, C. J. *Inorg. Nucl. Chem.* **1981**, *43*, 1381.
- (8) Sipos, S.; Sipos, E.; Dehany, A.; Deer, A.; Meisel, J.; Lakatos, B. *Acta Agron. Acad. Sci. Hung.* **1978**, *27*, 31.
- (9) Gamble, D. S. *Can. J. Chem.* **1972**, *50*, 2680.
- (10) Lee, S.; Langford, C. H.; Gamble, D. S.; Underdown, A. W., 1983, unpublished data.
- (11) Haughlin, M. B. "Light Scattering from Polymer Solutions"; Academic Press: New York, 1972.
- (12) Underdown, A. W. Ph.D. Thesis, Carleton, University, Ottawa, Canada, 1982.
- (13) Schnitzer, M.; Skinner, S. I. M. In "Isotopes and Radiation in Soil Organic Matter Studies"; I.A.E.A.: Vienna, 1968; p 41.
- (14) Hansen, E. H.; Schnitzer, M. *Anal. Chim. Acta* **1969**, *46*, 247.
- (15) Riffaldi, R.; Schnitzer, M. *Soil Sci. Soc. Am. Proc.* **1972**, *36*, 301.
- (16) Underdown, A. W.; Langford, C. H.; Gamble, D. S. *Anal. Chem.* **1981**, *53*, 2140.
- (17) Steelink, C.; Mikita, M. A.; Thorn, K. A. In "Aquatic and Terrestrial Humic Substances"; Christman, R. F.; Gjessing, E. T., Eds.; Ann Arbor Science: Ann Arbor, MI, 1983; Chapter 4.
- (18) Billingham, N. C. "Molar Mass Measurements in Polymer Science"; Wiley: New York, 1977; p 8.

Received for review August 2, 1983. Revised manuscript received September 6, 1984. Accepted September 14, 1984. This research was supported by the Natural Sciences and Engineering Research Council of Canada, and Les Fonds FCAC du Qu ebec.



All forward thinking environmental scientists depend on ES&T. They get the most authoritative technical and scientific information on environmental issues—and so can you! Have *your own*

subscription delivered directly to you each month!

YES! Enter my own subscription to *ENVIRONMENTAL SCIENCE & TECHNOLOGY* at the rate I've checked below:

1985

One Year	U.S.	Mexico & Canada	All Other Countries
ACS Members	<input type="checkbox"/> \$ 26	<input type="checkbox"/> \$ 34	<input type="checkbox"/> \$ 49
Nonmembers—Personal*	<input type="checkbox"/> \$ 35	<input type="checkbox"/> \$ 43	<input type="checkbox"/> \$ 58
Nonmembers—Institutional	<input type="checkbox"/> \$149	<input type="checkbox"/> \$157	<input type="checkbox"/> \$172

Payment Enclosed (Payable to American Chemical Society)
 Bill Me Bill Company Charge my: VISA MasterCard

Card No. _____ Interbank # _____ (Mastercard Only)

Exp. Date _____ Signature _____

Name _____ Title _____ Employer _____

Address _____ City, State, Zip _____

Employer's Business: Manufacturing, type _____

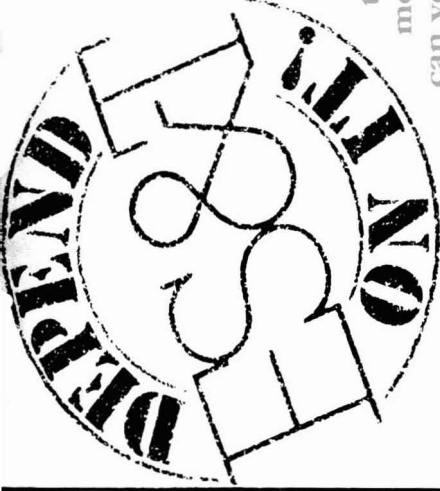
Academic Government Other _____

*Subscriptions at these rates are for personal use only.

All foreign subscriptions are now fulfilled by air delivery. Foreign payment must be made in U.S. currency by international money order, UNESCO coupons, U.S. bank draft, or order through your subscription agency. For nonmember subscription rates in Japan, contact Maruzen Co., Ltd.

Please allow 45 days for your first copy to be mailed. Redeem until December 31, 1985.

MAIL THIS POSTAGE-PAID CARD TODAY!



All forward thinking environmental scientists depend on ES&T. They get the most authoritative technical and scientific information on environmental issues—and so can you! Have *your own*

subscription delivered directly to you each month!

YES! Enter my own subscription to *ENVIRONMENTAL SCIENCE & TECHNOLOGY* at the rate I've checked below:

1985

One Year	U.S.	Mexico & Canada	All Other Countries
ACS Members	<input type="checkbox"/> \$ 26	<input type="checkbox"/> \$ 34	<input type="checkbox"/> \$ 49
Nonmembers—Personal*	<input type="checkbox"/> \$ 35	<input type="checkbox"/> \$ 43	<input type="checkbox"/> \$ 58
Nonmembers—Institutional	<input type="checkbox"/> \$149	<input type="checkbox"/> \$157	<input type="checkbox"/> \$172

Payment Enclosed (Payable to American Chemical Society)
 Bill Me Bill Company Charge my: VISA MasterCard

Card No. _____ Interbank # _____ (Mastercard Only)

Exp. Date _____ Signature _____

Name _____ Title _____ Employer _____

Address _____ City, State, Zip _____

Employer's Business: Manufacturing, type _____

Academic Government Other _____

*Subscriptions at these rates are for personal use only.

All foreign subscriptions are now fulfilled by air delivery. Foreign payment must be made in U.S. currency by international money order, UNESCO coupons, U.S. bank draft, or order through your subscription agency. For nonmember subscription rates in Japan, contact Maruzen Co., Ltd.

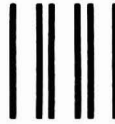
Please allow 45 days for your first copy to be mailed. Redeem until December 31, 1985.

MAIL THIS POSTAGE-PAID CARD TODAY!



**CALL
TOLL
FREE**

(800) 424-6747 (U.S. only)



NO POSTAGE
NECESSARY
IF MAILED
IN THE
UNITED STATES

BUSINESS REPLY CARD

FIRST CLASS PERMIT NO 10094 WASHINGTON D C

POSTAGE WILL BE PAID BY ADDRESSEE

American Chemical Society

Periodicals Marketing Dept.

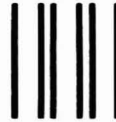
1155 Sixteenth Street, N.W.

Washington, D.C. 20036



**CALL
TOLL
FREE**

(800) 424-6747 (U.S. only)



NO POSTAGE
NECESSARY
IF MAILED
IN THE
UNITED STATES

BUSINESS REPLY CARD

FIRST CLASS PERMIT NO 10094 WASHINGTON D C

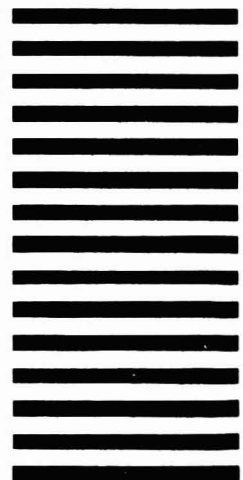
POSTAGE WILL BE PAID BY ADDRESSEE

American Chemical Society

Periodicals Marketing Dept.

1155 Sixteenth Street, N.W.

Washington, D.C. 20036



Differential Pulse Anodic Stripping Voltammetry of Cadmium(II) at a Membrane-Covered Electrode: Measurement in the Presence of Model Organic Compounds

Ronald B. Smart* and Edward E. Stewart

Department of Chemistry, West Virginia University, Morgantown, West Virginia 26506-6045

■ A rotating membrane-covered mercury film electrode (MCMFE) was constructed by placing a M_r 1000 cutoff dialysis membrane over a glassy carbon rotating disk electrode and plating a thin mercury film onto the electrode surface through the membrane. Differential pulse anodic stripping voltammetry (DPASV) was used to measure cadmium ion in the presence of eight surfactants, which were chosen to model ionic, nonionic, complexing, and polysaccharide compounds. The MCMFE eliminated many of the adsorption problems previously reported at a hanging mercury drop electrode as well as those seen at a bare mercury film electrode (MFE).

Dissolved organic material in natural waters adsorbs readily on a mercury electrode (1-6). For example, fulvic acid (FA) induces the adsorption of cadmium at mercury electrodes (5). Adsorption of organic material on a mercury electrode can cause serious problems when anodic stripping voltammetry (ASV) is used to measure trace metals in natural waters because even slow adsorption processes can reach equilibrium. Brezonik et al. (2) reported the effects of model surfactants on ASV of copper and cadmium at a hanging mercury drop electrode (HMDE). Sorption occurred at neutral and low pH, with some sorbents inhibiting the electrochemical reaction more strongly at low pH. Buffle et al. (6) found that organic adsorption could influence the electrochemistry at Hg electrodes and suggested the development of reproducible voltammetric electrodes capable of minimizing organic adsorption.

Covering a mercury film electrode with a dialysis membrane should prevent organic fouling of the electrode surface. In situ dialysis (7) and dialysis-ion exchange (8) have been used for determining the state of trace metals in natural water. Truitt and Weber (9) have effectively demonstrated that copper-FA complexes could be separated from "free" copper by using a dialysis membrane. In previous studies of membrane-covered mercury electrodes (10-16), only Schimpf (16) actually utilized it for trace metal measurement. He examined both specific (ion-exchange) and nonspecific (diffusion barrier) membranes. Nonspecific membranes generally reduced the sensitivity compared to the bare electrode; however, limited linear calibration curves $[(1-8) \times 10^{-7} \text{ M Cd}^{2+}]$ were still observed. Analysis time was shorter with the nonspecific membranes because of a shorter waiting period between successive analyses. Some selectivity was reported for the specific membranes, but no measurements were made with either membrane to evaluate the effects of organic matter.

We have developed a rotating membrane-covered mercury film electrode (MCMFE) for the purpose of measuring trace metals in the presence of surface active compounds. We have compared these results with those obtained with a bare mercury film electrode (MFE) and a HMDE. The optimum experimental parameters for the differential pulse ASV (DPASV) of Cd(II) have been reported previously (17).

Experimental Section

A Pine Instruments, Inc. (Grove City, PA), glassy carbon electrode (DD20) and PIR rotator were used in combination with an EG&G Princeton Applied Research Corp. (PAR, Princeton, NJ) Model 174A polarographic analyzer, a PAR Model 315 automated electroanalysis controller, and a Houston (Bellaire, TX) Omnigraphic Model 2000 X-Y recorder. A Metrohm (Sybron-Brinkman, Des Plaines, IL) pH stat was used for all work at pH 6. An Orion (Cambridge, MA) Model 701A digital ion analyzer was used for all other pH measurements. A microprobe combination pH electrode (Fisher, Pittsburgh, PA), an Ag/AgCl reference electrode (saturated KCl), a platinum wire counter electrode, and a 50-mL PAR jacketed polarographic cell were used for all measurements. Reagents and electrode polishing procedures have been previously described (17).

Membranes. The dialysis membranes were cut from Spectra/Por 6 cellulose dialysis tubing (Spectrum Medical Industries, Inc., Los Angeles, CA). This membrane has a nominal M_r 1000 cutoff. The bags were soaked in 70 °C deionized water for 20 min, thoroughly rinsed with deionized water, and finally soaked at room temperature in distilled deionized water for 48 h prior to their use. This procedure effectively removed the sodium benzoate preservative. Spectra/Por is most susceptible to attack by cellulytic microorganisms when thoroughly wet; therefore, the tubing was transferred to freshly boiled, doubly distilled, deionized water daily, and fresh tubing was prepared weekly. Unwashed tubing was stored in a refrigerator as per the manufacturer's instructions.

Surfactants. All surfactant solutions were prepared with deionized doubly distilled water. Agar, alginate acid, alkaline phosphatase, (+)-camphor, type IV gelatin, and polygalacturonic acid (Sigma Chemical Co., St. Louis, MO) were dissolved in water to give solutions of the highest possible concentration. (+)-Camphor was first dissolved in 1 mL of 95% EtOH and then diluted to 1 L. Triton X-100 (Rohm and Haas, Philadelphia, PA) was prepared by mixing the liquid with distilled water. The starch solution was prepared according to Standard Methods (18).

Ultrapure HNO₃ and KOH (passed through Chelex-100) were used to adjust the pH of the surfactants and the analyte solutions. The electrolyte was 0.01 M KNO₃ throughout.

Procedure. All analyses by DPASV were carried out in deaerated 0.01 M KNO₃ electrolyte, and ultrapure N₂ was continuously passed over the solution during analysis. The instrumental settings used for all DPASV measurements as well as electrode plating, preconditioning, and storage methods were previously reported (17). All polarographic cells were soaked in 6 M HNO₃ overnight and rinsed with deionized water prior to use. Stripping was done in a quiet solution at 25.0 ± 0.2 °C.

For all work with both the MFE and the MCMFE the concentration of Cd(II) was 8.90×10^{-7} M. Fifteen seconds of unstirred deposition time was used throughout, and

Table I. Summary of Effects of Surfactants on Cd(II) Peak Current and Peak Potential for the MFE, MCMFE, and HMDE^a

surfactant	concn range, ppm	electrode	neutral conditions ^b		acidic conditions ^c	
			$\Delta i_p(\text{max}),^d$ %	$\Delta E_p(\text{max}),$ mV	$\Delta i_p(\text{max}),$ %	$\Delta E_p(\text{max}),$ mV
agar	1-10	HMDE	-30	NC ^e	-30	NC
	1-10	MFE	-26	NC	+35	-17
	1-10	MCMFE	NC	NC	NC	NC
alginic acid	4-40	HMDE	-15	NC	-11	NC
	2-40	MFE	-49	NC	+19	-23
	2-40	MCMFE	-10	NC	NC	NC
APase	1-36	HMDE	-15	NC	-90	+40
	1-40	MFE	-73	NC	+98	+68
	1-40	MCMFE	NC	NC	-4	NC
camphor	1-100	HMDE	-17	NC	-25	+
	1-100	MFE	-22	NC	-14	NC
	1-100	MCMFE	NC	NC	NC	NC
gelatin	0.1-20	HMDE	NC	NC	-55	+56
	0.1-20	MFE	NC	NC	-85	+35
	0.1-20	MCMFE	NC	NC	NC	NC
PGUA	2-200	HMDE	-23	+23	-10	+17
	2-200	MFE	-64	-17	-11	NC
	2-200	MCMFE	-49	-20	NC	NC
starch	1-10	HMDE	-15	NC	-15	NC
	1-10	MFE	-4	NC	-8	NC
	1-10	MCMFE	NC	NC	NC	NC
Triton X-100	1-40	HMDE	-40	+100	-65	+100
	1-40	MFE	-51	+16	-94	+97
	1-40	MCMFE	-25	NC	-47	+30

^aData taken from ref 2. ^bHMDE, pH ~7; MFE and MCMFE, pH 6.00 ± 0.02. ^cHMDE, pH ~3; MFE and MCMFE, pH 3.00 ± 0.02. ^d $\Delta i_p(\text{max})$ and $\Delta E_p(\text{max})$ given relative to a control peak at the specified pH; $[\text{Cd}^{2+}] = 8.90 \times 10^{-7}$ M. ^eDenotes no change relative to a control peak at the specified pH.

prior to surfactant addition, a consistent i_p was demonstrated by obtaining four peaks varying less than 2%. Peak currents were corrected for any dilution.

Results and Discussion

We examined the effects of eight surfactants on the DPASV of Cd(II) at both the MFE and the MCMFE. The surfactants chosen were those previously investigated by Brezonik et al. (2), and our results at pH 3 and 6 are summarized in Table I together with theirs at pH 3 and 7. Clearly, the presence of these surfactants could lead to serious problems with data interpretations of the DPASV and ASV of Cd(II) at bare mercury electrodes.

The influence of agar and alginic acid was similar. Agar is composed of a complex range of polysaccharide chains, and alginic acid is a hydrophobic colloidal polysaccharide derived from seaweed with an average molecular weight of about 240 000. These compounds served as models for the polysaccharides secreted into natural water by phytoplankton. An agar concentration of 1 ppm had a definite effect (-16%) on peak current (i_p) at the MFE at pH 6, while 5 ppm alginic acid caused a 15% reduction in i_p . Small (<10 mV) negative shifts in peak potential (E_p) were also noted at this electrode with both compounds; however, the significance of this for stripping is not clear. The MCMFE exhibited no change in i_p or E_p for up to 10 ppm of agar and 5 ppm of alginic acid at pH 6; therefore, peak current attenuation at the MFE can probably not be attributed to complexation. The formation of labile reducible complexes or permeable complexes cannot be completely ruled out. Figure 1 shows peak current data for agar at the MFE and MCMFE at both pH 6 and pH 3.

At pH 3 the effects of agar and alginic acid at the MFE are perhaps even more serious. An agar concentration of 3 ppm caused about a 22% increase in i_p as well as a negative shift in E_p , while 2 ppm of alginic acid also caused negative E_p shifts and an increase in i_p of about 20%. Natural water samples are often analyzed by ASV or DPASV at neutral and acidic pH to differentiate between

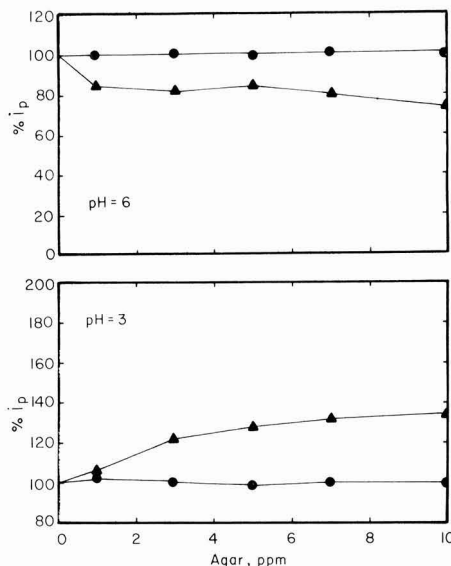


Figure 1. Effect of agar on percent initial peak current for Cd(II). (▲) MFE; (●) MCMFE; $[\text{Cd}^{2+}] = 8.90 \times 10^{-7}$ M.

free and total metal, and it again might be tempting to speculate about cadmium complexation. However, the data for the MCMFE indicated no change in i_p or E_p and, therefore, no cadmium complexation for up to 10 ppm of agar and 40 ppm of alginic acid. The increase in i_p observed at the MFE could be the result of surfactant adsorption, although we have no evidence of this.

The results with starch and gelatin are also similar although quite different from the previous two compounds. Gelatin (M_r 75 000) was used as a model of the colloidal proteinaceous matter present in natural water, and starch served as an additional model for polysaccharides secreted

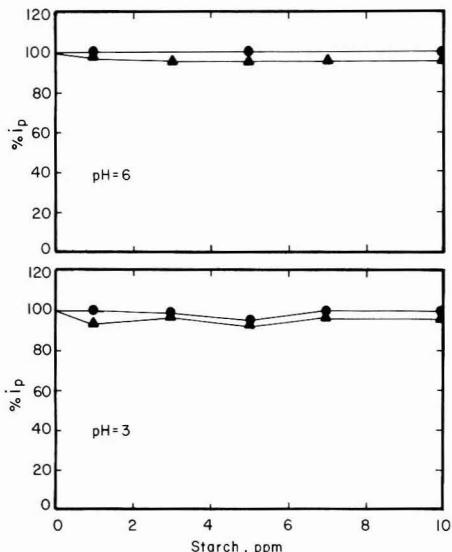


Figure 2. Effect of starch on percent initial peak current for Cd(II). (▲) MFE; (●) MCMFE; $[Cd^{2+}] = 8.90 \times 10^{-7}$ M.

by plankton. No effect on E_p was observed at pH 6 for either the MFE or MCMFE with up to 20 ppm of gelatin or 10 ppm of starch. Also, no i_p change was seen with either electrode for up to 20 ppm of gelatin, but 1 ppm of starch caused a slight decrease (4%) in i_p at the MFE possibly as a result of adsorption. Up to 10 ppm of starch had no effect on i_p at the MCMFE. The effect of starch at pH 6 and 3 on both the MFE and MCMFE is given in Figure 2.

At pH 3 an opposite effect to that noted with alginate and agar was seen. By use of the MFE, i_p was decreased by as much as 65% with 20 ppm of gelatin and 14% with 2 ppm of starch and was accompanied by positive shifts in E_p . No change in either i_p or E_p was observed at the MCMFE for up to 20 ppm of gelatin and 10 ppm of starch, again implying that cadmium complexation was not the cause for the observations at the MFE.

The data for alkaline phosphatase (APase; orthophosphoric-monoester phosphohydrolase), camphor, and Triton X-100 were also somewhat similar. APase is a water-soluble enzyme with an average molecular much greater than 1000 and served as a model for proteinaceous material. The results for APase at pH 6 and 3 are shown in Figure 3. A 73% decrease in i_p accompanied by a negative shift (30 mV) in E_p was seen at the MFE with 10 ppm of APase at pH 6; however, no effects on either i_p or E_p were observed at this pH with the MCMFE for up to 40 ppm of APase. This result again indicated that cadmium complexation was not the reason for the decreased i_p observed at the bare electrode. A decrease (13%) in i_p at the MFE with 10 ppm of camphor was also seen at pH 6; however, no shift in E_p was noted. No change in i_p or E_p occurred at the MCMFE at pH 6 for up to 100 ppm of camphor, which was surprising since camphor has a molecular weight of only about 152. Triton X-100 has a molecular weight of about 5000 and was used as a model nonionic surfactant. At pH 6, Triton X-100 (10 ppm) caused a 32% decrease in i_p and a slight (+18 mV) shift in E_p at the MFE. No change in i_p or E_p was seen at the MCMFE for up to 10 ppm of Triton X-100; however, a decrease in i_p (20%) was noted starting at 20 ppm. This was unexpected and must be the result of either cadmium

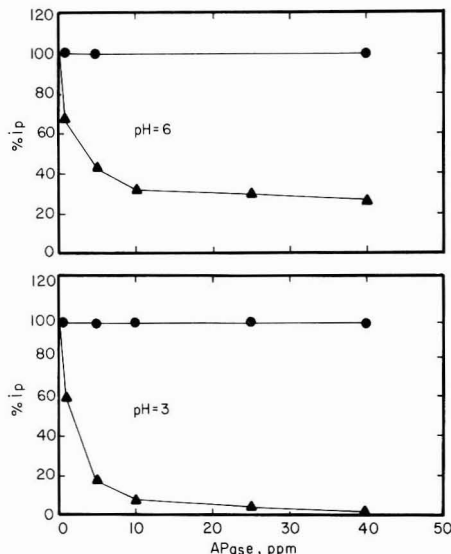


Figure 3. Effect of alkaline phosphatase on percent initial peak current for Cd(II). (▲) MFE; (●) MCMFE; $[Cd^{2+}] = 8.90 \times 10^{-7}$ M.

complexation by this surfactant or some sorption-induced interference, although it seems unlikely that Triton X-100 could diffuse through this membrane.

The influence of APase and Triton X-100 on both electrodes at pH 3 was similar to, but more pronounced than, that observed at pH 6. A 92% decrease in i_p and a positive (58 mV) shift in E_p were seen at the MFE for 10 ppm of APase, although no change in either i_p or E_p occurred at the MCMFE for up to 40 ppm. The decrease in i_p (86%) at the bare electrode caused by 10 ppm of Triton X-100 was markedly enhanced (similar to gelatin) at the lower pH. Triton X-100 also caused an almost linear decrease in i_p at the MCMFE (6% at 2 ppm up to 47% at 40 ppm). If this decrease in i_p was due to complexation of cadmium by this surfactant, the effect would be expected to be less rather than more pronounced at the lower pH. We can only speculate that this surfactant interfered with the mass transport of cadmium. Camphor (40 ppm) at pH 3 caused a 10% decrease in i_p at the MFE while up to 100 ppm caused no change i_p at the MCMFE.

The final surfactant examined, polygalacturonic acid (PGUA), behaved much differently than those compounds previously described. It is a long chain polymer of galacturonic acids with a molecular weight greater than 1000 and served as an additional model for the polysaccharides secreted by plankton. As shown in Figure 4, at pH 6 i_p at the MFE first increased (12%) with 2 ppm of PGUA and then decreased (15%) at 10 ppm. The decrease in i_p (14%) was also observed with the MCMFE for 10 ppm of PGUA and 34% for 50 ppm and 49% for 100 ppm of PGUA. Complexation of cadmium by PGUA is consistent with these data, and the larger decrease in i_p at the MFE might be a result of complexation coupled with adsorption.

At pH 3 i_p first increased 9% at the MFE with 10 ppm of PGUA and then decreased 11% with 100 ppm, while at the MCMFE no change in i_p was seen for up to 100 ppm of PGUA. This result lends further support for complexation as the reason for the reduction in i_p seen at the MCMFE at pH 6.

It is apparent that surfactants can cause problems with the interpretations of DPASV and ASV of cadmium at the bare mercury electrodes (HMDE, MFE). It is also inter-

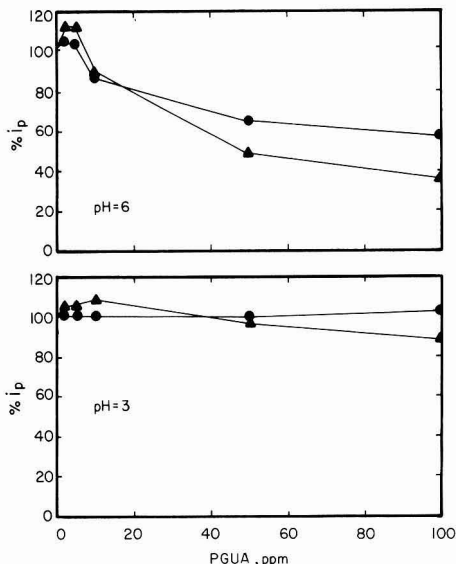


Figure 4. Effect of polygalacturonic acid on percent initial peak current for Cd(II). (▲) MFE; (●) MCMFE; $[Cd^{2+}] = 8.90 \times 10^{-7}$ M.

esting to note (see Table I) that, with some surfactants, the effects observed at the MFE are much different than those seen with the HMDE. This is especially noticeable for both agar and alginic acid at pH 3, where opposite effects occurred. The dialysis membrane provided a protective barrier on the MCMFE and eliminated the influence of the surfactants in most cases.

We are currently investigating the behavior of the MCMFE at pH greater than 6 with ASV and DPASV as well as studying the interactions of trace metals with soil-derived fulvic acid. It is hoped that the MCMFE will become a valuable tool for trace metal analysis in natural waters.

Acknowledgments

We thank Carl Wise, Robert Victor, Robert Shrout and

David Gover for their professional expertise in the maintenance and construction of equipment.

Literature Cited

- (1) Cominoli, A.; Buffle, J.; Haerdi, W. *J. Electroanal. Chem. Interfacial Electrochem.* **1980**, *110*, 259.
- (2) Brezonik, P. L.; Brauner, P. A.; Stumm, W. *Water Res.* **1976**, *10*, 605.
- (3) Cosovic, B.; Vojvodic, B. *Limnol. Oceanogr.* **1982**, *27*, 361.
- (4) Nelson, A.; Mantoura, R. F. C. *J. Electroanal. Chem. Interfacial Electrochem.* **1984**, *164*, 265.
- (5) Van Leeuwen, H. P. *Anal. Chem.* **1979**, *51*, 1323.
- (6) Buffle, J.; Cominoli, A.; Greter, F. L.; Haerdi, W. *Proc. Anal. Div. Chem. Soc.* **1978**, *15*, 59.
- (7) Benes, P.; Steinnes, E. *Water Res.* **1974**, *8*, 947.
- (8) Hart, B. T.; Davis, S. H. R. *Aust. J. Mar. Freshwater Res.* **1977**, *28*, 105.
- (9) Truitt, R. E.; Weber, J. H. *Anal. Chem.* **1981**, *53*, 337.
- (10) Bersier, P.; Bersier, J.; Hugli, F. *Helv. Chim. Acta* **1960**, *43*, 478.
- (11) Berge, H.; Kunkel, S. *Anal. Chim. Acta* **1971**, *54*, 221.
- (12) Bowers, R. C.; Wilson, A. M. *J. Am. Chem. Soc.* **1958**, *80*, 2968.
- (13) Pungor, E.; Feher, Zs. *J. Electroanal. Chem. Interfacial Electrochem.* **1977**, *75*, 241.
- (14) Chien, Y. W.; Olsen, C. L.; Sokoloski, T. O. *J. Pharm. Sci.* **1973**, *62*, 435.
- (15) Gough, D. A.; Leypoldt, J. K. *Anal. Chem.* **1979**, *51*, 439.
- (16) Schimpf, W. K. Ph.D. Dissertation, The University of Michigan, Ann Arbor, MI, 1971.
- (17) Stewart, E. E.; Smart, R. B. *Anal. Chem.* **1984**, *56*, 1131.
- (18) "Standard Methods for the Examination of Water and Wastewater"; APHA: Washington, DC, 1981.

Received for review October 17, 1983. Revised manuscript received June 25, 1984. Accepted September 13, 1984. Although the information described in this article has been partially funded by the U.S. Environmental Protection Agency under Assistance Agreement R810540-01-0, it has not been subjected to the Agency's required peer and administrative review and therefore does not necessarily reflect the views of the Agency, and no official endorsement should be inferred. Acknowledgment is made to the donors of the Petroleum Research Fund, administered by the American Chemical Society, for partial support of this research.

Voltammetric Methods for Distinguishing between Dissolved and Particulate Metal Ion Concentrations in the Presence of Hydrous Oxides. A Case Study on Lead(II)

María de Lurdes Simões Gonçalves

Centro de Química Estrutural, Instituto Superior Técnico, 1096 Lisboa, Portugal

Laura Sligg and Werner Stumm*

Institute for Water Resources and Water Pollution Control (EAWAG), Swiss Federal Institute of Technology, CH-8600 Dübendorf, Switzerland

■ Voltammetric techniques (differential pulse polarography, DPP, anodic stripping voltammetry, ASV, and differential pulse anodic stripping voltammetry, DPASV) were evaluated for their capability to distinguish between dissolved and particulate Pb(II) concentrations. Colloids of FeOOH, MnO₂, and SiO₂ were found to have no effect on the electrochemical reversibility (peak width, peak potential, and pseudopolarographic half-wave potential) of the Pb(II) reduction system. Soluble Pb(II) concentrations measured in the presence of colloids were consistent and independent of the voltammetric method used and the different time scales employed in these techniques. Equilibrium constants for the specific adsorption of Pb²⁺ on FeOOH, MnO₂, and SiO₂ surfaces were determined. Applicability of voltammetric techniques to other metals and in the presence of other colloids and in natural waters is discussed.

Introduction

In order to understand the factors that control the concentrations of metals in natural waters, their chemical reactivity, their bioavailability, and toxicity, we need to know the form of occurrence in which the metal is present; above all we should know whether the metal is present in solution or in particulate form. Analytically, however, one encounters difficulties in identifying unequivocally the various solute species and in distinguishing between dissolved and particulate concentrations. Much attention is paid to the influence of soluble complex formers on regulating the concentration of free metal ions, but the partition of chemical species between solid and liquid phases is of particular interest to aquatic and environmental chemists because particulate matter and colloidal matter play a dominant role in natural waters; in fresh waters, more than 95% of heavy metals that are transported from land to sea occurs in the form of particulate matter (1).

Operational Difficulties of Membrane Filters. Distinguishing chemical species between being "dissolved" and "particulate" is no trivial matter, especially for heavy metal ions occurring typically in concentrations much smaller than 10⁻⁶ M (often smaller than 10⁻⁹ M) and in presence of excesses of other ions. Often a decline in partition constants with higher suspended solids concentration has been reported (2), but laboratory artifacts derived from incomplete phase separations may explain the solids' concentration effect. The pore sizes of membrane filters provide an operational rather than a conceptual distinction between dissolved and particulate species. Metal ions, especially in fresh waters, are often present in the form of colloids or bound to colloids such as those of Fe(III) oxide hydroxides, which may have particle sizes smaller than 100 Å, sufficiently small to pass through a membrane filter. Furthermore, any filtration

operation is fraught with possibilities for contamination and adsorption loss. Changes in the concentration of particles and colloids, almost unavoidable during the filtration step or centrifugation, introduce changes in the partition of chemical species between the liquid and the (often electrically charged) surface phases, and this in turn may cause additional errors in the determination of the solute species. The best procedure will involve minimum sample manipulation. Obviously, the addition of acid or pH buffers to the system changes the solid solution partition.

Electrochemical Measurements. Ion selective electrodes (ISE) measure directly free metal ion activity and discriminate clearly against metal ions bound in a complex or adsorbed on particles or colloids. Unfortunately, ISE are usually not sufficiently sensitive to measure heavy metal ions in the concentration range typically encountered in natural waters. Electrode-kinetic measurements (polarographic and voltammetric techniques) are for many metals sufficiently sensitive and potentially able to distinguish different chemical species: First, there are detectable components of soluble trace metals that are mostly present as ionic forms and metal ion complexes that are kinetically labile at the Hg electrode; second, there are undetectable components of soluble trace metals, usually kinetically nonlabile organic ligand complexes; third, there are insoluble components often present as colloidal particles with incorporated or adsorbed metal ions that cannot be detected without prior treatment of the sample. Voltammetric methods are in principle able to differentiate without prefiltering the water sample between dissolved labile species, i.e., the metal ions electrochemically available within the diffusion layer and (in addition to other nonlabile complexes) those bound to particles or colloids.

Various investigations (3-8) have considered the effect of colloids and particles on electroanalytical measurements. Plavšić et al. (8) have carefully studied the effect of Al₂O₃ colloids on the voltammetric determination of labile Cu(II). Their interpretation and the subsequent quantitative treatment of their data on the titration of their samples with Cu(II) by Ružič (9) confirm the feasibility of the electroanalytical methodology for distinguishing between particular and soluble labile Cu(II) species.

Many investigators titrate natural waters directly with trace metals using voltammetric detection methods to determine the complexing capacity of the water or to gain information on the speciation of trace metals. One needs to know how colloidal matter often present in natural water samples (even if filtered or centrifuged) affects such titration curves.

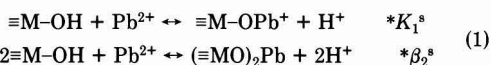
To obtain an in-depth knowledge of effects of colloids and particles on voltammetric measurements, we have carried out a careful case study using Pb(II) in the presence

of various metal oxide colloids. Pb^{2+} is known to be attached rather strongly to particles, especially in fresh waters (1, 6).

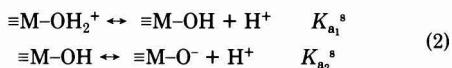
The objectives of this paper are (i) to present a case study on voltammetric measurements of solute $Pb(II)$ ions in the presence of lead ion adsorbable colloids, (ii) to discuss the effects of colloids upon the electrochemical reversibility and on the analytical determination of soluble labile Pb species, (iii) to illustrate the method's general feasibility to evaluate equilibria between dissolved and colloidal forms, and (iv) to elaborate to what extent this approach can be extended to other metal ions and other colloidal systems and to discuss the analytical applicability in real natural waters.

Since our primary concern was to assure that the voltammetric methods used do not respond to particulate forms of Pb , we used model systems where the variables were known or could be controlled; we omitted soluble organic ligands to avoid complications.

Solid-Solution Systems Investigated. Three types of hydrous oxides were used as model colloids for the particles typically encountered in fresh water systems: amorphous silica, goethite (α - $FeOOH$), and MnO_2 [manganate(IV)]. These colloids varied in particle size between 0.1 μm (MnO_2) and 1 μm (silica); $FeOOH$ and MnO_2 are, in principle (if in intimate contact with an electrode), electrochemically reducible. $Pb(II)$ was used as a representative heavy metal ion that can be easily determined by different voltammetric methods. The extent of surface binding (adsorption, or the distribution coefficient between particles and solution) on the hydrous oxide surface ($\equiv M-OH$) as a function of pH and other solution variables can be predicted with the help of surface complex formation constants which may be defined.



The degree of surface protonation depends on the acid-base equilibria:



Experimental Section

Colloids. Goethite (α - $FeOOH$) prepared according to ref 11 was used in an aqueous suspension without drying. The surface area of this material determined by BET was 14.7 $m^2 g^{-1}$. The concentration used in the adsorption experiments was 80 mg/dm^3 $FeOOH$.

MnO_2 prepared according to ref 12 was washed by centrifuging and resuspending in 0.01 M KNO_3 . (The pH of the suspension at the end of the washing procedure was 5.9.) The concentration of the material was determined by dissolution with oxalate and measurement of $Mn(II)$ by atomic absorption. The concentration used in the adsorption experiments was 4.2 mg/dm^3 MnO_2 .

SiO_2 was used as the commercial product Aerosil 200 (Degussa). The surface area determined by BET was 200 m^2/g^{-1} . A stock suspension of SiO_2 (4 g/dm^3) was prepared. The concentration used in the adsorption experiments was 16 mg/dm^3 .

Adsorption Experiments. For all experiments, the ionic medium was 0.01 M KNO_3 . All solutions were in 5×10^{-4} M tris(hydroxymethyl)aminomethane (Tris) buffer in order to obtain a buffering in the pH region 7-8.5; Tris was found to form no stable complexes with $Pb(II)$. pH was adjusted by adding 0.1 M HNO_3 or 0.1 M $NaOH$ to the suspensions, before adding the Pb solution. Adsorption

Table I. Experimental Conditions

method	scan rate, mV/s	initial potential, V	reduction potential, V	pulse height, mV	drop time, s	deposition time, min
DPP	4	-0.2		50	1 or 2	
ASV	4		-0.8			2
DPASV	5		-0.8	25		2

experiments were carried out either in solutions of constant $[Pb(II)]_T$ at varying pH or in solutions of constant pH with varying $[Pb(II)]_T$. Each experimental point records a measurement in an individual batch. Measurements of pH and $Pb(II)$ in solution were made after equilibration times of 1-2 h at room temperature ($25 \pm 2^\circ C$).

Voltammetric measurements were performed as differential pulse polarography at a dropping mercury electrode (DPP), as anodic stripping voltammetry with direct current measurement (ASV), or as differential pulse anodic stripping voltammetry (DPASV) at a hanging mercury drop electrode (Metrohm EA 590). A Metrohm E 506 polarograph and a PAR 174A polarograph were used. Experimental conditions used are given in Table I.

An $Ag/AgCl$ electrode was used as a reference electrode. In some experiments, an ion-selective Pb electrode (Orion) was used for comparison. All measurements were carried out at $25 \pm 2^\circ C$. For alternating current (ac) polarography measurements, the potential was varied between -400 and -1000 mV, frequency was 75 Hz, the current was measured at 90° and 0° phase angle shift, and the drop time was 1 s.

Calibration of Voltammetric Response to $[Pb^{2+}]$. In order to calibrate the voltammetric response, $Pb(II)$ solutions were kept at pH values below 7.2. For these solutions ($[Pb^{2+}] = 6 \times 10^{-5}$ to 10^{-7} M; $I = 10^{-2}$ M, 5×10^{-4} M Tris buffer), calibration plots of peak currents vs. $[Pb^{2+}]$ obtained by DPP, by DPASV, and by ASV(DC), respectively, gave excellent linear regressions ($r > 0.99$) with slopes of $i_p/[Pb^{2+}]$ of 9.68×10^3 , 2.54×10^6 , and $8.28 \times 10^4 \mu A/M$, respectively. At a given $[Pb^{2+}]$, the ASV peak current increased linearly with the deposition time (2-10 min) both in the presence and in the absence of the colloids studied.

Results and Discussion

Theoretically, one would infer that metal ions adsorbed or surface bound to particles or colloids are nonlabile; i.e., they will not to any extent, during a voltammetric measurement, be electrochemically available for cathodic reduction. First, from a physical point of view, the mass transfer of particles (by diffusion, settling, and interception) into the diffusion layer or to the electrode surface is, under the experimental conditions prevailing, not very efficient; diffusion coefficients for colloidal particles come out to be very small. A spherical 100- \AA particle has a diffusion coefficient D , which is approximately 100 times smaller than that of a metal ion. In DPP, for example, the peak current varies with $D_{1/2}$; thus, metal ions bound to such a particle could at best (i.e., if the metal particle complex were fully labile) account for one-tenth of the peak current that would be observed if all metal ions were present as dissolved labile metal ions. Second, from a chemical point of view, it is highly unlikely that metal ions become dissociated and released from the colloidal surface fast enough to become available to the electrode during depolarization.

The experimental verification of this inference is rendered very difficult especially if one wants to measure near

Table II. Conditional Surface Complex Formation Constants of Pb²⁺ with Hydrous Oxides

colloid ^c	C _{Pb} , M	pH	pK _{a1} ^{s,a}	pK _{a2} ^{s,a}	log K ₁ ^{s,b}	log β ₂ ^{s,b}
goethite, 1.5 × 10 ⁻⁵ M	2 × 10 ⁻⁶ to 10 ⁻⁵	7.25 ± 0.05	6.4 (18)	9.25	-2.0 ± 0.2 (DPASV) -1.8 ± 0.2 (DPP) -1.8 ± 0.2 (ASV)	
MnO ₂ , 1.3 × 10 ⁻⁵ M	2 × 10 ⁻⁶ to 10 ⁻⁵	5.0 ± 0.2	5.7		1.1 ± 0.2 (DPP) 1.4 ± 0.2 (DPASV)	
silica, 2.6 × 10 ⁻⁵ M	2 × 10 ⁻⁶ to 10 ⁻⁵	7.23 ± 0.02	7.3 (16)			-4.4 ± 0.1 (DPP)

^a pK_{a1}^s and pK_{a2}^s are the surface acidity constants as defined in eq 2. ^b K₁^s and β₂^s as defined in eq 3 and 4. ^c Concentrations refer to the surface =M-OH groups.

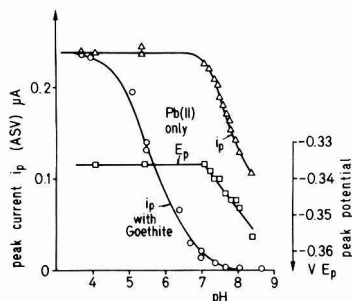


Figure 1. Pb(II) measurements by ASV as a function of pH in the presence and in the absence of goethite (α -FeOOH = 80 mg dm⁻³; [Pb]_T = 2 × 10⁻⁶ M). In the presence of goethite, peak currents decrease due to the strongly pH-dependent adsorption of Pb²⁺ on this hydrous oxide. In the absence of goethite, a pH-dependent adsorption on the glass wall occurs, causing a decrease of peak currents. The shift of the peak potential corresponds to the formation of PbOH⁺.

the concentration range encountered in aquatic systems. We used essentially three approaches: (i) to make measurements with voltammetric methods on the extent of adsorption on colloidal systems and assess whether consistent and comparable data on adsorption equilibria are obtained; (ii) to compare the agreement of the results obtained by using different voltammetric methods; (iii) to evaluate whether colloids had any effect on electrochemical reversibility.

Measurements on Adsorption by Voltammetric Methods. The pH dependence of the Pb(II) adsorption on α -FeOOH, MnO₂, and SiO₂ has been studied by measuring the residual solute Pb²⁺ concentrations by DPP, ASV/DC, and DPASV in the suspension without separation of the colloids. Figure 1 shows a representative curve of ASV peak current, *i_p*, as a function of pH, in the presence and in the absence of goethite. At high pH values, adsorption of Pb²⁺ on goethite occurs and a decrease in *i_p* is measured; in the absence of goethite, adsorption of Pb²⁺ on the glass wall occurs (as determined by atomic absorption measurements). The adsorption of metal ions to the glass wall shows a similar pH dependence as that observed on other oxide surfaces (cf. eq 1 and Figure 1). The hydroxo complexes of Pb(II) such as PbOH⁺ in our opinion, are fully labile. The shift in the peak potential *E_p* at pH ~ 7 is due to the formation of a hydroxo complex of Pb(II).

The shift in peak potential with increasing pH can be evaluated to determine the stability constant of PbOH⁺ (13). A value of log β₁ = 6.20 ± 0.03 (*I* = 10⁻² M KNO₃ and *t* = 25 °C) is obtained for the PbOH⁺ complex, a value which is in good agreement with those given by Baes and Messmer (14) and our own estimated value (log β₁ ≈ 6.4) obtained with the ion-selective Pb²⁺ electrode. Within the pH range considered, pH ≤ 8.4, Pb(OH)₂ is negligible [log β₂ = 10.9, *I* = 0 (14)]. The agreement with the literature data shows that the buffer "Tris" has a negligible effect

in complexing Pb(II) and that the buffer capacity, although small, is sufficient.

Equilibrium constants for the surface complexes have been calculated from experiments in which total concentration of Pb(II) was varied. The constants K₁^s and β₂^s are defined as follows:

$$K_1^s = \frac{[=M-OPb^+][H^+]}{[=M-OH][Pb^{2+}]} \quad (3)$$

$$\beta_2^s = \frac{[=(M-O)_2Pb][H^+]^2}{[=M-OH]^2[Pb^{2+}]} \quad (4)$$

For the complexation with α -FeOOH and with MnO₂, only 1:1 complexes are assumed and with SiO₂, only 1:2 complexes. The concentration of the different species is calculated from mass balances, assuming that the voltammetric measurements include the total Pb in solution, and with the help of surface acidity constants; values of K₁^s or β₂^s are calculated for each measured point, as in ref 15. The equilibrium constants given in Table II, are conditional for the pH range and the ionic strength used in the experiment, as the influence of surface charge was neglected in the calculation. Consistent values were obtained at different lead concentrations and by the different voltammetric methods used in this work. The adsorption curves obtained are comparable with literature results (16, 17), although an exact comparison of the equilibrium constants is not possible due to different experimental conditions (ionic strength etc.).

Behavior of Surface-Bound Metal Ions in Voltammetric Measurements. Pb(II) concentrations measured by DPP, ASV, and DPASV in the presence of colloids are internally consistent and independent of the voltammetric or polarographic method used and the different time scales employed in these methods. As shown in Figure 2, results obtained with DPP, ASV, and DPASV are in close agreement, independently whether the Pb(II) in solution is measured as the direct reduction current (DPP) or as the oxidation current after a preconcentration step (ASV).

The results of Figure 2 have been obtained by adding increments of Pb²⁺ to individual batches, containing dispersions of goethite (80 mg/L). After equilibration, each batch was analyzed by the various techniques for residual [Pb(II)_{aq}] by measuring the peak current directly in the suspension; *i_p* was converted into [Pb(II)] on the basis of the [Pb(II)] vs. *i_p* calibrations carried out in pure Pb(II) solutions. The shift in the "titration" curve was caused by the binding (specific adsorption) of Pb²⁺ to the goethite surface; at high Pb(II) concentrations the surface becomes saturated, and the Pb(II) concentration in solution is increasing linearly. As shown by the inset of Figure 2, the data can also be plotted as a Langmuir type of adsorption isotherm. The maximum adsorption of Pb²⁺, equivalent to the shift in the titration curve, implies a capacity of ~1.9 × 10⁻⁴ mol/g of goethite [which is in good agreement with a capacity of 2 × 10⁻⁴ mol/g determined by adsorption

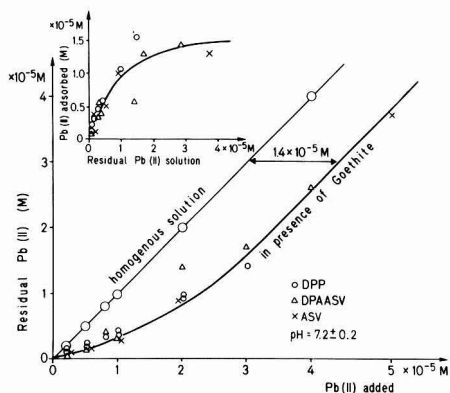


Figure 2. Pb(II) addition to goethite suspension at constant pH (α -FeOOH = 80 mg dm⁻³; pH 7.25 ± 0.05); residual Pb(II) concentrations in solution were measured by different voltammetric techniques. Different voltammetric techniques (DPP, DPASV, and ASV) were used for calibration (peak currents measured without prefiltration were converted into [Pb(II)_{aq}] on the basis of calibration plots obtained for each method in the absence of colloids). The curve obtained in the presence of colloids illustrates that the different measurements using reductive (DPP) as well as cathodic and anodic steps (ASV and DPASV) and characterized by different time scales give internally consistent measurements for [Pb(II)_{aq}].

of H⁺ and F⁻ on the goethite surface for the same type of goethite by Sigg (18)].

Effect of Colloids on Electrochemical Reversibility.

Peak potentials obtained in DPP measurements were not affected by the presence of colloids, although the reproducibility of the measurements of peak currents especially in the presence of MnO₂ was less than in the homogeneous solution at constant pH. (Peak potentials were reproducible within the precision of the instrument in the presence and in the absence of colloids.) Figure 3 gives an example of the signals obtained in the absence and in the presence of the MnO₂ by DPASV. Further evidence for the reversibility is the observation that the width of the peaks is the same in the presence and in the absence of colloids (64 ± 2 mV). Removal of the colloids by filtration did not influence the peak potentials. The influence on the peak heights was not systematic; errors due to filtration were partly responsible for these variations, as filtrated standard solutions also showed some changes in peak heights. The concentrations measured were also not affected by the drop time of Hg in DPP [in agreement with theory $i_p(1\text{ s}) = 0.63i_p(2\text{ s})$] or by changes in the length of the deposition times (ASV and DPASV).

The electrochemical reversibility of the Pb(II) system and the possible influence of colloids were also tested by constructing *pseudopolarograms* (19–21) from values of i_p at different deposition potentials, E_d , obtained in individual experiments.

The interpretation of pseudopolarograms is not straightforward because ASV is not strictly analogous to polarography (20–22). The morphology of the curves obtained reflects, in a qualitative sense, the typical cathodic wave for Pb²⁺ reduction having the appropriate half-wave potential. Although experimental points are more scattered in the presence of colloids, their presence does not result in a shift to more negative potentials.

The colloids, however, may affect the measured potential signals. Whenever measurements are made in a suspension, potentials can be generated, especially in cells containing liquid junctions. These potential shifts can be caused by the suspension effect and/or the sedimentation

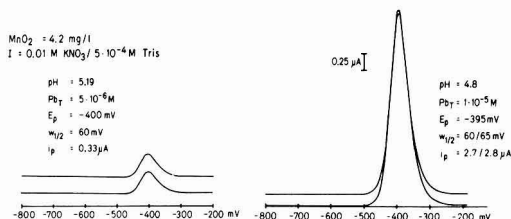
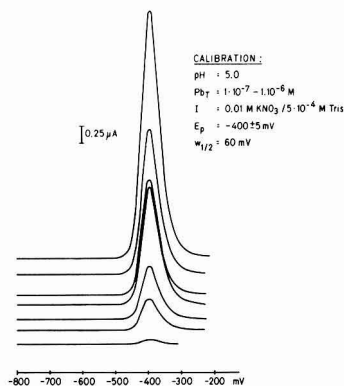


Figure 3. Voltammograms obtained in the absence and in the presence of a MnO₂ suspension. DPASV at the HMDE: deposition time 2 min; deposition potential -800 mV; pulse height 25 mV. The peak potentials (E_p) and the half-widths of the peaks are the same in the absence and presence of the MnO₂. In the presence of MnO₂ the peak heights are reduced due to adsorption of Pb(II) on MnO₂.

potential (23). The latter is induced if charged particles move or settle with respect to the solution; the potential shift caused by the suspension effect is related to the Donnan potential that would be observed between two reference electrodes, one submerged in the suspension and, hypothetically, another one in the same equilibrium solution containing no colloids. Thus, a potential induced on the reference electrode may introduce small deviations in the reading of the potential difference to the Hg electrode. Since concentrations of colloids found in most natural waters will be smaller than those in our test solutions, induced potentials are smaller or negligible, but it is nevertheless important to realize that colloids can affect the potential readings and may falsely give the appearance of an electrochemical kinetic control.

If colloids become attached to the electrode surface, other interferences are possible. Their effect on the capacity of the double layer can be assessed by using ac polarography (an elementary discussion of ac polarography may be found, for example, in ref 24).

Relatively high concentrations of MnO₂ caused a decrease of the current in ac polarography with 90° phase angle shift, between -400 and -1000 mV, in comparison with the supporting electrolyte alone. However, as at 10⁻² M ionic strength the ac current at 90° phase angle is influenced by the resistance of the solution, the intensity of current at 0 °C was also measured, and from these values the two components of admittance and impedance have been determined. After that the capacity of the double layer can be determined from the out-of-phase component of the impedance [$Z'' = 1/(\omega C_d)$]. A systematic decrease of the capacity with the concentration of the colloid was noticed, which may be due to some colloids attached to the electrode surface.

The MnO₂ colloids used were much smaller than the FeOOH and SiO₂ particles; they had a tendency to adhere

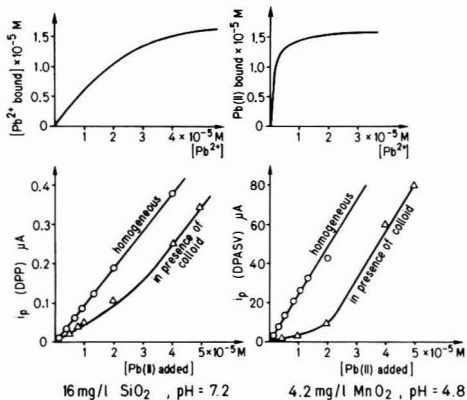


Figure 4. Pb(II) addition to MnO₂ and SiO₂ suspensions. The peak currents obtained in the presence of the suspensions are plotted vs. the Pb(II) concentrations added. The positive deviation from linearity is caused by surface complex formation (specific adsorption) of Pb²⁺ on the hydrous oxides. The shift, usually interpreted as "complex-forming capacity", is related to the metal ion binding capacity of the colloids and corresponds to the *adsorption isotherms*. These isotherms were obtained from the voltammetric results (ASV) measured in the presence of the particles.

and creep on the glass wall. Such forms of adhesion may correspond to the secondary minimum observed in the potential energy curve at relatively large interparticle distances (10).

Sequestering Surfaces vs. Complex Formation in Solution. As is evident from the titration curve with Pb²⁺ in Figure 2, the ligand atoms of the particles (usually O-donor atoms) bind metal ions in a similar way as soluble ligands. A smooth curve was obtained that tends toward a straight line parallel to the calibration plot at Pb values in excess of the surface OH group concentration (Figure 4). Then the metals bound to surfaces are electrochemically not available to the Hg electrode. This is a procedure analogous to the one used for determining "complexing capacity" of natural waters. Obviously, particles are, in addition to nonlabile organic complexes, an important part of the complexing capacity of natural waters, as shown by Allen et al. (25). In ideal cases, the tendency to coordination, i.e., the stability constant, can be estimated from such complexing capacity titrations (9, 20, 26).

The voltammetric measurement of [Me²⁺_{aq}] in the presence of particles and colloids is a particularly expedient method for evaluating the equilibrium partitioning between particles and the solution, determining surface coordination equilibrium constants and measuring the kinetics of adsorption or desorption. Such measurements can be carried out in colloidal dispersions that are very dilute in [Me²⁺_{aq}] (e.g., 10⁻⁵-10⁻¹⁰ M) without introducing the errors that are often encountered in filtration and centrifugation. Examples of adsorption isotherms, derived from the addition of various concentrations of Pb(II) to a colloid suspension, are given in Figure 4 and in the inset of Figure 2 for different colloids. Values for maximum adsorption obtained are in agreement with literature values of the adsorption capacity of the colloids (14, 18).

Other Electrochemical Methods. Also well suited for metal determinations in the presence of particles is the potentiometric stripping analysis (27); similar to ASV, the trace metal is preconcentrated in the amalgam by potentiostatic reduction. The reduced element is then titrated with an oxidant [often Hg(II) ions preadded to the sample]; from the resulting *E* vs. time curve (potentiometric stripping analysis, PSA), the concentration can be

calculated. Sigg and Jagner (28) have shown the general feasibility of using PSA to measure [Pb(II)_{aq}] in the presence of and undisturbed by colloids.

Application to Natural Waters. How can the findings reported here be extended to other metal ions and other colloidal systems and to what extent can the approach be applied to the determination of soluble metal ions in natural waters? To our knowledge, there is no report in the literature on the presence of electrode-kinetically labile associations of metal ions with (surface-bound or adsorbed) particles or colloids. Electrochemical reductions have been observed with electrically conducting colloids (29), but such colloids are not encountered typically in natural water systems. Although the specific adsorption and desorption steps involving metal ions are relatively fast, it is not plausible that metal ions are dissociated and released faster from the colloidal surface than metal ions are dissociated from many soluble nonlabile ligands. Another possibility is that the colloids themselves, if they get into intimate contact with the electrode, could become electrochemically reduced. This is unlikely because of too slow mass transfer of the colloids to the electrode surface and a lack of a true concentration gradient for the metal-carrying particles; our experiments confirm that very fine MnO₂ (~0.1-μm diameter) and FeOOH particles have no effect on the determination of soluble (labile) Pb(II). In view of the investigations by Plavšič et al. (8) and the theoretical interpretation of the data by Ružič (9) of Cu(II) in the presence of Al₂O₃ colloids and ethylenediaminetetraacetic acid (EDTA), it seems justified to imply that most other colloid-bound metals are nonlabile under the electrochemical conditions used. This appears to apply even more so in the presence of organic colloids. Since most higher molecular *soluble* organic metal complexes are nonlabile, it is improbable that metal ions bound to organic colloids are kinetically more dissociable.

Membrane filtration is often an unsatisfactory method for distinguishing between dissolved and particulate trace metals, due to contamination and adsorption problems and to the presence of colloidal particles smaller than filter pores. Further development of the voltammetric methodology exemplified here could be applied to natural waters for certain metals and yield results more interpretable in terms of dissolved concentrations. A possible analytical scheme could then include (a) direct voltammetric determination of labile dissolved metals in a natural water sample immediately after its collection, without pretreatment, and (b) total analysis after acidification and eventually destruction of organic matter, by voltammetry on any other method. Eventually, an *in situ* method where a voltammetric detector, e.g., a Hg-coated rotating electrode, is immersed directly into the natural water could be used.

Additional experiments on real natural water systems, especially also in the presence of soluble organic substances, need to be carried out. But it can already now be inferred that, in complexing capacity titrations of natural waters with Cu(II) or Pb(II), the particle-bound metal ions are not detectable voltammetrically. One must not forget that it is difficult to establish a reference method for natural waters because all existing analytical methods used to distinguish between dissolved and particulate trace metals suffer from many drawbacks.

Conclusions

Voltammetric methods (DPP, ASV, and DPASV) allowed measurement of the soluble Pb(II) concentration in the presence of colloids of α-FeOOH, MnO₂, and SiO₂; the different voltammetric methods gave consistent results and

appeared to be well suited to distinguish between soluble and particulate-bound Pb(II). Voltammetric methods thus offer the possibility of measuring the distribution of metal ions between soluble and particulate phase without separation of the solid phase.

Further work is needed in order to apply this method to the determination of soluble metal ions in natural waters; in this case, the situation is complicated by the presence of strong organic complexes.

Acknowledgments

We are indebted to Jacques Buffle, Božena Čosović, and W. Davison for valuable advice.

Registry No. α -FeOOH, 1310-14-1; MnO₂, 1313-13-9; SiO₂, 7631-86-9; Pb, 7439-92-1; water, 7732-18-5.

Literature Cited

- (1) Martin, J. M.; Meybeck, M. *Mar. Chem.* **1979**, *7*, 173.
- (2) O'Connor, D. J.; Connolly, J. P. *Water Res.* **1980**, *14*, 1517.
- (3) Davison, W. *Limnol. Oceanogr.* **1977**, *22*, 746.
- (4) Batley, G. E. *Mar. Chem.* **1983**, *12*, 107.
- (5) Sunda, W. G.; Hanson, P. J. In "Chemical Modelling in Aqueous Systems"; Jenne, E. A., Ed.; American Chemical Society: Washington, DC, 1979; p 147.
- (6) Turner, D. R.; Whitfield, M. In "Marine Electrochemistry"; Whitfield, M.; Jagner, D., Eds.; Wiley-Interscience: Chichester, 1981; p 67.
- (7) Van den Berg, C. *Mar. Chem.* **1982**, *11*, 323.
- (8) Plavšić, M.; Kozar, S.; Krznarić, D.; Bilinski, H.; Branica, M. *Mar. Chem.* **1980**, *9*, 175.
- (9) Ružić, I. *Anal. Chim. Acta* **1982**, *104*, 99.
- (10) Stumm, W.; Morgan, J. J. "Aquatic Chemistry", 2nd ed.; Wiley-Interscience: New York, 1981; p 625.
- (11) Atkinson, R. J.; Posner, A. M.; Quirk, J. P. *J. Phys. Chem.* **1967**, *71*, 550.
- (12) Morgan, J. J.; Stumm, W. *J. Colloid Sci.* **1964**, *19*, 347.

- (13) De Ford, D. D.; Hume, D. N. *J. Am. Chem. Soc.* **1951**, *73*, 5321.
- (14) Baes, C. F.; Messmer, R. E. "The Hydrolysis of Cations"; Wiley-Interscience: New York, 1976.
- (15) Hohl, H.; Stumm, W. *J. Colloid Interface Sci.* **1976**, *55*, 281.
- (16) Schindler, P. W.; Fürst, B.; Dick, R.; Wolf, P. U. *J. Colloid Interface Sci.* **1976**, *55*, 469.
- (17) Balistieri, L. S.; Murray, J. W. *Geochim. Cosmochim. Acta* **1982**, *46*, 1253.
- (18) Sigg, L. Ph. D. Thesis, Swiss Federal Institute of Technology, Zürich, 1979.
- (19) Branica, M.; Novak, D. M.; Bubic, S. *Croat. Chem. Acta* **1977**, *49*, 539.
- (20) Shuman, M. S.; Cromer, J. L. *Anal. Chem.* **1979**, *51*, 1546.
- (21) Zirino, A.; Kounaves, S. P. *Anal. Chem.* **1977**, *49*, 56.
- (22) Buffle, J. "Electroanalytical Measurement of Trace Metals Complexation in Natural Aquatic Conditions"; IUPAC Commission: 1984; Vol. 5.
- (23) Brezinski, D. P. *Analyst (London)* **1983**, *108* (No. 1285), 425.
- (24) Bard, A. J.; Faulkner, L. R. "Electrochemical Methods"; Wiley: New York, 1980.
- (25) Allen, H. E.; Boonlayangoor, C.; Noll, K. E. *Environ. Int.* **1982**, *7*, 337.
- (26) Chau, Y. K.; Gächter, R.; Lum-Shue-Chan, K. *J. Fish. Res. Board Can.* **1974**, *31*, 1515.
- (27) Jagner, D. *Anal. Chem.* **1978**, *50*, 1924.
- (28) Sigg, L.; Jagner, D., University of Gothenburg, unpublished results, 1980.
- (29) Faul, W.; Kastening, B. *Oberflaeche-Surf.* **1981**, *22* (10), 327.

Received for review November 14, 1983. Revised manuscript received August 3, 1984. Accepted September 26, 1984. This work was supported by EAWAG and a subsidy of Fundação Calouste Gulbenkian. The work is within the context of JNICT Research Contract 315.81.57 of Junta Nacional de Investigação Científica et Tecnológica.

Environmental Neutralization of Polonium-218

Scott D. Goldstein and Phillip K. Hopke*

Institute for Environmental Studies and Department of Civil Engineering, University of Illinois, Urbana, Illinois 61801

■ Previous work has indicated that two mechanisms of neutralization of the singly charged polonium ion exist. Charged Polonium-218 can be neutralized by reacting with oxygen to form a polonium oxide ion with a higher ionization potential than that of the polonium metal and then accepting an electron transferred from a lower ionization potential gas. In this present work, this mechanism has been verified by determining that the polonium oxide has an ionization potential in the range 10.35–10.53 eV. It was also previously reported that ²¹⁸Po can be neutralized, in the absence of oxygen, by the scavenging of electrons by a trace gas such as water or nitrogen dioxide and their diffusion to the polonium ion. To verify this second neutralization mechanism, concentrations of nitrogen dioxide in nitrogen in the range of 50 ppb–1 ppm were examined for their ability to neutralize the polonium ion. Complete neutralization of ²¹⁸Po was observed at nitrogen dioxide concentrations greater than 700 ppb. For concentrations below 700 ppb, the degree of neutralization was found to increase smoothly with the nitrogen dioxide concentration.

Introduction

Interest in the study of radon daughter chemistry, as well as other radioactive isotopes, has escalated in the

recent past for a variety of reasons. A major area of concern is their potential adverse health effects of workers in the uranium industry and on the general public. The release of radon-222, a natural decay product of uranium-238, is a common occurrence in the uranium mining process. Radon is also released from coal-fired power plants, naturally emanates from the soil and building materials, and may be dissolved in groundwater. It may adversely affect the health of the general population. Radon is an inert gas, but its decay products are chemically active. Radon-222, having a half-life of 3.825 days, undergoes four rapid, successive decays to polonium-218 (RaA), lead-214 (RaB), bismuth-214 (RaC), and polonium-214 (RaC'). Each of these radioactive daughters has a relatively short half-life. Polonium-214 then decays to 22.3 year lead-210 (RaD).

It is to these decay products that the adverse health effects are attributed. These radionuclides have a tendency to become attached to or plateout on environmental surfaces. The attachment of the radioactivity to small, respirable particles is an important mechanism for the retention of activity in the air and its transport to people. One of the parameters controlling plateout is the ionic charge of these decay products induced by their decay. To better understand and control airborne radioactivity levels

resulting from the radon decay products, investigation of the neutralization pathways for Po-218 was undertaken in the present study.

Polonium-218 (RaA) has the longest half-life of the available polonium isotopes formed directly from naturally occurring radon isotopes. The ^{218}Po nucleus has a recoil energy of 110 keV and, in dry air, is found to be a singly charged, positive ion 88% of the time (1, 2). The neutral species occurs the remaining 12% of the time. Charged ^{218}Po can be formed by the stripping of orbital electrons by the departing α particle or by the recoil motion (3). Before its subsequent nuclear decay, charged ^{218}Po ions may be neutralized by interactions with the ambient atmosphere.

Study of radon daughter chemistry is difficult because of the short half-life of these products. Also, only relatively low concentrations of precursor radon can be used in such studies. In their study of thoron decay products, Porstendorfer and Mercer (2) indicated the necessity of using relatively low concentrations when studying the neutralization of radon decay products since neutralization can occur rapidly in the higher ion density that is present in high concentrations of radon or thoron. Also, Leong et al. (4) found that, in the presence of a strong radioactive source, the rate of ion formation and radiolysis is sufficient to permit the formation of measurable particles even in clean air. At the low concentrations required to minimize these effects, conventional spectroscopic techniques cannot be used to examine radon decay product chemistry, and an indirect approach is needed. The value of the molecular diffusion was found by Porstendorfer (5) to be a good indicator of the degree of neutralization of the radon daughters. To gain chemical knowledge of the processes controlling neutralization, an understanding of the variation of the diffusion coefficient under controlled gas-phase composition is required.

There has been considerable confusion in the literature over the value of the diffusion coefficient for radon decay products. Dating back to the early 1900s, the molecular diffusion coefficients of radon and thoron decay products have been studied under a variety of conditions. Using an apparatus consisting of a cylindrical vessel with a central electrode, Wellisch (6) measured the diffusion coefficient of ^{218}Po in air and in ethyl ether. By drawing the experimental gas and radon mixture into the vessel, he was able to measure the amount of radioactive deposit on the central electrode using a simple electrometer. He found the diffusion coefficient of ^{218}Po in air to be $0.045\text{ cm}^2/\text{s}$. He also found neutralization of the decay products occurring in ethyl ether (IP = 10.04 eV) in air since there was no longer an increased collection of active deposit on the central charged rod.

Chamberlain and Dyson (7) estimated the diffusion coefficient of ^{218}Po in air to be $0.054\text{ cm}^2/\text{s}$ in reasonable agreement with Wellisch's value. In a study of ^{212}Pb , Porstendorfer (5) found a 33% reduction in the diffusion coefficient of the charged species relative to the neutral one. This reduction in diffusivity was suggested to be due to clustering of molecules around the ion, leading to a larger effective mass of the polonium ion. However, it may be that the decreased mobility is simply due to the increased interaction of the ionic charge with induced dipoles in the gas molecules (8).

Many studies have examined radon and thoron daughters in air at various relative humidities, and contradictory values for the molecular diffusion coefficient have been obtained. Raabe (9) used a technique outlined by Townsend and Dublin (10) to determine the diffusion coefficient

of ^{218}Po in various relative humidities. The radon daughters are drawn from a larger chamber through cylindrical tubes of various lengths, and the fractions of polonium atoms penetrating through the tube are measured. Corrections were made for the production of radon daughters during the passage of the radon gas through the tube. Raabe observed that the diffusion coefficient of ^{218}Po decreased with increasing humidity. He found it to be $0.047\text{ cm}^2/\text{s}$ at a partial pressure of 0.49 kPa of water vapor or a relative humidity of 15% and $0.035\text{ cm}^2/\text{s}$ at a partial pressure of 0.92 kPa of water vapor or a relative humidity of 35%.

Thomas and LeClare (11) used a method similar to that of Raabe's called the two-filter method to measure the diffusion coefficient of ^{218}Po . However, with the two-filter method, a filter is positioned at the inlet port of the diffusion tube assuring that the only source of ^{218}Po in the tube is from the decay of radon within the tube. Because of the long half-life of ^{222}Rn compared to the sampling and counting times used with this method and a constant inlet radon concentration, it can be assumed that the rate of formation of ^{218}Po in the tube is constant. Thomas and LeClare found that ^{218}Po atoms with an average age of less than 15–20 s had diffusion coefficients of $0.085\text{ cm}^2/\text{s}$ for humidities over 20% and $0.053\text{ cm}^2/\text{s}$ under very dry conditions. Raabe reported that the ratio of ^{218}Po atoms to ^{214}Pb atoms was about 2.4 to 1, indicating that the age of his ^{218}Po was of the order of 25 min. This difference in the results of Raabe and of Thomas and LeClare indicates the necessity of controlling the age of the decay products.

Raghunath and Kotrappa (12) used a diffusional sampler to study the effect of relative humidity and ventilation rate in a large carboy on the diffusion coefficients of radon and thoron daughters in air and in argon. They observed that the diffusion coefficient decreased substantially as the residence time of the radionuclide in the diffusion carboy increased. They also determined that the diffusion coefficient decreased with increasing humidity and decreasing ventilation rates. The diffusion coefficient was found to range from $0.005\text{ cm}^2/\text{s}$ for ^{214}Bi in humid air to $0.095\text{ cm}^2/\text{sec}$ for ^{218}Po in dry argon. The highest values were found for an age of 1 min, their minimum residence time.

In their study of the molecular diffusion coefficients of ^{212}Pb (ThB), Porstendorfer and Mercer (2) used a method similar to that of Thomas and LeClare. With their method, decay products that formed within the diffusion tube either diffused to the wall, where they were collected on a thin paper liner, or were collected on a membrane filter at the tube exit. Unlike the two-filter method, Porstendorfer and Mercer designed their system to also collect activity on a central electrode in the diffusion tube so to allow for the analysis of the charged atoms. They found the neutral species to have a value of $0.068\text{ cm}^2/\text{s}$ independent of the relative humidity. The diffusion coefficient of the charged species was not determined conclusively but was estimated as $0.024\text{ cm}^2/\text{s}$ in dry air and was found to increase with increasing humidity. It was found that, at relative humidities between 30% and 90%, the diffusion coefficient increased to $0.068\text{ cm}^2/\text{s}$, the value observed in the neutral case.

Busigin et al. (13) studied the diffusion coefficient of ^{218}Po using a method similar to that used by Raabe. They observed complex transmission curves for the passage of ^{218}Po through a diffusion tube. They also concluded from their humidity studies that the fraction of initially charged ^{218}Po is higher at 0% relative humidity and decreases as

the relative humidity increases. Busigin also suggested that it is likely that charged ^{218}Po in air reacts with oxygen to form polonium dioxide ions, and he estimated that the ionization potential of this species to be approximately 10 eV.

Frey et al. (14) used the Thomas and LeClare two-filter method to study the diffusion coefficient of ^{218}Po in a variety of experimental gases of known composition. They assumed that the formation of polonium dioxide ions occurs when charged ^{218}Po is in an atmosphere with oxygen present. Charged ^{218}Po undergoes about 10^8 collisions/s with gas molecules; therefore, it is quickly thermalized. Thermodynamic data predict that the polonium metal should also react with oxygen to form polonium dioxide ions and release a further 3.7 eV of chemical energy (13). This reaction was also suggested by Raabe (8) and by Billard et al. (15).

Polonium dioxide is expected to have a higher ionization potential than the polonium metal, and it was estimated to be 10 eV (13). Thus, if a polonium oxide ion is mixed with a trace gas of lower ionization potential, neutralization will result. Frey et al. (14) demonstrated this mechanism with nitric oxide (IP = 9.25 eV) in a nitrogen/oxygen atmosphere. They estimated the diffusion coefficient of the neutral species to be $0.079 \text{ cm}^2/\text{s}$. The actual value of the ionization potential of the polonium oxide species was not determined.

Frey et al. (14) also examined humidity effects and found ^{218}Po is completely neutralized at relative humidities between 20% and 80% in nitrogen. Frey et al. (14) found that pure oxygen (IP = 12.10) did not neutralize the polonium oxide ion. Thus, water vapor (IP = 12.36 eV) also cannot directly neutralize the ion via an electron transfer. They suggested that there are two mechanisms for neutralization. In oxygen, the electron transfer mechanism to the polonium oxide ion can take place in the presence of lower ionization potential gases like nitric oxide or nitrogen dioxide. The neutralization by water vapor in nitrogen was suggested to occur by the scavenging of electrons from the recoil path of the polonium by water molecules. The negative water ion then diffuses to the positive polonium ion and yields neutralization. The data of Thomas and LeClare (11) show a smoothly increasing diffusion coefficient with increasing water vapor concentration over the range of 0–20% relative humidity, suggesting that increasing numbers of water molecules in the vicinity of the recoil path leads to an increasing rate of neutralization. It appears from these results that it is necessary to have some scavenger present to prevent the loss of electrons from the region of the recoil path since neutralization is not observed in the absence of a scavenger species. However, calculations indicate that water molecules are not capable of binding an electron (16). Thus, some other process must be providing the electron scavenger. Radiolysis of the water molecules leads to the formation of OH (17), and OH is a good electron acceptor (18). For ^{218}Po in 10 ppm of nitrogen dioxide gas in dry nitrogen, Frey et al. (14) also found complete neutralization. This result was not understood at the time of their publication.

In review, it has been previously proposed that charged ^{218}Po reacts readily in air to form polonium dioxide ions. This ion can then be neutralized by accepting an electron from a lower ionization potential gas. The ionization potential of the polonium dioxide ions has yet to be firmly determined. In their investigation of the diffusion coefficient of ^{218}Po in water vapor in nitrogen and in 10 ppm of nitrogen dioxide gas in dry nitrogen, Frey et al. found

complete neutralization. These results indicate another neutralization mechanism of ^{218}Po may exist. Thus, the purpose of this investigation is 2-fold: first, to determine the ionization potential of the polonium dioxide ion; second, to explore the neutralization of ^{218}Po by nitrogen dioxide gas in dry nitrogen as observed by Frey et al. and to confirm the existence of the scavenging mechanism proposed by Frey et al.

Experimental Section

The two-filter method of Thomas and LeClare (11) was used to study the molecular diffusion coefficient of ^{218}Po in a variety of experimental gases. The basic sampling unit is a $75 \text{ cm} \times 3.17 \text{ cm}$ diameter stainless steel cylinder with a glass fiber filter on each end. The inlet filter removes all of the decay product activity, including free atoms of radon daughters, but permits the radon to pass. In the diffusion tube, radon decays to form ^{218}Po . Since the half-life of radon is long compared to the sampling time used with the two-filter method, a constant formation rate for ^{218}Po can be assumed to occur in the tube. A fraction of the ^{218}Po atoms formed in the tube reaches the exit port glass fiber filter and is captured, while some of the ^{218}Po atoms will diffuse to the inner walls of the tube. The activity collected on the exit filter can be counted and related to the decay product behavior in the diffusion tube. Considering the two-filter method conceptually, it would be expected that at a fixed flow rate, Q , the number of disintegrations, X , observed on the exit port filter would decrease with increasing diffusion coefficient, D , since more of the molecules will diffuse to the walls.

The mass diffusion equation for forced axial flow of a decaying radioisotope through a cylinder has been solved for simple velocity profiles by Tan (19). The basic equation derived relates the inlet radon concentration, C_{Rn} , to the number of counts detected on the exit filter during a fixed period of time following the sampling interval. This equation derived by Tan (19) is given as

$$C_{\text{Rn}} = 0.450x / (ZEVF_f) \quad (1)$$

where x is the number of counts on the exit filter determined in a single count beginning at a fixed time after the sampling interval, Z is a constant that takes into account the growth and decay of the radioactive chain and is given by Thomas and LeClare (11), E is the detector efficiency, V is the volume of the diffusion tube, and F_f is the fraction of ^{218}Po atoms penetrating through the tube. The values of F_f were calculated by Tan (19) and depend on the value of μ given by

$$\mu = \pi DL / Q \quad (2)$$

where D is the diffusion coefficient, L is the length of the tube, and Q is the volumetric flow through the tube. For each experiment, the value of D could be determined by developing a zero-slope, straight-line relationship between the inlet radon concentration and the variable, μ , for the various flow rates used. An iterative computer program had been developed for this purpose (20).

The experimental apparatus is schematically outlined in Figure 1. With the two-filter method, a constant radon concentration is generated by purging a constant flow of $4.0 \text{ cm}^3/\text{s}$ of nitrogen gas through a humidifier and then through the acidic radium chloride solution. The radon-laden flow is dehumidified since it has been observed that water vapor will result in the neutralization of ^{218}Po .

The diffusion coefficient of ^{218}Po was determined in a variety of gases including dry nitrogen, dry oxygen, 3 ppm of butane in dry oxygen, 5 ppm of isobutane in dry oxygen, 1.5 ppm of cyclopentane in dry oxygen and in dry nitrogen,

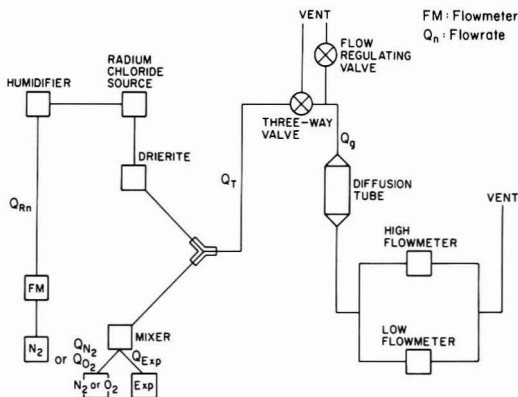


Figure 1. Experimental apparatus.

16 ppb of *n*-pentane in dry nitrogen, 40 ppb of *n*-pentane in dry oxygen, 1.25 ppm of ammonia in dry nitrogen and dry air, 50 ppb of nitric oxide in dry oxygen, and various concentrations of nitrogen dioxide in dry nitrogen and dry oxygen. Except for the organic liquids (pentane and cyclopentane), all the trace species were obtained as trace gases in pure nitrogen from commercial vendors. The volatile organic liquids, pentane and cyclopentane, were used in a diffusion cell system like that described by Miguel and Natusch (21) to permit the careful control of their gaseous concentrations. Sufficient concentrations of the experimental gases need to be present to permit rapid neutralization, but the concentrations must be small enough to prevent the occurrence of substantial radiolysis and molecular clustering that would result in an erroneously low molecular diffusion coefficient.

During a 5-min sampling period, the mixture of radon and experimental gas was directed through the diffusion tube. The radon decay products were collected on a glass fiber filter located at the exit port of the diffusion tube. Samples were taken at various flow rates ranging from 6.83 to 55.0 cm³/s. The sample was then removed from the tube during a 2-min handling period, and it was then counted for 10 min with a flow proportional counter.

At least three trials were made at each flow rate. When a constant inlet radon concentration and experimental gas composition were maintained, the number of disintegrations observed varied only with the flow rate through the diffusion tube since the length of the diffusion tube was held constant. The value of the diffusion coefficient was then calculated as previously described.

Results and Discussion

The neutralization of charged ²¹⁸Po can be inferred from the magnitude of its molecular diffusion coefficient. Low values indicate that the majority of the polonium atoms are charged, while the higher values are attributed to the neutral species. Frey et al. (14) and Raghunath and Koprappa (12) both proposed that a diffusion coefficient of roughly 0.072 cm²/s constitutes complete neutralization. Frey found that the mixture of charged and neutral species has an average value of 0.039 cm²/s in dry nitrogen. The first objective was to measure the ionization potential of polonium dioxide by using the electron-transfer mechanism.

In neutralization via the electron-transfer mechanism, the charged polonium species accepts electrons from trace gases having appropriately low ionization potentials. The ionization potential of the polonium metal is 8.43 eV (22). The ionization potentials of the compounds used in this

Table I. Diffusion Coefficients of ²¹⁸Po in a Variety of Gas Mixtures

experimental gas	IP, eV ^a	diffusion coefficient, cm ² /s
dry N ₂	15.58	0.0340 ± 0.0009
dry oxygen	12.10	0.0310 ± 0.0008
3.0 ppm of <i>n</i> -C ₅ H ₁₀ in dry O ₂	10.63	0.0370 ± 0.0020
5.0 ppm of isobutane in dry O ₂	10.57	0.0375 ± 0.0033
1.5 ppm of C ₆ H ₁₀ in dry N ₂	10.53	0.0355 ± 0.0032
1.5 ppm of C ₆ H ₁₀ in dry O ₂		0.0375 ± 0.0032
16 ppb of <i>n</i> -C ₅ H ₁₂ in dry N ₂	10.35	0.0365 ± 0.0013
40 ppb of <i>n</i> -C ₅ H ₁₂ in dry O ₂		0.0700 ± 0.0015
1.25 ppm of NH ₃ in dry N ₂	10.2	0.0345 ± 0.0009
1.25 ppm of NH ₃ in dry air		0.0725 ± 0.0016
100 ppb of NO ₂ in dry O ₂	9.79	0.0730 ± 0.0053
50 ppb of NO ₂ in dry O ₂		0.0715 ± 0.0048
10 ppm of NO in dry N ₂ ^b	9.2	0.0320 ± 0.0006
8.3 ppm of NO in dry O ₂ ^b		0.0720 ± 0.0006
50 ppb of NO in dry O ₂		0.0670 ± 0.0035

^aRef 22. ^bRef 14.

investigation are given in Table I. No compounds were investigated that could directly neutralize the charged ²¹⁸Po because each has an ionization potential greater than 8.43 eV. As shown in Table I, ²¹⁸Po was not neutralized by any of the trace gases in an atmosphere of dry nitrogen.

The experimental plan was to examine the effects of different compounds with increasing ionization potential until the value of the polonium dioxide ionization potential was bracketed by compounds that do and do not cause neutralization. As shown in Table I, it was found that in an oxygen atmosphere, neutralization occurred in nitric oxide gas (IP = 9.25 eV), in nitrogen dioxide gas (IP = 9.79 eV), in ammonia gas (IP = 10.2 eV), and in pentane gas (IP = 10.35 eV). However, no neutralization was observed in cyclopentane (IP = 10.53 eV) in oxygen or in butane (IP = 10.63 eV) in oxygen. Therefore, the ionization potential of the polonium dioxide species must be in the 10.35–10.53-eV range.

Ethylene (IP = 10.5 eV) and hydrogen sulfide (IP = 10.4 eV) were also investigated in an attempt to further narrow the ionization potential range of polonium dioxide. An intermediate molecular diffusion coefficient of approximately 0.05 cm²/s was found in each case, indicating that additional unknown processes are occurring. It will be difficult to further narrow the ionization potential range since the obvious gases with ionization potentials in the 10.35–10.53-eV range are reactive organic compounds or good electron acceptors.

Since it is thermodynamically impossible, the electron transfer mechanism cannot explain the neutralization of ²¹⁸Po either in 20–80% relative humidity with nitrogen or in 10 ppm of nitrogen dioxide in nitrogen. The alternate mechanism was suggested to be the electron-scavenging mechanism. Depending on the electron affinity of the trace gas, a higher concentration of the electron scavenger would be needed for complete neutralization by this mechanism compared to the electron-transfer mechanism. It would also be expected that there would be an increasing rate of neutralization with increasing concentration of the electron scavenger.

The values of the molecular diffusion coefficient for ²¹⁸Po in nitrogen dioxide gas in dry nitrogen can be found in Table II. Nitrogen dioxide in a dry nitrogen atmosphere cannot directly transfer electrons to the charged ²¹⁸Po. However, neutralization was observed at nitrogen dioxide in dry nitrogen concentrations greater than 700 ppb. No neutralization was observed at a nitrogen dioxide concentration of 50 ppb. In Figure 2, the diffusion coefficient

Table II. Diffusion Coefficients of ^{218}Po in Nitrogen Dioxide/Nitrogen Mixtures

experimental gas	diffusion coefficient, cm^2/s
10 ppm of NO_2 in dry N_2^a	0.0720 ± 0.004
1.0 ppm of NO_2 in dry N_2	0.0705 ± 0.0015
700 ppb of NO_2 in dry N_2	0.0705 ± 0.0029
400 ppb of NO_2 in dry N_2	0.0630 ± 0.0031
200 ppb of NO_2 in dry N_2	0.0500 ± 0.0026
75 ppb of NO_2 in dry N_2	0.0395 ± 0.0027
50 ppb of NO_2 in dry N_2	0.0350 ± 0.0026
pure dry N_2	0.0340 ± 0.0009

^aRef 14.

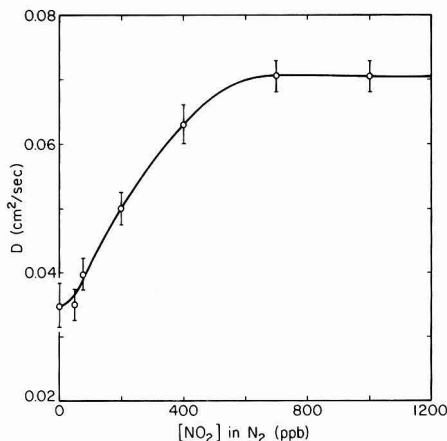


Figure 2. Diffusion coefficient of ^{218}Po as a function of nitrogen dioxide concentration in dry nitrogen.

values of ^{218}Po are plotted vs. their respective nitrogen dioxide concentrations. This characteristic smooth increase in the diffusion coefficient, similar to that observed by Thomas and LeClare (11) for low concentrations of water vapor, indicates that the electron-scavenging mechanism was responsible for the neutralization of ^{218}Po in nitrogen dioxide in dry nitrogen.

To demonstrate that there are two distinct mechanisms, it is possible to examine the ability of the nitrogen dioxide to neutralize ^{218}Po via the electron-transfer mechanism in the presence of oxygen. It is expected that even low concentrations of nitrogen dioxide in dry oxygen could efficiently neutralize charged ^{218}Po by the electron-transfer mechanism. When charged ^{218}Po was mixed with 50 ppb of nitrogen dioxide in dry oxygen (Table I), neutralization was observed in clear contrast to the lack of neutralization observable with 50 ppb of nitrogen dioxide in dry nitrogen.

It is not clear exactly what is occurring in the electron-scavenging process. Nitrogen dioxide is known to be an excellent electron acceptor to form a negative ion. However, some additional process must be occurring in the case of neutralization by water vapor, and further studies are needed to identify how neutralization is obtained.

Conclusion

The magnitude of the diffusion coefficient has been used to determine the degree of neutralization of ^{218}Po . In studying the molecular diffusion coefficient of ^{218}Po , careful attention must be directed toward the age of the decay products being studied and the composition of the atmosphere surrounding the radon decay products. The diffusion coefficient for the neutral ^{218}Po was measured to be $0.072 \text{ cm}^2/\text{s}$, while the value for the initial mixture of

charged and neutral species is $0.037 \text{ cm}^2/\text{s}$. These values are in close agreement to those observed by Frey, by Thomas and LeClare, and by Porstendorfer and Mercer.

Polonium reacts with oxygen to form polonium dioxide ions. In an electron-transfer mechanism, charged ^{218}Po accepts an electron from a gas with a lower ionization potential. The ionization potential of the polonium dioxide was determined to be in the range 10.35–10.53 eV.

The neutralization of ^{218}Po in nitrogen dioxide in dry nitrogen has also been studied to test the electron-scavenging mechanism previously proposed by Frey et al. (14). In dry nitrogen, the fractional neutralization of ^{218}Po was observed to increase with increasing nitrogen dioxide concentrations above 50 ppb and was complete at concentrations greater than 700 ppb. In contrast in oxygen where the electron-transfer mechanism can occur, 50 ppb of nitrogen dioxide yielded complete neutralization, showing that there are two distinct neutralization mechanisms for charged ^{218}Po ions in the atmosphere.

Acknowledgments

We express our appreciation to Keng Leong for his advice throughout the course of the investigation. We also thank Robert Holub of the Denver Research Center, U.S. Bureau of Mines, for useful discussions of the results.

Registry No. $n\text{-C}_4\text{H}_{10}$, 106-97-8; C_5H_{10} , 287-92-3; $n\text{-C}_6\text{H}_{12}$, 109-66-0; NH_3 , 7664-41-7; NO , 10102-43-9; NO_2 , 10102-44-0; O_2 , 7782-44-7; $^{218}\text{PoO}_2$, 93862-54-5; $^{218}\text{Po}^+$, 93862-53-4; ^{218}Po , 15422-74-9; isobutane, 75-28-5.

Literature Cited

- (1) Wellisch, E. M. *Philos. Mag.* **1913**, *26*, 623–635.
- (2) Porstendorfer, J.; Mercer, T. T. *Health Phys.* **1979**, *15*, 191–199.
- (3) Szucs, S.; Delfosse, J. M. *Phys. Rev. Lett.* **1965**, *15*, 163–165.
- (4) Leong, K. H.; Hopke, P. K.; Stukel, J. J.; Wang, H. C. *J. Aerosol. Sci.* **1983**, *14*, 23–27.
- (5) Porstendorfer, J. Z. *Phys.* **1968**, *213*, 384–386.
- (6) Wellisch, E. M. *Philos. Mag.* **1914**, *28*, 417–439.
- (7) Chamberlain, A. C.; Dyson, E. D. *Br. J. Radiol.* **1956**, *No. 29*, 317–334.
- (8) Ridge, D. P. "Kinetics of Ion-Molecule Reactions"; Ausloos, P., Ed.; Plenum Press: New York, NY, 1979; pp 55–68.
- (9) Raabe, O. *Nature (London)* **1963**, *217*, 1143–1145.
- (10) Townsend, J. S.; Dublin, M. A. *Philos. Trans. R. Soc. London*, **1900**, *193*, 129–158.
- (11) Thomas, J. W.; LeClare, P. C. *Health Phys.* **1970**, *18*, 113–122.
- (12) Raghunath, B.; Kotrappa, P. *J. Aerosol. Sci.* **1979**, *10*, 133–138.
- (13) Busign, A.; van der Vooren, A. W.; Babcock, J. C.; Phillips, C. R. *Health Phys.* **1980**, *40*, 333–343.
- (14) Frey, G.; Hopke, P. K.; Stukel, J. J. *Science (Washington, D.C.)* **1981**, *211*, 480–481.
- (15) Billard, F.; Madelaine, G. J.; Chapus, A.; Fontan, J.; Lopez, A. *Radioprotection* **1971**, *6*, 45–54.
- (16) Jordan, K. D.; Wendoloski, J. J. *Chem. Phys.* **1977**, *21*, 145–154.
- (17) Melton, C. E. *J. Phys. Chem.* **1970**, *74*, 582–587.
- (18) Mohnen, V. *J. Geophys. Res.* **1970**, *75*, 1717–1721.
- (19) Tan, C. W. *J. Heat Mass Transfer.* **1969**, *12*, 471–478.
- (20) Beck, H. A. Senior Thesis, University of Illinois, Urbana, IL, 1983.
- (21) Miguel, A. H.; Natusch, D. F. S. *Anal. Chem.* **1975**, *47*, 1705–1707.
- (22) "CRC Handbook of Chemistry and Physics", 50th ed.; CRC Press: Cleveland, OH, 1969; pE-74.

Received for review March 28, 1984. Revised manuscript received June 18, 1984. Accepted September 17, 1984. This work was supported by the U.S. Department of Energy under Contract DE-AC02-83ER60186.

Hydroxyl Radical Oxidation of Isoprene

Chee-Ilang Gu, Carolyn M. Rynard, Dale G. Hendry,[†] and Theodore Mill*

Physical Organic Chemistry Department, SRI International, Menlo Park, California 94025

■ We have used the low total pressure (10 torr) flowing gas system and the high total pressure (760 torr) CH₃ONO-NO photolysis system to study the reaction of OH with isoprene. Both systems give methyl vinyl ketone, methacrolein, and 3-methylfuran as the major products; 1,2-addition is favored over 1,4-addition by a factor of 7. From the proposed mechanism and reaction pathways, we conclude that more than 2 mol of NO will be oxidized to NO₂ for each mole of isoprene oxidized by OH. Direct reaction of isoprene with NO₂ was also measured.

Introduction

Two general types of natural hydrocarbon emissions have been identified (1). The first type is low molecular weight hydrocarbons including ethylene, produced in minor amounts by decaying organic matter. The second and more important type is largely isoprene and a variety of terpenes emitted from living plants (2, 3).

The significance of natural hydrocarbons as a source of ozone in the atmosphere is a subject of recent controversy (3-9). Arnts and Gay (5) have reported smog chamber results using isoprene and a number of terpenes as the reactive hydrocarbons. They find that these hydrocarbons are very reactive, with most of them having half-lives of about 1-2 h; however, little ozone was generated in these experiments. This is believed to be due in part to the rapid reaction of these compounds with ozone, as long as the hydrocarbons are present in significant amounts.

Killus and Whitten (10) recently have established that outdoor smog chamber experiments of isoprene can be computer modeled with available kinetic data and known principles of structure-reactivity for hydrocarbons. Unlike Arnts and Gay (5), they believe that isoprene alone can yield as much as 50% of the peroxy radicals formed in ambient rural air even though isoprene might be only 6% of the ambient hydrocarbon level. With sufficient NO_x all peroxy radicals will produce ozone; however, in typical rural environments NO_x is low, and the efficiency of ozone production by this route is unknown.

Our own analyses (6) of smog chamber experiments leads us to suggest that one must be extremely careful in extrapolating the smog chamber experiments to the environment primarily for three reasons. First, smog chambers favor reaction of organics with ozone because chamber experiments are typically run with higher than normal atmospheric concentrations of reactants and initially generate ozone faster than would be observed in the atmosphere. Consequently, smog chambers tend to over-emphasize ozone chemistry at the expense of the free radical chemistry initiated by OH.

Second, the higher initial concentrations of reactants and higher proportion of O₃ to OH reactions in a smog chamber generate higher concentrations of aerosol precursors and ultimately a larger fraction of aerosol. The limited amount of data on the reaction of terpenes and ozone indicates that aerosols are formed in most cases (11) and that aerosol formation is concentration dependent (12). In smog chamber experiments, aerosol formation removes organic

carbon from further reaction and thereby limits ozone formation. Thus, the hydrocarbons may appear to have less ability to form ozone in the smog chambers than in the environment.

Third, the chamber experiments are short in duration and do not provide an adequate test of the ability of initially formed, less reactive, products to generate ozone over a long period. In the environment, where aerosol loading is smaller and the time scale is longer, organics that form the aerosol particulate may revolatilize to provide hydrocarbons for the free radical reactions that lead to ozone formation.

Thus, information from smog chambers regarding the chemistry of isoprene and terpene is limited, and conclusions may be misleading. We believe that the most effective way to understand the chemistry of these compounds is to study their reactions with OH and O₃ individually rather than in smog chambers where the proportion of OH and O₃ chemistries is uncontrolled.

This paper reports the product analysis of OH reaction with isoprene. We have used two types of experimental systems to study the reaction: (1) a low total pressure (10 torr) flowing gas H-atom-NO₂ system and (2) a high total pressure (760 torr) CH₃ONO-NO photolysis system. We discuss the mechanism of product formation as well as the implication of the significance of the reaction to atmospheric chemistry.

Experimental Procedures

Materials. Isoprene (Aldrich, gold label, 99+%) was distilled through a 75-cm Heli-Pak column before use. Bromoethane (Baker) was distilled through a 12-in. Vigreux column. Nitric oxide was purified by vacuum distillation before use. Nitrogen dioxide was supplied by Liquid Carbonic as a 0.698% custom mixture in helium, and the concentration was determined to be 0.58% by ultraviolet absorption. Oxygen, synthetic air, argon, and hydrogen were obtained from Liquid Carbonic.

Synthesis of Methyl Nitrite (CH₃ONO). CH₃ONO was prepared by following the procedure of Hortung and Eressley (13) and Taylor et al. (14) using NaNO₂ and 60% H₂SO₄ in MeOH. The trapped and dried CH₃ONO was vacuum distilled and stored in the dark. The UV absorption cross section at 339 nm is 3.3×10^{-19} cm² mol⁻¹.

Low-Pressure Flowing Gas System. The flowing gas system used in these studies was described elsewhere (15) and is shown in Figure 1. Total pressures in the system were 10 torr, and the temperature was 22 ± 2 °C. Typically, a Datametrics Barocell Pressure Sensor was used to measure the pressure. Hydrogen was added to the system to 0.6 torr, and mixed with argon to total pressures of 2-3 torr. A scintillonic Model HV15A microwave generator produced a plasma and dissociated molecular hydrogen. The resulting hydrogen atoms reacted with 5-6 torr of 0.5% NO₂ in the He to produce hydroxyl radicals and nitric oxide. The NO₂/He inlet consisted of a linearly adjustable diffuser that allowed variation of the position of hydroxyl radical generation relative to the inlet positions for other gases.

Isoprene vapor was admitted from a gas sample bulb to 0.05 torr and mixed with 1.5 torr of oxygen. After a reaction was complete, the system was cleaned by rinsing

[†]Deceased.

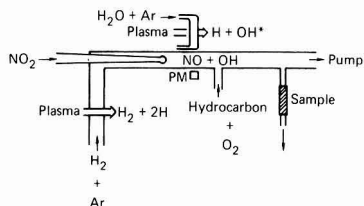


Figure 1. Flowing gas system used in the experiments.

first with acetone, then with alcoholic KOH, and finally with distilled water.

From the position of discharge to the point of addition of NO_2 , the walls of the system were coated with phosphoric acid (Baker, 85%) to minimize recombination of H. At the position of generation of OH radicals, the walls were coated with Halocarbon Series 6-00 wax. Reaction mixtures from the flow system were collected by drawing the gases through absorbent cartridges with a vacuum pump. Cartridges were prepared with 10 cm long by 0.4 cm i.d. Pyrex tubes and packed with glass wool and Poropak Q (50–80 or 100–200 mesh, Waters Associates) or Tenax GC (60–80 mesh, Applied Science Laboratories). The cartridges were spliced into the injector system of the gas chromatograph using a vacuum-tight gas sampling valve. Products were desorbed by rapidly heating the columns, which were flushed with carrier gas.

Products were analyzed with a Varian 3700 gas chromatograph using a flame ionization detector, and the data were collected by a Varian CDS 111 integrator. Reaction products and authentic samples were separated on a 15 ft by $1/8$ in. o.d. Poropak QS (80–100 mesh) column and on a 18 ft by $1/8$ in. o.d. 10% OV-17 column. Gas chromatography/mass spectrometry (GC/MS) was performed with similar columns on a LKB 9000 GC/MS using 70-V ionization.

Atmospheric Pressure $\text{CH}_3\text{ONO-NO-Isoprene Photolysis Experiments.}$ Experiments at 760 torr were performed by irradiating mixtures of NO , CH_3ONO , and isoprene (16) in 760 torr of synthetic air in 5-L Pyrex reaction bulbs. Irradiations were performed with an Oriel Model 6153 2500-W mercury lamp adjusted to give light intensity equivalent to a rate of photolysis of NO_2 of 0.32 min^{-1} in N_2 at the bulb center.

Reaction mixtures were analyzed by gas chromatography using bromoethane as internal standard under the same conditions as used for low-pressure experiments.

Before photolysis, the reaction bulb was rinsed first with HF solution and then with distilled water, and finally baked at 80°C under 0.01 torr. A Bendix ozone monitor, 8002, and a Bendix $\text{NO-NO}_2\text{-NO}_x$ analyzer, 8101-B, were used to monitor NO_x and O_3 during the reaction.

Dark Reaction between Isoprene and NO_2 . Known amounts of purified NO_2 and isoprene were injected into a 10-cm-path UV cell at an initial concentration of $(1.5\text{--}2.6) \times 10^{16}$ and $(0.4\text{--}1.2) \times 10^{16}$ molecule/ cm^3 of NO_2 and isoprene, respectively. Synthetic air was used to pressurize the cell to 1 atm, and loss of NO_2 was followed spectrally at 400 nm.

Results and Discussion

In most experiments, the amounts of isoprene collected from the flow system were a few percent less than the amounts expected from the concentration of the starting material, even in the absence of reaction. This may be a consequence of unequal rates of evaporation of isoprene relative to bromoethane from the starting mixture or of reaction of isoprene with NO_2 .

Table I. Products of the Reaction of Isoprene with OH at 10.0 torr and 15–20% Conversion (Averaged Results of 20 Reactions)^a

compound	% of total reaction products ^b
methyl vinyl ketone (MVK)	48.9 ± 5.1
methacrolein (MA)	41.7 ± 5.0
3-methylfuran (MF)	7.6 ± 6.3
formaldehyde (FA)	1.8 ± 1.8

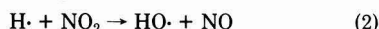
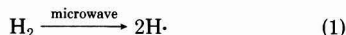
^a See Experimental Procedures for detailed flow system conditions; [isoprene] = 0.05 torr, $[\text{H}_2] = 0.03\text{--}0.3$ torr, $[\text{NO}_2/\text{HO}] = 4.5\text{--}6.2$ torr, and $[\text{O}_2] = 4.50$ torr. All reactions were conducted at ambient temperature, $22 \pm 2^\circ\text{C}$. ^b Percent based on moles of total products.

Table II. Rate Constants for Relevant OH Reactions

compound	SAR $k_{\text{OH}} \times 10^{12}$, ^a $\text{cm}^3 \text{ mol}^{-1} \text{ s}^{-1}$	environmental lifetime, ^b $t_{1/2}(\text{OH}), \text{h}^{-1}$
bromoethane	0.39	258
isoprene	96 ^c	1.1
MVK	17.9 ^d	3.7
MA	31.4 ^d	1.5
MF	130	0.77

^a SAR (structure activity relationship) (17). ^b $[\text{OH}] = 1.9 \times 10^6 \text{ mol cm}^{-3}$ in the atmosphere (18). ^c Measured value (16). ^d Measured value (19).

The flow and static systems used in this study provide two different ways to study HO–isoprene oxidation. The flow system produces HO by the sequence



If properly designed, the system can provide a clean source of OH and NO with few secondary reactions, but only at relatively low pressure and under slow-flow conditions where product analyses are difficult. The static system uses continuous photolysis of CH_3ONO in 1 atm. of air to form HO, but secondary reactions and aerosol formation complicate interpretation of the results and typically make product mass balances difficult to attain. We believe that use of both systems described here adds considerable confidence to our analyses and conclusions.

A number of flow experiments were performed under the following conditions: [isoprene] = 0.05 torr, $[\text{H}_2] = 0.04$ torr, $[\text{NO}_2/\text{He}] = 4.5$ torr, and discharge power 30 W; [Ar] was varied to keep the total pressure constant at 10.0 torr. Oxygen was varied from 0.5 to 2.5 torr. Over this small range, there was no observable change in the product yields or branching ratios.

Products of the reaction of hydroxyl radical, OH, with isoprene at 10.0 torr are listed in Table I. Products were identified by GC/MS and by comparing the observed spectra with published mass spectra.

The addition of extra NO (to 0.03 torr) did not change the products or their relative amounts appreciably. Although OH and NO are initially produced in equal amounts, reaction 2, OH is lost in wall and disproportionation reactions; thus, NO is already in excess, and added NO is not expected to have an effect. Table II summarizes estimated rate constants for reaction of OH with bromoethane, isoprene, and the observed oxidation products, on the basis of the Hendry structure–activity relationship (SAR) method (17). Bromoethane is only $1/300$ as reactive as isoprene toward OH radical and thus should be unreactive and a suitable standard for use in these flow experiments.

Table III. Products of the Reaction of Isoprene with OH in Air at 30–40% Conversion and 760 torr^a

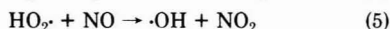
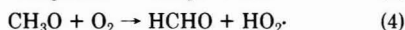
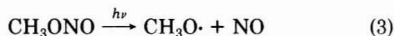
[isoprene], ppm	gas	% products ^b				% yield ^c
		MVK	MA	MF		
4.3	Air	32	54	14		44 ± 12
4.0	O ₂	34	50	16		40
100	Air	43	46	11		52 ± 10

^a See Experimental Procedures for detailed photolysis system; the initial concentration ratio for NO:CH₃ONO:isoprene:bromoethane was kept at 1:2.5:1:0.2. All reactions were conducted at ambient temperature, 22 ± 3 °C. ^b Percent based on moles of total products. ^c Yield based on moles of product per mole of isoprene consumed.

The material balance for the reaction of OH with isoprene was determined by measuring the amount of unreacted isoprene and collected products relative to the internal standard, bromoethane.

Material balances obtained for isoprene oxidations in molar units indicate that methyl vinyl ketone (MVK), methacrolein (MA), and 3-methylfuran (MF) account for 72 ± 10% (molar) of the total isoprene reacted. The mass balance is not as high as reported for oxidation of toluene or xylene (93%) (15). However, the primary products from isoprene are both very reactive toward OH (see Table II) and are subject to wall interactions and aerosol formation.

HO Oxidation of Isoprene at 760 torr. The experimental technique of CH₃ONO–NO–isoprene photolysis was based on the modified procedure of Atkinson et al. (16). OH radical was generated by irradiating CH₃ONO at ≥290 nm in the presence of air.



NO was added to the system to minimize the concentration of ozone and its reaction with isoprene.



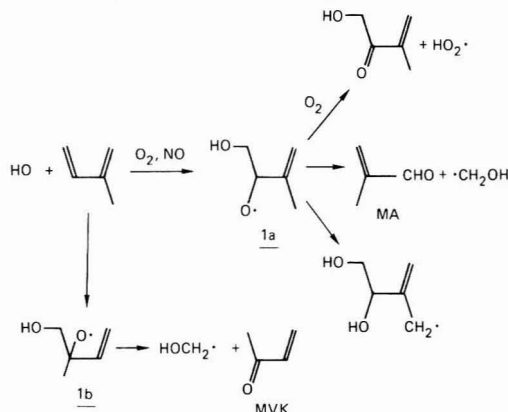
A series of experiments was performed at 23 ± 3 °C in which isoprene concentrations were varied from 4.3 to 100 ppm. Irradiation times were carefully controlled so that O₃ formation was below that detectable by an O₃ monitor (<0.01 ppm) and the [NO₂]/[NO] ratio did not exceed 2 (16). The latter criterion cannot be determined in our high concentration ([isoprene] = 100 ppm) experiments because the NO analyzer was overscaled by the presence of high levels of CH₃ONO (20).

Products of the reaction of OH with isoprene at 760 torr total pressure at two isoprene concentrations are listed in Table III. In agreement with the low pressure studies, MVK, MA, and MF are the major products observed.

The low average mole percent yield (48%) of products may be caused by aerosol formation in static experiments, although we have no direct evidence for this. Small amounts of CO₂, HCHO, CH₃OH, CH₃CHO, HCOOCH₃, CH₃COCH₃, CH₃CH₂OH, and CH₃COOH were detected by GC/MS. These products probably come from further reactions of the primary products and from CH₃ONO photolysis.

In view of the fast reaction between butadiene and NO₂ (21) and the fact that NO₂ is generated quickly in the system (16), the dark reaction between isoprene and NO₂ also was studied. The reaction is first order with respect

Scheme I. 1,2-Addition of HO to Isoprene



to both components and gives a second-order rate constant of 98 + 8 M⁻¹ s⁻¹. This rate is about 5 times slower than that reported by Gryaznou and Rozolvskii (22) where a higher concentration of starting materials and indirect analytical methods were used. By use of our rate constant, the maximum NO₂ detected in each experiment, and the short photolysis time (<4 min), we calculate that the interference of the NO₂ dark reaction with isoprene is less than 1.5% and can be neglected.

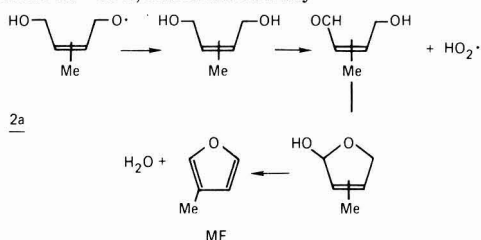
Oxidation Pathways and Mechanisms. The oxidation of isoprene by HO radical occurs both by addition and by abstraction; however, SAR analysis indicates that well over 95% of HO radicals react with isoprene by addition at carbons 1 and 4 to give 1,2- and 2,3-allylic radicals (17). The discussion will be facilitated by considering separately the products of reaction of the two kinds of radicals (shown in Scheme I).

1,2-Addition leads to two allylic radicals and, on reaction with O₂ and NO, two possible alkoxy radicals, 1a and 1b. The rate of a depends on the competition between three possible modes of reaction: cleavage, oxidation, and isomerization. 1b can only cleave to give methyl vinyl ketone (MVK) (Scheme I).

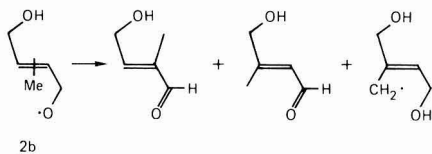
Thus, the proportion of MVK is probably a good measure of 1,2-addition to form the tertiary alkoxy radical, but MA gives only the minimum proportion of 1,2-addition to give the secondary alkoxy radical. Kinetic analysis of these RO reactions following the methodology of Baldwin et al. (23) indicates that all three processes are of comparable importance for 1a. However, our product analyses and balances both in the low- and the high-pressure experiments suggest that both isomeric alkoxy radicals mostly cleave. The material balances do leave room for intervention by both isomerization and oxidation of 1a to give a dihydroxyaldehyde or hydroxy ketone. Both products are polar, nonvolatile, and difficult to identify by our analysis and probably contribute to some extent to the deficit in material balance.

In this connection the work of Niki et al. (24) on oxidation of ethylene is instructive. They found that of the β-hydroxyalkoxy radical HOCH₂CH₂O· cleaves about 80% of the time and oxidizes only about 20% of the time in air, contrary to expectations of >95% oxidation based on kinetic analysis. Pitts et al. (25) reported that the 2-butoxy radical cleaves only half as fast as it oxidized to 2-butanone, whereas kinetic analysis led to the expectation of 10 times more cleavage than oxidation (22). For the oxy radical (1a), we would expect a faster rate of oxidation to methacrolein than for the 2-butoxy radical owing to formation

Scheme II. Cis 1,4-Addition Pathway



Scheme III. Trans 1,4-Addition Pathway



of the conjugated vinyl ketone. This process requires participation by oxygen, but since we have found no effect of oxygen pressure on the proportion of methacrolein (Table III), we conclude that oxidation is much too slow to compete with cleavage. We note that the suggested mechanism for 1,2-addition (Scheme I) to isoprene also predicts the formation of CH_2OH ; this radical should oxidize rapidly to HCHO and $\text{HO}_2\cdot$ with O_2 .

We now consider 1,4-addition and note that both *cis*- and *trans*-1,4-hydroxyalkoxy radicals can be formed. As shown in Scheme II, the *cis*-1,4-hydroxyalkoxy radicals will probably undergo rapid 1,6-H atom isomerization (21) followed by oxidation, cyclization, and loss of water to yield the observed product, 3-methylfuran.

cis-1,4-Hydroxyalkoxy radicals can also form 3-methylfuran by oxidation to the hydroxyaldehyde followed by ring closure and loss of water. Competition between isomerization and oxidation would appear to favor the former by a factor of 10^4 . However, as we saw from the example of Niki et al., the kinetic parameters for these reactions are not well characterized, and without additional experiments we cannot unequivocally assign the origin of the methylfuran to one or another of these reactions of the alkoxy radical.

The *trans*-1,4-hydroxyalkoxy radicals, on the other hand, can undergo oxidation, cleavage, or isomerization and lead to various multifunctional products as suggested in Scheme III. Again, these products are difficult to find and probably account for ~6 mol % of consumed isoprene, equivalent to the yield of 3-methylfuran (Tables II and III). Isomerization of either 1,4-alkoxy radical, via 1,6-H atom transfer, can form trifunctional oxy radicals, which in turn can also oxidize or cleave.

Thus, although the material balance leaves considerably room for uncertainty, our analysis shows that, for OH reaction with isoprene, 1,2-addition is favored over 1,4-addition by a factor of 7. This result is only qualitatively in accord with the liquid-phase oxidation of isoprene by peroxy radicals, where 55% of the products result from 1,2-addition (26).

Also of interest is whether the proportion of 1,2- vs. 1,4-addition is under kinetic or thermodynamic control. Allylic carbon radicals are rapidly but reversibly scavenged by oxygen; therefore, the effect of NO, which irreversibly captures peroxy radicals, on the proportion of 1,2- vs. 1,4-addition could be significant. However, our experiments show that NO has no significant effect on the proportion of carbonyls and furan, suggesting that in our

experiments, the reaction is under thermodynamic control.

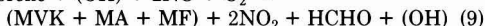
To summarize then, 1,2-addition is the dominant pathway in the oxidation of isoprene, but the more complex polar products, probably formed by 1,4-addition, prevent more quantitative assessment of their relative importance. In 1,2-addition, cleavage of the alkoxy radical appears to be the dominant process for producing the methacrolein, but some fraction of the alkoxy radical probably oxidizes to the as yet undetected hydroxy vinyl ketone.

Conclusions

The reported rate constant for O_3 reaction with isoprene (5) is $1.28 \times 10^{-17} \text{ cm}^3 \text{ mol}^{-1} \text{ s}^{-1}$. Because average concentrations for O_3 in the boundary layer are believed to be about $1.0 \times 10^{12} \text{ molecule/cm}^3$ (14), the environmental lifetime for reaction of isoprene with O_3 is around 15 h. By comparison of this lifetime with that of the isoprene reaction with OH (Table II), it is evident that the latter reaction will predominate in the environment even if the ozone concentration increases substantially without a corresponding increase in the OH concentration.

From the measured emission rate of isoprene in the Houston area and the assumption that 2 mol of ozone can form by oxidation of 1 mol of isoprene, Zimmerman estimated that approximately $4.92 \times 10^{11} \text{ molecule/cm}^3$ (20 ppb) of ozone can be generated in 1 day from oxidation of isoprene (2). However, this estimate assumes high NO_x concentrations which in most rural areas is not true (8).

Our product analysis as given in eq 9 shows that for each isoprene + (OH) + 2NO + $\text{O}_2 \rightarrow$



mole of isoprene oxidized to MA, MVK, and MF, 2 mol of NO_2 will be produced if enough NO is present, a result consistent with Zimmerman's estimate but again subject to availability of NO_x .

From the UV absorption spectra of MVK and MA (6), the lower limit lifetimes for these two compounds in sunlight can be calculated by using the known solar irradiance values (18) in the wavelength region where these compounds absorb. The calculations give environmental photolysis half-lives of 0.96 h for MA and of 1.12 h for MVK. Thus, photolysis probably will compete with OH for the oxidation of MVK and MA in the atmosphere. There is no significant UV absorption for MF beyond 290 nm. The dominant loss mechanism for MF in the atmosphere has to be reaction with OH. Because more NO will be oxidized when primary products MA, MVK, and MF are oxidized by OH, more than 2 mol of NO_2 could be formed from OH oxidation of isoprene. 3-Methylfuran (MF) was reported by Saunders et al. (27) as a major organic component in a sample of rain water collected in Washington, DC, in 1974 following a sustained photo-oxidant alert. Although the GC/MS analytical technique used by Saunders et al. could not distinguish 3-MF from 2-MF formed possibly by oxidation of aromatics (28), our results suggest a distinctive route to its formation in the atmosphere, from isoprene. The fate of 3-MF as well as those of MVK and MA deserves further investigation.

Finally, Winer et al. (29) recently suggested that NO_3 could be the dominant oxidant for isoprene as well as some monoterpenes especially at night. The effect of this reaction on the rural environment, especially for O_3 formation, should be explored.

Acknowledgments

We thank Richard A. Kenley for helpful discussions and David Thomas for identification of many products by GC/MS.

Registry No. MVK, 78-94-4; MA, 78-85-3; MF, 930-27-8; FA, 50-00-0; OH, 3352-57-6; NO₂, 10102-44-0; NO, 10102-43-9; isoprene, 78-79-5.

Literature Cited

(1) Research Triangle Institute "Nature Emissions of Gaseous Organic Compounds and Oxides of Nitrogen in Ohio and Surrounding States". 1974, Final Report, Contract No. 68-02-1096.
 (2) Zimmerman, P. R. *Spec. Conf. Ozone/Oxid.: Interact. Total Environ., [Proc.]*, 2nd 1979, 257.
 (3) Rasmussen, R. A. *J. Air Pollut. Control Assoc.* 1972, 22, 537.
 (4) Graedel, T. E. *Rev. Geophys. Space Phys.* 1979, 17, 937.
 (5) Arnsts, R. R.; Gay, B. W., Jr. "Photochemistry of Some Naturally Emitted Hydrocarbons". 1979, EPA Final Report EPA-600/3-79-081.
 (6) Gu, C.-L.; Mill, T., SRI, Menlo Park, CA, unpublished data, 1984.
 (7) Budiansky, S. *Environ. Sci. Technol.* 1980, 14, 901.
 (8) Dimitriadis, B. *J. Air. Pollut. Control Assoc.* 1981, 31, 229.
 (9) Altshuller, A. P. *Atmos. Environ.* 1983, 17, 2131.
 (10) Killus, J. P.; Whitten, G. Z. *Environ. Sci. Technol.* 1984, 18, 142.
 (11) Schuetzle, D.; Rasmussen, R. A. *J. Air Pollut. Control Assoc.* 1978, 28, 236.
 (12) Lipeles, M.; Landis, D. A.; Hidy, G. M. *Adv. Environ. Sci. Technol.* 1977, 8, 69.
 (13) Blatt, A. H., Ed. "Organic Synthesis"; Wiley: New York, 1943; Collect. Vol. 2, p 112.
 (14) Taylor, W. D.; Allston, T. D.; Moscato, M. J.; Fazekas, G. B.; Kozlowski, R.; Takacs, G. A. *Int. J. Chem. Kinet.* 1980, 12, 231.
 (15) Kenley, R. A.; Davenport, J. E.; Hendry, D. G. *J. Phys. Chem.* 1981, 85, 2746.

(16) Atkinson, R.; Aschmann, S. M.; Winer, A. M.; Pitts, J. N., Jr. *Int. J. Chem. Kinet.* 1982, 14, 507.
 (17) Davenport, J. E.; Gu, C.-L.; Hendry, D. G.; Mill, T., unpublished results, 1984.
 (18) Hendry, D. G. "Laboratory Protocols for Evaluating the Fate of Organic Chemicals in Air and Water". 1982, EPA Final Report EPA 600/3-82-022.
 (19) Kleindienst, T. E.; Harris, W. G.; Pitts, J. N., Jr. *Environ. Sci. Technol.* 1982, 16, 844.
 (20) Winer, A. M.; Peters, J. W.; Smith, J. P.; Pitts, J. N., Jr. *Environ. Sci. Technol.* 1974, 8, 1118.
 (21) Cadle, R. D.; Littman, F. F.; Eastman, R. H.; Silverstein, R. M. Stanford Research Institute, Menlo Park, CA, 1952, Interim Technical Report Project C-466.
 (22) Gryaznov, V. A.; Rozlovskii, A. I. *Dokl. Akad. Nauk. SSSR* 1975, 220, 1099; Chem. Abs. '82, 138856h.
 (23) Baldwin, A. C.; Barker, J. R.; Golden, D. M.; Hendry, D. G. *J. Phys. Chem.* 1977, 82, 2483.
 (24) Niki, H.; Maker, P. D.; Savage, C. M.; Bretenach, L. P. *Chem. Phys. Lett.* 1981, 80, 499.
 (25) Pitts, J. N., Jr.; Darnall, K. R.; Winer, A. M.; McAfee, J. M. "Mechanisms of Photochemical Reactions in Urban Air". 1977, Chamber Studies, EPA Final Report EPA 600/3-77-0146.
 (26) Hendry, D. G.; Gould, C. W.; Mayo, F. R., SRI, Menlo Park, CA, unpublished data, 1972.
 (27) Saunders, R. A.; Griffith, J. R.; Saalfeld, F. E. *Biomed. Mass Spectrom.* 1974, 1, 192.
 (28) We thank the referee for pointing this out.
 (29) Winer, A. M.; Atkinson, R.; Pitts, J. N., Jr. *Science (Washington, D.C.)* 1984, 224, 156.

Received for review April 2, 1984. Accepted August 27, 1984. This research was supported by the Environmental Protection Agency, Washington, DC, under Grant R8081-10010.

Fluorescence Characteristics of Polychlorinated Biphenyl Isomers in Cyclodextrin Media

Robert A. Femla, Stephen Scypinski, and L. J. Cline Love*

Department of Chemistry, Seton Hall University, South Orange, New Jersey 07079

■ The fluorescence characteristics of several polychlorinated biphenyl (PCB) isomers in α - and β -cyclodextrin (CD) are discussed and contrasted. The steric hindrance of PCBs imposed by the positions of the chlorine atoms on the rings determines the overall stability of the resulting inclusion complexes with cyclodextrin which is reflected in the fluorescence intensities. Less substituted homologues include into the CD cavity equally well in both cyclodextrins, but very heavily substituted molecules show drastic differences between their fluorescence intensities in the α - and β -cyclodextrin solutions. This behavior can be employed as a method for spectral fractionation of PCB isomers. Separation is demonstrated here for two variably substituted molecules, and the photophysical limitations of this approach are discussed.

Introduction

Polychlorinated biphenyls (PCBs) are a source of global concern because of their widespread contamination of the earth's environment. The vast literature on this subject attests to the prevalence of this environmental problem (1-3). Much attention has been focused on developing suitable analyses for these toxic materials (1), with one of the most widely used methods for separation and detection

of PCBs in the environment being capillary gas chromatography with electron capture detection (4, 5). Even this powerful technique suffers from problems of nonlinear response to the highly substituted PCB homologues and interferences due to chlorinated pesticides such as DDT which often necessitates time-consuming preparatory separations and cleanup steps (6). For these reasons, among others, the search for a universal PCB analysis scheme continues.

In the past, luminescence spectroscopy has not been regarded as an attractive method for PCB determinations. The characteristic broad, featureless fluorescence bands are generally of low intensity, due partially to the internal heavy atom effect that actually makes PCBs more amenable to determination by phosphorescence. Weinberger has shown that micelle-stabilized room temperature phosphorescence (MS-RTP) is effective as a screening tool for the identification of the presence of PCBs, as a family, in Aroclor blends and microscope oils (7). The results of Donkerbroek and co-workers indicate that sensitized/quenched phosphorescence of biacetyl is useful as a detection mode in the liquid chromatographic separation of PCBs (8). However, identification of individual isomers in complex mixtures of PCBs by luminescence remains a challenging problem.

This paper reports the fluorescence excitation and emission characteristics of several PCB isomers in α - and β -cyclodextrin (CD). Cyclodextrins are macrocyclic glucose polymers containing a hollow interior which can include various molecules if certain stringent size criteria are met, resulting in a "host-guest" interaction or complex (9). This unique feature of CDs allows a microscopic *in situ* separation to take place based on the molecular dimensions of the guest and provides a scheme by which a mixture of substitutional isomers can be fractionated (10). PCBs are ideal candidates for such a study as substitution of chlorine atoms onto the biphenyl rings results in increased bulkiness of the molecule which is dependent not only on the number of chlorine atoms attached to the ring(s) but also on the specific positions of substitution. This leads to selective complexation based on whether or not the particular PCB isomer can physically enter the CD cavity. Enhanced fluorescence is observed from those which can be included.

We have evaluated the feasibility of employing CD's in this capacity to separate various PCB isomers in aqueous solution with subsequent identification by fluorescence emission spectroscopy. The fluorescence characteristics of the individual PCBs in α - and β -CD are discussed in terms of their photophysical properties that adversely affect their positive identification by this technique. Possible separation schemes for two or more PCBs based on their substitution sites are demonstrated.

Experimental Section

Reagents. Ultrahigh purity polychlorinated biphenyl isomers were obtained from Ultra Scientific (Hope, NJ) and were used as received. Biphenyl (MCB) was once recrystallized from ethanol. The α - and β -cyclodextrins (Aldrich) were once recrystallized from boiling water. Spectroscopic grade methanol and *p*-dioxane (Fisher Scientific, Springfield, NJ) were used without further purification. The water was deionized and triply distilled.

Apparatus. Fluorescence spectra were obtained on a Fluorolog 2+2 (SPEX Industries, Metuchen, NJ) with a 450-W continuous xenon light source, double excitation and emission monochromators (spectral band-pass 1.8 nm/mm), and a Peltier-cooled Hammamatsu R928 photomultiplier tube (PMT). Data acquisition and instrumental parameters were controlled by using a SPEX Datamate microcomputer interfaced to the spectrofluorometer. A Houston Instruments digital *x,y* plotter was used to obtain hard copies of spectra. All fluorescence spectra are uncorrected for lamp intensity and PMT response.

Procedure. All cuvettes and glassware were soaked in nitric acid and were then rinsed with methanol and distilled water prior to use. Stock solutions of all analytes were prepared in methanol. Inclusion complexes were prepared by adding an aliquot of the appropriate stock solution to a 10-mL volumetric flask and allowing the solvent to evaporate gently on a hot plate. The solution was then diluted to the mark with a 0.01 M aqueous cyclodextrin solution and sonicated for 5 min. Polarity references in *p*-dioxane were prepared in a similar manner. Cuvettes were filled with the samples, stoppered, and transferred to the fluorometer. Degaeration of the sample did not have any observable effect on the fluorescence intensity and was not included in the experimental procedure.

Results and Discussion

Steric and Size Effects. Selectivity via complexation with cyclodextrin based on steric nonbonding interactions

Table I. Fluorescence Characteristics of PCBs in α -Cyclodextrin

compound	maxima, nm		intensity, counts	C^a	deg of inclusion into cavity
	λ_{ex}	λ_{em}			
biphenyl (6.5×10^{-5} M)	268	322	2.94E5	1.40	total
4-chloro- (8.5×10^{-5} M)	272	330	3.04E4	0.344	partial
4,4'-dichloro- (2.9×10^{-5} M)	280	345	6.76E4	0.0935	none
3-chloro- (6.8×10^{-5} M)	265	325	2.91E4	0.519	partial
3,3'-dichloro- (5.6×10^{-5} M)	282	346	6.07E4	0.121	partial
2,3,5,6-tetrachloro- (5.5×10^{-5} M)	300	360	8.93E3	1.03	partial
3,3',4,4'-tetrachloro- (1.1×10^{-5} M)	300	378	8.73E3	0.15	none
2,2',3,3',4,4',5,5'- octachloro- (1.2×10^{-5} M)	300	349	1.02E4	0.423	none

^a Calculated by using eq 1 in the text. Concentrations of PCBs were the same in α -CD, β -CD, and *p*-dioxane.

Table II. Fluorescence Characteristics of PCBs in β -Cyclodextrin

compound	maxima, nm		intensity, counts	C^a	deg of inclusion into cavity
	λ_{ex}	λ_{em}			
biphenyl	268	324	3.01E5	1.43	total
4-chloro-	272	332	2.06E5	2.33	total
4,4'-dichloro-	392	364	6.41E5	0.887	total
3-chloro-	278	330	7.00E4	1.25	partial
3,3'-dichloro-	287	346	7.20E3	0.143	partial
2,3,5,6-tetrachloro-	300	360	1.09E4	1.27	partial
3,3',4,4'-tetrachloro-	300	387	6.98E4	1.24	partial
2,2',3,3',4,4',5,5'- octachloro-	300	347	1.23E4	0.510	none

^a Calculated by using eq 1 in the text. Concentrations of PCBs were the same as in Table I.

is not novel (10). Differences in the binding abilities between host and guest molecules give cyclodextrins an inherent natural ability to distinguish between isomeric series of molecules based on guest size. Although a battery of analytical techniques has been employed in the study of this phenomena, the use of luminescence spectroscopy as a probe for discriminating between included and free molecules has not been used to any great extent.

Cyclodextrin-induced room temperature phosphorescence (CD-RTP) is a unique method of distinguishing between parent molecules and derivatives based on the nature of their emission spectra (11). It was thought that the PCBs would be good examples of the selectivity offered by CD-RTP, but they were found to be weak phosphors in cyclodextrin medium, a phenomenon that is characteristic of the biphenyl class of compounds (12). However, fluorescence spectroscopy was found to be an excellent qualitative measure of the complexing ability of PCBs with cyclodextrins. Although fluorescence is not as selective as phosphorescence, the intensity of the singlet-state emission of the PCBs reflects the ability of α - and β -cyclodextrin to form stable inclusion complexes of varying strengths with this series of molecules.

Tables I-III first the pertinent spectral data for the PCB isomers examined in this study in α -cyclodextrin, β -cyclodextrin, and *p*-dioxane, respectively. The latter solvent was chosen as a reference as its polarity is comparable to

Table III. Fluorescence Characteristics of PCBs in *p*-Dioxane^a

compound	maxima, nm		intensity, counts
	λ_{ex}	λ_{em}	
biphenyl	275	325	2.01E5
4-chloro-	287	331	8.83E4
4,4'-dichloro-	301	360	7.23E5
3-chloro-	292	355	5.61E4
3,3'-dichloro-	283	331	5.02E4
2,3,5,6-tetrachloro-	305	353	8.59E3
3,3',4,4'-tetrachloro-	288	340	5.63E4
2,2',3,3',4,4',5,5'-octachloro-	340	392	2.41E4

^a Concentrations of PCBs were the same as in Table I.

that of the cyclodextrin interior (13). Also given in Tables I and II are the qualitative degree of inclusion of the PCBs expected with α - and β -CD. Estimation of the length and width of the molecules based on bond angles and lengths and van der Waals radii allows these predictions to be made.

In probing the effect of the CD cavity size on the fluorescence intensity, a control solvent is necessary because the fluorescence of PCBs not only is dependent on the degree of complexation but also is governed by photophysical characteristics (to be discussed later). In order to separate these two effects, it is necessary to examine the fluorescence of these molecules in a medium that will completely dissolve them irrespective of their molecular dimensions. *p*-Dioxane was selected to be used as the solvent in which the PCB fluorescence characteristics would be determined solely by photophysical reasons, not by molecular size matching. A useful method for comparing fluorescence emission in the three media and obtaining a numerical value proportional to the degree of inclusion involves applying a correction factor to the spectra in α -CD and β -CD that will take into account the photophysical effects on intensity which are manifested in *p*-dioxane. This was done by using the following equation:

$$C = \frac{\text{fluorescence peak intensity in cyclodextrin}}{\text{fluorescence peak intensity in } p\text{-dioxane}} \quad (1)$$

where the concentration of PCB was identical in the two media. The numerical *C* value is a relative measure of the degree of complexation of a particular PCB isomer in α - or β -cyclodextrin. A value of *C* greater than unity signifies an enhancement in the intensity due to the inclusion process. A number less than unity denotes destabilization of the excited singlet state, i.e., fluorescence in a more polar medium in which PCBs are weak emitters. The values of *C* for the PCBs reported in this study are listed in Tables I and II. In *p*-dioxane the major factor contributing to the fluorescence intensity is the number and position of the chlorine substituents. However, in α - and β -CD, the ability of the lumiphor to fit into the CD cavity, as dictated by its molecular dimensions, will also have a profound effect on the observed intensity. Note from the Tables that the unsubstituted parent biphenyl molecule exhibits comparable fluorescence in both the α -CD ($C_\alpha = 1.40$) and β -CD ($C_\beta = 1.43$), most probably due to an unhindered axial entrance into both cavities. A fluorescence intensity enhancement in cyclodextrin medium compared to *p*-dioxane is observed, which may be attributed to isolation of the excited-state lumiphor from quenchers in the bulk solution and to motional restraints. The 4.5-Å diameter of the α -CD cavity is sufficiently small to include totally only the

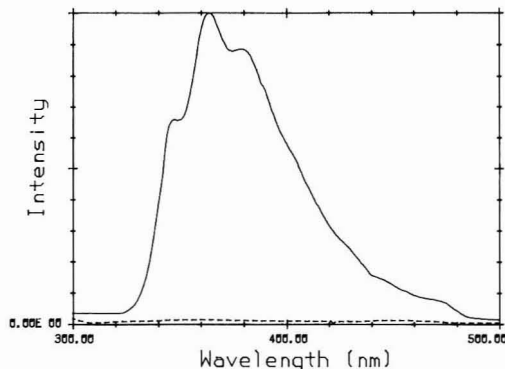


Figure 1. Fluorescence emission spectrum of a mixture of 2.9×10^{-5} M 4,4'-dichlorobiphenyl and 1.5×10^{-4} M 3,3'-dichlorobiphenyl in 0.01 M β -cyclodextrin (solid line). Fluorescence emission spectrum of 1.5×10^{-5} M 3,3'-dichlorobiphenyl (dashed line). Excitation wavelength, 301 (4,4') and 283 nm (3,3'); slits, 14.4 nm for EX and 3.6 nm for EM; scan rate, 1 nm/s.

biphenyl molecule. Substitution of only a single chlorine in a para ring position, as in the case of 4-chlorobiphenyl, results in almost an order or magnitude of difference between its fluorescence intensity in α -CD ($C_\alpha = 0.344$) and that in β -CD ($C_\beta = 2.33$). In the case of the 4-chloro isomer, there is an unsubstituted ring available to enter the α -CD cavity, but the bulky chlorine probably prevents total inclusion so that some protrusion into the bulk solution occurs and also depopulates the excited-singlet state via enhanced spin-orbit coupling. Previous work has shown that the maximum fluorescence intensity is obtained from a molecule which is totally encapsulated inside the cyclodextrin cavity and that the more a molecule is subjected to the aqueous medium surrounding the cyclodextrin, the lower the fluorescence intensity (11, 12).

Although 4-chlorobiphenyl is used here as a representative example of the differences in singlet-state emission characteristics of the α - and β -CD complexes, the tables show that a general trend exists for the other PCB isomers. As the biphenyl rings become more heavily chlorinated, only the β -CD whose interior dimensions measure approximately 7.0 Å can include these bulky molecules. In the case of 2,2',3,3',4,4',5,5,6-octachlorobiphenyl, whose molecular dimensions forbid entrance into even the β -CD, a close similarity exists between the fluorescence intensity for the two media, reflecting the fact that the fluorophor is in the bulk aqueous phase outside the cyclodextrin cavity.

As can be seen from these data, the size of the cyclodextrin, coupled with the position(s) of the chlorine atom(s) on the rings, can drastically affect the fluorescence intensity of a particular PCB isomer. Although the fluorescence intensity is not strong, differences of an order of magnitude exist between the two cyclodextrin media, as PCBs do not fluoresce strongly in the α -CD polar bulk aqueous phase where the heavily substituted PCBs would reside. This behavior can be used to develop spectral identification patterns for specific isomers by using the relative intensity as a "fingerprint" of the molecules. For example, 4,4'-dichlorobiphenyl exhibits intense fluorescence emission in aqueous β -CD solution as substitution at the para position does not hinder complexation into the β -CD cavity. In the case of 3,3'-dichlorobiphenyl, the fluorescence intensity is approximately 2 orders of magnitude less than that of the 4,4'-biphenyl species as shown in Figure 1. This difference, which is not as dramatic in

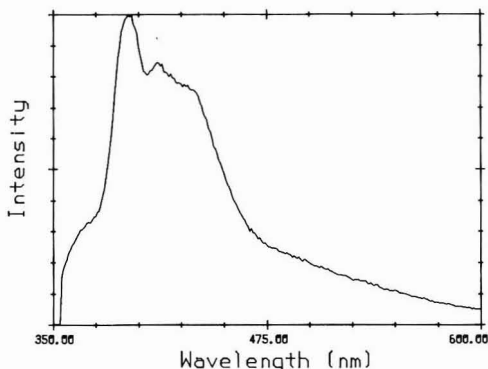


Figure 2. Fluorescence emission spectrum of 1.1×10^{-5} M 2,2',3,3',4,4',5,5'-octachlorobiphenyl in *p*-dioxane. Excitation wavelength, 340 nm; slits, 14.4 nm for EX and 3.6 nm for EM; scan rate, 1 nm/s.

p-dioxane, may be attributed to the steric hindrances of the bulky chlorines in the meta positions on the rings which would inhibit axial inclusion into the β -CD cavity. In addition, substitution at the meta sites perturbs the excited-state transition moment which results in decreased fluorescence intensity (14). This second factor will be dealt with in the next section.

Photophysical Effects. In addition to the effect on fluorescence emission intensity of complexing ability based on size, there are also photophysical properties indigenous to PCB isomers that can drastically affect the ability of these compounds to luminesce. The PCBs are weak fluorescence emitters due, in part, to the heavy atom substituents that can increase nonradiative depopulation of the excited-singlet state via internal conversion and intersystem crossing to the triplet state. In addition, nonradiative deactivation from the triplet state is the dominant process of depopulation in aerated solutions. Extensive studies on the parent biphenyl have revealed differences in the geometries of the molecule in its ground and excited states which can partially account for drastic changes in the fluorescence profiles of the PCB isomers (15). It is postulated that the biphenyl moiety becomes more planar upon excitation via rotation of the aromatic rings about the shared σ bond (16). This is supported by examination of the absorption spectra of the PCBs which are broad and featureless, while their fluorescence spectra are significantly narrower and well-resolved vibrationally. This suggests an increase in rigidity of the PCB isomers upon excitation, most probably through increased planarity, producing well-resolved bands. Indeed, many resonance structures can be written for biphenyl that have considerable double bond character in the interannular bond joining the two aromatic rings. On the basis of these arguments and on Berlman's classification of molecules based on geometry changes (17), biphenyl would be a class three molecule, a class which is nonplanar in the S_0 state and planar in the S_1 state.

The dynamic interactions of the biphenyl moiety upon excitation can be influenced by the number and position of the chlorine substituents. For example, ortho substitution of chlorine atoms can result in some steric hindrance to rotation of the two aromatic rings relative to one another. For the isomer 2,2'-dichlorobiphenyl, if it is a class two molecule (nonplanar in both S_0 and S_1), one would predict its fluorescence intensity to be weak and broad in shape. Indeed, Figure 2 shows such a spectrum for a sterically hindered PCB isomer. The spectrum is broad,

which is likely due to emission from many slightly different PCB geometrical isomers, each having a slightly different S_1 energy. Isomers other than ortho substituted also exhibited varying degrees of steric hindrance affecting their fluorescence spectra. For example, Figure 1 contains the spectra of 4,4'- and 3,3'-dichlorobiphenyl. The meta-substituted species has a spectrum that is broader and less intense and is blue shifted 23 nm relative to the para-substituted species spectrum. It has been proposed on the basis of symmetry arguments that the primary excited-state emissions of biphenyl and its chloro derivatives are long axis polarized (18, 19). Our experimental results show that the most intense fluorescence emission is obtained for PCB isomers with substituents symmetrically placed on the long axis of the molecule.

The selective complexation of PCB isomers with α - and β -cyclodextrins appears to be governed not only by size constraints on the inclusion process but also on the photophysical parameters imposed by the specific chlorine substitutions which can be approximately factored out by using the *C* values. Thus, spectral interpretation of PCB fluorescence emissions must be done with care. It is possible that other sterically hindered lumiphors such as drugs and their metabolites may be amenable to this combined separation/detection method. Many molecules of this type have larger fluorescence quantum yields so that the resulting spectra would be more useful analytically.

Registry No. α -CD, 10016-20-3; β -CD, 7585-39-9; biphenyl, 92-52-4; 4-chlorobiphenyl, 2051-62-9; 4,4'-dichlorobiphenyl, 2050-68-2; 3-chlorobiphenyl, 2051-61-8; 3,3'-dichlorobiphenyl, 2050-67-1; 2,3,5,6-tetrachlorobiphenyl, 33284-54-7; 3,3',4,4'-tetrachlorobiphenyl, 32598-13-3; 2,2',3,3',4,4',5,5'-octachlorobiphenyl, 35694-08-7.

Literature Cited

- (1) Cairns, T.; Siegmund, E. G. *Anal. Chem.* **1981**, *53*, 1183A.
- (2) Koeman, J. H.; Debrauw, M. S.; DeVos, R. H. *Nature (London)* **1969**, *221*, 1126.
- (3) Hutzinger, O.; Safe, S.; Zitko, V. "The Chemistry of PCBs"; CRC Press: Boca Raton, FL, 1974; p 14.
- (4) Sissons, D.; Welti, D. *J. Chromatogr.* **1971**, *60*, 15.
- (5) Teichman, J.; Bevenue, A.; Hylin, J. W. *J. Chromatogr.* **1978**, *53*, 761.
- (6) Amour, J.; Burke, J. J. *Assoc. Off. Anal. Chem.* **1970**, *53*, 761.
- (7) Weinberger, R. Ph.D. Dissertation, Seton Hall University, South Orange, NJ, 1983.
- (8) Donkerbroek, J. J.; Van Eikema Hommes, N. J. R.; Gooijer, C.; Velthorst, N. H.; Frei, R. W. *J. Chromatogr.* **1983**, *255*, 581.
- (9) Szejtli, J. "Cyclodextrins and Their Inclusion Complexes"; Akademiai Kiado: Budapest, Hungary, 1982; Chapter 3.
- (10) Hinze, W. L. *Sep. Purif. Methods* **1981**, *10* (12), 159.
- (11) Scypinski, S.; Cline Love, L. J. *Anal. Chem.* **1984**, *56*, 322.
- (12) Scypinski, S.; Cline Love, L. J. *Anal. Chem.* **1984**, *56*, 331.
- (13) VanEtten, R. L.; Sebastian, J. F.; Clowes, G. A.; Bender, M. L. *J. Am. Chem. Soc.* **1967**, *89*, 3242.
- (14) Parker, C. A. "Photoluminescence of Solutions"; Elsevier: Amsterdam, The Netherlands, 1968; pp 428-429.
- (15) Wagner, P. J.; Scheve, B. J. *J. Am. Chem. Soc.* **1977**, *99*, 2888.
- (16) Skrilec, M.; Cline Love, L. J., submitted for publication in *J. Phys. Chem.*
- (17) Berlman, I. B. *J. Phys. Chem.* **1970**, *74*, 3085.
- (18) Momicchioli, F.; Bruni, M.; Baraldi, I. *J. Phys. Chem.* **1972**, *76*, 3983.
- (19) Berlman, I. B. *J. Chem. Phys.* **1970**, *52*, 5616.

Received for review April 5, 1984. Accepted September 20, 1984. This work was supported in part by National Science Foundation Grant CHE-8216878 and the U. S. Environmental Protection Agency. Although the research described in this article has been

funded, in part, by the U.S. Environmental Protection Agency under Assistance Agreement R 809474 to L.J.C.L., it has not been subjected to the Agency's required peer and administrative review and, therefore, does not necessarily reflect the view of

the Agency, and no official endorsement can be inferred. This work was presented in part at the 1984 Pittsburgh Conference on Analytical Chemistry Spectroscopy, Atlantic City, NJ; March 8, 1984, Abstract No. 776.

Kinetics and Atmospheric Implications of the Gas-Phase Reactions of NO₃ Radicals with a Series of Monoterpenes and Related Organics at 294 ± 2 K

Roger Atkinson,* Sara M. Aschmann, Arthur M. Winer, and James N. Pitts, Jr.

Statewide Air Pollution Research Center, University of California, Riverside, California 92521

Rate constants for the gas-phase reactions of the NO₃ radical, an important constituent of both clean and polluted nighttime atmospheres, with the naturally emitted monoterpenes myrcene, *cis*- and *trans*-ocimene, α- and γ-terpinene, and α-phellandrene have been determined in air at atmospheric pressure and 294 ± 2 K. On the basis of our recently determined equilibrium constant of 3.4 × 10⁻¹¹ cm³ molecule⁻¹ at 298 K for the reactions NO₂ + NO₃ ⇌ N₂O₅, the following rate constants (in units of 10⁻¹¹ cm³ molecule⁻¹ s⁻¹) were obtained: myrcene, 1.1 ± 0.3; *cis*- and *trans*-ocimene, 2.4 ± 0.6; α-terpinene, 19.4 ± 4.7; γ-terpinene, 3.1 ± 0.7; α-phellandrene, 9.1 ± 2.3. By use of these and our previous data for α- and β-pinene, Δ³-carene, and *d*-limonene, NO₃ radical rate constants are estimated for a further series of monoterpenes and related organics. It is shown that nighttime NO₃ radical reactions for these and other monoterpenes can be dominant loss processes for these naturally emitted organics and/or for NO₃ radicals. In addition, rate constants for the reaction of NO₂ with myrcene and *cis*- and *trans*-ocimene were also determined.

Introduction

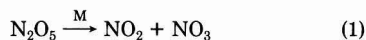
Long path-length differential optical absorption spectroscopic techniques have recently been used to identify and measure the gaseous NO₃ radical in nighttime atmospheres at a variety of locations in the United States and Europe (1-6). Observed NO₃ radical concentrations have ranged from the detection limit of the technique [~1 part per trillion (ppt)] up to ~350 ppt at a downwind receptor site in the Los Angeles Air Basin (1). These ambient atmospheric data, together with the available kinetic data for NO₃ radical reactions with a wide variety of organics (7-14), show that the reaction of the NO₃ radical with the more reactive alkenes (including the monoterpenes), the hydroxy-substituted aromatics, and dimethyl sulfide can be an important nighttime loss process for NO₃ radicals and/or these organics (8-12, 14, 15). Indeed, our recent data for the kinetics of the reactions of the NO₃ radical with the monoterpenes α- and β-pinene, Δ³-carene, and *d*-limonene (12) showed that these reactions would lead to large reductions in either the nighttime NO₃ radical or the monoterpene concentrations, depending on the relative magnitude of the NO₃ radical formation rates and the monoterpene emission rates (15).

In this work, we have extended our previous measurements of the rate constants for the reaction of NO₃ radicals with α- and β-pinene, Δ³-carene, and *d*-limonene (12) to a further series of monoterpenes. These kinetic measurements, together with our previous data (12), permit predictions to be made of NO₃ radical rate constants for other monoterpenes and related organics for which experimental data are not available. These experimental or estimated NO₃ radical rate constants, together with the

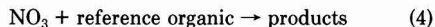
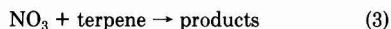
corresponding OH radical and O₃ reaction rate constants, then allow the dominant atmospheric fates and lifetimes of these organics to be assessed under both ambient daytime and nighttime conditions.

Experimental Section

The experimental technique used for the determination of NO₃ radical reaction rate constants was a relative rate method which has been described in detail previously (10-14). This technique is based upon monitoring the relative decay rates of a series of organics, including at least one organic whose NO₃ radical reaction rate constant is reliably known, in the presence of NO₃ radicals. NO₃ radicals were generated by the thermal decomposition of N₂O₅ (16) in air:



Providing that the monoterpenes and the reference organics reacted negligibly with N₂O₅ and NO₂ (see below), then under the experimental conditions employed the sole chemical loss process for these organics was reaction with NO₃ radicals:



Additionally, small amounts of dilution occurred from the incremental additions of N₂O₅ to the reactant mixture. During these experiments, the dilution factor *D_t* was typically 0.0025 (i.e., ~0.25%) per N₂O₅ addition. Thus (10-14)

$$\ln \left(\frac{[\text{terpene}]_{t_0}}{[\text{terpene}]_t} \right) - D_t = \frac{k_3}{k_4} \left[\ln \left(\frac{[\text{reference organic}]_{t_0}}{[\text{reference organic}]_t} \right) - D_t \right] \quad (I)$$

where [terpene]_{t₀} and [reference organic]_{t₀} are the concentrations of the monoterpene and the reference organic, respectively, at time *t₀*, [terpene]_{*t*} and [reference organic]_{*t*} are the corresponding concentrations at time *t*, *D_t* is the dilution factor at time *t*, and *k₃* and *k₄* are the rate constants for reactions 3 and 4, respectively. Hence, plots of [ln ([terpene]_{t₀}/[terpene]_{*t*}) - *D_t*] vs. [ln ([reference organic]_{t₀}/[reference organic]_{*t*}) - *D_t*] should yield a straight line of slope *k₃/k₄* and a zero intercept.

With this experimental technique, the initial concentrations of the terpenes and the reference organics were ~1 ppm (1 ppm = 2.41 × 10¹³ molecule cm⁻³ at 294 K and 735 torr total pressure), and up to five incremental

amounts of N_2O_5 [$\sim(0.1-1)$ ppm per addition] were added to the chamber during an experiment. In order to extend the reaction times beyond the mixing time, 1–4 ppm of NO_2 was also included in the reaction mixtures in order to derive the equilibrium between NO_3 radicals, NO_2 and N_2O_5 toward N_2O_5 . The reference organics 2-methyl-2-butene and 2,3-dimethyl-2-butene and the monoterpenes were quantitatively monitored during these experiments by gas chromatography with flame ionization detection (GC-FID), using the columns described previously (12).

All rate constant determinations were carried out at 294 ± 2 K and atmospheric pressure (~ 735 torr) in a ~ 4000 -L all-Teflon chamber, with the diluent gas being dry purified matrix air (17). As described previously (10–14), N_2O_5 was prepared by the method of Schott and Davidson (18). Known pressures of N_2O_5 (as measured by an MKS Baratron capacitance monometer) in 1.0-L Pyrex bulbs were flushed into the chamber for 5 min by a 2 L min^{-1} flow of N_2 ($\geq 99.995\%$ purity level), with simultaneous rapid stirring by a fan rated at 300 L s^{-1} . Initial NO_2 concentrations were measured by using a chemiluminescence $NO-NO_2$ analyzer.

Since several conjugated dialkenes react with NO_2 at nonnegligible rates (19), the rate constants for the reactions of myrcene and *cis*- and *trans*-ocimene with NO_2 were also determined as an integral part of this study [those for α - and γ -terpinene and α -phellandrene had been measured previously (19)]. In these experiments, ~ 4 ppm of NO_2 was added to a myrcene or *cis*- and *trans*-ocimene (~ 1 ppm)-air mixture, and the monoterpene concentrations were monitored by GC-FID as a function of time after the addition of NO_2 , as described in detail previously (19).

α -Phellandrene was obtained from Fluka Chemical Corp. with a stated purity level of $>99\%$. Myrcene (technical grade) and α - and γ -terpinene (with stated purity levels of $\geq 98\%$) were obtained from the Aldrich Chemical Co. Ocimene (a *cis*- and *trans*-mixture) was generously donated by Givaudan. While the *cis*- and *trans*-ocimene isomers were resolved by GC-FID, the *cis* or *trans* identities of these isomers were not established. However, since these isomers reacted at essentially identical rates (within $<10\%$) with both NO_2 and NO_3 radicals (see below), this was not necessary.

Results

Reactions with NO_2 . We have previously determined rate constants, or upper limits thereof, for the reaction of NO_2 with α - and γ -terpinene and α -phellandrene at room temperature (19). In this study, rate constants at 294 ± 2 K were similarly determined for myrcene and *cis*- and *trans*-ocimene. As observed previously, the monoterpene decays in the presence of excess concentrations of NO_2 were exponential, and rate constants at 294 ± 2 K and ~ 735 torr of air were determined to be


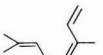
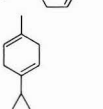
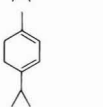
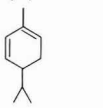
$$k(NO_2 + \text{myrcene}) = (2.6 \pm 0.2) \times 10^{-19} \text{ cm}^3 \text{ molecule}^{-1} \text{ s}^{-1}$$

$$k(NO_2 + \text{cis- or trans-ocimene}) = (8.9 \pm 0.4) \times 10^{-19} \text{ cm}^3 \text{ molecule}^{-1} \text{ s}^{-1}$$

with the rate constants for the *cis*- and *trans*-ocimene isomers being identical within $\sim 7\%$. The above indicated errors are two least-squares standard deviations.

NO_3 Radical Reactions. By use of our relative rate constant technique, rate constants for the reactions of NO_3 radicals with the monoterpenes α - and γ -terpinene, α -phellandrene, myrcene, and *cis*- and *trans*-ocimene (the structures of these are shown in Tables I and II) were determined, with 2-methyl-2-butene and 2,3-dimethyl-2-

Table I. Rate Constant Ratios k_3/k_4 for the Reaction of NO_3 Radicals with a Series of Monoterpenes at 294 ± 2 K

monoterpene	structure	k_3/k_4^a relative to	
		2-methyl-2-butene	2,3-dimethyl-2-butene
myrcene		1.13 \pm 0.02	
<i>cis</i> - and <i>trans</i> -ocimene		2.38 \pm 0.06 ^b	
γ -terpinene		3.14 \pm 0.05	
α -terpinene			3.18 \pm 0.13
α -phellandrene			1.49 \pm 0.11

^a Indicated errors are two least-squares standard deviations of the slopes of the plots shown in Figures 1 and 2. ^b The rate constant ratios for the *cis*- and *trans*-isomers were essentially identical (within 8%). The value given is that obtained by least-squares analyses of the data for both isomers.

butene being used as the reference organics.


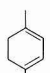



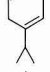
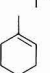
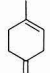
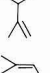
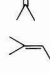
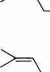
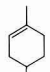
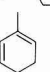

Previous work in these laboratories using in situ Fourier transform infrared absorption spectroscopy (10) has shown that, in $N_2O_5-NO_2$ -alkene-air mixtures, the NO_2 concentration remains essentially constant throughout these reactions. Hence, the present and previous (19) room temperature rate constants for the reaction of NO_2 with the conjugated dialkenes and the initial NO_2 concentrations in these $N_2O_5-NO_2$ -alkene-air experiments were used to correct the observed amounts of consumption of the monoterpenes for loss due to reaction with NO_2 . Relative to the total observed monoterpene decay rates this correction was negligible ($<1\%$) for γ -terpinene and amounted to $\sim 18\%$ for myrcene, $\sim 12\%$ for *cis*- and *trans*-ocimene, $\sim 10-47\%$ for α -terpinene, and $\sim 29-46\%$ for α -phellandrene. For α -terpinene and α -phellandrene, in order to minimize the loss of these monoterpenes due to reaction with NO_2 , the reaction times were kept as short as possible (≤ 28 min), and the added NO_2 concentrations were ≤ 2 ppm. For example, for α -phellandrene, the fastest reacting of these monoterpenes with NO_2 (19), the decay rate due to reaction with NO_2 was $\sim 0.02 \text{ min}^{-1}$ (i.e., $2\% \text{ min}^{-1}$) at an NO_2 concentration of 1 ppm. Thus, these corrections for reaction with NO_2 ranged from being completely negligible for γ -terpinene to being a significant fraction of the observed monoterpene disappearance rates for α -phellandrene and α -terpinene.

Plots of eq I (with the data for the conjugated monoterpenes corrected for reaction with NO_2 as described above) are shown in Figures 1 and 2, and the rate constant ratios k_3/k_4 obtained by least-squares analyses of these data are given in Table I. In all cases the intercepts of these plots as derived by least-squares analyses were within two standard deviations of zero.

Discussion

NO_2 Reactions. The reactions of NO_2 with the monoalkenes and nonconjugated dialkenes have been shown to be negligibly slow [with rate constants $\leq 5 \times 10^{-20} \text{ cm}^3$

Table II. Experimental and Estimated Rate Constants k_3 for the Reactions of NO_3 Radicals with a Series of Monoterpenes and Related Organics at Room Temperature and Atmospheric Pressure

organic	structure	$10^{12}k_3, \text{cm}^3 \text{ molecule}^{-1} \text{ s}^{-1}$		organic	structure	$10^{12}k_3, \text{cm}^3 \text{ molecule}^{-1} \text{ s}^{-1}$	
		observed ^a	estimated ^b			observed ^a	estimated ^b
α -pinene		6.1 ± 1.5 (12)	10	α -terpinene		194 ± 47 (this work)	
β -pinene		2.5 ± 0.6 (12)	0.4	γ -terpinene		31 ± 7 (this work)	20
Δ^3 -carene		10.6 ± 2.4 (12)	10	terpinolene			71
<i>d</i> -limonene		13.9 ± 3.1 (12)	10	dihydromyrcene			10
myrcene		11 ± 3 (this work)	11	carvomenthene			10
<i>cis</i> -ocimene		24 ± 6 (this work)	23	<i>p</i> -cymene			~ 0.0003
α -phellandrene		91 ± 23 (this work)					
β -phellandrene			~ 13				

^a Based upon a equilibrium constant for the reactions $\text{NO}_2 + \text{NO}_3 \rightleftharpoons \text{N}_2\text{O}_5$ of $2.4 \times 10^{-27} (T/300)^{0.32} e^{11080/T} \text{cm}^3 \text{ molecule}^{-1}$ (16, 21). The indicated errors are two least-squares standard deviations. Rate constants k_4 of $(9.9 \pm 2.2) \times 10^{-12} \text{cm}^3 \text{ molecule}^{-1} \text{ s}^{-1}$ for 2-methyl-2-butene and $(6.1 \pm 1.5) \times 10^{-11} \text{cm}^3 \text{ molecule}^{-1} \text{ s}^{-1}$ for 2,3-dimethyl-2-butene (12, 16, 21) were used to derive these rate constants k_3 . ^b These estimates are based upon the rate constants for the alkenes with the same degree of configuration and substitution around the double bond(s); i.e. (in units of $10^{-12} \text{cm}^3 \text{ molecule}^{-1} \text{ s}^{-1}$) $\text{CH}_2=\text{CH}-$ (propene), 0.008; $\text{CH}_2=\text{C}-$ (isobutene), 0.4; $\text{CH}_2=\text{C}(\text{CH}=\text{CH}_2)-$ (isoprene), 0.6; $(\text{CH}_3)_2\text{C}=\text{CH}-$ (2-methyl-2-butene), 10; $-\text{CH}=\text{C}(\text{CH}=\text{CH}_2)-$ and $\text{CH}_2=\text{C}(\text{CH}=\text{CH}-)$ (approximated by 1,3-cyclohexadiene), 13; $(\text{CH}_3)_2\text{C}=\text{C}-$ (2,3-dimethyl-2-butene), 61 [where the model alkene for a given structural unit (see text) is given in parentheses]. The estimate for *p*-cymene is based upon our experimental data for *p*-xylene (14). Since α -phellandrene and α -terpinene are the first conjugated dialkenes with three and four substituents, respectively, to be studied, their reaction rate constants cannot be a priori estimated.

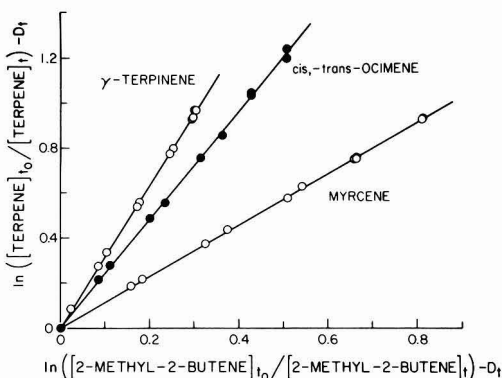


Figure 1. Plot of eq 1 for myrcene, *cis*- and *trans*-ocimene, and γ -terpinene, with 2-methyl-2-butene as the reference organic.

$\text{molecule}^{-1} \text{ s}^{-1}$ at room temperature (19, 20)]. Furthermore, for the acyclic conjugated dialkenes the rate constants increase with the degree of substitution around the $\text{C}=\text{C}=\text{C}$ structure (19,20). Thus, the rate constants for myrcene and *cis*- and *trans*-ocimene are expected, a priori, to be similar to those for isoprene and 2,3-dimethyl-1,3-

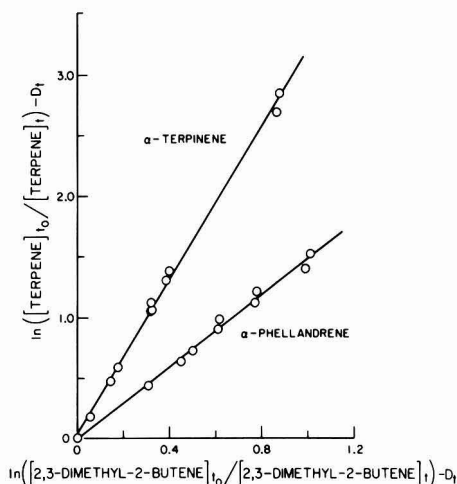


Figure 2. Plot of eq 1 for α -terpinene and α -phellandrene, with 2,3-dimethyl-2-butene as the reference organic.

butadiene, respectively. However, while, as expected, the NO_2 reaction rate constant for *cis*- and *trans*-ocimene is

Table III. Rate Constants and Lifetimes for a Series of Monoterpenes and Related Naturally Emitted Organics due to Reaction with O₃ and OH and NO₃ Radicals at Room Temperature

naturally emitted organic	rate constant, cm ³ molecule ⁻¹ s ⁻¹			lifetime ^a		
	O ₃ ^b	OH ^c	NO ₃ ^d	O ₃ (24 h)	OH (daytime)	NO ₃ (nighttime)
α-pinene	8.4 × 10 ^{-17e}	6.0 × 10 ⁻¹¹	6.1 × 10 ⁻¹²	4.6 h	4.6 h	11 min
β-pinene	2.1 × 10 ^{-17e}	7.8 × 10 ⁻¹¹	2.5 × 10 ⁻¹²	18 h	3.6 h	28 min
Δ ³ -carene	1.2 × 10 ⁻¹⁶	8.7 × 10 ⁻¹¹	1.1 × 10 ⁻¹¹	3.2 h	3.2 h	6.3 min
d-limonene	6.4 × 10 ⁻¹⁶	1.4 × 10 ⁻¹⁰	1.4 × 10 ⁻¹¹	36 min	2.0 h	5.0 min
myrcene	1.2 × 10 ⁻¹⁵	1.9 × 10 ⁻¹⁰	1.1 × 10 ⁻¹¹	19 min	1.5 h	6.3 min
cis-ocimene	2.0 × 10 ⁻¹⁵	2.3 × 10 ⁻¹⁰	2.4 × 10 ⁻¹¹	12 min	1.2 h	2.9 min
α-phellandrene	1.2 × 10 ⁻¹⁴	~1.7 × 10 ⁻¹⁰	9.1 × 10 ⁻¹¹	1.9 min	1.6 h	45 s
β-phellandrene	1.8 × 10 ⁻¹⁶	~1.4 × 10 ⁻¹⁰	~1.3 × 10 ⁻¹¹	2.1 h	2.0 h	5.3 min
α-terpinene	8.8 × 10 ⁻¹⁴	~2.1 × 10 ⁻¹⁰	1.9 × 10 ⁻¹⁰	16 s	1.3 h	22 s
γ-terpinene	2.8 × 10 ⁻¹⁶	1.7 × 10 ⁻¹⁰	3.1 × 10 ⁻¹¹	1.4 h	1.6 h	2.2 min
terpinolene	1.0 × 10 ⁻¹⁴	2.0 × 10 ⁻¹⁰	7.1 × 10 ⁻¹¹	2.3 min	1.4 h	1.0 min
p-cymene	≤10 ^{-2f}	~1.5 × 10 ⁻¹¹	~3 × 10 ⁻¹⁶	≥4.4 year ^f	19 h	160 day

^a Calculated for clean tropospheric concentrations of 7.2 × 10¹¹ molecule cm⁻³ (30 ppb) of O₃ (25), 1 × 10⁶ cm⁻³ (0.04 ppt) of OH radicals (during daytime hours) (26), and 2.4 × 10⁸ cm⁻³ (10 ppt) of NO₃ radicals (during nighttime hours) (5). ^b From ref 23 except as noted. ^c From ref 22. ^d From Table II. ^e From ref 24. ^f Estimated by analogy to *p*-xylene (28).

significantly higher than that for myrcene, the rate constants for myrcene [(2.6 ± 0.2) × 10⁻¹⁹ cm³ molecule⁻¹ s⁻¹] and *cis*- and *trans*-ocimene [(8.9 ± 0.4) × 10⁻¹⁹ cm³ molecule⁻¹ s⁻¹] are somewhat higher (by a factor of ~2.5-3) than the literature data for isoprene (19, 20) and 2,3-dimethyl-1,3-butadiene (20). The reasons for these higher reactivities for these two monoterpenes, as compared to the simpler conjugated dialkenes with the same number of substituents around the C=C—C=C structure, are not known at present.

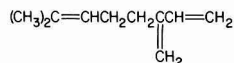
NO₃ Radical Reactions. The data shown in Figures 1 and 2 are in good accord with eq I. The simple alkenes such as 2-methyl-2-butene and 2,3-dimethyl-2-butene have been shown to react with NO₃ radicals, and not with N₂O₅ (8, 10). Since the [N₂O₅]/[NO₂], and hence [N₂O₅]/[NO₃], ratios were varied by factors of 1.5–2 in the present study, the excellent straight line plots in Figures 1 and 2 show that the monoterpenes investigated here also react with NO₃ radicals, and not with N₂O₅.

The rate constant ratios *k*₃/*k*₄ given in Table I can be placed on an "absolute" basis (but still linearly dependent on the value of the equilibrium constant used for the reactions NO₂ + NO₃ ⇌ N₂O₅) by using the rate constants, *k*₄, for 2-methyl-2-butene and 2,3-dimethyl-2-butene (12). While in our previous NO₃ radical rate constant studies (10–14) we used the NO₂ + NO₃ ⇌ N₂O₅ equilibrium constant given by Malko and Troe (16), in this work we use our recently determined equilibrium constant of 3.4 × 10⁻¹¹ cm³ molecule⁻¹ at 298 K (21), which is a factor of 1.8 higher than that given by Malko and Troe (16). The rate constants *k*₃ so obtained are given in Table II.

The data in Tables I and II show that, as observed previously for α- and β-pinene, Δ³-carene, and d-limonene (12), the monoterpenes studied here are highly reactive toward the NO₃ radical. Indeed, these six monoterpenes are as reactive, or more reactive, toward the NO₃ radical than are the four monoterpenes studied previously. α-Terpinene is the most reactive organic toward the NO₃ radical studied to date, with a room temperature rate constant of *k*₃ = 1.9 × 10⁻¹⁰ cm³ molecule⁻¹ s⁻¹.

On the basis of these and our previously measured NO₃ radical reaction rate constants at room temperature for a series of alkenes and dialkenes (10, 12), it appears, analogous to the situation for the corresponding OH radical reactions (22), that the room temperature rate constants for the monoalkenes and nonconjugated dialkenes can be estimated with some degree of accuracy from the configuration and degree of substitution around the double

bond(s). A similar situation occurs for the conjugated dialkenes. For example, myrcene



contains a trisubstituted double bond [(CH₃)₂C=CH—] plus a monosubstituted conjugated dialkene entity [CH₂=C(CH=CH₂)—]. Hence, the NO₃ radical rate constant for myrcene should be approximated by the sum of those for 2-methyl-2-butene [for the (CH₃)₂C=CH— group] and isoprene (for the [CH₂=C(CH=CH₂)—] group).

Rate constants *k*₃ estimated in this manner for the monoterpenes studied to date are also given in Table II, and apart from β-pinene [as discussed previously (12)], these estimated rate constants are in good agreement (i.e., within a factor of 2) with our experimental values. Thus, we have also included in Table II estimates of the NO₃ radical rate constants for a number of other monoterpenes and related organics for which experimental data are not yet available (i.e., dihydromyrcene, carvomenthene, *p*-cymene, β-phellandrene, and terpinolene) (see footnote *b* of Table II for further details of this estimation technique). Since *p*-cymene is an aromatic hydrocarbon, with *p*-alkyl substituents, we have estimated its NO₃ radical rate constant to be essentially identical with that for *p*-xylene.

In Table III, the room temperature rate constants for reaction of a series of naturally emitted organics with O₃ (23, 24) and with OH (22) and NO₃ radicals and their corresponding atmospheric lifetimes under "clean" tropospheric conditions are given. Ozone, OH radical, and NO₃ radical concentrations of 7.2 × 10¹¹ molecule cm⁻³ (25), 1 × 10⁶ cm⁻³ (26), and 2.4 × 10⁸ cm⁻³ (5), respectively, were used in these calculations. It is obvious from this table that the reactions of the naturally emitted monoterpenes with the NO₃ radical can be an extremely important loss process, with lifetimes being measured in terms of minutes or less for a nighttime concentration of NO₃ radicals of 10 ppt. Only for *p*-cymene, a naturally emitted aromatic hydrocarbon (27), is the NO₃ radical reaction expected to be of minor or negligible importance as a sink process, based upon our previous kinetic data for the aromatic hydrocarbons (14).

Recently Winer et al. (15) have shown that the effects of the reactions of NO₃ radicals with the monoterpenes depend on the relative source strengths for the NO₃ radical and the monoterpenes. Under conditions where the mo-

monoterpene emission rates are greater than the NO₃ radical formation rate (e.g., in "pristine" forested areas), the nighttime NO₃ radical concentrations will be markedly decreased relative to their levels in the absence of monoterpene emissions. Conversely, under conditions where the NO₃ radical formation rates are greater than the monoterpene emission rates (e.g., urban or arid/semidesert areas), the nighttime monoterpene concentrations are greatly reduced [by factors of ~100–150 (15)] over those in the absence of NO₃ radicals. Clearly, as discussed in detail by Winer et al. (15), these NO₃ radical reactions must be taken into account in chemical computer models of the atmospheric chemistry of the monoterpenes.

Registry No. NO₃, 12033-49-7; NO₂, 10102-44-0; myrcene, 123-35-3; *cis*-ocimene, 27400-71-1; *trans*-ocimene, 27400-72-2; α -terpinene, 99-86-5; γ -terpinene, 99-85-4; α -phellandrene, 99-83-2; α -pinene, 80-56-8; β -pinene, 127-91-3; Δ^3 -carene, 13466-78-9; *d*-limonene, 5989-27-5; β -phellandrene, 555-10-2; terpinolene, 586-62-9; dihydromyrcene, 2436-90-0; carvomenthene, 5502-88-5; *p*-cymene, 99-87-6.

Literature Cited

- (1) Platt, U.; Perner, D.; Winer, A. M.; Harris, G. W.; Pitts, J. N., Jr. *Geophys. Res. Lett.* **1980**, *7*, 89–92.
- (2) Noxon, J. F.; Norton, R. B.; Marovich, E. *Geophys. Res. Lett.* **1980**, *7*, 125–128.
- (3) Platt, U.; Perner, D.; Schroder, J.; Kessler, C.; Toennissen, A. *J. Geophys. Res.* **1981**, *86*, 11965–11970.
- (4) Platt, U.; Perner, D.; Kessler, C. "The Importance of NO₃ for the Atmospheric NO_x Cycle from Experimental Observations". Proceedings of the 2nd Symposium of the Composition of the Non-urban Troposphere, Williamsburg, VA, May 25–28, 1982.
- (5) Platt, U. F.; Winer, A. M.; Biermann, H. W.; Atkinson, R.; Pitts, J. N., Jr. *Environ. Sci. Technol.* **1984**, *18*, 365–369.
- (6) Pitts, J. N., Jr.; Biermann, H. W.; Atkinson, R.; Winer, A. M. *Geophys. Res. Lett.* **1984**, *11*, 557–560.
- (7) Morris, E. D., Jr.; Niki, H. *J. Phys. Chem.* **1974**, *78*, 1337–1338.
- (8) Japar, S. M.; Niki, H. *J. Phys. Chem.* **1975**, *79*, 1629–1632.
- (9) Carter, W. P. L.; Winer, A. M.; Pitts, J. N., Jr. *Environ. Sci. Technol.* **1981**, *15*, 829–831.
- (10) Atkinson, R.; Plum, C. N.; Carter, W. P. L.; Winer, A. M.; Pitts, J. N., Jr. *J. Phys. Chem.* **1984**, *88*, 1210–1215.
- (11) Atkinson, R.; Pitts, J. N., Jr.; Aschmann, S. M. *J. Phys. Chem.* **1984**, *88*, 1584–1587.
- (12) Atkinson, R.; Aschmann, S. M.; Winer, A. M.; Pitts, J. N., Jr. *Environ. Sci. Technol.* **1984**, *18*, 370–375.
- (13) Atkinson, R.; Plum, C. N.; Carter, W. P. L.; Winer, A. M.; Pitts, J. N., Jr. *J. Phys. Chem.* **1984**, *88*, 2361–2364.
- (14) Atkinson, R.; Carter, W. P. L.; Plum, C. N.; Winer, A. M.; Pitts, J. N., Jr. *Int. J. Chem. Kinet.* **1984**, *16*, 887–898.
- (15) Winer, A. M.; Atkinson, R.; Pitts, J. N., Jr. *Science (Washington, D.C.)* **1984**, *224*, 156–159.
- (16) Malko, M. W.; Troe, J. *Int. J. Chem. Kinet.* **1982**, *14*, 399–416.
- (17) Doyle, G. J.; Bekowies, P. J.; Winer, A. M.; Pitts, J. N., Jr. *Environ. Sci. Technol.* **1977**, *11*, 45–51.
- (18) Schott, G.; Davidson, N. *J. Am. Chem. Soc.* **1958**, *80*, 1841–1853.
- (19) Atkinson, R.; Aschmann, S. M.; Winer, A. M.; Pitts, J. N., Jr. *Int. J. Chem. Kinet.* **1984**, *16*, 697–706.
- (20) Glasson, W. A.; Tuesday, C. S. *Environ. Sci. Technol.* **1970**, *4*, 752–757.
- (21) Tuazon, E. C.; Sanhueza, E.; Atkinson, R.; Carter, W. P. L.; Winer, A. M.; Pitts, J. N., Jr. *J. Phys. Chem.* **1984**, *88*, 3095–3098.
- (22) Atkinson, R.; Aschmann, S. M.; Carter, W. P. L. *Int. J. Chem. Kinet.* **1983**, *15*, 1161–1177.
- (23) Grimsrud, E. P.; Westberg, H. H.; Rasmussen, R. A. *Int. J. Chem. Kinet.* **1975**, *Symp. 1*, 183–195.
- (24) Atkinson, R.; Winer, A. M.; Pitts, J. N., Jr. *Atmos. Environ.* **1982**, *16*, 1017–1020.
- (25) Singh, H. B.; Ludwig, F. L.; Johnson, W. B. *Atmos. Environ.* **1978**, *12*, 2185–2196.
- (26) Crutzen, P. J. In "Atmospheric Chemistry"; Goldberg, E. D., Ed.; Springer-Verlag: Berlin, 1982; pp 313–328.
- (27) Graedel, T. E. *Rev. Geophys. Space Phys.* **1979**, *17*, 937–947.
- (28) Pate, C. T.; Atkinson, R.; Pitts, J. N., Jr. *J. Environ. Sci. Health* **1976**, *A11*, 1–10.

Received for review May 11, 1984. Accepted August 27, 1984. This work was financially supported by National Science Foundation Grant ATM-8209028-02.

Evaluating Two-Resistance Models for Air Stripping of Volatile Organic Contaminants in a Countercurrent, Packed Column

Paul V. Roberts,* Gary D. Hopkins, Christoph Munz, and Arturo H. Rlojas

Department of Civil Engineering, Stanford University, Stanford, California 94305

■ Mass transfer of six volatile organic solutes during gas stripping in a countercurrent, packed column was studied experimentally to assess the validity of previously proposed, generalized correlations for predicting the stripping behavior of trace organic contaminants. The simplifying assumption of liquid-phase control of the transfer rate was found to be warranted for the most volatile solutes, oxygen and dichlorodifluoromethane. However, for moderately volatile solutes such as carbon tetrachloride, tetrachloroethylene, trichloroethylene, and chloroform, the gas-phase resistance was found to affect the overall rate to an increasing degree with decreasing solute volatility. A two-resistance model consistent with the penetration theory, previously suggested by Onda and co-workers, adequately predicted the results. The Onda model predicted the transfer rate constants within an average standard deviation of 21%. Nonetheless, the mixed-resistance region remains a troublesome domain, where substantial errors in prediction must be anticipated.

Introduction

Air stripping in a countercurrent, packed contactor has been shown to be effective in controlling trace organic contaminants such as trihalomethanes, chlorinated solvents, and other volatile constituents (1-8). The theory of countercurrent, gas-liquid absorption and desorption processes is well understood (9, 10). Air stripping, as practiced for water treatment and water pollution control, in most instances corresponds to the relatively simple case of desorption from dilute solution. Moreover, in many cases the solutes are sufficiently volatile for the gas-phase resistance to be neglected in mass transfer calculations; indeed, this simplifying assumption generally has been made in previous studies of air stripping of volatile trace organic solutes from water (3, 6, 8). This paper assesses the validity of several previously proposed mass-transfer models for countercurrent air stripping in a packed column and compares model predictions with experimental data from a laboratory-scale packed column. The objective is to evaluate whether it is justified to neglect the gas-phase resistance, or whether two-resistance mass-transfer models offer a significant improvement over a single-resistance model that neglects the gas-phase resistance.

Theory of Countercurrent Air Stripping

Design Equations. Air stripping can be effectively achieved in a packed tower in which air and water flow countercurrent to one another, with the water flowing downward over the packing as a film, while the air flows upward as the continuous phase (Figure 1). The design equations are derived elsewhere (5, 9-11) for the general cases of absorption and desorption (stripping). The design equation given here is for the simple case of isothermal desorption of a trace, volatile solute. The packed height, Z , required to achieve a desired separation is

$$Z = \text{HTU} \times \text{NTU} \quad (1)$$

According to eq 1, Z is the product of two groups, HTU and NTU. HTU, the height of a transfer unit (m), is the

ratio of the superficial velocity, u_0 (m/s), to the transfer rate constant, $K_L a$ (s^{-1}):

$$\text{HTU} = u_0 / (K_L a) = L_m / (\rho_L K_L a) \quad (2)$$

where L_M = liquid mass flux ($kg \cdot m^{-2} \cdot s^{-1}$), ρ_L = liquid density ($kg \cdot m^{-3}$), and $K_L a$ = overall transfer rate constant (s^{-1}) based on the liquid-phase driving force. The transfer rate constant, $K_L a$, is the product of the overall coefficient, K_L ($m \cdot s^{-1}$) times the specific interfacial area, a ($m^2 \cdot m^{-3}$). NTU, the number of transfer units (dimensionless), is defined as

$$\text{NTU} = \frac{S}{S-1} \ln \left[\frac{(C_{L,2} - C_{G,1}/H_c)(S-1) + 1}{(C_{L,1} - C_{G,1}/H_c)S} \right] \quad (3)$$

where $C_{L,2}$ and $C_{L,1}$ are the solute concentrations in the influent and effluent liquid, respectively, and $C_{G,1}$ is the concentration in the influent gas (Figure 1). H_c is the Henry constant, a dimensionless partition coefficient expressed as the ratio of the mass (or molar) concentration in the gas phase to that in the liquid phase; the ratio $S = (Q_G H_c / Q_L)$ is the stripping factor; Q_G and Q_L are the volumetric flow rates ($m^3 \cdot s^{-1}$) of gas and liquid, respectively.

In the present work, as in many water treatment applications, the stripping gas can be considered devoid of the contaminant of interest. Substituting $C_{G,1} = 0$ into eq 3, we can simplify to

$$Z = \left(\frac{L_M}{\rho_L K_L a} \right) \left(\frac{S}{S-1} \right) \ln \left[\frac{(C_{L,2}/C_{L,1})(S-1) + 1}{S} \right] \quad (4)$$

Equation 4 can be used in design calculations to estimate the packed height necessary to achieve a given treatment objective, or rearranged to solve for the liquid-phase concentration ratio. In any case, the value of S must be chosen. Treybal (10) presents solutions to eq 3 in convenient graphical form.

Stripping Factor. The stripping factor can be thought of as an equilibrium capacity factor, i.e., the product of the volumetric air:water ratio (Q_G/Q_L) times the partition coefficient (H_c). If $S > 1$, there is sufficient gas-phase capacity to convey away all of the solute in the entering liquid; complete removal by stripping is then possible, given a sufficiently tall column. If $S < 1$, however, the system performance is limited by equilibrium, and the fractional removal is asymptotic to the value of the stripping factor, i.e.

$$(1 - C_{L,1}/C_{L,2}) \rightarrow S \quad Z \rightarrow \infty \quad (5)$$

Clearly, the stripping factor is a crucial criterion for air stripping performance (5, 9-11). The quantitative influence of the stripping factor on effluent quality and on required packed height is demonstrated elsewhere (12, 13).

Two-Resistance Theory. The overall resistance to interphase mass transfer can be considered as the sum of two resistances, a gas-phase and a liquid-phase resistance (14). For present purposes, the two-resistance theory can be stated as

$$R_T = R_L + R_G \quad (6)$$

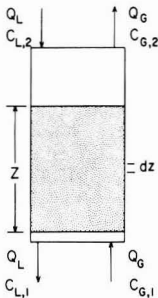


Figure 1. Schematic of countercurrent packed column.

where the subscripts T, L, and G refer to the total, liquid-phase, and gas-phase resistances, respectively. Defining the resistance as the reciprocal of the respective rate constant, and assuming phase equilibrium governed by Henry's law at the interface, we obtain (15)

$$(K_L a)^{-1} = (k_L a)^{-1} + (H_c k_G a)^{-1} \quad (7)$$

where K = overall coefficient and k = coefficient for an individual phase. Accordingly, the ratio of resistances is given by

$$\frac{R_L}{R_G} = \frac{H_c k_G a}{k_L a} = \frac{H_c k_G}{k_L} \quad (8)$$

or

$$\frac{R_L}{R_T} = \left(1 + \frac{k_L}{H_c k_G} \right)^{-1} \quad (9)$$

If $(H_c k_G / k_L) \gg 1$, the gas-phase resistance can be considered sufficiently small to be neglected, a condition termed liquid-phase control. If the two resistances are of roughly equal magnitude, then both must be taken into account in predicting and interpreting mass transfer.

Models for Predicting Mass-Transfer Rate Constants

In this paper, three models are evaluated for predicting the mass-transfer rate constant: those of Sherwood and Holloway (16), Shulman et al. (17, 18), and Onda et al. (19). The Sherwood-Holloway model (16) presumes that the liquid-phase resistance controls, thus neglecting the gas-phase resistance; it is the model most widely used to date in studies of volatile organic stripping for water treatment (6, 8, 11). The models of Shulman et al. (17) and Onda et al. (19) evaluate the gas-phase as well as the liquid-phase resistance and hence qualify as two-resistance models.

Sherwood-Holloway Model. Sherwood and Holloway (16) studied the desorption of H_2 , CO_2 , and O_2 from water into a countercurrent flow of air in columns filled with a variety of packing materials, over a range of water and air flow rates: $0.27 < L_M < 43 \text{ kg-m}^{-2}\text{-s}^{-1}$ and $0.04 < G_M < 1.8 \text{ kg-m}^{-2}\text{-s}^{-1}$. The solutes were all gases, with Henry constants sufficiently large ($H_c > 1$) such that the liquid-phase resistance controlled; this was indeed confirmed by the absence of an effect of gas flow rate on the mass-transfer rate constant (16). Accordingly, the transfer rate constant was correlated with the liquid rate and liquid-phase properties only (16) and is given as

$$\frac{k_L a}{D_L} = 10.746 \alpha \left(\frac{0.3048 L_M}{\mu_L} \right)^{1-n} \left(\frac{\mu_L}{\rho_L D_L} \right)^{0.5} \quad (10)$$

where D = molecular diffusivity ($\text{m}^2\text{-s}^{-1}$), μ = fluid viscosity (Pa·s), and ρ = fluid density (kg-m^{-3}). The coefficient α

and exponent n in eq 10 are empirically determined packing parameters. Values of α and n are given by Sherwood and Holloway (16) and others (9, 10); for the packing used in this work, $1/2$ -in. ceramic Berl saddles, the values are $\alpha = 150$ and $n = 0.28$. Equation 10 is not dimensionally consistent, as the group containing L_M / μ_L has units of $(\text{length})^{-1}$ and $k_L a / D_L$ has units of $(\text{length})^{-2}$; the constant, 10.764, converts from the English units used by Sherwood and Holloway (16) to the SI units used in the present work. The exponent, 0.5, of the dimensionless Schmidt number, $Sc = \mu_L / (\rho_L D_L)$, is in accordance with the penetration theory (20, 21).

Shulman Model. The model of Shulman et al. (17) entails separate estimation of k_L , k_G , and a . The Shulman model is recommended by Treybal (10) for cases where both the liquid-phase and gas-phase resistance must be taken into account.

Shulman's correlation (17) for the liquid-phase coefficient k_L was expressed as a relationship between dimensionless groups, the Sherwood number, $Sh = k_L d_s / D_L$, the Reynolds number, $Re = d_s L_M / \mu_L$, and the Schmidt number, $Sc = \mu_L / (\rho_L D_L)$:

$$\frac{k_L d_s}{D_L} = 25.1 \left(\frac{d_s L_M}{\mu_L} \right)^{0.45} \left(\frac{\mu_L}{\rho_L D_L} \right)^{0.5} \quad (11)$$

with the characteristic length chosen as d_s = diameter of a sphere having the same surface area as a unit of packing. The coefficient, 25.1, is an empirically determined constant, whose value is independent of the units chosen. Equation 11 was verified by Shulman et al. (17) using previously reported data covering the same range of L_M as Sherwood and Holloway (16).

Shulman et al. (17) also developed a correlation for the gas-phase coefficient, k_G , based on vaporization of packing prepared from solid naphthalene, in the range $0.14 < G_M < 1.4 \text{ kg-m}^{-2}\text{-s}^{-1}$. They reported the result in a dimensionless form which, for a dilute gas mixture, can be rearranged to

$$\frac{k_G d_s}{D_G} = 1.195(1 - \epsilon)^{0.36} \left(\frac{d_s G_M}{\mu_G} \right)^{0.64} \left(\frac{\mu_G}{D_G \rho_G} \right)^{0.33} \quad (12)$$

Equation 12 for k_G can be seen to be analogous to eq 11 for k_L , in that both represent relations between the same dimensionless groups: Sh , Re , and Sc . However, whereas k_L is proportional to $D^{1/2}$ as predicted by penetration theory, k_G depends on $D_G^{2/3}$, in accordance with expectations for mass transfer in a turbulent boundary layer at small values of Sc (22, 23).

Shulman et al. (17) also described a means of estimating the interfacial contact area, but the data were presented in a cumbersome graphical form (10, 17) not amenable to presentation here.

Onda Model. The model of Onda et al. (19) also entails separate estimation of k_L , k_G , and a . The specific interfacial area is taken to be the specific wetted packing area, a_w , which is estimated as a function of the liquid flow rate, packing properties, and liquid properties:

$$\frac{a_w}{a_t} = 1 - \exp[-1.45(\sigma_c / \sigma_L)^{0.75} \times [L_M / (a_t \mu_L)]^{0.1} [L_M^2 a_t / (\rho_L^2 g)]^{-0.05} [L_M^2 / (\rho_L \sigma_L a_t)]^{0.2}] \quad (13)$$

where a_t = total specific surface area of packing, σ_c = critical surface area of packing material, and ρ_L , μ_L , and σ_L are the liquid density, viscosity, and surface tension, respectively. The last three factors within the argument of the exponential in eq 13 are the Reynolds, Froude, and Weber numbers, all dimensionless. Equation 13 is claimed

to be accurate within $\pm 20\%$ for saddles, spheres, and rods made of ceramic, glass, and PVC, as well as wax-coated material (19). For a given packing material, liquid, and temperature, the specific interfacial area increases with increasing liquid rate and asymptotically approaches a_t as L_M becomes very large.

The correlation for the liquid-phase coefficient, k_L , was determined from interpretation of a large data base (including the work of Sherwood and Holloway (16)), encompassing rings, spheres, rods, and saddles from 4- to 50-mm size, covering the liquid flow range $0.8 < L_M < 43 \text{ kg}\cdot\text{m}^{-2}\cdot\text{s}^{-1}$. The result was reported in dimensionless form by Onda et al. (19)

$$k_L \left(\frac{\rho_L}{\mu_L g} \right)^{1/3} = 0.0051 \left(\frac{L_M}{a_w \mu_L} \right)^{2/3} \left(\frac{\mu_L}{\rho_L D_L} \right)^{0.5} (a_t d_p)^{0.4} \quad (14)$$

where d_p = nominal packing size (m). The accuracy of the estimate of k_L was given as $\pm 20\%$ (19). The form of eq 14 was rationalized by Onda et al. (24), who showed that the left-hand side can be expressed as

$$k_L \left(\frac{\rho_L}{\mu_L g} \right)^{1/3} = \frac{\left(\frac{k_L}{a_t D_L} \right) \left(\frac{\mu^2 a_t^3}{\rho^2 g} \right)^{1/3}}{\left(\frac{\mu_L}{\rho_L D_L} \right)} = \frac{\text{Sh}\cdot\text{Ga}}{\text{Sc}} \quad (15)$$

where Sh = Sherwood number, defined by using a_t^{-1} as the characteristic length, Sc = Schmidt number, and Ga = Galileo number, which can be viewed as a ratio of viscous forces to gravitational acceleration forces. Equation 14 predicts the same square-root dependence on D_L as do eq 10 and 11, in accordance with the penetration theory (20, 21), but the dependence on L_M , namely, $k_L \propto L_M^{2/3}$, is stronger than that according to eq 11, namely, $k_L \propto L_M^{0.45}$.

For the gas-phase coefficient, Onda et al. (19) correlated mass-transfer data for absorption and vaporization in the gas flow range $0.014 < G_M < 1.7 \text{ kg}\cdot\text{m}^{-2}\cdot\text{s}^{-1}$ and various packing shapes in the size range 4–50 mm, obtaining the following relationship in dimensionless form

$$\frac{k_G}{a_t D_G} = 5.23 \left(\frac{G_M}{a_w \mu_G} \right)^{0.7} \left(\frac{\mu_G}{\rho_G D_G} \right)^{1/3} (a_t d_p)^{-2} \quad (16)$$

but recommended that the value of the constant in eq 16 be changed for small packings ($d_p < 15 \text{ mm}$) from 5.23 to 2.0. The Onda model for k_G (eq 16) agrees closely with the Shulman model (eq 12) in terms of the dependence of k_G on G_M and D_G .

Summary. Three models are proposed as being potentially useful for predicting and interpreting mass transfer in the air stripping of volatile, trace organic contaminants from water. The Shulman model (17) is recommended by Treybal (10), whereas the Onda relations (19) are recommended in the Chemical Engineers' Handbook (25) for absorption and stripping design calculations. However, the data bases from which the models were developed did not encompass stripping of trace organic solutes from aqueous solution. Hence, their validity must be verified under appropriate conditions before they may be used with confidence for such applications.

Umphres et al. (6) found that air stripping data for trihalomethanes (CHCl_3 , CHBrCl_2 , CHBr_2Cl , and CHBr_3) at high air:water ratios could be correlated adequately with a model of the Sherwood–Holloway form (eq 10), but the observed values were smaller by a factor of 2 than those predicted by using Sherwood and Holloway's values of the

fitting parameters (16). Ball et al. (8) also successfully correlated air stripping data for a group of halogenated aliphatic compounds using the Sherwood–Holloway model (16) but found it necessary to adjust the parameters α and n to obtain a good fit. Cummins and Westrick (7) showed that the predictions of the Onda model (19) agreed well with stripping data for $\text{CHCl}=\text{CCl}_2$ in the range $6 < L_M < 20 \text{ kg}\cdot\text{m}^{-2}\cdot\text{s}^{-1}$, reporting a relative standard error of 17.8% as a measure of the discrepancy between prediction and experiment, but found it necessary to reduce the Henry constant by a factor of 3 to obtain good agreement.

This paper is a summary of the work of Roberts et al. (5), who tested the three mass-transfer models described above by applying them without parameter adjustment. Numerous other single-resistance models reviewed elsewhere (26) are not considered here.

Experimental Methods

Air stripping experiments were conducted in a column of 0.22 m inside diameter, which could be assembled in 0.5-m sections. The column was packed with 12.5-mm ($1/2$ -in.) ceramic Berl saddles, giving a ratio of column diameter to packing size, $d_c/d_p = 18$, which is believed to be adequate to assure satisfactorily uniform liquid distribution (10). The packing was supported on a Teflon plate with holes drilled to give 9% open area for fluid passage. Liquid was distributed at the top of the bed through a six-spoked stainless steel distributor. The packed height was varied from 0.2 to 1.4 m, giving a bed height-to-diameter ratio in the range 1:1 to 7:1, which is well within the range considered favorable from the viewpoint of equal liquid distribution (10).

A concentrated aqueous solution of the organic solutes was provided from a 50-L reservoir, consisting of a gas-free Teflon bag filled with Milli-Q water, saturated with dissolved oxygen and containing halogenated organic compounds. The concentrated solution was mixed with aerated tap water, which had been preadjusted to the experimental temperature, in a ratio of approximately 1:10 (v/v) to attain the desired influent concentration. The influent concentrations were in the range 50–200 $\mu\text{g}/\text{L}$ for the organic solutes, well below their solubility limits, and approximately 7–9 mg/L for oxygen. The liquid feed flow was measured with a rotameter and controlled with a rheostat on the feed pump. All tubing was of Teflon, except for short lengths of Viton in the peristaltic pump. The flow of gas, research-grade (99.99%) nitrogen, was controlled by two gas pressure regulators in series and measured with a precision mass flow meter (Matheson Models 602 and 603). Experiments were conducted at ambient temperature, $22 \pm 2^\circ \text{C}$.

Experiments were carried out to measure the stripping of dissolved oxygen and six halogenated organic solutes: dichlorodifluoromethane (CCl_2F_2 (Freon-12)); chloroform (CHCl_3); 1,1,1-trichloroethane (CH_3CCl_3); carbon tetrachloride (CCl_4); trichloroethylene ($\text{CHCl}=\text{CCl}_2$); tetrachloroethylene ($\text{CCl}_2=\text{CCl}_2$). The relevant properties of the solutes are summarized in Table I. Concentrations of organic solutes were determined by gas chromatography of pentane extracts with 1,2-dibromoethane as an internal standard. The precision of the organic analysis within a given experiment was generally better than $\pm 3\%$.

The nitrogen flow rate was held constant, in a given experiment, at one of the following values: $Q_G = 1, 2, 4, 8, \text{ or } 16 \text{ L}/\text{min}$, corresponding to a range of gas mass flux between 5.2×10^{-4} and $8.2 \times 10^{-3} \text{ kg}\cdot\text{m}^{-2}\cdot\text{s}^{-1}$. Likewise, the water flow rate was held constant in a given experiment at one of the following values: $Q_L = 1, 4, \text{ or } 10 \text{ L}/\text{min}$, corresponding to a range of liquid mass flux between 0.44

Table I. Solute Properties Used for Mass Transfer Predictions

compd	H_c^a	properties at 293 K	
		$D_L^b \times 10^9, \text{m}^2\text{-s}^{-1}$	$D_G^c \times 10^6, \text{m}^2\text{-s}^{-1}$
oxygen	30	2.03	2.19 ^d
CCl_2F_2	10.9 ^e	0.99	0.93 ^d
CCl_4	1.01	0.86	0.81
$\text{CCl}_2=\text{CCl}_2$	0.63	0.79	0.77
CH_2CCl_3	0.62	0.83	0.77
$\text{CHCl}=\text{CCl}_2$	0.41	0.86	0.85
CHCl_3	0.22	0.94	0.87

^a Experimental values (15); H_c is expressed as a dimensionless mass concentration ratio. ^b Calculated by using the Wilke-Chang correlation (27), with molecular volumes estimated as described in Table A-3 of ref 15. ^c Experimental data of Lugg (28), except where noted. ^d Calculated by using the Wilke-Lee correlation (29). ^e Experimental data of Munz (30).

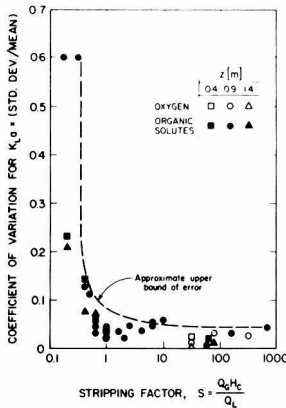


Figure 2. Dependence of experimental precision on the stripping factor.

and 4.4 $\text{kg}\cdot\text{m}^{-2}\cdot\text{s}^{-1}$. The corresponding gas:water ratios were between 1:1 and 16:1 (v/v). The packing height was 0.2, 0.4, 0.9, or 1.4 m. Further details of the experimental apparatus and procedure are described elsewhere (5).

Data Interpretation

For each set of flow conditions (L_M, G_M), the amount of mass transfer was measured in the empty column (without packing) and expressed as a number of transfer units, $\text{NTUC} = \text{NTU}$ correction for end effects. For a given experiment with a packed column, the net number of transfer units, NTUN , due to mass transfer in the packed section was obtained by subtracting NTUC from NTUT :

$$\text{NTUN} = \text{NTUT} - \text{NTUC} \quad (17)$$

where NTUT is the total number of transfer units calculated by using eq 3 with the measured values of $C_{L,2}$ and $C_{L,1}$. The experimentally observed overall transfer rate constant based on the liquid-phase driving force, $K_L a$, was calculated by combining eq 1 and 2 and rearranging to obtain

$$(K_L a)_{\text{obsd}} = \frac{L_M \text{NTUN}}{\rho_L Z} \quad (18)$$

The precision of the experimental estimates of $K_L a$ was approximately $\pm 5\%$ (Figure 2), so long as the stripping factor, S , exceeded unity. However, the experimental

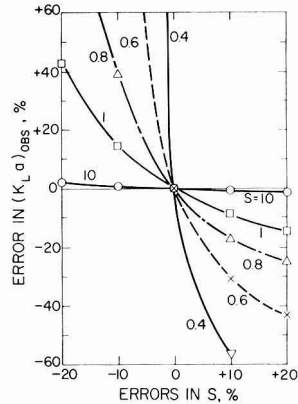


Figure 3. Sensitivity of the observed values of $K_L a$ to errors in the stripping factor estimate used in the data analysis.

precision deteriorated badly for $S < 1$ (Figure 2). The basic reason is that the estimation of $K_L a$ from experimental data becomes very sensitive to errors in S in the region $S < 1$. This is shown for a particular set of conditions, typical of the present experiments, in Figure 3; the abscissa represents the deviation of the value of S assumed in the data analyses from the true value

$$\% \text{ error in } S = \left(\frac{S_{\text{assumed}} - S_{\text{true}}}{S_{\text{true}}} \right) 100 \quad (19)$$

and the ordinate is the resulting error in the experimentally estimated $K_L a$. Errors in the stripping factor result in errors of the opposite sign in the estimated value of $K_L a$. The value of $K_L a$ is insensitive to errors in S for $S \approx 10$, and at $S \approx 1$, errors of the order $\pm 10\%$ in S result in errors in $K_L a$ of approximately equal magnitude. But for $S < 1$, the error in $K_L a$ becomes relatively larger than the corresponding error in S , especially for negative errors in S , where the error in $K_L a$ goes to infinity as the assumed value of S approaches the limiting value implicit in eq 3.

For the above reasons, data corresponding to $S < 0.8$ were omitted from the data analysis, as were any data for which the end effects accounted for more than half of the total mass transfer, i.e., $\text{NTUC} > 0.5 \text{ NTUT}$. Such conditions were encountered most commonly with the less volatile solutes (e.g., CHCl_3) in experiments with a short packed section (e.g., $Z = 0.2$ or 0.4 m) at a low gas:water ratio (i.e., $Q_G/Q_L = 1$).

Results

Number of Transfer Units. The dependence of the total number of transfer units on the packed height is illustrated for six solutes in Figure 4. The packed column data show the anticipated linear dependence of NTUT on Z , especially for the more volatile solutes: oxygen ($H_c = 30$); dichlorodifluoromethane (Freon-12, $H_c = 11$); carbon tetrachloride ($H_c = 1.0$). For those compounds, the linear regressions of NTUT on Z ($Z = 0.4, 0.9, \text{ and } 1.4 \text{ m}$) result in coefficients of determination, r^2 , greater than 0.99. For the moderately volatile compounds, 1,1,1-trichloroethane ($H_c = 0.6$), tetrachloroethylene ($H_c = 0.6$), and trichloroethylene ($H_c = 0.4$), the regressions are acceptably linear, but the correlations are weaker, $r^2 = 0.974, 0.949, \text{ and } 0.687$, respectively.

This demonstrates directly the sensitivity of the results to the stripping factor in the regions $S < 1$: under the conditions of the experiments shown in Figure 4 ($Q_G/Q_L = 1$), the stripping factor exceeded unity for $\text{O}_2, \text{CCl}_2\text{F}_2,$

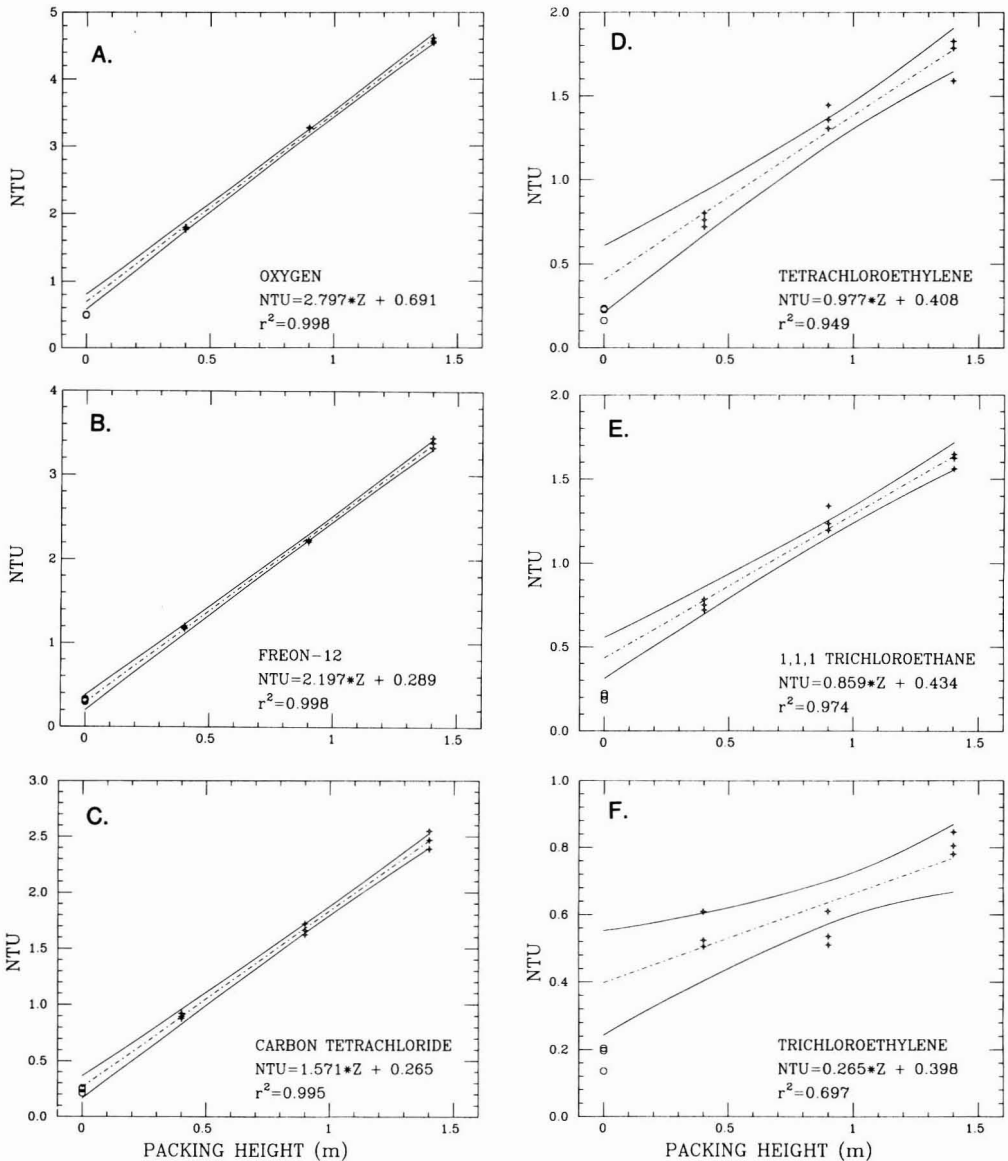


Figure 4. Dependence of total number of transfer units on packed height. Results of linear regression (dashed line), with 95% confidence limits (solid curves). The data from the empty column (open symbols) were not included in the regressions. Compounds in descending order of H_c : A, O₂; B, CCl₂F₂; C, CCl₄; D, CCl₂=CCl₂; E, CH₃CCl₃; F, CHCl=CCl₂.

and CCl₄, whereas the values were in the critical range ($S < 1$) for Cl₃CCH₃ ($S = 0.6$), CCl₂=CCl₂ ($S = 0.6$), and CHCl=CCl₂ ($S = 0.4$). For CHCl₃ (not shown in Figure 4), the packed height had no significant effect on NTU ($r^2 = 0.33$), indicating that, at a very low value of the stripping factor ($S = 0.2$), the stripping gas is nearly saturated with solute even before entering the packed section.

The intercepts of the regressions in Figure 4 are generally higher than the empty-column data (open symbols, $Z = 0$), although the differences are not statistically significant in some cases (CCl₂F₂, CCl₄, and CCl₂=CCl₂). We can offer only the speculative explanation that the mass transfer in the chamber below the packing support does not behave in an additive manner with that in the packed section, because the flow conditions below the packing

support deviate strongly from the plug flow, countercurrent regime believed to prevail in the packed section and presumed in the analysis. We have used the empty column data to estimate NTUC (eq 17), in the belief that this procedure provides a more stringent test of the mass transfer model than does the alternative (6, 8) of estimating $K_L a$ from a linear regression of NTU on Z .

Transfer Rate Constants. The experimentally determined values of the overall transfer rate constant, $K_L a$, are summarized in Table II; each value of $K_L a$ is the average of triplicate experimental values. The missing values, denoted by a footnote, denote conditions where $S < 0.8$ and/or NTUC > 0.5 NTU, for which the estimation methods used here are considered unreliable. The variability, quantified as the standard deviation divided by the

Table II. Experimental Values of the Overall Transfer Rate Constant^a

Z, m	Q _L , L/min	Q _G , L/min	observed K _L a × 10 ³ , s ⁻¹						
			O ₂	CCl ₂ F ₂	CHCl ₃	CH ₃ CCl ₃	CCl ₄	CHCl=CCl ₂	CCl ₂ =CCl ₂
0.9	1	10	2.35	1.97	0.96	1.78	1.82	1.64	1.89
0.9	4	10	6.78	4.94	0.52	3.65	4.10	2.21	3.89
0.9	10	10	13.58	9.31	b	5.14	6.97	1.82	5.67
0.4	10	10	14.09	9.59	b	6.00	7.25	4.03	6.03
1.4	10	10	12.79	9.62	b	4.41	6.99	1.98	4.78
0.4	1	1	2.34	1.70	b	0.87	1.16	b	0.89
0.4	1	2	2.30	1.89	b	1.31	1.51	1.03	1.34
0.4	1	4	2.52	2.14	0.78	1.70	1.79	1.61	1.68
0.4	1	8	2.43	2.08	1.21	1.87	1.87	1.71	1.85
0.4	1	16	2.48	1.97	1.40	1.84	1.83	1.74	1.83
0.2	1	1	2.94	1.97	b	b	b	b	b
0.9	1	1	1.86	2.28	b	1.05	1.56	0.36	1.11

^a All values shown are averages of triplicate experiments. ^b Data not analyzed because of NTUC > NTUT or S < 0.8.

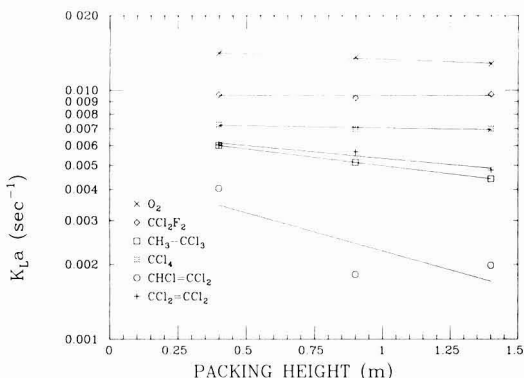


Figure 5. Effect of packed height on the observed transfer rate constants. Q_L = Q_G = 10 L/min.

mean, is depicted in Figure 2.

Effects of Packed Height. The packed height, Z, has relatively little effect on the observed K_La values, as shown in Figure 5. Indeed, it is expected that the observed K_La values should be independent of Z, according to eq 10–16. This expectation was confirmed by the data, most clearly for the most volatile solutes (O₂, CCl₂F₂, and CCl₄), but also for the less volatile solutes (CCl₂=CCl₂, CH₃CCl₃, CHCl=CCl₂, and CHCl₃). Although the latter group exhibited apparent negative trends (Figure 5) that were statistically significant at the 95% confidence level, the dependence of K_La on Z was slight except for the least volatile solute shown, namely, CHCl=CCl₂, for which S = 0.4 under these conditions.

Effect of Gas Flow Rate. The influence of the gas flow rate on the observed transfer rate constants is illustrated in Figure 6. For the two most volatile solutes—O₂ and CCl₂F₂—the observed K_La values are independent of Q_G, according to the expectation for liquid-phase control of the overall rate. For the other solutes, however, the observed values of K_La decrease with decreasing Q_G; the effect becomes more pronounced with decreasing solute volatility, with the sensitivity to Q_G increasing in the order CCl₄ < CCl₂=CCl₂ and CH₃CCl₃ < CHCl=CCl₂ < CHCl₃. The above order is identical with the descending rank order of the Henry constants (Table I). This points toward increasing gas-phase resistance as the underlying cause, according to eq 8.

Effect of Liquid Flow Rate. The dependence of the observed transfer rate constants on the liquid flow rate is shown in Figure 7. The observed K_La values increase with increasing Q_L for the more volatile solutes, as predicted

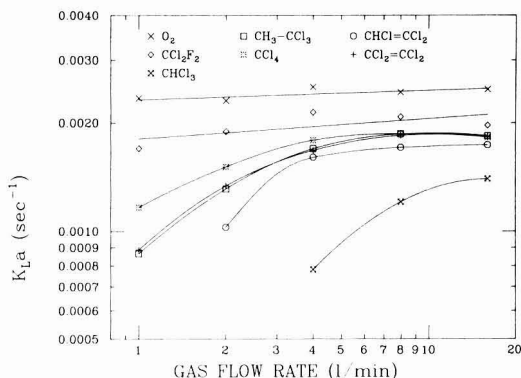


Figure 6. Effect of gas flow rate on the observed transfer rate constants. Q_L = 0.96 L/min; Z = 0.4 m.

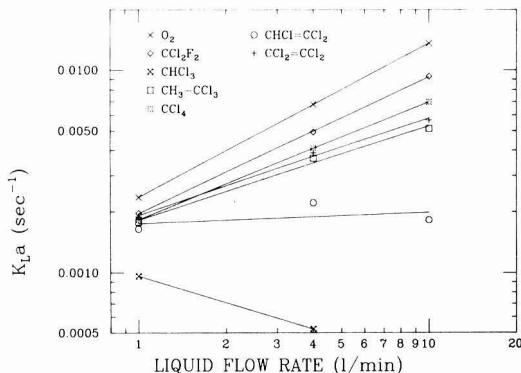


Figure 7. Effect of liquid flow rate on the observed transfer rate constants. Q_G = 10 L/min; Z = 0.9 m.

by all of the mass-transfer models described above. The dependence of K_La on Q_L is weaker for the less volatile solutes (CHCl₃ and CHCl=CCl₂) than for the more volatile ones (O₂, CCl₂F₂, CCl₄, CCl₂=CCl₂, and CH₃CCl₃). Indeed, the observed values of K_La for CHCl=CCl₂ are not significantly dependent on Q_L, and those for CHCl₃ actually show a negative dependence; these anomalies again demonstrate the difficulty of analyzing experiments conducted at low values of S. Under conditions leading to low values of S, the accuracy of the Henry constant estimate used in the data analysis is critically important, as illustrated in Figure 3.

Table III. Measures of Goodness-of-Fit for Comparing Transfer Rate Constant Predictive Models

model	regression equation	r^2	SEE ^a
Sherwood-Holloway	$\log(K_{La})_{\text{pred}} = 0.936 \log(K_{La})_{\text{obsd}} - 0.118$	0.865	0.125
Shulman	$\log(K_{La})_{\text{pred}} = 1.377 \log(K_{La})_{\text{obsd}} + 0.893$	0.909	0.198
Onda	$\log(K_{La})_{\text{pred}} = 1.108 \log(K_{La})_{\text{obsd}} + 0.274$	0.951	0.0845

^aSEE = standard error of estimate, defined in eq 20.

Discussion

Predicted Values of K_{La} . The value of K_{La} was predicted for each set of experimental conditions by using the Sherwood-Holloway, Shulman, and Onda models, as described above. The required solute properties are summarized in Table I. The values of the liquid and gas properties needed for prediction were as follows at 20 °C: $\mu_L = 0.001 \text{ Pa}\cdot\text{s}$; $\rho_L = 998 \text{ kg}\cdot\text{m}^{-3}$; $\sigma_L = 0.073 \text{ kg}\cdot\text{s}^{-2}$; $\mu_G = 1.75 \times 10^{-5} \text{ Pa}\cdot\text{s}$; $\rho_G = 1.166 \text{ kg}\cdot\text{m}^{-3}$. However, the predictions were made for the actual experimental temperatures by using the corresponding values of the properties. The packing properties used in eq 14-16 for 1/2-in. ceramic Berl saddles were $d_p = 0.0125 \text{ m}$, $a_T = 465 \text{ m}^{-1}$, and $\sigma_c = 0.061 \text{ kg}\cdot\text{s}^{-2}$ (19, 25). Detailed results of the model predictions are given elsewhere (5).

Comparison of Observed and Predicted K_{La} Values. The relation between the predicted and observed values of K_{La} is shown in Figure 8 for each of the models tested. Shown are the 36 individual experiments (triplicates), whose averages are reported in Table II, giving a total of $N = 216$ experimental data points. The data encompass a range of approximately 20-fold in the observed values of K_{La} . The Onda model (19) gives the best overall fit, as evidenced by the tighter grouping of data around the diagonal line representing perfect agreement. This contradicts the widely accepted view (26) that Onda (19) erred in presuming that the interfacial area is proportional to the wetted area and that Shulman's approach to estimating the interfacial area (17) is intrinsically superior. The Shulman model (17) tends to underpredict K_{La} at the low end of the range and to overpredict at the high end. The Sherwood-Holloway (16) model predictions show a wide range of observed values corresponding to a single predicted value, especially at the low end of the range, as a result of improperly neglecting the gas-phase resistance.

The coefficients of determination, r^2 , for linear regressions of $\log(K_{La})_{\text{pred}}$ vs. $\log(K_{La})_{\text{obsd}}$ are given in Table III. The standard error of estimate, SEE, defined as

$$\text{SEE} = \left[\frac{(\log(K_{La})_{\text{pred}} - \log(K_{La})_{\text{obsd}})^2}{N} \right]^{1/2} \quad (20)$$

where N = number of observations, also is given in Table III. Goodness of fit can be inferred from high values of r^2 (approaching unity) and low values of SEE. By both measures, the Onda model fits the data better than either the Shulman or the Sherwood-Holloway models. Shulman's two-resistance model does not fit the data as well as does the single-resistance Sherwood-Holloway model, having a higher SEE value. The degree of difference can be quantified by comparing the SEE values: for Onda, SEE = 0.0845; for Shulman, SEE = 0.1983; for Sherwood-Holloway, SEE = 0.1257. Since SEE is expressed in log units, a value of SEE = 0.0845 implies that, for the

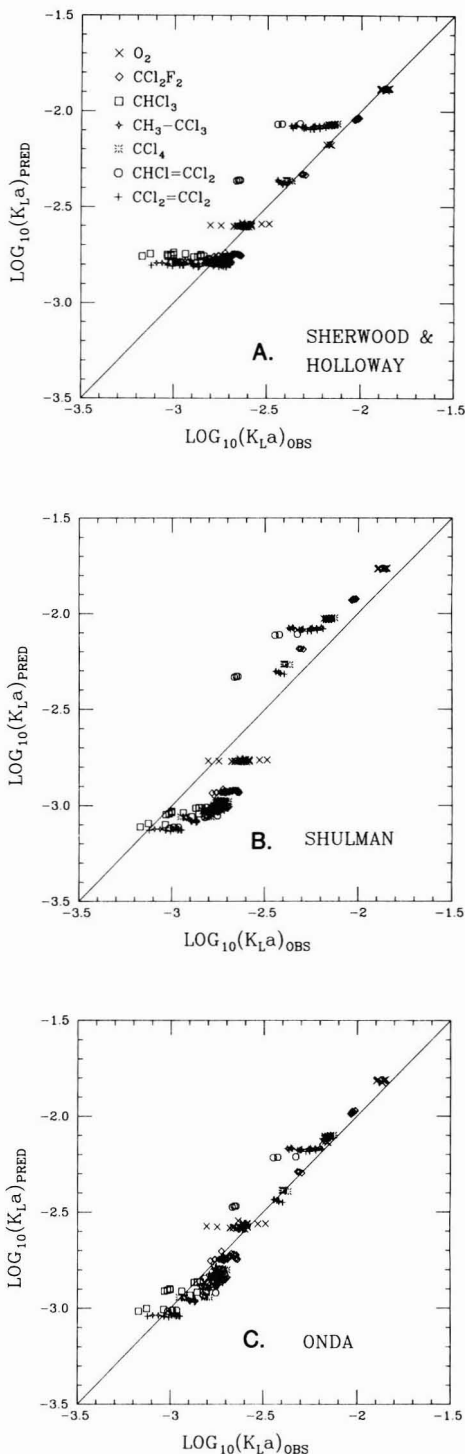


Figure 8. Agreement between observed and predicted values of the transfer rate constant. A, Sherwood-Holloway model (16); B, Shulman model (17); C, Onda model (19).

Onda model, 68% of the predicted values lie within a factor $10^{0.0845} = 1.21$ of the observed value. This statement of accuracy agrees closely with Onda's own assessment (19)

Table IV. Resistance Ratios for Gas Stripping in a Countercurrent Packed Tower

compd	H_c	Onda model predictions ^a					
		k_G/k_L at Q_G/Q_L			R_L/R_G at Q_G/Q_L		
		1	2.5	10	1	2.5	10
O ₂	30	4.2	6.3	11	120	190	330
CCl ₂ F ₂	10.9	3.6	5.5	9.7	39	60	105
CCl ₄	1.01	3.3	5.0	8.9	3.2	4.9	8.7
CCl ₂ =CCl ₂	0.63	3.5	5.4	9.4	2.1	3.2	5.7
CH ₂ CCl ₃	0.62	3.5	5.3	9.4	2.1	3.2	5.6
CHCl=CCl ₂	0.41	3.5	5.4	9.5	1.4	2.1	3.7
CHCl ₃	0.22	3.4	5.1	9.0	0.68	1.0	1.8

^a $L_M = 4.4 \text{ kg}\cdot\text{m}^{-2}\cdot\text{s}^{-1}$; $T = 293 \text{ K}$; packing = $1/2$ -in. ceramic Berl saddles.

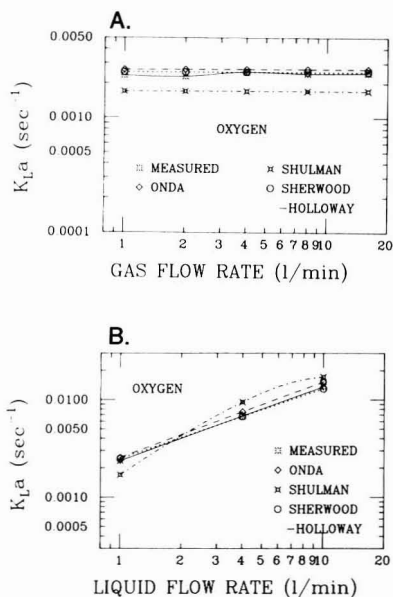


Figure 9. Dependence of predicted and observed K_La values for oxygen on the gas (A) and liquid (B) flow rates.

that the accuracy of the predictive model is on the order of $\pm 20\%$.

Further insight into the features of the models can be gained from comparing the responses of the predicted and observed K_La values to changes in the liquid and gas flow rates for individual compounds. These comparisons are shown in Figures 9 and 10 for two compounds: oxygen, a highly volatile constituent for which complete liquid-phase control is clearly demonstrated, and tetrachloroethylene, a moderately volatile compound for which the gas-phase resistance can be expected to exert some degree of influence on the transfer rate. With oxygen, both the Onda and Sherwood-Holloway models give a reasonable representation of the observed effects on Q_G and Q_L on K_La ; the value of K_La is independent of Q_G , as expected in a situation where the liquid-phase resistance controls. For tetrachloroethylene, on the other hand, the observed K_La shows an incipient decrease with decreasing Q_G at the low end of the range, symptomatic of increasing influence of the gas-phase resistance. The Onda model predicts this influence better than either of the two alternative models; the Onda model also predicts the effect of Q_L on tetrachloroethylene's K_La value better than do the other two models. Similar qualitative evidence of the superiority of the Onda model was seen with other compounds, under conditions where substantial influence of the gas-phase

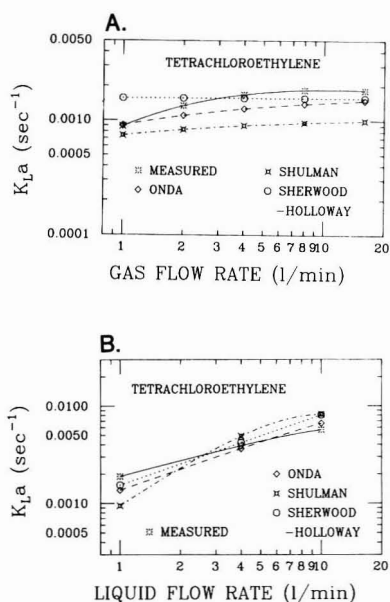


Figure 10. Dependence of predicted and observed K_La values for tetrachloroethylene on the gas (A) and liquid (B) flow rates.

resistance was predicted (5). However, the Sherwood-Holloway model predictions also agreed closely with observed values under conditions where neglecting the gas-phase resistance was justified (5).

Influence of Gas-Phase Resistance. Having validated the Onda model as an acceptable predictor of K_La under the conditions of this work, we now use the model in exploratory fashion to quantify the relative magnitudes of the liquid- and gas-phase resistances for the experiments reported here. The results of these calculations are given in Table IV. The significance of the gas-phase resistance is greatest for the less volatile solutes at low gas:liquid flow ratios, in accordance with two-resistance theory. The effect of gas:liquid flow ratio derives from the velocity dependence of k_L and k_G (eq 14 and 16). The ratio k_G/k_L accordingly decreases with decreasing gas:liquid ratio (Table IV). The values of k_G/k_L given in Table IV are in the range $3 < k_G/k_L < 11$, somewhat lower than the average value, $k_G/k_L \approx 25$, reported earlier for mechanical surface aeration (31) and at least an order of magnitude lower than is generally recommended (11, 32, 33). A lower value of the ratio k_G/k_L implies stronger influence of the gas-phase resistance. Equation 8 implies that the minimum value of H_c for assuring liquid-phase control by using the criterion $R_L/R_G > 10$ is in the range $0.3 < H_c < 1$ for gas:liquid ratios in the range $1 < Q_G/Q_L < 10$; the value of H_c

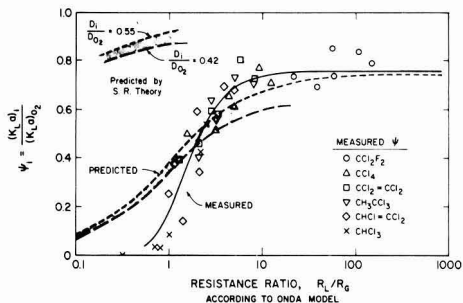


Figure 11. Test of the two-resistance theory in the mixed-resistance transition region.

must exceed the cited values of H_c to assure liquid-phase control. Concomitantly, for conditions similar to those in this work, the stripping factor must exceed a lower limit of approximately 10 to justify neglecting the gas-phase resistance.

Test of the Two-Resistance Theory. The Onda model, eq 13-16, in conjunction with the assumption of additivity of the individual phase resistances (eq 6-7) serves well for overall prediction of the transfer rate constants in this work (Figure 8 and Table III). To further test the model, the organic solute data were compared to those of oxygen by computing the ratio $\psi_i = (K_L a)_i / (K_L a)_{O_2}$, where ψ is a ratio of transfer rate constants, i is the solute index, and $(K_L a)_i$ and $(K_L a)_{O_2}$ are the observed values of $K_L a$ for compound i and oxygen in a given experiment. For oxygen, the liquid-phase resistance is thought to have controlled rate for all conditions in this work (Table IV). Hence, the ratio ψ_i is anticipated to rise with increasing $(R_L/R_G)_i$, beginning at $\psi_i = 0$ for $(R_L/R_G)_i = 0$ and asymptotically approaching a limit equal to $(D_i/D_{O_2})^{0.5}$, according to eq 14, as $(R_L/R_G)_i$ goes to infinity. The predicted values, estimated as

$$\psi_i = \left[\frac{(D_L)_i}{(D_L)_{O_2}} \right]^{0.5} \left(\frac{R_L/R_G}{1 + R_L/R_G} \right) \quad (21)$$

are shown in Figure 11 as a shaded sigmoidal band, corresponding to the range of ratios, $0.42 < (D_i/D_{O_2}) < 0.55$, that embraces the organic compounds in this work (Table I). The observed values, shown for comparison in Figure 11, are characterized by a similar sigmoidal shape. The predicted and measured relations both conform to the criterion that ψ_i reaches half its maximum value (i.e., $\psi_i = 0.5 \times 0.76 = 0.38$) at approximately $R_L/R_G = 1$, as anticipated. However, the measured values show a sharper transition from gas-phase to liquid-phase control than predicted by the Onda model. Whether this discrepancy represents a real deficiency of the model or an experimental artifact is not known, as the data in the region of low R_L/R_G ratios correspond to low values of S , for which the reliability is questionable. Nonetheless, this perspective serves as a warning that the two-resistance model recommended in this work, while offering an improvement over the simplistic assumption of liquid-phase control, may not predict behavior accurately over the mixed-resistance transition. The two-resistance model, although widely used over six decades, has been questioned on fundamental grounds by King (34), who pointed out the likelihood of significant deviations resulting from local differences in hydrodynamic conditions. The present study reaffirms the usefulness of the two-resistance approach but also documents the kind of deviation in the mixed-resistance domain that was anticipated on theoretical grounds by King (34).

Conclusions

Three semiempirical mass-transfer models—Onda, Shulman, and Sherwood-Holloway—were tested for their ability to predict, without adjustment of fitting parameters, the gas stripping of trace organic contaminants from aqueous solution. The two-resistance model of Onda provided the best overall fit, with a standard deviation of $\pm 21\%$ for the agreement between predicted and observed values of the transfer rate constant over a 20-fold range. For conditions similar to this work, the gas-phase resistance significantly affects the transfer rate and cannot be neglected (with less than 10% error) unless the stripping factor exceeds a minimum value of approximately 10. The two-resistance approach using the Onda correlations offers a satisfactory predictive ability in the range of conditions studied here, so long as the stripping factor exceeds unity. If the stripping factor decreases below unity, errors in experiment and estimation are magnified to such an extent that neither prediction nor quantitative interpretation is reliable. The two-resistance model predictions appear to deviate qualitatively from experimental behavior in the mixed-resistance region, indicating a more gradual transition from gas-phase to liquid-phase control than is observed. However, the present study was not designed to provide a rigorous test of two-resistance theory, because the gas-phase resistance was not directly measured. In any event, the two-resistance approach incorporating the Onda relations represents a significant improvement over the simplistic assumption of liquid-phase control.

Registry No. CH_2Cl_2 , 71-55-6; CCl_2F_2 , 75-71-8; CCl_4 , 56-23-5; $CCl_2=CCl_2$, 127-18-4; $CHCl=CCl_2$, 79-01-6; $CHCl_3$, 67-66-3; O_2 , 7782-44-7.

Literature Cited

- (1) McCarty, P. L.; Sutherland, K. H.; Graydon, J.; Reinhard, M. Proceedings of the AWWA Seminar on Controlling Organics in Drinking Water, AWWA, Denver, CO, 1979.
- (2) McCarty, P. L.; et al. Department of Civil Engineering, Stanford University, Stanford CA, 1980, Technical Report 236.
- (3) Singley, J. E.; Ervin, A. L.; Mangone, M. A.; Allan, J. M.; Land, H. H. "Trace Organics Removal by Air Stripping"; Environmental Science and Engineering, Inc.; Gainesville, FL, 1980.
- (4) Mumford, R. L.; Schnoor, J. L. *Annu. Conf. Proc. Am. Water Works Assoc.* 1982, 601-617.
- (5) Roberts, P. V.; Hopkins, G. D.; Munz, C.; Riojas, A. H. Office of Water Research and Technology, Washington, DC, 1982, Technical Report OWRT/RU-82/11.
- (6) Umphres, M. D.; Tate, C. H.; Kavanaugh, M. C.; Trussell, R. R. *J.-Am. Water Works Assoc.* 1983, 75, 414-418.
- (7) Cummins, M. D.; Westrick, J. J. *Proc. ASCE Environ. Eng. Conf.* 1983, 442-449.
- (8) Ball, W. P.; Jones, M. D.; Kavanaugh, M. C. *J. Water Pollut. Control Fed.* 1984, 56, 127-136.
- (9) Sherwood, T. K.; Pigford, R. L.; Wilke, C. R. "Mass Transfer"; McGraw-Hill: New York, 1975.
- (10) Treybal, R. "Mass Transfer Operations", 3rd ed.; McGraw-Hill: New York, 1980.
- (11) Kavanaugh, M. C.; Trussell, R. R. *J.-Am. Water Works Assoc.* 1980, 72, 684-692.
- (12) Kavanaugh, M. C.; Trussell, R. R. *Proc.-AWWA Semin. Org. Chem. Contam. Ground Water: Transp. Removal* 1981, 83-106.
- (13) Roberts, P. V.; Levy, J. A. *J.-Am. Water Works Assoc.*, in press.
- (14) Lewis, W. K.; Whitman, W. G. *Ind. Eng. Chem.* 1924, 16, 1215-1220.
- (15) Roberts, P. V.; Munz, C.; Dändliker, P.; Matter-Müller, C. Department of Civil Engineering, Stanford University, Stanford, CA, 1983, Technical Report 274.

- (16) Sherwood, T. K.; Holloway, F. A. L. *Trans. Am. Inst. Chem. Eng.* 1940, 36, 39-70.
- (17) Shulman, H. L.; Ulrich, C. F.; Proulx, A. Z.; Zimmerman, J. O. *AIChE J.* 1955, 1, 253-258.
- (18) Shulman, H. L.; Ulrich, C. F.; Wells, N. *AIChE J.* 1955, 1, 247-253.
- (19) Onda, K.; Takeuchi, H.; Okumoto, Y. *J. Chem. Eng. Jpn.* 1968, 1, 56-62.
- (20) Higbie, R. *Trans. Am. Inst. Chem. Eng.* 1935, 31, 265-388.
- (21) Vivian, J. E.; King, C. J. *AIChE J.* 1964, 10, 221-226.
- (22) Toor, H. L.; Marchello, J. M. *AIChE J.* 1958, 4, 97-101.
- (23) Skelland, A. H. P. "Diffusional Mass Transfer"; Wiley-Interscience: New York, 1974.
- (24) Onda, K.; Sada, E.; Murase, Y. *AIChE J.* 1959, 5, 235-239.
- (25) Fair, J. R.; Steinmeyer, D. E.; Penney, W. R.; Brink, J. A. "Chemical Engineers' Handbook", 5th ed.; Chilton, C. H., Ed.; McGraw-Hill: New York, 1973; Chapter 18.
- (26) Au-Yeung, P. H.; Ponter, A. B. *Can. J. Chem. Eng.* 1983, 61, 481-493.
- (27) Wilke, C. R.; Chang, P. *AIChE J.* 1955, 1, 264-270.
- (28) Lugg, G. A. *Anal. Chem.* 1968, 40, 1072-1077.
- (29) Wilke, C. R.; Lee, C. Y. *Ind. Eng. Chem.* 1955, 47, 1253-1257.
- (30) Munz, C., Stanford University, Stanford, CA, 1984, unpublished data.
- (31) Roberts, P. V.; Dändliker, P. G. *Environ. Sci. Technol.* 1983, 17, 484-489.
- (32) Mackay, D.; Leinonen, P. J. *Environ. Sci. Technol.* 1975, 9, 1178-1180.
- (33) Mackay, D.; Shiu, W. Y.; Sutherland, R. P. *Environ. Sci. Technol.* 1979, 13, 333-337.
- (34) King, C. J. *AIChE J.* 1964, 10, 671-677.

Received for review May 29, 1984. Accepted September 5, 1984. This research was supported by the Office of Water Research and Technology, Department of Interior, under Contract OWRT-14-34000-10474, Robert H. Madancy, Project Officer.

Lake Ontario Oxygen Model. 1. Model Development and Application

William J. Snodgrass* and Robert J. Dalrymple†

Department of Geography and Environmental Engineering, Johns Hopkins University, Baltimore, Maryland 21218

■ A mathematical model for dissolved oxygen has been formulated for Lake Ontario. The lake is treated as one box during winter circulation but as two boxes (epilimnion, hypolimnion) during summer stratification; inflows, outflows, vertical transport across the thermocline, atmospheric reaeration, photosynthesis, and decomposition are considered. For each year, temperature data are used to estimate the vertical exchange coefficient and the thermocline depth as a function of time. Predictions of the oxygen model show reasonable agreement with observations for a 9-year period. This agreement provides some verification for the model and for the application of the oceanic stoichiometry of Redfield to lakes. Model predictions and observations suggest that oxygen is transported from the hypolimnion to the epilimnion and from the epilimnion to the atmosphere during summer stratification. Vertical transport accounts for ca. 10% of the hypolimnetic loss of oxygen.

Introduction

The rapid loss of oxygen from the hypolimnia of lakes is a major water-quality problem of concern. In the extreme, it can induce fish kills, allow the development of noxious smells associated with methane and hydrogen sulfide production, and enhance the transport of substances from the sediments such as reduced metals (iron, manganese) and nutrients (phosphorus, ammonia).

Hypolimnetic oxygen consumption is usually attributed to the oxidation of organics from allochthonous and autochthonous sources and to sediment consumption. Allochthonous sources include eroded or soluble organics from woodland and agricultural areas and discharges from wastewater treatment plants and storm sewers. Autochthonous sources include particulate organic carbon (POC) derived from lysed algal and zooplanktonic cellular remains and soluble forms released during cell breakup.

Sediment consumption describes the flux of oxygen into the sediments for organic decay and the oxidation of reduced substances.

Other consumptive mechanisms which may be significant include algal respiration and the oxidation of ammonia. Algal respiration is particularly important in the euphotic zone; it may swamp the magnitude of bacterial respiration (1). Ammonia oxidation is caused by the use of ammonia as an energy source for growth by nitrifiers (e.g., *Nitrosomonas*, *Nitrobacter*). The nitrifiers may compete with phytoplankton for ammonia in the euphotic zone. They become particularly important in a small class of water bodies subjected to discharges of ammonia from wastewater treatment plants and industrial sources such as integrated steel mills (e.g., Hamilton Harbor (1)).

The development of quantitative tools for predicting the rate of development of hypolimnetic oxygen deficits has been long sought by managers of water quality and fisheries. This paper describes the development and application of one such tool for a class of lakes which are relatively deep, show only a small degree of hypolimnetic oxygen depletion during summer stratification, and are hypothesized to have their oxygen consumption controlled by the decomposition of organic substances formed in situ (i.e., autochthonous sources). Such lakes represent one of the spectrum of various lake classes (e.g., oligotrophic; eutrophic; allochthonous vs. autochthonous sources) which will need to be used over the long term for model testing.

Previous Work

Models for predicting the oxygen concentration in aqueous systems have received widest application in riverine and estuarine systems. The earliest models considered allochthonous sources of organics (e.g. (2) the discharge of sewerage) and physically described the river as a horizontal plug flow or dispersed plug flow system. Later efforts included autochthonous sources of organics, nitrification, and sediment oxygen demand (3-6) in deterministic models, or stressed stochastic aspects (7-9).

For lakes, the basic concepts stress autochthonous sources of organics and result from the work of several early limnologists (10-13). These concepts suggest that

* To whom correspondence should be addressed at Department of Chemical Engineering, McMaster University, Hamilton, Ontario, Canada, L8S 4L7.

† Present address: Ontario Ministry of Environment, West Central Region, Hamilton, Ontario, Canada, L8N 3Z9.

organic matter formation via algal growth and its subsequent sedimentation and decay can be related to the rate of nutrient supply from land-based sources and internal recycling. Empirical multiple regression models (14-16) have been used to relate hypolimnetic oxygen depletion rates to morphometry, nutrient inputs from land based sources, and nutrient retention factors.

Predictive oxygen models based upon mass balance concepts are much more scarce. One work assumes that oxygen decay in a reservoir is controlled by allochthonous sources (17, 18); consideration of sediment oxygen demand (19-21) improves the model fit in hypolimnetic waters. Whether allochthonous sources are the main determinant of oxygen decay requires further assessment. A few mass balance models have considered aspects of the oxygen question including relationships of oxygen production to consumption (22) and the significance of SOD to hypolimnetic oxygen concentrations (23, 24).

The physical description of oxygen models for lakes can be divided into two main forms—box models and dispersed plug flow (DPF) models. The former (24-26) typically describe the epilimnion overlying the hypolimnion (a two-box model) while the latter (17-24) provide further physical resolution by dividing the lake vertically into many slices of equal thickness. In the limit, as the thickness of slices increases, the DPF approaches the description of the box model.

Box models, the approach adopted in this work, have received less usage for oxygen than for other biochemical substances. Examples of relatively simple box models for oxygen include those of O'Connell and Thomas (4) and Bhagat et al., (25). The model of Chen and Smith (26) divides the lake into several layers and uses several boxes for each layer to provide horizontal resolution for biochemical substances (21 ecological entities and 14 chemical parameters). The utilization of simpler models provides insight into complex models and can suggest priorities for calibration of models such as those of ref 26 and 27.

The objective of the model described in this paper is to predict the seasonal and annual variations of oxygen in the epilimnion and hypolimnion of a lake. For this purpose, a two-box model is applied to Lake Ontario. The model assumes that oxygen consumption in the water column is controlled by autochthonous sources of organics and that the rate of formation of organics can be explained by the cycling of phosphorus between two forms: sol. orthophosphate and particulate phosphorus. It assumes that the ratio of oxygen consumption to particulate phosphorus decomposition can be explained by Redfield stoichiometry derived from the oceans. The model development, its application to Lake Ontario, and its testing are described comprehensively in Dalrymple (28); relevant details are summarized here. A similar model has also been subsequently tested in Hamilton Harbor (1) and two reservoirs in Southern Ontario (29).

Model Development

A two-box model for summer stratification and a one-box model for the nonstratified period are constructed for oxygen (see Figure 1). Stream inputs, hydraulic outflow, net production, reaeration, and vertical exchange across the thermocline influence epilimnetic oxygen concentrations ($[DO_e]$); net decomposition, sediment oxygen demand, and vertical exchange across the thermocline affect hypolimnetic oxygen concentrations ($[DO_h]$) during summer stratification. The winter model uses similar reactions except that production is confined to the euphotic zone while decomposition occurs throughout the lake. The models are coupled at the vernal and autumnal overturns.

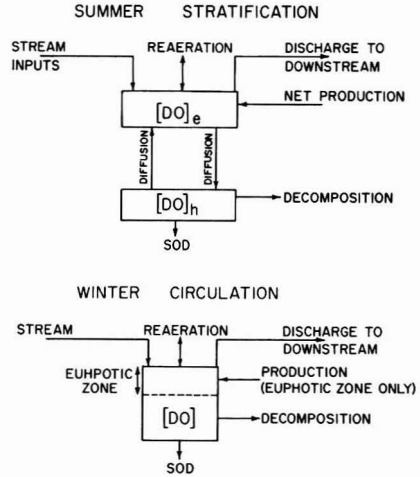


Figure 1. Oxygen transport mechanisms.

Because measurements of stream concentrations were not readily available, saturation conditions for riverine inflows are assumed.

The rate of oxygen production and oxygen consumption are estimated respectively from the rate of formation and rate of decomposition of particulate phosphorus predicted by a phosphorus model developed previously (30, 31). They are

$$\text{oxygen production} = Fp_e[OP_e]V_e \quad (1)$$

$$\text{oxygen decomposition} = Fd_n[PP_h]V_h \quad (2)$$

for summer stratification. The symbols are defined under Glossary. These formulations assume that, on a seasonal basis, the rate of autochthonous formation of organics and their subsequent decay is controlled by the rate of cycling of phosphorus within the lake.

Three fluxes across interfaces require formulation for summer stratification. Reaeration is described similarly to the Streeter-Phelps formulation as a mass transfer coefficient (\hat{k}_{aw}) times the difference between saturation and actual epilimnetic oxygen concentrations. It is

$$\text{reaeration} = \hat{k}_{aw}A_{\text{surf}}(DO_s - [DO_e]) \quad (3)$$

A similar expression is used to describe transport across the thermocline:

$$\text{vertical transport} = \hat{k}_{th}A_{th}([DO_e] - [DO_h]) \quad (4)$$

Both expressions (eq 3 and 4) describe net upward transport of oxygen if the oxygen concentration of deeper waters is larger. A zero-order expression is adopted to describe the flux of oxygen into the sediment:

$$\text{sediment transport} = \text{SOD} \cdot A_s \quad (5)$$

These developments result in a model consisting of six simultaneous, interdependent, linear differential equations for the stratification period and four for the winter circulation period. The equations are given in Table I. The model has several coefficients which require calibration (see next section) and requires estimates of the depth of the thermocline (Z_{th}), the vertical transport coefficient (\hat{k}_{th}) across the thermocline, and the surface temperature (to permit calculation of DO_s).

The Canada Centre for Inland Waters and its processor organizations have obtained measurements of water chemistry and temperature for Lake Ontario since 1966 in a routine fashion. Data stored on the CCIW computer

Table I. Equations for Oxygen Model

Summer Stratification

(i) epilimnion

$$[DO_e]: V_e d[DO_e]/dt = DO_{sat}Q - Q[DO_e] + Fp_e V_e [OP_e] + \hat{k}_{aw} A_{surf}(DO_s - [DO_e]) + \hat{k}_{th} A_{th}[DO_h] -$$

net rate of change input: from tributaries output: hydraulic discharge net production atmospheric reaeration vertical exchange from hypolimnion

$$\hat{k}_{th} A_{th}[DO_e]$$

vertical exchange to hypolimnion

(1)

$$[OP_e]: V_e d[OP_e]/dt = \Sigma Q_j [TP_j] - Q[OP_e] - p_e V_e [OP_e] + \hat{k}_{th} A_{th}[OP_h] - \hat{k}_{th} A_{th}[OP_e]$$

net rate of change input: loading from land-based sources output: hydraulic discharge net production vertical exchange from hypolimnion vertical exchange to hypolimnion

(2)

$$[PP_e]: V_e d[PP_e]/dt = -Q[PP_e] + p_e V_e [OP_e] - g_e A_{th}[PP_e] + \hat{k}_{th} A_{th}[PP_h] - \hat{k}_{th} A_{th}[PP_e]$$

net rate of change output: hydraulic discharge net production settling to hypolimnion vertical exchange from hypolimnion vertical exchange to hypolimnion

(3)

(ii) hypolimnion

$$[DO_h]: V_h d[DO_h]/dt = -F d_h V_h [PP_h] - SODA_s + \hat{k}_{th} A_{th}[DO_e] - \hat{k}_{th} A_{th}[DO_h]$$

net rate of change decomposition sediment demand vertical exchange from epilimnion vertical exchange to epilimnion

(4)

$$[OP_h]: V_h d[OP_h]/dt = d_h V_h [PP_h] + \hat{k}_{th} A_{th}[OP_e] - \hat{k}_{th} A_{th}[OP_h]$$

net rate of change decomposition vertical exchange from epilimnion vertical exchange to epilimnion

(5)

$$[PP_h]: V_h d[PP_h]/dt = g_e A_{th}[PP_e] - g_h A_s [PP_h] - d_h V_h [PP_h] + \hat{k}_{th} A_{th}[PP_e] - \hat{k}_{th} A_{th}[PP_h]$$

net rate of change input: settling from epilimnion output: settling to sediments decom- position vertical exchange from epilimnion vertical exchange to epilimnion

(6)

Winter Circulation

$$[DO]: Vd[DO]/dt = DO_{sat}Q - Q[DO] + Fp_{eu} V_{eu}[OP] - FdV[PP] - SODA_s + k_{aw} A_{surf}(DO_s - [DO])$$

net rate of change input: from tributaries output: hydraulic discharge gross production decom- position sediment demand atmospheric reaeration

(7)

$$[OP]: Vd[OP]/dt = \Sigma Q_j [TP_j] - Q[OP] - p_{eu} V_{eu}[OP] + dV[PP]$$

net rate of change input: loading from land-based sources output: hydraulic discharge production in euphotic zone decom- position

(8)

$$[PP]: Vd[PP]/dt = -Q[PP] + p_{eu} V_{eu}[OP] - dV[PP] - gA_s [PP]$$

net rate of change output: hydraulic discharge production in euphotic zone decom- position settling to sediments

(9)

system were obtained and analyzed (see ref 28 for details). The general approach was to estimate lake wide average temperature with depth for any one cruise, estimate the thermocline depth, and then resolve the data into epilimnetic and hypolimnetic components. The rate of deepening of the thermocline varies from 0.8 m/month in 1967 to 5.8 m/mon in 1972; the average rate for all years is 3.6 m/month (28, 32).

From a heat balance upon the hypolimnion, seasonal estimates for the vertical exchange coefficient (\hat{k}_{th}) give values which range from 0.07 (1968) to 0.15 m/day (1972). These estimates do not include the effects of thermocline deepening upon \hat{k}_{th} . A comparison of including or excluding entrainment in the parameterization of \hat{k}_{th} (see ref 33) shows that the different parameterizations have small effects upon the predictions of hypolimnetic dissolved

oxygen (DO_h) and of epilimnetic dissolved oxygen (DO_e) in Lake Ontario.

Inspection of the values of \hat{k}_{th} and the rate of thermocline deepening show some correlation with wind conditions. For example, the rate of deepening is highest in 1966 and in 1972 (post-Hurricane Agnes) and lowest in 1967. Average wind speeds are higher in 1966 than 1967 (34).

The variation in DO_e is estimated from the mean surface temperatures (0–1 m) for 1966–1973 and the relationship (17) $DO_e = 14.48 - 0.36T + 0.0043T^2$. Analysis of the surface temperature data (28) for the period 1966–1974 gives a relationship as a function of time.

for $0.1 \leq t \leq 5.31$ and $D = t$

$$T = (0.1584D - 0.5972)D + 2.6058 \quad (6a)$$

for $5.31 \leq t \leq 6.61$, and $d = t - 5.31$

$$T = [(-1.4288D + 1.9278)D + 6.9978]D + 9.1264 \quad (6b)$$

for $6.61 \leq t \leq 12.00$ and $D = t - 6.61$

$$T = [(0.4278D - 3.6162)D + 4.8140]D + 18.3106 \quad (6c)$$

where t = time (months), T = surface temperature ($^{\circ}C$), and D = dummy variable. The curve is obtained by fitting a third-order polynomial using a least-squares procedure (CUBIC SPLINES, a software package available on the CDC Computer System).

Analysis of the hypsometric curve for the lake (obtained with thanks from CCIW) gives the following relationship between surface area or lake volume and lake depth.

for $0 < Z \leq 43$ m

$$A = (-126Z + 18300) \times 10^6 \quad (7a)$$

$$V = (-63Z^2 + 18300Z) \times 10^6 \quad (7b)$$

for $34 < Z \leq 182$ m

$$A = (-86.4Z + 16920) \times 10^6 \quad (7c)$$

$$V = (-43.2Z^2 + 16920Z) \times 10^6 \quad (7d)$$

for $Z > 182$ m

$$A = (-41.4Z + 9100) \times 10^6 \quad (7e)$$

$$V = (-20.7Z^2 + 9100Z) \times 10^6 \quad (7f)$$

A has units of m^2 and V of m^3 . These equations are used to describe the time trend of the volume of the epilimnion and hypolimnion from the thermocline–time relationship.

Model Calibration and Verification

The approach of this research is to adopt the model coefficients developed previously for the phosphorus model (30, 31) because, although it was calibrated with Lake Ontario data, its application to other lakes provided verification of its predictions for total phosphorus. The actual seasonal variation of Z_e and actual values of \hat{k}_{th} are used in place of those of ref 31. The model assumes that summer stratification commences on June 15 and ends on Oct 15 of each year (28) and that the phosphorus loading rate is constant [$0.68 \text{ g}/(\text{m}^2 \cdot \text{year})$; see ref 31]. With adoption of these coefficient values and external data, the only model coefficients requiring calibration are F , k_{aw} , and SOD. The coefficients are calibrated by using literature data and/or data on Lake Ontario for 1966 and 1969 and verified by using data from other years.

For oceanic conditions, relationships between algal formation, oxygen production, and nutrient uptake have

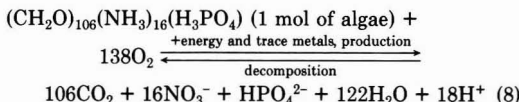
Table II. Ratios of C, N, and P (A) and Concentration Data (B) in Particles for Lake Ontario during IFYGL^a

(A) Ratios of C, N, and P						
depth in lake, m	C:N:P			C:N		
	ratio	C.V.		ratio	C.V.	
		C:P	N:P			
0–20	123:16.3:1	0.29	0.36	7.7 ^b	0.16	
20–40	118:16:1	0.22	0.19	7.5 ^b	0.16	
>40	134 ^b :17:1	0.27	0.31	7.8 ^b	0.22	

(B) Concentration Data						
depth in lake, m	POC		PN		PP	
	[POC], μM	C.V.	[PN], μM	C.V.	[PP], μM	C.V.
0–20	18	0.31	3.9	0.58	0.22	0.28
20–40	19	0.29	2.6	0.27	0.16	0.16
>40	15	0.17	1.8	0.24	0.11	0.22

^aC.V., coefficient of variation = standard deviation/mean; POC, particulate organic carbon; PN, particulate nitrogen; particulate phosphorus. ^bThese values are significantly different than Redfield stoichiometry (C:P = 106; N:P = 16; C:N = 6.6) at the 5% level of significance (two-tailed, Student's t test).

been quantified and incorporated into the Redfield stoichiometric equation. It can be expressed as follows (35):



Stoichiometrically, the equation predicts that production or decomposition of 1 μg of particulate phosphorus is associated with the production or consumption of 0.14 mg of oxygen.

The validity of this equation cannot be assessed directly for oxygen, but observations about other aspects can be made by examining concentrations of POC, particulate nitrogen (PN), and particulate phosphorus (PP) and their ratios in these particulate fractions in Lake Ontario (see Table II). The data of Table II are averages from 17 quasihomogeneous zones in Lake Ontario (see ref 36 for raw data) during the period April 1972–April 1973. The coefficient of variation for the ratios (Table IIA) is somewhat larger than that for the concentration data (Table IIB), suggesting that the ratios explain some variability in the concentration data. Of the various ratios, only the C:P ratio for depths greater than 40 m and all N:P ratios are significantly different from that of Redfield stoichiometry at the 5% level of significance. The C:P ratios and all of the N:P ratios are not significantly different.

F is calibrated by assigning it a value of 0.14 mg of $\text{O}_2/\mu\text{g}$ of P. Successful prediction of the rate of hypolimnetic oxygen depletion without recalibration of F or d_h will provide some verification for the flux predicted by the phosphorus model and for the application of Redfield stoichiometry derived from the oceans to large lakes. If the C:P ratio in the lake is 123:1 (C:N = 7.7:1, N:P = 16:1) as suggested by the data of Table I rather than 106:1, the rate of oxygen consumption would increase by 17% [$(7.7/6.6 - 1)100\%$] and F would equal 0.16.

Values for SOD typically range from 0.1 to 0.2 g/($\text{m}^2 \cdot \text{day}$) (37) for freshwater sediments although values to 1.0 g/($\text{m}^2 \cdot \text{day}$) are observed in eutrophic water bodies (38). It was hypothesized that SOD would be low because the lake bottom is covered by large areas of postglacial muds con-

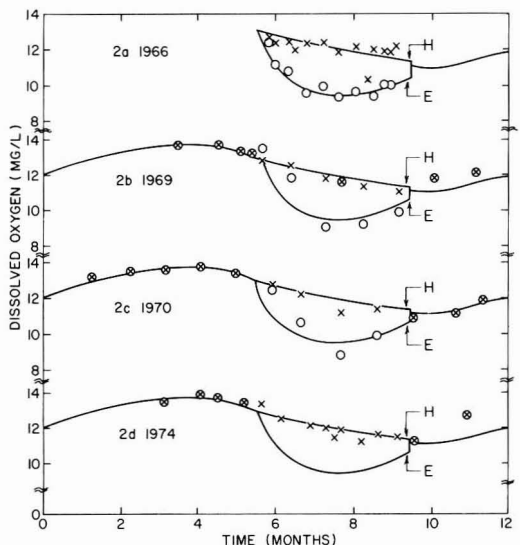


Figure 2. Model predictions of dissolved oxygen compared to observations for Lake Ontario. (O) Epilimnion; (X) hypolimnion; (—) model; E, epilimnion; H, hypolimnion. (a, b) Calibration; (c, d) verification.

sisting of 2–6% organic matter. A value for SOD of 0.1 g/(m²-day) was chosen for use by Dalrymple (28). Sulfate reduction (39) is equivalent to 0.022 g of O₂/(m²-d); an oxygen-sulfate model if available could be used to refine estimates of SOD.

SOD measurements subsequently reported (40) give a lake-wide average of 0.24 g of O₂/(m²-day). Because current velocities employed in a similar SOD chamber appear to cause high estimates for SOD in Lake Erie (41), these measured values are probably high. The value for SOD of 0.1 g/(m²-day) is retained because model predictions show good agreement with observations—the model overpredicts the rate in 1966 and underpredicts the rate in 1969 (see Figure 2) by small amounts.

Compared to measurements for k_{th} and SOD, estimates in the lake literature for k_{aw} are much more sparse. Values for rivers of the order of 0.5–37 m/day (42–46) have been formalized into relationships as a function of such parameters as stream velocity (e.g. ref 47). These relationships assume that the energy of river flow control the rate of reaeration. For lakes, it is expected that wind conditions would be the energy source controlling reaeration. Preliminary efforts in this direction are being formalized (e.g., ref 48). The typical range for k_{aw} is 0.3–9 m/day (see Table III). For initial calibration trials, 7.5 m/day was selected.

Model calibration studies for k_{aw} are carried out by using 1966 data for the stratification period and 1969 data for the circulation period. Model verification is attempted by comparing model predictions for the period 1966–1974. The calibration studies suggested that $k_{aw} = 7.5$ m/day gives good results during the winter circulation period but underpredicts DO_o, particularly during the first half of the stratification period. A value of k_{aw} of 2 m/day gave the most reasonable results for summer stratification. This correlates with climatological information which shows winds to be stronger in winter than in summer (51).

Representative model predictions for the period 1966–1974 are shown in Figures 2a–d for 1966, 1969, 1970, and 1974, respectively. Parts a and b of Figure 2 represent calibration studies while parts c and d are verification figures. The agreement between model prediction and

Table III. Representative Values of Reaeration Coefficients Observed for Lakes

investigator	description of study	range of K, m/day
Bella (23)	modeling study on oxygen in Lake Sammamish	1–8.6
Rumer and Melfi (49)	modeling study of Lake Sammamish	7.5
Sivakumar and Herzog (48)	field data	0.25–3
Torgersen et al. (50)	measurement using tritium-helium-3 ^a	
	Lake Huron (August)	1–1.8
	Lake Erie (early September)	1.4
	Lake Ontario	0.8–1.0

^a Calculations made herein. They (50) calculated a value for the ³He mass transfer coefficient from experimental measurements. This work assumes similar resistance properties in surface film for ³He and O₂ but corrects for differences in molecular diffusivity coefficients (4.42 × 10⁻⁵ for ³He and 2.11 × 10⁻⁵ cm²/s for O₂ at 20 °C).

observations is generally good; the fit is significant at the 5% level. This provides some verification for the reaeration rates selected and the application of Redfield stoichiometry to decomposition processes in lakes (see ref 52 and 53 for discussion concerning the modeling process and model verification). Some deviation between model predictions and observations for [DO_o] is noted during the early stratification period in 1969 and 1970; this deviation is caused by the assumption that stratification commences each year on June 15 rather than on the actual date.

Model predictions and observations show that the epilimnetic concentrations of oxygen are always lower than those for the hypolimnion. Accordingly vertical exchange transports (“pumps”) oxygen from the hypolimnion to the epilimnion during stratification, and reaeration transports (“pumps”) oxygen from epilimnion to the atmosphere during the first portion of summer stratification. These transport features are characteristic of a few of the Great Lakes and opposite of that observed for most lakes. The slow rates of loss explain the observation of Chen and Smith (26) that the high DO content of the cooler hypolimnetic waters appears to be “locked inside” the lake system.

For the hypolimnion, there are three main sources of oxygen loss: vertical exchange, decomposition, and SOD. For the 1966–1974 period, the model predicts that the average loss rates are respectively 0.20, 0.84, and 0.1 g/(m²-day). Observations indicate that the loss rates are 0.19 and 1.0 g/(m²-day), respectively, for vertical exchange and decomposition when SOD is assumed to be 0.1 g/(m²-day). This comparison provides some additional validation of the model's predictions, although the comparison of observations and predictions are connected; the same vertical exchange coefficients are used both for calculating the values of the observations and in the model for its predictions.

Accordingly the model can be considered to be verified for one class of lakes. Model verification should be achieved by using a data set which is independent of the data set used for model calibration (see ref 52). By obtaining agreement with observations for the 1966–1974 period, model predictions are not initial value governed, suggesting that the data for 1974 is independent of those for 1966 and 1969. Model testing on lakes with higher rates of hypolimnetic oxygen consumption would more severely test the model and hence provide more confidence in its predictions.

Model Analysis

This section (i) presents a sensitivity analysis and (ii) examines three aspects of the model (phosphorus loading, $[DO_h]$ entrainment by the epilimnion, and reaeration).

A sensitivity analysis of the model's predictions at 60 and 120 days after the start of stratification to variations of the model's coefficients has been made (28). The analysis proceeded by changing the coefficient from its standard value to the new value at the beginning of summer stratification. The overall changes in model predictions (0–9%) are small even for a 100% perturbation of model coefficients because the model is strongly initial value governed. Model predictions for $[DO_h]$ are sensitive in decreasing order of significance to the following: (1) F , the dissolved oxygen/phosphorus stoichiometric factor; (2) k_{th} , the vertical exchange coefficient; (3) d_h , the particulate phosphorus decomposition coefficient; (4) SOD, the rate of consumption of oxygen by the sediments. Model predictions for $[DO_e]$ at the end of stratification are insensitive to all parameters.

Inspection of eq 2 would suggest that predictions of dissolved oxygen should be equally sensitive to F and to d_h . They are not because a change in d_h also induces changes in $[PP_h]$. For example, an increase in d_h causes a decrease in $[PP_h]$ and results in a decomposition flux, $d_h[PP_h]$, which does not linearly respond to a change in d_h .

The sensitivity analysis also provides information for assessing errors associated with the use of a constant annual phosphorus loading W . The model assumes a constant annual loading for 1966–1974, whereas the actual loadings are estimated to have increased from 31 ton/day (0.61 g/(m²·day)) in 1967 to 40 ton/day in 1969 and to have decreased to 25 ton/day in 1977 (36, 54, 55). The peak loading is 15% higher than that used in the model; for a step change in loading, the phosphorus model predicts that 88% of a new steady-state concentration is achieved in 7 years (30). For one stratification period, the sensitivity analysis indicates a decrease of 0.2% in DO_h , while over 7 years, the decrease would be 13%. The error associated with not considering a variable loading pattern is less than 13%.

Another error of concern is the mathematical treatment of entrainment. The formulation given (Table I) allows the epilimnion to increase and the hypolimnion to decrease with time due to entrainment, but the new epilimnetic waters are assumed to have the same concentration as the remainder of the epilimnion. Entrainment should be formulated such that the epilimnetic concentration after entrainment is equal to the mass of oxygen in the old volume of the epilimnion plus the mass of oxygen in the entrained water divided by the new epilimnetic volume. Assessment of this error (33) shows that it is insignificant for predictions of $[DO_h]$.

The last analysis to be considered concerns the role of reaeration upon epilimnetic oxygen concentrations. For $[DO_e]$, the preliminary calibration for 1966 (28) suggested that a value for k_{aw} of 7.5 m/day caused model predictions for $[DO_e]$ to level off too early during summer stratification whereas a value of 2 m/day gave a longer response time (ca. 2 months). But analysis of the response time (33) suggests that the new pseudo-steady-state concentration is reached within days with either the value of 2 or 7.5 m/day. This is explained as follows. The value for $[DO_e]$ is always above saturation—when there is a net source of oxygen in the epilimnion (photosynthesis) and when $[DO_h]$ is pumped into the epilimnion by vertical exchange, the steady-state concentration of $[DO_e]$ is always higher than

DO_s . Larger values of k_{aw} cause $[DO_e]$ to approach closer to saturation conditions than lower values of k_{aw} . The value of k_{aw} for 2 m/day gives a steady-state value for $[DO_e]$ which is 0.6 mg/L larger than does a value of 7.5 m/day. Hence, the calibration of k_{aw} controls the predicted value of $[DO_e]$ but not its time trend; the time trend $[DO_e]$ in Figure 2 is controlled by the time trend of DO_s .

Summary

The development of a two-box model for oxygen in Lake Ontario is presented in this paper. Prediction of the rate of oxygen production in the epilimnion and oxygen decomposition in the hypolimnion is made by using Redfield stoichiometry and a two-box, two-compartment model for phosphorus previously verified to make predictions for total phosphorus concentration. Of the remaining model coefficients, vertical transport across the thermocline and the rate of descent of the thermocline are calculated from temperature data, and SOD and the reaeration coefficient are selected by calibration studies.

The following statements are made based on these analyses.

(1) Model predictions show reasonable agreement with observations for a 9-year period. This provides some verification for the oxygen depletion flux predicted by the phosphorus model and the application of Redfield stoichiometry derived from the oceans to lakes. This also provides some verification for using box models for predicting seasonal trends of dissolved oxygen. This verification is viewed as incomplete.

(2) For further refinement of this model or that of others (26), the sensitivity analysis suggests that the following is the order of priority: the quantity of oxygen consumed per unit of organics oxidized, the rate of vertical transport across the thermocline, the rate of consumption of organics (particulate phosphorus decomposition), and the SOD.

(3) The model and observed data imply that oxygen is pumped from the hypolimnion to the epilimnion and to the atmosphere throughout summer stratification in Lake Ontario. Of the mean hypolimnetic oxygen depletion rate of 1.3 g of O₂/(m²·day), vertical transport accounts for ca. 10% of the loss.

Acknowledgments

The cooperation of various scientists at CCIW and especially Robert Duffield of the CCIW Computer Centre in providing the cruise data is gratefully acknowledged. Conversations concerning various aspects of this work with F. Boyce, D. Lam, M. F. Holloran, D. M. DiToro, P. J. Dillon, and C. R. O'Melia are gratefully acknowledged.

Glossary

Species

[DO]	concentration of dissolved oxygen, ML ⁻³
DO_s	saturation concentration of dissolved oxygen, ML ⁻³
[OP]	concentration of orthophosphate, ML ⁻³
[PP]	concentration of particulate phosphorus, ML ⁻³

Parameters

A	interfacial area, L ²
BOD	biochemical oxygen demand
d	decomposition rate coefficient, T ⁻¹
DPF	dispersed plug flow
F	redfield stoichiometric factor
g	effective settling velocity, LT ⁻¹
k	vertical exchange coefficient, LT ⁻¹
L_a	areal phosphorus loading rate, ML ⁻² T ⁻¹
P	net production rate coefficient, T ⁻¹

Q	volumetric rate of lake discharge, L^3T^{-1}
Q_j	volumetric rate of inflow of water from tributary j , L^3T^{-1}
SOD	sediment oxygen demand, $ML^{-2}T^{-1}$
V	volume, L^3
W	phosphorus input rate, MT^{-1}
Z	mean depth, L

Subscripts

aw	air water interface
e	epilimnion
eu	euphotic zone
h	hypolimnion
th	thermocline region
s	sedimentation-water interface
surf	lake surface

Registry No. O₂, 7782-44-7; P, 7723-14-0.

Literature Cited

- Ng, P. M. Eng. Thesis, McMaster University, Hamilton, Ontario, 1981, pp 1-236.
- Streeter, H. W.; Phelps, E. B. "A Study of the Pollution and Natural Purification of the Ohio River". U.S. PHS, Washington, DC, 1925, Public Health Bulletin 146.
- Dobbins, W. E., *J. Sanit. Eng. Div., Am. Soc. Civ. Eng.* **1964**, *90* (SA3), 53-78.
- O'Connell, R. L.; Thomas, N. A. *J. Sanit. Eng. Div., Am. Soc. Civ. Eng.* **1965**, *91* (SA3), 1-16.
- Edwards, R. W.; Rolley, H. L. *J. Ecol.* **1965**, *53*, 1-19.
- O'Connor, D. J. *Water Resour. Res.* **1967**, *3* (1), 65-79.
- Thayer, R. P.; Krutchkoff, R. G. *J. Sanit. Eng. Div. Am. Soc. Civ. Eng.* **1967**, *93* (SA3), 59-72.
- Thomann, R. V. *J. Sanit. Eng. Div., Am. Soc. Civ. Eng.* **1967**, *93* (SA1), 1-23.
- Huck, P. M.; Farquhar, G. J. *J. Environ. Eng. Div. (Am. Soc. Civ. Eng.)* **1974**, *100* (EE3), 733-752.
- Thienemann, A.; *Der Nahrungskrieslauf im Wasser. Verh. Dtsch. Zool. Ges.* **1926**, *2*, 29-79.
- Hutchinson, G. F. *Int. Rev. Gesamtem Hydrobiol.* **1938**, *36*, 336-355.
- Hutchinson, G. F. "A Treatise on Limnology"; Wiley: New York, 1957; Vol. 1.
- Ohle, W. *Limnol. Oceanogr.* **1956**, *1*, 139-149.
- Cornell, R. J.; Rigler, F. H. *Science (Washington, D.C.)* **1979**, *205*, 580-581.
- Cornell, R. J., & Rigler, F. H. *Limnol. Oceanogr.* **1980**, *25* (4), 672-679.
- Vollenweider, R. A.; Janus, L. L. *Mem. Ist. Ital. Idrobiol.* **1982**, *40*, 1-24.
- Markofsky, M.; Harleman, D. R. F. "Predictive Model for Thermal Stratification and Water Quality in Reservoirs". Ralph M. Parsons Laboratory, Massachusetts Institute of Technology, Boston, MA, 1971, Technical Report No. 134.
- Markofsky, M.; Harleman, D. R. F. *J. Hydraul. Div., Am. Soc. Civ. Eng.* **1973**, *99*, 729-745.
- Snodgrass, W. J.; Holloran, M. F. *Water Pollut. Res. Can.* **1977**, *12*, 135-156.
- Snodgrass, W. J.; Holloran, M. F. *Can. Water Resour. J.* **8**(3), 1-25.
- Snodgrass, W. J. *J. Environ. Eng. Div. (Am. Soc. Civ. Eng.)* **1983**, *109*, 1424-1429.
- Wright, J. C. *Limnol. Oceanogr.* **1961**, *6*, 330-337.
- Bella, D. R. *J. Sanit. Eng. Div., Am. Soc. Civ. Eng.* **1970**, *96* (SA5), 1129-1146.
- Newbold, J. D.; Higgett, J. A. *J. Environ. Eng. Div. (Am. Soc. Civ. Eng.)* **1974**, *100* (EE1) 41-59.
- Bhagat, S. K.; Fink, W. H.; Johnstone, D. L. "Correlated Studies of Vancouver Lake-Water Quality Prediction Study" 1972, EPA-R2-72-111.
- Chen, C. W.; Smith, D. J. In "Perspectives on Lake Ecosystem Modelling"; Scavia, D., Robertson, A., Eds.; Ann Arbor Science: Ann Arbor, MI, 1979; pp 249-279.
- Scavia, D. *Ecol. Modell.* **1980**, *8*, 49-78.
- Dalrymple, R. J. M. Eng. Thesis, McMaster University, Hamilton, Ontario, 1977, pp 1-184.
- Snodgrass, W. J. *Can. Water Resour. J.* **1982**, *7* (1), 397-415.
- Snodgrass, W. J. Ph.D. Dissertation, University North Carolina, Chapel Hill, NC, 1974, pp 1-309.
- Snodgrass, W. J.; O'Melia, C. R. *Environ. Sci. Technol.* **1975**, *9*, 937-944.
- Snodgrass, W. J. In "Transport Processes in Lakes and Oceans"; Gibbs, R. J. Ed.; Plenum Press: New York, 1977; pp 175-199.
- Snodgrass, W. J. *Environ. Sci. Technol.*, following paper in this issue.
- Sweers, H. E. *Limnol. Oceanogr.* **1970**, *15*, 273-280.
- Stumm, W.; Morgan, J. J. "Aquatic Chemistry"; Wiley: New York, 1981.
- CCIW (Canada Centre for Inland Waters) "Assessment of Water Quality Simulation Capability for Lake Ontario"; CCIW: Burlington, Ontario, 1979.
- Sonzogri, W. C.; Larsen, D. P.; Malueg, K. N.; Schuldt, M. D. *Water Res.* **1977**, *11*, 461-464.
- Walker, R. R. M. Eng. Thesis, McMaster University, Hamilton, Ontario, 1980, pp 1-244.
- Nriagu, J. O.; Coker, R. D. *Limnol. Oceanogr.* **1976**, *21* (4), 485-489.
- Thomas, N. A. "Sediment Oxygen Demand and Dissolved Oxygen Properties of Lake Ontario during IFYGL". Large Lakes Research Station, U.S. EPA, Grosse Ile, MI, 1982, unpublished data.
- Snodgrass, W. J.; Faye, L. "Measurement of Sediment Oxygen Demand in Lake Erie using Two Different Chambers". 1983, unpublished data.
- Banks, R. B. *J. Environ. Eng. Div. (Am. Soc. Civ. Eng.)* **1975**, *101* (EES), 813-827.
- Banks, R. B. *J. Environ. Eng. Div. (Am. Soc. Civ. Eng.)* **1977**, *103*, 489-504.
- Churchill, M. A.; Elmore, H. L.; Buckingham, R. A. *J. Sanit. Eng. Div., Am. Soc. Civ. Eng.* **1962**, *88* (SA4), 1-46.
- Churchill, M. A.; Nicholas, W. R. *J. Sanit. Eng. Div., Am. Soc. Civ. Eng.* **1967**, *93* (SA6), 73-90.
- Juliano, D. W. *J. Sanit. Eng. Div., Am. Soc. Civ. Eng.* **1969**, *95* (SA6), 1165-1178.
- O'Connor, D. J.; Dobbins, W. E. *Trans. Am. Soc. Civ. Eng.* **1958**, *64*, 6-66.
- Sivakumar, M.; Herzog, A. In "Hydrodynamics of Lakes"; Graf, W. H.; Mortimer, C. H., Eds.; Elsevier: Amsterdam, 1979; pp 331-340.
- Rumer, R. R.; Melfi, D. paper presented at the 1973 Northeast Regional Meeting of the American Chemical Society, Rochester, NY 1973.
- Torgersen, T.; Top, A.; Clarke, W. B.; Jenkins, W. J.; Broecker, W. S. *Limnol. Oceanogr.* **1977**, *22*, 181-193.
- Phillips, D. W.; McCulloch, J. A. W. "Climate of the Great Lakes Basin". Atmospheric Environmental Services, Environment Canada, Downsview, 1972, Climatological Studies No. 20.
- Snodgrass, W. J. In "Perspectives in Lake Ecosystem Modelling"; Scavia, D.; Robertson, A., Eds.; Ann Arbor Science: Ann Arbor, MI, 1979.
- Thomann, R. V. *J. Environ. Eng. Div. (Am. Soc. Civ. Eng.)* **1982**, *108*, 923-940.
- Willson, K. E. "Nutrient Loadings to Lake Ontario 1967-1978". Canada Centre for Inland Waters, 1978, unpublished report.
- Fraser, A. S. *J. Great Lakes Res.* **1980**, *6* (1), 83-87.

Received for review February 17, 1983. Revised manuscript received November 16, 1983. Accepted September 13, 1984. This research was supported by a Canadian National Research Council fellowship to R.J.D. while he was a master's candidate, by computer funds provided by a NRC operating grant to W.J.S., and by the financial support of McMaster University and The Johns Hopkins University.

Lake Ontario Oxygen Model. 2. Errors Associated with Estimating Transport across the Thermocline

William J. Snodgrass*

Department of Geography and Environmental Engineering, The Johns Hopkins University, Baltimore, Maryland 21218

■ Errors associated with ignoring entrainment of hypolimnetic waters into the epilimnion in two-box models are examined for dissolved oxygen. The effects of entrainment upon modeling and estimating the mass transfer coefficient across the thermocline are also analyzed. Use of Eulerian and semi-Lagrangian box models are contrasted. For epilimnetic dissolved oxygen, neglecting the upward transport of oxygen by entrainment has a maximum error of 5%. A model for estimating the vertical transport coefficient, which uses a heat budget for the hypolimnion and which includes the entrainment process, is developed. For estimation of this coefficient, the temperature either in the hypolimnion or in the thermocline may be used; qualitative arguments are presented for selection of the thermocline temperature. Available data suggest that the entrainment rate in Lake Ontario varies from 1 to 6 m/month and that values for the seasonal vertical transport coefficient are of the order of 0.05–0.1 m/day.

Introduction

The objective of this work is to examine the errors associated with estimating transport across the thermocline of lakes. In particular, including or ignoring the entrainment of hypolimnetic waters is examined. Heat and dissolved oxygen in Lake Ontario are used for illustrative purposes.

Estimates of vertical diffusivity in the waters about the thermocline suggest that the rates are much lower than those of the epilimnion or hypolimnion (1–4). This permits one to view transport across the thermocline as the rate-limiting step and thus to use box models (epilimnion, hypolimnion) for modeling purposes. While box models assume that the rate of mixing within the box is infinite and while the vertical rate of mixing in the hypolimnion is often less than that in the epilimnion, the approximation is often appropriate.

For some substances, the thermocline of a lake is viewed as a seal, preventing transport of soluble materials between the hypolimnion and epilimnion. For example, it is often assumed that the transport of oxygen across the thermocline is insignificant when estimates of the hypolimnetic oxygen deficit are made (5). Some studies (modeling; measurement programs, e.g., see ref 6–12) suggest that oxygen transport in a few lakes is not negligible and that the phosphorus loading to the epilimnion from the hypolimnion may equal or exceed that from land-based sources during summer stratification. An accurate modeling description of mechanisms of and values for the coefficients of vertical transport is essential.

One common method for describing transport is by analogy to a Fickian diffusion process, reparameterized as a mass-transfer process. By making a mass balance on the rate of change of heat in the hypolimnion, an estimate of the diffusivity or mass transfer coefficient can be made. The development of this procedure is given in the Ap-

pendix (eq 7). Then by assuming that the diffusivity or mass transfer coefficient is the same as heat, an estimate of mass transport can be made. The coefficient thus derived incorporates all physical processes into one coefficient; these processes include molecular diffusion, eddy diffusion, entrainment of the hypolimnion by the epilimnion, internal seiches, and leakage around the side of the thermocline (see Figure 1).

There are at least two problems with this description of vertical transport. First, in some lakes, the true diffusivity coefficient for mass may be less than the heat conduction coefficient, because the transport process is essentially molecular. For example, using radon as a tracer (molecular diffusivity coefficient = 0.2×10^{-4} cm²/s), Hesslein and Quay (3) demonstrate that the diffusivity coefficient for the transport of mass in the area of the thermocline was less than the heat conduction coefficient (whose value is approximately 12×10^{-4} cm²/s) in a small Canadian Shield lake. Second, some transport processes incorporated into the diffusivity coefficient are one directional (e.g., entrainment, analogous to a velocity parameter) whereas diffusivity is a two-directional process. For example, Sweers (13) demonstrates that much of the noise in values of diffusivity coefficients for Lake Ontario (positive then negative then positive) and the actual magnitude of their value was substantially reduced when the movement and the tilting of the thermocline was included—this was accomplished by transforming the conventional heat transport equation with fixed origin onto a quasi-Lagrangian coordinate system whose origin moves with the mean depth of the thermocline.

This paper examines the errors associated with including or excluding entrainment in a two-box model format upon (i) predictions of mass balance models and (ii) estimates of the diffusivity coefficient.

Alternative perspectives to the two-box model structure include three-box and higher resolution models. In the extreme, these higher resolution models approach a finite differencing scheme. All perspectives provide some information for answering the question "how much spatial and temporal resolution is required to allow the fulfillment of a model's objectives?" A philosophy that one-box, two-box, and three-box, and higher resolution models need information from each other is used by Simons and Lam (12) and Lam et al. (14), e.g., diffusivity coefficient estimates from multibox models and net sedimentation from one-box models. This paper retains the perspective of a two-box model since many of the essential variations of water quality in lakes can be described by an epilimnetic-hypolimnetic discretization. Particular attention is paid to the use of Eulerian box models and semi-Lagrangian box models for characterizing transport through the metalimnion.

Effect of Entrainment upon Oxygen Models

Figure 1 shows a conceptual sketch of three processes affecting transport through the thermocline: entrainment (or erosion) of hypolimnetic waters by epilimnetic waters, leakage around the side, and eddy diffusivity. Entrain-

*To whom correspondence should be addressed at the Department of Civil Engineering, McMaster University, Hamilton, Ontario, Canada L8S 4C7.

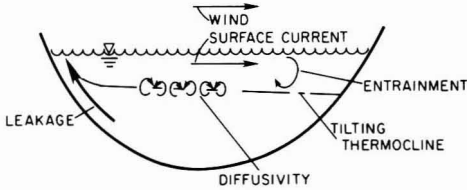


Figure 1. Conceptual sketch of entrainment, leakage around the side, and diffusivity across the thermocline.

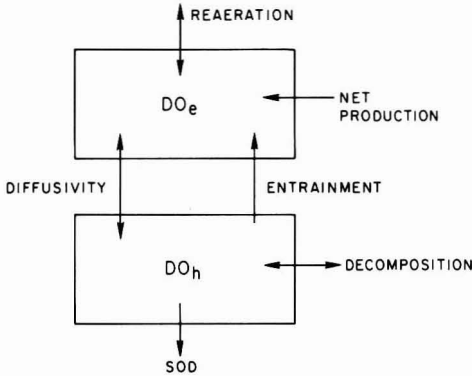


Figure 2. Mass flows for DO compartments.

ment may be described as resulting from the situation where vertical convective currents in the epilimnion have a higher kinetic energy than the potential energy of buoyancy forces caused by vertical density differences; the currents entrain or erode the upper waters of the mesolimnion until an energy balance is reattained. Such an energy balance concept is used in many one-dimensional temperature models for lakes and reservoirs (e.g., see ref 15). The energy of the convective currents originates from two sources: (i) wind energy and (ii) surface cooling. Leakage around the side is associated with a tilting thermocline around which hypolimnetic waters flow, to enter the epilimnion. Both processes result in an increase in the volume of the epilimnion. They both affect the average concentration of materials in the epilimnion without affecting the average concentration of material in the hypolimnion; this is contrasted by the diffusivity concept which argues that the concentrations of material in both the hypolimnion and epilimnion are affected by transport across the thermocline. This differentiation is amplified below.

A definitional sketch for dissolved oxygen in the epilimnion and hypolimnion is given in Figure 2. Transport across the thermocline is divided into diffusivity and entrainment processes: entrainment and leakage around the side are treated as the same process. Entrainment is assumed to be downward (i.e., incorporation of metalimnetic/hypolimnetic waters into the epilimnion). It is assumed that vertical entrainment of metalimnetic/epilimnetic waters by the hypolimnion such as occurs in Lake Erie (e.g., see ref 7 and 14) is not significant; such entrainment represents a transfer of mass from the epilimnion to the hypolimnion. Reversal entrainment events which involve repeated upward and downward thermocline movements can occur; they are caused by alternative episodes of entrainment of epilimnetic and hypolimnetic waters. For several reversal entrainment events, the overall transport could be treated as a diffusivity type process for a suitably long time scale.

From mass balance principles, one obtains the following equations for Figure 2:

$$d(V_e DO_e)/dt = \text{rate of change of mass} = k_{aw} A_{aw} (DO_s - DO_e) + k_{th} A_{th} (DO_h - DO_e) + r_e V_e + \omega_{ze} A_{th} DO_h \quad (1)$$

re-aeration diffusivity photosyn-thesis entrainment

$$d(V_h DO_h)/dt = \text{rate of change of mass} = k_{th} A_{th} (DO_e - DO_h) - r_h V_h + \omega_{zh} A_{th} DO_h - SOD A_s \quad (2)$$

diffusivity decom-position entrainment sed. oxygen demand

The magnitude of ω_{ze} , the rate of increase of the epilimnion due to entrainment (e.g., m/day), is numerically equal to the magnitude of ω_{zh} , the rate of decrease of the hypolimnion due to entrainment. The other symbols are defined in the Glossary. The left-hand side of the two equations are expanded as

$$\frac{d(V_e DO_e)}{dt} = V_e \frac{dDO_e}{dt} + DO_e \frac{dV_e}{dt} = V_e \frac{dDO_e}{dt} + DO_e A_{th} \omega_{ze} \quad (3)$$

$$\frac{d(V_h DO_h)}{dt} = V_h \frac{dDO_h}{dt} + DO_h \frac{dV_h}{dt} = V_h \frac{dDO_h}{dt} + DO_h A_{th} \omega_{zh} \quad (4)$$

Substitution into (1) and (2) yields

$$\frac{dDO_e}{dt} = \frac{k_{aw}}{\bar{Z}_e} (DO_s - DO_e) + \left(\frac{\hat{k}_{th}}{\bar{Z}_e} + \frac{\omega_{ze}}{\bar{Z}_e} \right) (DO_h - DO_e) + r_e \quad (5)$$

$$\frac{dDO_h}{dt} = \frac{\hat{k}_{th}}{\bar{Z}_h} (DO_e - DO_h) - r_h - \frac{SOD}{\bar{Z}_h} \quad (6)$$

assuming that $A_{aw} = A_{th} = A_s$.

Inspection of eq 5 and 6 shows that the entrainment term is found in the equation describing oxygen in the epilimnion (eq 5), but not in the equation describing oxygen in the hypolimnion (eq 6). This makes sense because the continual removal of a surficial layer of water from the hypolimnion by entrainment (e.g. 1 m each month) would not be expected to affect the concentration of the hypolimnion, but it would that of the epilimnion.

Mathematically, the lack of inclusion of an entrainment term in the hypolimnion equation 6 is obtained in the following manner. If all fluxes, biochemical reactions, etc. in the epilimnion (i.e., the right side of eq 1) are zero, the concentration of DO_e would decrease if the volume of the epilimnion increased; the main effect of an expansion of the epilimnion (see eq 3) is that the same mass of oxygen is distributed over a larger volume, resulting in the decrease of concentration. Similarly, if the right side of eq 2 equals zero, the concentration of oxygen in the hypolimnion would increase because the same mass is distributed over a smaller volume (see eq 4). When entrainment is considered in eq 2 and all other fluxes and reactions are zero, the

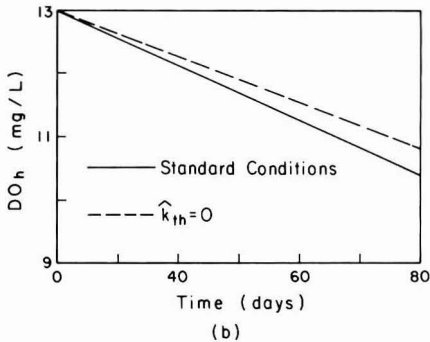
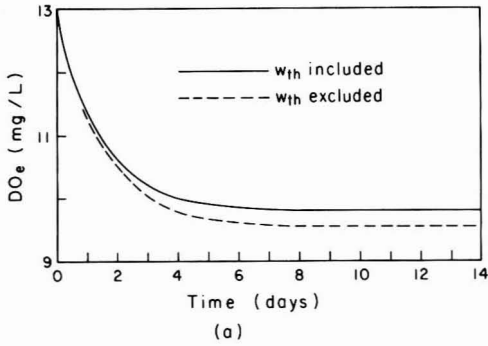


Figure 3. DO predictions over time (a) DO_e for inclusion and exclusion of ω_{ze} and (b) DO_h for standard conditions ($\hat{k}_{th} = 0.15$ m/day) and for $\hat{k}_{th} = 0$.

change in concentration is zero when eq 2 and 4 are combined because the amount of mass lost via entrainment ($\omega_{zt}A_{th}DO_h$) exactly compensates for any increase in concentration due to the reduction of volume [$DO_h(dV_h/dt)$].

The model (eq 5 and 6) shows that entrainment does not directly affect the predictions of DO_h . Only to the extent to which DO_e is affected, and hence the extent to which the diffusivity flux [$\hat{k}_{th}(DO_e - DO_h)$] is affected, will DO_h be influenced.

In a dissolved oxygen model developed previously for Lake Ontario (16,17), the modeling of entrainment was not considered. Their model reduces to eq 5 and 6 without the ω_{ze}/Z_e term of eq 5; inspection of their (16,17) equations shows that the predictions of photosynthesis and decomposition, based upon a total phosphorus model, have pseudo-constant values for r_e and r_h , respectively, of 0.040 and 0.017 g of $O_2/(m^3\cdot day)$. Their (16,17) vertical transport coefficient was estimated using a heat balance (method 1, under Appendix, which is described in more detail below). The rate of deepening of the thermocline was estimated from temperature data and incorporated into the model by changing the epilimnetic and hypolimnetic volume over time. This of course does not change the concentration of either the epilimnion or hypolimnion because, as the epilimnion increases, the additional volume assumes the same concentration as the rest of the epilimnion.

Calculations using eq 5 and 6 are given in Figure 3, for cases which consider the inclusion or exclusion of the ω_{ze}/Z_e term and different values of \hat{k}_{th} . A simplification of Lake Ontario's geometry and the values of $DO_e = DO_h = 13$ g/m³ at time zero, $\hat{k}_{th} = 0.14$ m/day, $\omega_{ze} = 5.5$ m/month, $DO_s = 9.2$ g/m³, $k_{aw} = 2$ m/day, $Z_e = 5.5t - 24$ (t = time in months from January 1) and $Z_h = 89 - Z_e$ are taken as standard conditions for Figure 3; these conditions are typical of 1966. The difference between the presence

Table I. Steady-State Values for DO_e as a Function of Parameter Values ($DO_s = 9.2$; $DO_h = 13$)

case	coefficient values					
	k_{aw} m/day	\hat{k}_{th} m/day	ω_{th} m/month	r_e , g/ (m ³ ·day)	Z_e m	DO_e , g/m ³
1	2	0.14	5.5	0.04	6	9.83
2	2	0.14	5.5	0.20	6	10.24
3	2	0.14	0	0.04	6	9.56
4	2	0.14	5.5	0.04	15	9.99
5	7.5	0.14	5.5	0.04	6	9.38
6	2	0.14	0	0	6	9.45

and absence of the ω_{ze}/Z_e term is small (ca. 0.25 mg/L at 2 weeks; see Figure 3a). The time to attain a near constant value for DO_e is rapid (less than 2 weeks); 95% of the change in DO_e occurs within 5 days. The effect upon hypolimnetic concentrations is insignificant. Similar effects result from variations in the value of \hat{k}_{th} : a maximum change in DO_h of 0.4 mg/L at the end of stratification is predicted if $\hat{k}_{th} = 0$ (see Figure 3b).

A sensitivity analysis of the steady-state value of DO_e is given in Table II. The value of DO_e for standard conditions defined as case 1 in Table I is 9.83 g/m³, compared to a saturation value of 9.2. The concentration in excess of saturation, 0.63 g/m³, is due to fluxes associated with vertical transport (k_{th}), thermocline erosion (ω_{ze}), and photosynthesis (r_e). Comparison of cases 1 (standard conditions), 3 (no entrainment), and 4 (the epilimnetic thickness at the end of stratification) suggests that vertical transport accounts for 40%, thermocline erosion for 43%, and photosynthesis for 17% of the concentration in excess of saturation. Increasing the rate of photosynthesis by 4 times (case 2) increases DO_e by 0.4 mg/L while increasing k_{aw} to 7.5 m/day (case 5) decreases DO_e by 0.45 mg/L. Errors associated with ignoring the entrainment flux of oxygen into the epilimnion for predicting DO_e are small (ca. 3%; compare case 1 to case 3).

The calculations also show that, for a net production of oxygen and transport from the hypolimnion, the epilimnion should always be supersaturated. Hence, if a lake is observed to have daily average concentrations which are below saturation, either (i) net production is negative (i.e., decay is greater than gross daily production), (ii) oxygen loss via bubble formation during daylight hours and decomposition over 24 h are sufficient to give the average DO_e a value less than DO_s , or (iii) gross production is greater than decay and vertical transport occurs to the hypolimnion because the DO_h is less than DO_e in contrast to conditions of Lake Ontario.

Estimation of Vertical Exchange under the Influence of Vertical Entrainment

Estimates of the vertical exchange coefficient (eq 2; Table I) are also influenced by entrainment. Errors associated with these estimates can be classified as (i) model formulation and interpretation and (ii) parameter estimation. This paper is concerned solely with model formulation and interpretation.

A conceptual sketch of temperature profiles over time for pure diffusivity and pure convective overturn (entrainment) is given in parts a and b of Figure 4, respectively, assuming that the epilimnetic temperature remains constant. Both processes cause the thermocline to deepen. The diffusivity profile is analogous to heat conduction in a bar (18) while convective overturn is analogous to plug flow in a river with no transport across a front. Diffusivity acts to cause the front to become more diffuse. Two possible combinations of diffusivity and convective over-

turn are given in Figure 4c,d. The first (Figure 4c) shows a nonparallel movement of the temperature profile and a change of isotherm at which the thermocline is located. The second (Figure 4d) shows the temperature profile remaining parallel to its original position as it moves downward. A direct consequence of this parallel movement is that both the bottom temperature and the heat content below the thermocline remain constant with time (13).

The actual lake will have entrainment (epilimnetic overturn) and thermocline diffusivity occurring simultaneously. Both will vary with time and depth. The vertical diffusivity coefficients above, in the region of, and below the thermocline will differ from each other. *Diffusivity transports heat into the hypolimnion below the thermocline, lowering the thermocline; entrainment that is largely episodic will erode the upper warmed waters, returning some of the heat which has entered the upper hypolimnetic water, via diffusion, to the epilimnetic waters but not causing a temperature increase.* For a seasonal time scale, the intensity and frequency of entrainment is expected to be greater during late summer due to surface cooling and lesser during early summer when surface heating occurs. Only if mixing of the upper hypolimnetic waters with deeper waters is sufficiently fast is a significant fraction of the heat transported by diffusion effectively incorporated into the hypolimnion.

A detailed analysis of the shape of the temperature curve as well as the rate of deepening of the thermocline is a powerful tool for separating diffusivity from convective overturn. This work simplifies the approach, by analyzing the rate of deepening of the thermocline and the transport of heat across the thermocline via diffusivity; this is made possible by the assumption that the two processes are linearly additive. This assumption fails for conditions such as when the scale of vertical diffusivity in the thermocline is a function of the rate of entrainment.

Two different methods for estimating vertical transport across the thermocline are given in the Appendix. They respectively exclude and include entrainment in addition to vertical diffusivity as processes affecting transport between the hypolimnion and epilimnion. Vertical transport due to diffusivity processes is described in terms of a mass transfer coefficient (the vertical exchange coefficient, k_{th} with units m/day) rather than a diffusivity coefficient. Temperature data used for calculating k_{th} are given in Figure 5 for Lake Ontario (June 10 and 25 and Sept 14, 1966); calculations of k_{th} are given in Table II.

The first method (see Appendix) assumes that all transport is due to diffusivity processes: the rate of change of heat below the average depth of the thermocline (lhs, eq 7) is equal to the diffusional flux times the average thermocline area (rhs, eq 7). The average depth of the thermocline, obtained from the relationship of Z_e over time from several cruises in 1966 is 11 m, while examination of the vertical temperature curves suggests a thermocline located at ca. 6 m on June 25 and at ca. 21 m on Sept 16 (the value for June 8 is taken as that of June 25). The temperature of the thermocline in 1966 increases from ca. 7 to 15 °C and then decreases to 9 °C in September. By use of the data for June 8 and Sept 16 and eq 7, k_{th} is 0.15 m/day (see Table IIA).

But if entrainment is significant, there is hypolimnetic water included in the estimate of \bar{T}_e for June 8 and a substantial portion of epilimnetic water included in the estimate of \bar{T}_h for Sept 16 (see Figure 5). By use of the actual positions of the thermocline on June 8 and Sept 16, the estimates of \bar{T}_h on June 8 increases and on Sept 16 decreases (see Table IIB). When these values of Table IIB

Table II. Calculated Values of \hat{k}_{th} Using Different Methods

(A) Method 1 Applied to Illustrative Data Given in Figure 5^a

	$t = 0$ days	$t = 98$ days
\bar{T}_e , °C	7.76	19.29
\bar{T}_h , °C	4.19	5.71

(B) Temperature Data When Account Is Taken for Seasonal Depth of Thermocline

	$t = 0$ days	$t = 98$ days
\bar{T}_e , °C	8.69	17.2
\bar{T}_h , °C	4.31	4.29
T_{th} , °C	7	9

(C) Comparison of Data for Years 1966–1972
(a) Calculations Using Methods 1 and 2

year	no. of days for calculation	Eulerian method 1 \hat{k}_{th} , m/day	quasi-Lagrangian method			
			ω_{th} , m/month	T_{th} , °C	method 2 \hat{k}_{th} , m/day	method 2A \hat{k}_{th} , m/day
1966	98	0.15	5.5	8	0.09	0.01
1967	111	0.12	0.84	11	0.14	0.13
1968	47	0.07	1.1	13	0.11	0.08
1969	116	0.12	2.8	11	0.10	0.04
1970	83	0.13	3.7	13	0.10	-0.01
1972	92	0.15	5.8	8	0.07	-0.01

(b) Sweets' (1970) Estimates

	Eulerian method		quasi-Lagrangian method	
	k_{th} , m ² /day	\hat{k}_{th} ^b , m/day	k_{th} , m ² /day	\hat{k}_{th} ^b , m/day
1966	1.1	0.22	0.63	0.10
1967	0.52	0.10	0.20	0.04

^aCalculations: for $Z_e = 10$ m, $\hat{k}_{th} = 0.15$ m/day. ^bBased upon assuming that the thickness of the temperature gradient is 5 m.

are used in eq 7, \hat{k}_{th} becomes slightly negative because [T_h (Sept 16) - T_h (June 8)], a measure of the increase in heat over the period, becomes slightly negative.

Method 2 (see eq 10 in the Appendix) assumes that transport is due to diffusivity processes (first term on the rhs) and to entrainment (second term on the right-hand side). The integrated form (eq 11) accounts for both the temporal variation of the heat content of the hypolimnion and the variation of the thermocline area. Equation 11 is valid for any lake. Use of morphometric and other data for Lake Ontario (eq 12–14) result in eq 15 which is specific for Lake Ontario.

One question remains: should T_{th} or \bar{T}_h be used to estimate entrainment effects upon k_{th} ? That is, should $T_{th} = \bar{T}_h$ be used in method 2? Viewed strictly from a two-box perspective (transport due to diffusivity being a function of the average concentration of each box expressed physically at its midpoint), method 2A (i.e., $T_{th} = \bar{T}_h$) appears most appropriate. But if transport is viewed from a three-box perspective (epilimnion, metalimnion, and hypolimnion), then both \hat{k}_{th} and T_{th} describe the effects of an essential component of transport, the metalimnion on the other two boxes. Defining \hat{k}_{th} as a parameter describing transport in the vicinity of the thermocline argues for the use of T_{th} . Method 2 is viewed as most appropriate by this writer.

Seasonal estimates of \hat{k}_{th} using methods 1, 2, and 2A are given in Table IIC for 6 years for Lake Ontario. Overall, there is not much difference in the estimates obtained for

method 1 [that used by Snodgrass and Dalrymple (17)] and method 2 (that which accounts for entrainment). Accordingly, the error associated with not considering entrainment in estimating \hat{k}_{th} (17) is small. A larger difference results between methods 2 and 2A than between methods 1 and 2; hence, the interpretation of what temperature parameter to use for describing the temperature of the water being entrained into the epilimnion is quite critical.

Discussion

There are no data available in the literature which allow for a direct comparison of values of \hat{k}_{th} calculated herein. An indirect comparison can be made using the work of Sweers (13). His estimates for the vertical diffusivity coefficient (k_{th} for 1966 and 1967) are given in Table IIC(b). Biweekly estimates of k_{th} were obtained by Sweers (13) and averaged to give these estimates. The continuous traces from bathythermograph readings provided Sweers much more data for calculating vertical profiles than was used herein (e.g., see Figure 5; temperature data from the beginning and end of stratification have been used herein). Sweers also argues that the quasi-Lagrangian method gives values that are smaller and more consistent than those using the Eulerian method.

Sweers' estimates suggest that 1967 was a quieter year than 1966; this is correlated with lower wind velocities in 1967. While the values for \hat{k}_{th} estimated by method 2 are the reverse of Sweers, the differences are plausible because of the different time periods and procedures used. Sweers used data between July 6 and Sept 14, while the calculations using method 2 (i) are for June 8-Sept 14, (ii) are derived from much less data, and (iii) do not use the mean-depth-of-the-isotherm procedure of Sweers. The isotherm mean-depth procedure avoids variability caused by a tilting thermocline.

The comparison with Sweers's data suggests that the estimates of Table II for \hat{k}_{th} (method 2) should not be used to examine for trends, but they do appear to provide proximal estimates of the numerical value of \hat{k}_{th} corresponding to the calculations of Sweers' data [Table IIC(b)] when a metalimnion thickness of 5 m is invoked.

Summary

The error associated with not considering the flux of mass and heat into the epilimnion due to entrainment is assessed. The equations show that, for Lake Ontario conditions, the concentration of mass and heat in the hypolimnion is nearly independent of whether or not the flux is considered. Small indirect effects occur because the entrainment flux influences the epilimnetic concentration, which in turn influences the diffusivity flux across the thermocline. The main error caused by lack of consideration of hypolimnetic entrainment by metalimnion erosion is the prediction of the concentration of epilimnetic constituents. For dissolved oxygen in Lake Ontario, the maximum error is ca. 5%.

Two methods for calculating the vertical transport coefficient across the thermocline for box models are presented and analyzed. The two main methods (Appendix) depend upon whether strictly diffusivity or diffusivity plus entrainment control the shift of the thermocline. The analysis presented herein suggests that, for Lake Ontario, the diffusivity assumption gives values which are slightly higher than, but similar to, those from the diffusivity plus entrainment assumption. The analyses conducted herein suggest seasonal values for ω_{th} which vary from 1 to 6 m/month and values for \hat{k}_{th} of the order of 0.05-0.1 m/day for Lake Ontario.

Appendix

Methods for Estimating Vertical Transport Coefficients across the Thermocline from Box Model Perspective. Method 1: Eulerian Frame of Reference. Formulating a heat balance upon the hypolimnion gives

$$\begin{aligned} \frac{\partial[V_h T_h]}{\partial t} &= -k_{th} A_{th} \left. \frac{\partial T}{\partial z} \right|_{z=\text{thermocline}} \\ \frac{d[V_h T_h]}{dt} &= -k_{th} A_{th} \frac{(\bar{T}_h - \bar{T}_e)}{\Delta z} \\ \frac{d[V_h T_h]}{dt} &= -\hat{k}_{th} A_{th} (\bar{T}_h - \bar{T}_e) \end{aligned} \quad (7)$$

Assuming that the volume of the hypolimnion is constant and that T_h is a measure of the heat in the hypolimnion gives

$$\hat{k}_{th} = \frac{\bar{Z}_h dT_h/dt}{\bar{T}_h - \bar{T}_e} = \frac{\bar{Z}_h}{\Delta t} \left[\frac{T_h(t) - T_h(0)}{\bar{T}_e - \bar{T}_h} \right] \quad (8)$$

$$\bar{Z}_h = \frac{\bar{V}_h}{A_{th}} \quad (9)$$

Method 2: Quasi-LaGrangian Frame of Reference; V_h is Constant. A heat balance upon the hypolimnion gives

$$\frac{d[V_h T_h]}{dt} = -\hat{k}_{th} A_{th} (\bar{T}_h - \bar{T}_e) - \omega_{th} A_{th} \bar{T}_{th} \quad (10)$$

by way of analogy to eq 7 and 8 of Sweers (1970). Here, the product $V_h T_h$ is equivalent to Sweers definition of the mean heat control at time t , in a water column extending from the thermocline to the lake bottom.

Integrating (10) gives

$$[V_h T_h]_0^t = -[\omega_{th} T_{th} + \hat{k}_{th} (\bar{T}_h - \bar{T}_e)] \int_0^t A_{th} dt \quad (11)$$

For Lake Ontario conditions in which the thermocline deepens with time in an approximately linear fashion (see ref 10), i.e.

$$\bar{Z}_e = \omega_{th} t + C \quad (12)$$

and for its morphometry in the thermocline area of

$$A_{th} = (18300 - 126\bar{Z}_e)10^6 \quad (13)$$

one obtains

$$A_{th} = C_1 - C_2 \omega_{th} t \quad (14)$$

$$C_1 = (18300 - 126C)10^6$$

$$C_2 = 126 \times 10^6$$

The substitution of (14) into (11) and integration gives

$$\hat{k}_{th} = \frac{[V_h(t)T_h(t) - V_h(0)T_h(0)]/[\Delta t(C_1 - C_2 \omega_{th}(\Delta t/2))]}{\bar{T}_e - \bar{T}_h} + \omega_{th} T_{th} \quad (15)$$

Method 2A: Alternative Interpretation of T_{th} . T_{th} is interpreted as $T_{th} = \bar{T}_h$.

Glossary

A_{aw}	area of air-water interface, L^2
A_{th}	area of thermocline, L^2
$A_{th}(0)$	value of A_{th} at $t = 0$ and $t = t$ for calculating \hat{k}_{th}
$A_{th}(t)$	

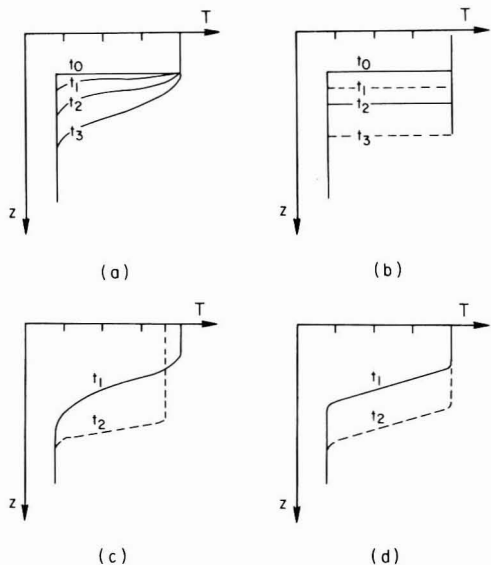


Figure 4. Idealized temperature profiles: (a) diffusivity as the only mechanism; (b) entrainment as the only mechanism; (c) typically observed profile; (d) constant vertical profile.

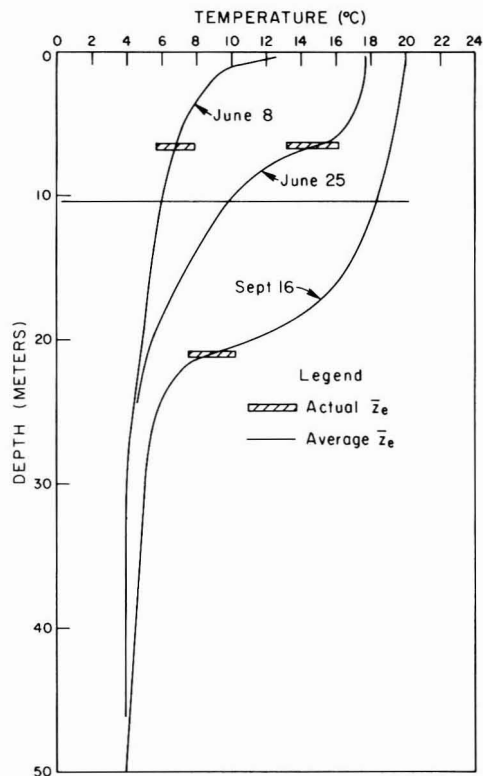


Figure 5. Temperature data for Lake Ontario used for calculations of k_{th} .

d/dt rate of change with respect to time
 d/dz rate of change with respect to depth
 DO_e dissolved oxygen concentration in epilimnion, ML^{-3}
 DO_h dissolved oxygen concentration in hypolimnion, ML^{-3}

DO_s saturation concentration of DO_e , ML^{-3}
 k_{aw} reaeration coefficient at air-water interface, LT^{-1}
 k_{th} diffusivity coefficient in thermocline, L^2T^{-1}
 k_{th} vertical exchange coefficient in thermocline, LT^{-1}
 r_e rate of epilimnetic production of oxygen, $ML^{-3}T^{-1}$
 r_h rate of hypolimnetic production of oxygen, $ML^{-3}T^{-1}$
 T_e temperature of epilimnion, $^{\circ}C$
 T_h temperature of hypolimnion, $^{\circ}C$
 \bar{T}_e, \bar{T}_h average value of T_e and T_h between $t = 0$ and $t = t$, $^{\circ}C$
 $T_h(0), T_h(t)$ value of T_h at $t = 0$ and $t = t$, $^{\circ}C$
 SOD sediment oxygen demand, $ML^{-2}T^{-1}$
 t time, T
 Δt time between $t = 0$ and $t = t$, T
 V_e volume of epilimnion, L^3
 V_h volume of hypolimnion, L^3
 \bar{V}_h average value of V_h between $t = 0$ and $t = t$, L^3
 $V_h(0), V_h(t)$ value of V_h at $t = 0$ and $t = t$, L^3
 ω_{th} rate of entrainment of thermocline waters, LT^{-1}
 ω_{ze} rate of deepening of epilimnion (dZ_e/dt), LT^{-1}
 ω_{zh} rate of decrease of depth of hypolimnion (dZ_h/dt), LT^{-1}
 Z depth, L
 Z_e mean depth of epilimnion at a point in time, L
 Z_h mean depth of hypolimnion at a point in time, L
 $Z_h(0), Z_h(t)$ value of Z_h at $t = 0$ and $t = t$, L
 Δz thickness of temperature gradient across thermocline, L

Registry No. Oxygen, 7782-44-7.

Literature Cited

- Hutchinson, G. E. "A Treatise on Limnology"; Wiley: New York, 1980; Vol. II.
- Lerman, A.; Stiller, M. *Verh. Int. Ver. Limnol.* **1969**, *17*, 323-333.
- Hesslein, R.; Quay, P. *J. Fish. Res. Board Can.* **1973**, *30*, 1491-1500.
- Li, Y.-H. *Schweiz. Z. Hydrol.* **1973**, *35*, 1-7.
- Cornett, R. J.; Rigler, F. H. *Limnol. Oceanogr.* **1980**, *25*, 672-679.
- Burns, N. M.; Ross, C. "Project HYPO"; 1972, Canada Centre for Inland Waters Paper No. 6, pp 85-119.
- Burns, N. M. *J. Fish. Res. Board Can.* **1976**, *33*, (a) 512-519, (b) 520-536.
- Seip, K. L. *Verh. Int. Ver. Limnol.* **1981**, *21*, 394-398.
- Stauffer, R. E.; Lee, G. F. In "Modelling the Eutrophication Process"; Middlebrooks, E. J., et al., Eds.; Utah State University: Logan, UT, pp 73-82.
- Snodgrass, W. J. In "Transport Processes in Lakes and Oceans"; Gibbs, R. J., Ed.; Plenum Press: New York, 1977; pp 179-202.
- CCIW (Canada Centre for Inland Waters) "Assessment of Water Quality Simulation Capability for Lake Ontario"; CCIW: Burlington, Ontario, Canada, 1979; Scientific Series No. 111, Environment Canada, pp 1-220.
- Simons, T. J.; Lam, D. C. L. *Water Resour. Res.* **1980**, *16* (1), 105-116.
- Sweers, H. E. *Limnol. Oceanogr.* **1970**, *15*, 273-280.
- Lam, D. C. L.; Schertzer, W. H.; Fraser, A. S. *Hydrobiologia* **1980**, *91*, 217-225.
- Octavio, K. A. H.; Jirka, G. H.; Harleman, D. R. F. "Vertical Heat Transport Mechanisms in Lakes and Reservoirs"; R. M. Parson Laboratory, Massachusetts Institute of Technology, 1977, Report No. 227, 131 pp 131.
- Dalrymple, R. J. Master's Thesis, McMaster University, Hamilton, Ontario, 1977, pp 1-184.
- Snodgrass, W. J.; Dalrymple, R. J. *Environ. Sci. Technol.*, preceding paper in this issue.
- Crank, J. "Mathematics of Diffusion"; Oxford University Press: London, 1970

Received for review February 17, 1983. Revised manuscript received November 16, 1983. Accepted September 13, 1984.

Comparison of Organic Combustion Products in Fly Ash Collected by a Venturi Wet Scrubber and an Electrostatic Precipitator at a Coal-Fired Power Station

Florence L. Harrison,* Dorothy J. Bishop, and Barbara J. Mallon

Environmental Sciences Division, Lawrence Livermore National Laboratory, University of California, Livermore, California 94550

■ Organic compounds recovered from fly ash collected by an electrostatic precipitator (ESP) and a Venturi wet scrubber (WS) at the Four Corners Coal-Fired Power Station at Fruitland, NM, were analyzed. Organic constituents in extracts of solid waste included large numbers of aliphatic and aromatic compounds. A series of normal C₁₅-C₃₀ paraffins was found in the aliphatic fractions. The aromatic compounds were of one, two, three, and four rings; no compounds containing more than four rings were identified. However, our studies on recovery of radio-labeled naphthalene and benzo[a]pyrene added to scrubber fly ash indicate that polynuclear aromatic hydrocarbons containing more than four rings are poorly recovered. Comparison of organic constituents in extracts of fly ash from the WS and the ESP showed that ESP extracts contained more compounds in greater quantities. The types and quantities of organic compounds recovered are not expected to present any environmental hazard.

Introduction

The Power Plant and Industrial Fuel Act of 1979 was designed to minimize the use of petroleum and natural gas and to emphasize the use of coal. Implementation of this act will increase the contaminant load to local environments from the combustion products of coal. Fly ash and bottom ash will be produced in greater amounts. This is of concern because these ashes are enriched in trace metals and potentially contain carcinogenic organic combustion products such as aromatic amines, heterocyclic nitrogen compounds, and polynuclear aromatic hydrocarbons (PAHs). The amount of unsubstituted PAHs has decreased in soil sediments in the last 30 years, probably because of the change from coal to fuel oil (1).

Emission-control devices are effective in reducing the total suspended solids discharged from the stack. Generally, less than 5% of the airborne particles produced are released in the plume. Electrostatic precipitation and wet scrubbing processes are two major strategies employed to control particulate emissions at coal-fired, electrical utility stations (2, 3). Particles of respirable size constitute a greater proportion of the mass of aerosols from wet scrubbers (WSs) than from electrostatic precipitators (ESPs) (2).

The availability to adjacent ecosystems of the organic and inorganic contaminants associated with collected fly ash depends on the discharge pathway of the contaminants. Fly ash collected by ESPs and WSs is deposited in holding ponds or pits. Fly ash collected by WSs is of special interest because these devices are designed to remove both gaseous and particulate material, require large volumes of water, and operate at relatively low temperatures.

Our objective was to characterize the kinds and quantities of organic combustion products from pollution control wastes released from a coal-fired power station. This information will be used to predict the impact on man of

potentially hazardous organic combustion products released with WS and ESP ash.

Experimental Section

Description of Power Station. The Four Corners Coal-Fired Power Station, located in northwestern New Mexico, consists of five steam electric-generating units that burn pulverized coal and have a combined power capacity of 2100 MW. Coal burned at the plant comes from the nearby Navajo Mine. The coal is classified as subbituminous with an average heat content of 9000 Btu/lb, an average ash content of 22.5%, and an average sulfur content of 0.67%. Daily coal consumption averages 18 500 ton (28 000 ton maximum at peak output).

At the time of sample collection, atmospheric emissions from the plant were controlled by Venturi WSs with rated efficiencies for total suspended particles (TSP) of 99.6% (units 1-3) and by ESPs with rated efficiencies of 97.6% (TSP) (units 4 and 5). Two of the units that were fitted with WSs contained 180-MW generators; the third unit had a 240-MW generator. Each of the units that was fitted with ESP collectors had a 750-MW capacity. Water for the WSs was obtained from Morgan Lake, a 1260-acre man-made reservoir fed via aqueduct from the San Juan River.

Ash material from coal combustion was handled in one of two ways. Ash collected by ESPs was trucked to the Navajo Mine and buried in the scar left from the mining operation. Ash collected by the Venturi WSs was pumped to the distribution tank where slaked lime (calcium hydroxide) was added. The slurry was next pumped to the thickener tank, where water was continuously removed and recycled to the Venturi WSs. The slurry from the thickener tank was pumped through a trench to ash-settling ponds adjacent to the power plant; these ponds support little or no life. Water overflowed from the ash ponds into a duck pond and then into Chaco Wash where it was returned to the San Juan River via groundwater and surface water systems. Considerable vegetation was found in and around the duck pond and Morgan Lake.

Collection of Samples. Samples were collected at the Four Corners Power Station during the afternoon of Dec 12, 1979. The WS fly ash was collected in 19-L glass carboys from the distribution tank as a slurry. This slurry was at a pH of 5.6 at 31.1 °C. After the slurry was returned to the laboratory, the solution was decanted and filtered. The solids were frozen in 1-L jars, freeze-dried, well mixed, and repacked in 1-L amber glass jars for storage. The ESP ash was collected from unit 4 from a hopper midrange between the inlet and outlet. The 5-kg sample was returned to the lab in a sealed polyethylene container. It was well mixed to ensure homogeneity, and subsamples were packed into 1-L amber jars. Both WS and ESP ash samples were stored at 0-4 °C until analysis.

Reagents and Preparation Procedures. All reagents were used as received. Methylene chloride, pentane, and

Table I. Relative Efficiency of Solvent Extraction, in Percent Recovery of Compounds Added to Fly Ash^a

expt	compound	method	solvent	no. of extractions				
				1	2	3	4	total
1	[¹⁴ C]BaP	shaker	methylene chloride	0.11	0.07			0.18
	[¹⁴ C]BaP	shaker	toluene-methylene chloride (1:1)			0.5		0.5
	[¹⁴ C]BaP	shaker	toluene-methanol (4:1)				0.39	0.39
2	[¹⁴ C]BaP	sonifier	methylene chloride	0.16	0.19	0.14		0.49
3	[¹⁴ C]BaP	sonifier	toluene-methanol (4:1)	1.52	1.33	0.72		3.57
4	[¹⁴ C]BaP	sonifier	toluene-methylene chloride (1:1)	1.1				1.1
5	[¹⁴ C]naphthalene	shaker	methylene chloride	74.2	12.5	4.5	6.2	97.4
6	[¹⁴ C]naphthalene	shaker	toluene-methylene chloride (1:1)	81.7	10.3	2.4	1.9	96.3
7	[¹⁴ C]naphthalene	sonifier	methylene chloride	46	19.5			65.5
8	[¹⁴ C]naphthalene	sonifier	toluene-methanol (4:1)	38.6	13.4			52

^a Concentration of ¹⁴C-labeled compounds was 6 ppb.

Table II. Percent [¹⁴C]BaP Recovered by Rotary Shaker Extraction

amount of BaP added, ppm	% recovered
10	94
0.10	23
0.001	5

hexane were distilled in glass. Reagent-grade methanol, toluene, hydrochloric acid, and sodium hydroxide were used. The ¹⁴C-labeled phenol, naphthalene, and benzo[*a*]pyrene (BaP) were purchased from Amersham Corp. (Arlington Heights, IL).

All glassware and other implements were washed thoroughly with detergent and rinsed repeatedly with tap water, distilled water, methanol, and finally methylene chloride. All bottles were fitted with Teflon-lined screw caps. Glass-fiber filters of nominal 1- μ m pore size were used in all filtering procedures.

Before the samples were extracted, we performed tests to compare the effectiveness of rotary shaking and sonication methods using various solvents for recovering naphthalene and BaP that were added separately to fly ash in different experiments. Whereas naphthalene was readily recovered by several solvents, BaP was extracted best by a 4:1 mixture of toluene and methanol, but the recovery was poor (Table I). In another experiment, addition of larger quantities of BaP resulted in progressively better percentages of recovery (Table II). A Model W185E Branson Sonifier (Danbury, CT) fitted with a Model H419 microtip (Heat Systems, Plainview, NY) was used as the ultrasonic generator.

Samples included WS fly ash from the distribution tank and ESP fly ash from the hopper that had been stored for 1¹/₂ years in the dark at 0-4 °C and sand that had been ashed at 500 °C for 2 days. Before the samples were extracted, they were spiked with internal standards of anthracene-*d*₁₀ and 1-chloronaphthalene that were dissolved in acetone. The mixture was homogenized by using a sonifier, rotary evaporated, and then freeze-dried. The 25-g aliquots were shaken with 100 mL of methylene chloride at 220 rpm for 5 h and centrifuged at 2500 rpm, and then the supernatant was decanted and filtered. Each aliquot was extracted 3 times, and a total of 12 aliquots (300 g) was processed. The supernatants from all aliquots were combined and rotary evaporated to approximately 25 mL. The volume was reduced to 0.5 mL by evaporation with cooled nitrogen gas and then stored in Teflon-lined screw-cap vials at -30 °C until analysis.

All aliquots of each sample were further extracted by using the ultrasonic generator. Three extractions were again performed. We added 50 mL of dried toluene-methanol (4:1) to the residue from the methylene chloride

extraction. The sample was sonicated at >100 W for 3 min, the mixture centrifuged, and then the supernatant removed and filtered. The combined extracts were rotary evaporated to approximately 25 mL. Because methanol is undesirable for gas chromatography (GC) and gas chromatography-mass spectrometry (GC-MS) analysis, the rotary-evaporated samples were carefully evaporated to dryness and then reconstituted to 0.5 mL with methylene chloride before storage at -30 °C.

Gas Chromatography. Quantitative separations of hydrocarbon mixtures were performed on Models 5840A and 5880 Hewlett-Packard gas chromatographs (Palo Alto, CA) equipped with flame ionization detectors. The instruments were fitted with fused silica, wall-coated 25-m SP2100 and 25-m DB-5 columns (0.25 mm i.d.), respectively, from J & W Scientific (Rancho Cordova, CA). The oven was programmed to hold at 35 °C for 5 min, then increase from 35 to 260 °C at 3 °C/min, and hold at 260 °C for 20 min. The carrier gas was helium, and the flow rate was 3.2 cm³/min.

Concentrations of compounds extracted from the ashes were calculated from response factors determined by analysis of known standard compounds. One group of standards used was a mixture of nine PAHs that ranged in size from that of naphthalene to that of BaP. Repeated injections of these standards in the gas chromatograph produced coefficients of variation of ≤ 0.04 . Another group of standards was a mixture of eight phthalates ranging in molecular weight from 194 to 390; the coefficient of variation was also ≤ 0.04 . A mixture of four paraffins ranging from C₁₆ to C₂₂ made up the last group; these produced coefficients of variation of ≤ 0.03 . The compound 1-chloronaphthalene was used as an internal standard by adding known concentrations to the sediments before extraction. The coefficient of variation for this compound was ≤ 0.03 . An average response factor was determined from all of the standards and used in the Model 3350 Hewlett-Packard Laboratory Automation System to quantify GC peaks. Because the response to a column for a given concentration of a compound is not the same for compounds of different molecular weight, the use of an average response factor generates bias in the data. The average response factor value used would tend to underestimate the concentration of high molecular weight compounds by up to 18% and overestimate some low molecular weight compounds by approximately 10%. All data reported in tables list quantities based on average response factors.

Gas Chromatography-Mass Spectrometry. Major components in the Four Corners samples were identified on the Hewlett-Packard 5985B GC-MS system. The GC conditions and column type were the same as for the 5880 system described above. The mode of ionization was by

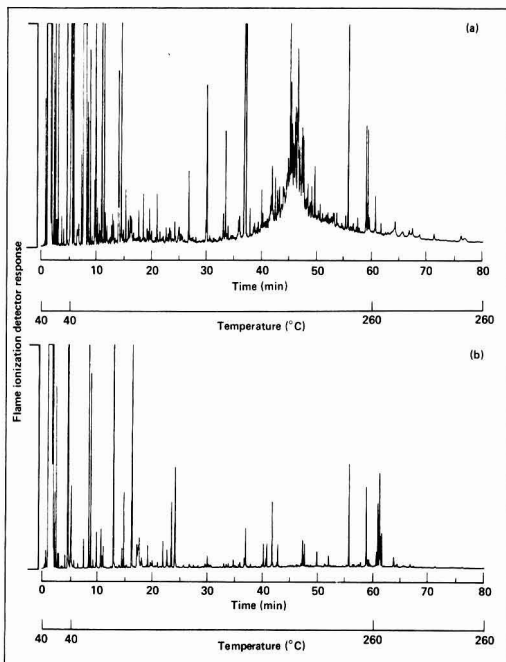


Figure 1. Gas chromatograms of (a) the rotary shaker extracts of fly ash from the Venturi wet scrubber collected at the Four Corners Power Station on Dec 12, 1979, and (b) the sonicated extracts of fly ash from the Venturi wet scrubber collected at the Four Corners Power Station on Dec 12, 1979.

electron impact at 70 eV. The ion-source temperature was 200 °C, and the scan cycle time was 1.5 s.

Compounds were identified by comparing mass spectra acquired during a run with reference spectra contained in a library. The Wiley and National Bureau of Standards Libraries we have on file contain over 40 000 different spectra for organic compounds. The computer searches these libraries for the spectra that best match those contained in the run. Visual comparisons of the unknown and reference spectra allow the analyst to identify most of the major components in the sample.

A technique known as reverse searching allows the analyst to search the entire run for specific compounds. Alteration of the search parameters allows the components to be detected in the presence of contaminants or noise.

The molecular ion of a compound may be plotted vs. run time to determine the presence or absence of a compound at a particular time in the run. The presence of a particular ion is only a fair indication of the presence of a given compound, but the absence of the ion is strong evidence against the presence of that compound. This technique was used to detect the presence of trace levels of some PAHs in a sample.

The relative quantities of PAHs required for detection by GC and GC-MS were examined. The amounts of the individual compounds needed for detection differed by a factor of 20 (Table III).

Results

Large numbers of compounds were extracted from WS and ESP fly ash by a combination of shaking and sonicating (Table IV; Figures 1 and 2). Some compounds were extracted easily by just shaking, whereas others were removed better by sonicating. Characteristic of the GC scan

Table III. Gas Chromatography-Mass Spectrometry Detection Limits

compound	concn, ppm	compound	concn, ppm
naphthalene	1	fluoranthrene	6.5
acenaphthene	4	pyrene	4.5
fluorene	6	benzo[a]pyrene	16
phenanthrene	4.5	perylene	20
anthracene	6.5		

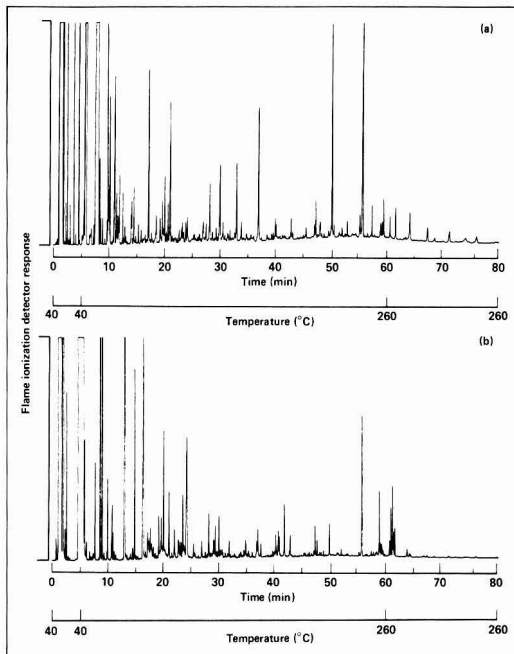


Figure 2. Gas chromatograms of (a) the rotary shaker extracts of fly ash from the electrostatic precipitator collected at the Four Corners Power Station on Dec 12, 1979, and (b) the sonicated extracts of fly ash from the electrostatic precipitator collected at the Four Corners Power Station on Dec 12, 1979.

of the WS fly ash extracts was a hump at retention times between 45 and 60 min (Figure 2a). These terpene-type compounds (M_r 268–274), which are not present in the ESP fly ash, constitute about one-third of the total concentration of hydrocarbons extracted from WS fly ash.

The total quantities of aromatic compounds and the quantities of those of each ring size were greater in ESP than in WS fly ash (Table V). Among the nonaromatic compounds, a greater number of high molecular weight compounds ($M_r > 170$) were extracted from the WS fly ash than from the ESP fly ash.

Discussion

Our study established identities and quantities of some of the organic compounds in WS and ESP fly ash from the Four Corners Coal-Fired Power Station. A large number of compounds were identified, but concentrations were generally low. We will discuss our results with regard to coal composition, fly ash analyses, extraction methods, and potential environmental hazard from drinking water.

Coal Combustion. In a review chapter, Davidson states that coal contains small molecular weight fragments that can be extracted by various solvents, flash heating, or supercritical gas extraction (4). He lists the following types of low molecular weight substances: aliphatic hydro-

carbons up to C₃₁, aromatic hydrocarbons, partly hydrogenated aromatic structures, and those with high oxygen content (mainly phenols). Davidson (4) noted a change in both types and quantities of low molecular weight compounds in progressing from lignite (low rank) to anthracite (high rank) coals; the most volatile components were found in the intermediate bituminous coals. The Navajo Coal used in our study is classified as subbituminous or between lignite and bituminous (5). Berkowitz reported that the products of destructive distillation of highly volatile bituminous coal include aromatics, naphthalenes, monoolefins, dienes, cycloolefins, paraffins, indane, carbon disulfide, and thiophenes and that the yield of these compounds varied with type of retort and temperature (6). Above 700 °C, initial products react and become aromatized. Davidson and Berkowitz both reported branched and alicyclic hydrocarbons predominated in compounds <C₁₈ for lower ranked coals (4, 6). Possible precursors of these hydrocarbons are the original terpenoids forming the coal (4).

Our analyses revealed hydrocarbons very similar to those described by Davidson and Berkowitz (4, 6). We found higher concentrations of the branched or cyclic compounds in the WS than in the ESP ash. Many of these compounds were terpene type with molecular weights of about 170. In the ESP ash, however, normal paraffins predominated. Davidson noted that paraffin distributions >C₁₈ were dominated by odd-number carbon compounds (4). We found this also, but it was more pronounced in WS than in the ESP ash. Our study also revealed the presence of aromatic hydrocarbons of one or more condensed rings and their partly hydrogenated counterparts as well as phenols and other oxygenated compounds. It is possible that many of the hydrocarbons we detected were direct distillation products from the coal. An extraction of the Navajo Coal would likely result in a list similar to that given in Table IV.

Fly Ash Analyses. The aliphatic hydrocarbons we found in fly ash from Four Corners were mainly paraffins and terpenoids. Griest and Guerin (7) and Bennett et al. (8) reported normal paraffins up to C₃₀ (tricontane) in fly ash from ESPs. We found these compounds in both ESP and WS fly ash, but the quantities and distributions of the paraffins differed from theirs. These differences could be due to the types of coal used and methods of burning, heating regimes, temperature of the ESPs, and particle size. These workers did not report terpene-type compounds in their ESP fly ash. We likewise found none in the ESP extracts but did in the WS extracts. We suspect that collection of these compounds by the WS is due to the heating regime of the burner. Terpenes and terpanes distill from coal at <300 °C; they are unstable at higher temperatures (9).

Our results show low concentrations of PAHs with two, three, and four rings, and no PAHs with five or more rings in both ESP and WS ash. The amounts of aromatic as well as the aliphatic compounds were lower in the WS ash than in the ESP ash, as would be predicted from the greater efficiency of the ESP. The PAH emissions from coal-fired power stations are influenced by many factors, from the type of coal to the rate of burning (7). The BaP emissions may range from 0.00002 to 0.352 lb/ton (from 10 to 176 000 µg/kg) depending on whether the station is mechanically or manually fired (10). Hangebrauck et al. report low gross output of BaP emissions (19 × 10⁻⁶ µg/BTU) for a large, pulverized coal-burning plant (11). If the ESP or WS is efficient, we would expect some BaP in the collected particulates of the Four Corners Power Station. Using

figures from Hangebrauck et al. (11), we would expect an emission of 0.14 g/h or 3.4 g/day BaP.

Low amounts of aromatic compounds in fly ash might not be unexpected. Griest and Guerin showed that the majority of organic compounds are apparently still volatile at temperatures of the ESP units and that they pass up the stack (7). Griest and Guerin also compared the 0–3.3-µm ESP and stack ash and found more PAHs in greater quantities in the stack ash than in ESP ash. Also, Ondov et al. (12) found the WS system 6 times less efficient than the ESP in removing the submicron respirable particles (<1 µm) from the Four Corners Coal-Fired Power Station; the WS is more efficient for larger particles. Natusch (10) reported PAHs condense or adsorb preferentially to these submicron particles. Consequently, it is probable that more PAHs would escape up the stack by their association with respirable particles than in coal-fired power plants fitted with WSs than in those fitted with ESPs.

Extraction Methods. Because PAHs adhere strongly to the ash, the kinds and quantities recovered are related to the extraction procedures that are used. Studies on effects of extraction procedures on recoveries were performed by Rohrbach and Reed on marine sediments (13) and by Griest and Guerin on fly ash (7). Rohrbach and Reed recovered the highest concentrations of organic compounds using a toluene-methanol Soxhlet procedure. These results contrasted with those of Griest and Guerin, who compared the effectiveness of using a Soxhlet apparatus, refluxing baths, and an ultrasonic microtip apparatus (1). They found the Soxhlet procedure to be relatively ineffective—no more than 18% of the PAHs was recovered. They also tested the extraction efficiency of several solvents and concluded that, in a Soxhlet apparatus, benzene was superior to methylene chloride, tetrahydrofuran, methanol, or acetone.

Our studies on the effectiveness of extraction of [¹⁴C]-naphthalene and [¹⁴C]BaP from fly ash indicated that, in removing naphthalene, rotary shaking was as effective or more effective than sonicating. The BaP, on the other hand, was removed more effectively by sonicating than rotary shaking. These results are in agreement with those of Rohrbach and Reed, who reported that rotary shaking was almost as effective as using a Soxhlet for extracting marine sediments (13), and those of Griest and Guerin, who found sonicating better than using a Soxhlet for removing PAHs from ESP fly ash (7).

We found the recovery of radiolabeled BaP to increase with increases in the quantities of the compound added with the spike. These data indicate that preferential binding sites on the particles decrease when an excess of the compound is available. Griest and Guerin (7) suggested that π bonding of the electrons in the larger PAHs causes the difficulty in extraction. Because recoveries of some PAHs are still low even when the best current methods are used, there is a need to investigate better extraction techniques.

Low recoveries of PAHs may occur because they are lost or degraded during analysis. When we injected known concentrations of nine PAHs into our gas chromatograph-mass spectrometer, the results indicated that there were large losses of PAHs of more than four rings. It is not known whether the compounds were degraded or adhered to the column.

Some of the compounds listed in the tables may not be coal derived but are possibly contaminants in the water system at the power plant or contaminants introduced during the extraction procedure. The phthalates, which

Table IV. Concentrations in ppb of Organic Compounds Identified in Wet Scrubber and Electrostatic Precipitator Fly Ash Collected from the Four Corners Power Station on Dec 12, 1979^a

compound	GC ^b retention time, min	M _r	wet scrubber fly ash			electrostatic precipitator fly ash		
			shaker	sonic	total	shaker	sonic	total
isopropylbenzene	11.2	120	150		150			
propylbenzene	11.7	120		14	14			
ethylmethylbenzene	13	120	13		13			
<i>n</i> -propylbenzene	13.1	120	6	10	16			
ethylmethylbenzene	13.4	120		4	4			
methylnonane	13.6	142		9	9			
methylstyrene	14	118	29		29	46	23 ^c	69
trimethylbenzene	14.6	120				36	37	74
decane	14.8	140		19	19			
decane	14.9	142		120	120		390	390
trimethylbenzene	15.4	120				11		11
dimethylphenol	16	122		12	12			
methyl butylacetate	16.2	130	12		12			
(methylheptanol)	16.4	130	12		12			
α -hydroxytoluene	16.5	108				14		14
(methylcyclohexenone)	16.6	110				300		300
decalin	16.7	138	9		9			
methylcyclohexenone	17.4	110					66	66
(methyldecanes)	17.4-18.1	156		74	74			
trimethylbenzene	17.6	120					34	34
cresol	18.2	108	13		13			
phenylpropanol	18.6	136	21		21			
undecane	19.2	152				35	94	129
dimethylheptadienone	19.6	138		8	8	53	180	233
isophorone	20.1	138				87	403	490
artemisia ketone	21.1	152					32	32
(hydroxymethyl)tetrahydrofuran	22	128					90	90
naphthalene	22.6	128	9	trace	9	13	81	93
dodecane	23.3	170				22	72	94
dimethylhydroxyheptene	23.7	142				34	93	127
trimethylcyclohexenone	24.2	138				42		42
decanol	24.2	168	9	44	53			
(decanol type)	24.9	168	9		9			
dimethyl- <i>tert</i> -butylphenol	25.5						60	60
(acetoxyphenol)	27						83	83
2-methylnaphthalene	27.1	142				24	12	36
1-methylnaphthalene	27.6	142				37	32 ^c	69
[butylmethyl(methylenedioxy)benzene]	27.6						32	32
tridecane	28.2	184				95	170	265
diisopropylphenol	29.3	178				31 ^b	110	141
(diisopropylphenol)	30	178					140	140
(cyclic tetrahydroadipate type)	30.4	200	67		67			
(diisopropylphenol)	30.6	178				47		47
tetradecane	31.2	198				poss ^d	42	42
(amylanisole)	31.5						41	41
dimethyloctahydronaphthalenone	31.8	178					62	62
dimethylnaphthalene	31.8	156				19		19
dimethyl phthalate	32.8	156				26 ^c	20	46
(2,6-Di- <i>tert</i> -butylbenzoquinone)	33	220				130		130
acenaphthene	33.6	154					16	16
pentadecane	33.8	212	7		7			
triphenylpropane							16	16
<i>tert</i> -butylmethoxyphenol	33.9	180	34	39	63			
(dimethylbiphenol)	34.2	182					16	16
(aristolone)	34.8	218				29 ^c	92	121
methyl diphenylmethane	35.2	182				8 ^c	22	30
(aristolone)	35.3	218				18 ^c	42	52
trimethylnaphthalene	35.6	170				24		24
fluorene	36.7	166					72	72
diethyl phthalate	37.1	222	900	46	946	190	97	287
diphenylamine	37.8	169	20	4	24			
substituted naphthalene	39.3	198				13		13
heptadecane	39.9	240			21			
heptadecane	40	240				31		31
pristane	40.2	268				28		28
styrene dimer	40.2	208					68	68
methyl butyl phthalate	40.6	236				9 ^c	95	104
thunbergene types:	41.5-48		1400		1400			
(dihydrosilarene)		274						
(podocarpene)		272						
(anhydroretinol)		268						
(dehydroabietane)		270						
(kaurene)		272						

Table IV (Continued)

compound	GC ^b retention time, min	M _r	wet scrubber fly ash			electrostatic precipitator fly ash		
			shaker	sonic	total	shaker	sonic	total
			phenyltetrahydronaphthalene	41.8	236			
phenanthrene	42.6	178				poss	poss	poss
anthracene	42.8	178		poss	poss	poss	poss	poss
octadecane	42.9	254	poss		poss	poss	poss	poss
nonadecane	45.5	268	85		85	13 ^e	20	33
dibutyl phthalate	47.5	278	65	18	83	46	94	140
eicosane	48.1	282	30	1	31			
(vinyl decanoate)	48.6			2	2			
juvabione	48.8	234				7 ^c	21	28
di- <i>n</i> -pentyl phthalate	49.8	306				13 ^c	94	107
fluoranthrene	50	202					23	23
heneicosane	50.5	296			34	19		19
pyrene	51.4	202	poss				20	20
docosane	52.9	310	13		13	22		22
tricosane	55.1	324	24		24	43 ^c	3	46
butyl butoxyethyl phthalate	55.6	336	97	100	197	400	440	840
tetracosane	57.4	338				38		38
(substituted phenol)	58.3	312		28	28			
benzophenanthridine	58.9	229	57		57			
(carbomethoxybenzophenone)	59	312				40	40	40
pentacosane	59.4	352	24		24	47		47
(methylphenylcyclopropanyl phenyl sulfides)	59.1–59.4	316					10	10
dioctyl phthalate	60.6	390	25	6	31	13	32	45
hexacosane	61.5–61.6	366	15		15	45	57	102
(substituted phenol)	63.7	312					33	33
heptacosane	64.5–64.2	380	38		38	46		46
octacosane	67.3	394	20		20			
triphenylbenzene	68.5	306	55		55			
nonacosane	71.2	408				27		27
triacontane	76.1	422	7	2	9	26		26

^a Compounds tentatively identified are shown in parentheses. All organic compounds in the fly ash have been corrected for amounts found in sand ashed at 500 °C for 2 days. ^b Gas chromatography. ^c Peak seen on gas chromatogram but not identified by gas chromatography–mass spectrometry. ^d Possible occurrence. The as chromatography–mass spectrometry showed some ions in reverse ion search. ^e The gas chromatography peaks found in this region had the molecular weight indicated but were not identified as the compound shown.

Table V. Concentrations in ppb of Different Classes of Organic Compounds Identified in Extracts of Fly Ash Collected at the Four Corners Power Station on Dec 12, 1979

class	wet scrubber fly ash	electrostatic precipitator fly ash
aromatic compounds		
one ring	1800	2400
two ring	10	520
three ring	60	210
four ring	trace	40
nonaromatic compounds		
M _r < 170	330	2100
M _r > 170	1800	680
total	4000	6000

are ubiquitous plasticizers, are especially suspect. Also, the identification of compounds was incomplete; some of the compounds could not be identified by GC–MS because it could only positively identify those compounds for which known spectra exist.

Potential Environmental Hazard. Compounds reported in the extracts of fly ash were checked against lists of toxic water pollutants and toxic chemicals (3, 17). Chemicals that matched were generally radically lower in concentration in the extracts than the permissible concentration in water. Most of the 129 priority water pollutants listed by the U.S. Environmental Protection Agency were not found in our extracts (20). Those found of concern are PAHs and nitrogen-containing compounds. The PAHs found in largest concentrations in the extracts

were naphthalene and its derivatives. Recently, we measured the partitioning of [¹⁴C]naphthalene between fly ash and scrubber water. For ESP fly ash and scrubber water, the ratio was 1100:1, and for WS fly ash and scrubber water, it was 2400:1. Therefore, we would expect the naphthalene concentrations in water equilibrated with the ESP fly ash to be about 0.08 µg/L and that equilibrated with WS fly ash to be about 0.004 µg/L. These concentrations are lower than those found in some drinking water (14). Because all PAHs larger than naphthalene were lower in concentration in the extracts and are expected to be less soluble in water, the naphthalene concentration in water probably represents a maximum PAH concentration. The average concentration of PAHs in drinking water is 0.014 µg/L, but exposure to PAH from all sources is 1.6 µg/day (15). However, some drinking water supplies have been found to contain as much as 1.4 µg/L PAHs (15). These data indicate that the equilibrium concentrations of PAH in ESP or WS leachates would probably not be a hazard according to current standards.

The other group of compounds of concern are those containing nitrogen. Clark et al. analyzed extracts of synfuels from coal (16). Their results from Ames tests indicate that primary arylamines are extremely mutagenic and other arylamines and heterocyclic compounds are less mutagenic. Of all the multitude of aromatic, nitrogen-containing compounds found in coal synfuels, only diphenylamine at 24 ppb and benzophenanthridine at 51 ppb were found in extracts of WS fly ash; none were found in extracts of the ESP fly ash.

A permissible concentration in air for diphenylamine of 10.0 mg/m³ was proposed by the American Conference of

Industrial Hygienists (17). If it is assumed that a 70-kg man breathes 12.1 m³ of air each working day and consumes 2 L of water/day, we can convert a work exposure to full-time exposure (28.8 mg/day) and calculate an equivalent permissible water concentration of 14.4 mg/L (18). Because the octanol-water partition coefficient of this compound is similar to that of naphthalene (3), a leachate in equilibrium with the WS ash would be predicted to have a concentration of 0.01 µg/L. This concentration is well within that calculated to be permissible for drinking water purposes.

No permissible water concentrations were found for benzophenanthridine. However, some data are available for acridine, which has a similar structure but one less aromatic ring. Let us assume that acridine is present in fly ash. Acridine has a log octanol-water partition coefficient of 3.4 (similar to that of naphthalene), from which a water concentration of 0.02 µg/L is predicted. Dacre et al. (18) suggest a safe daily dose to be (1.155 × 10⁻⁵)LD₅₀. In the 1980 edition of the *Registry of Toxic Effects of Chemical Substances*, intravenous LD₅₀ for a rabbit of 100 mg/kg is listed (19). Using human weight and consumption values, we can calculate an equivalent dose to man to be 1.15 × 10⁻³ mg/kg or 40 µg/L. This value is much greater than the concentration predicted for this compound in the leachate of fly ash. Let us now consider the potential impact of benzophenanthridine in fly ash. Because it has another ring, it would be expected to be less soluble and more tightly bound to the fly ash than acridine and therefore be present in lower concentration in the water. However, because of the additional ring, it would be expected to be more mutagenic.

Ahlberg et al. studied mutagenicity of the emission above an ESP of a coal-fired power plant (21). They found it to be below the detection limit of the Ames test. They pointed out that the PAH concentration was up to 3 orders of magnitude higher in smoke from residential wood burning and in diesel and gasoline exhausts than it was in emissions from coal-fired power plants.

Anderson found more sister chromatid exchange (SCE) induced by ash collected above pollution control equipment than from it (22). Only one sample from an ESP unit of a coal-fired power plant showed increased SCEs. This emission passed through a cyclone unit prior to the ESP, thereby probably allowing more cooling and condensation of the organic compounds with higher boiling points.

Conclusions

Comparison of extracts of fly ash from WS and ESP collectors showed higher concentrations of low molecular weight organic compounds as well as more PAHs in the ESP fly ash. The WS fly ash contained a series of high molecular weight terpenes which were absent from the ESP ash.

Significant amounts of *n*-alkanes through C₃₀ and PAHs up to four rings were found. No compounds containing more than four rings were identified. Radiolabel studies performed on extraction techniques indicated poor recovery of BaP added to fly ash; therefore, absence of PAHs containing more than four rings in the GC-MS analyses may not imply that they are not present in the fly ash.

The amounts of solvent-extractable organic compounds present in WS and ESP fly ash were small, and we do not anticipate that any single compound will constitute an environmental hazard. However, potential adverse effects posed by the complex mixture of organic compounds present in fly ash are not understood and need to be in-

vestigated. Also, before this waste is classified as nonhazardous, more information is required on chemical reactions and microbial transformations occurring under storage conditions that may enhance the mobility and increase the mutagenicity of constituents in the waste.

Acknowledgments

We thank George Cameron, Fred Dietrich, Clay Scott, and Molly Barker for technical assistance on this project and Daniel Stuermer and Charles Morris for their advice and assistance in the analysis and identification.

Literature Cited

- Wakeham, S. G.; Farrington, J. W. In "Contaminants and Sediments"; Baker, R. A., Ed.; Ann Arbor Science: Ann Arbor, MI, 1960; pp 3-32.
- Ondov, J. M.; Ragaini, R. C.; Biermann, A. H. *Environ. Sci. Technol.* 1979, 13, 946-953.
- Verschueren, K. "Handbook of Environmental Data on Organic Chemicals"; Van Nostrand Reinhold: New York, 1983.
- Davidson, R. M. In "Coal Science"; Gorbaty, M. L.; Larsen, J. W.; Wender, I., Eds.; Academic Press: New York, 1982; pp 120-126.
- Noyes, R., Ed. "Coal Resources, Characteristics and Ownership in U.S.A."; Noyes Data Corp.: Park Ridge, NJ, 1978; p 216.
- Berkowitz, N. "An Introduction to Coal Technology"; Academic Press: New York, 1979; pp 137-142.
- Griest, W. H.; Guerin, M. R. "Identification and Quantification of Polynuclear Organic Matter (POM) on Particulates from a Coal-Fired Power Plant". Oak Ridge National Laboratory, Oak Ridge, TN, 1979, interim report.
- Bennett, R. L.; Knapp, K.; Jones, P. W.; Wilkerson, J. A. E.; Strup, P. E. *Polynucl. Aromat. Hydrocarbons, Int. Symp. Chem. Biol.—Carcinog. Mutagen.*, 3rd, 1979, 419-428.
- Bartle, K. D.; Jones, D. W.; Pakdel, H. In "Analytical Methods for Coal and Coal Products"; Karr, C., Jr., Ed.; Academic Press: New York, 1978; pp 250-254.
- Natusch, D. F. S. *Environ. Health Perspect.* 1978, 22, 79-90.
- Hangebrauck, R. P.; Von Lehmden, D. J.; Meeker, J. E. *J. Air Pollut. Control Assoc.* 1974, 14, 267-278.
- Ondov, J. M.; Ragaini, R. C.; Biermann, A. H. *Environ. Sci. Technol.* 1979, 13, 598-607.
- Rohrbach, B. G.; Reed, W. E. "Evaluation of Extraction Techniques for Hydrocarbons in Marine Sediments". Institute of Geophysics and Planetary Physics, University of California at Los Angeles, Los Angeles, CA, 1976, Publication 1537.
- Environmental Criteria and Assessment Office "Ambient Water Quality Criteria for Naphthalene"; Environmental Criteria and Assessment Office, U.S. Environmental Protection Agency: Washington, DC, 1980; EPA-440/5-80-059, p C-31.
- Environmental Criteria and Assessment Office "Ambient Water Quality Criteria for Polynuclear Aromatic Hydrocarbons (PAHs)"; Environmental Criteria and Assessment Office, U.S. Environmental Protection Agency: Washington, DC, 1980; EPA-440/5-80-069, pp C-110-C-111.
- Clark, B. R.; Ho, C.; Greist, E. H.; Guerin, M. R. "Abstracts of Papers", 179th National Meeting of the American Chemical Society, Houston, TX, March 1980; American Chemical Society: Washington, DC, 1980; CONF-800303-13.
- Sittig, M. "Handbook of Toxic and Hazardous Chemicals"; Notes Publications: Park Ridge, NJ, 1981.
- Dacre, J. C.; Rosenblatt, D. H.; Cogley, D. R. *Environ. Sci. Technol.* 1980, 14, 778-784.
- Lewis, R. J., Sr.; Tatken, R. L., Eds. "Registry of Toxic Effects of Chemical Substances", 1980 ed.; U.S. Government Printing Office: Washington, DC, 1982; Publication 81-226.
- Callahan, M.; Simak, M.; Gabel, N.; May, I.; Fowler, C.; Freed, R.; Jennings, P.; Durfee, R.; Whitmore, F.; Maestri,

B.; Mabey, W.; Holt, B.; Gould, C. "Water Related Environmental Fate of 129 Priority Pollutants"; U.S. Environmental Protection Agency: Washington, DC, 1979; EPA 440/4-79-029a, Vol. 1 and 2.

- (21) Ahlberg, M.; Bergheim, L.; Nordberg, G.; Persson, S.; Rudling, L.; Steen, B. *Environ. Health Perspect.* 1983, 47, 85-102.

- (22) Anderson, O. *Environ. Health Perspect.* 1983, 47, 239-253.

Received for review February 17, 1984. Revised manuscript received September 24, 1984. Accepted October 1, 1984. This work was performed under the auspices of the U.S. Department of Energy by the Lawrence Livermore National Laboratory under Contract W-7405-Eng-48.

NOTES

Influence of pH and Ionic Strength on the Aqueous-Nonaqueous Distribution of Chlorinated Phenols

John C. Westall*

Department of Chemistry, Oregon State University, Corvallis, Oregon 97331

Christian Leuenberger and René P. Schwarzenbach

Swiss Federal Institute for Water Resources and Water Pollution Control (EAWAG), CH-8600 Dübendorf, Switzerland

■ The distribution ratio of hydrophobic ionizable organic compounds (HIOC's) between aqueous and nonaqueous phases is shown to depend on the pH and ionic strength of the aqueous phase. Four models are presented to describe the association of the HIOC with the nonaqueous phase: (i) transfer of the neutral organic species from the bulk of the aqueous phase to the bulk of the nonaqueous phase; (ii) transfer of the ionic organic species with inorganic counterions to the bulk of the nonaqueous phase; (iii) transfer of the ionic organic species to the aqueous-nonaqueous interface with inorganic counterions in the aqueous phase; (iv) association of the organic species with specific functional groups of the nonaqueous phase. The distribution of 2,3,4,5-tetrachlorophenol and pentachlorophenol in the two-phase system composed of KOH, KCl, H₂O, octanol, and the chlorophenol was determined as a function of ionic strength and interpreted quantitatively in terms of models i and ii. For aqueous phases with high pH values and ionic strengths, the dominant species of the chlorophenols in the octanol phase were the chlorophenolate ions in association with K⁺ counterions.

Introduction

The distribution ratios of nonpolar organic compounds between water and natural sorbents have been estimated with satisfactory accuracy from their relationships to the organic carbon content of the sorbent and the octanol-water partition constant of the solute. These correlations have been of great value in the estimation of the degree of sorption of a wide variety of compounds on a wide variety of sorbents. However, it has been noted in some of the correlation studies that polar and especially ionizable organic compounds do not fit to the same pattern as the nonpolar compounds.

In a recent study on the sorption of chlorinated phenols by sediments and aquifer materials, Schellenberg et al. (1) demonstrated that sorption of not only the neutral phenol but also the anionic phenolate occur. In certain cases the phenolate species contributes significantly to the overall distribution ratio of the compounds. Kaiser and Vald-

Table I. Properties of Some Hydrophobic Ionizable Organic Compounds

compound	log K_a^a	log K_{ow}^a
2-chlorophenol	8.52	2.17
2,4-dichlorophenol	7.85	2.75
2,4,6-trichlorophenol	5.99	3.38
pentachlorophenol	4.74	5.01
2-nitrophenol	7.21	1.76
4-nitrophenol	7.15	1.91
2,4-dinitrophenol	4.09	1.53
2,4-dimethylphenol	10.60	2.50
3-methyl-4-chlorophenol		2.95
2-methyl-4,6-dinitrophenol	4.35	2.85

^a Values from Callahan et al. (3).

manis (2) have reported the dependence on pH of the distribution ratio of pentachlorophenol between water and octanol, but no systematic study of the effect of ionic strength was made. Experimental results of Schellenberg et al. (1) indicate that phenolate sorption is strongly influenced by the organic carbon content of the sorbent and by the ionic composition of the aqueous phase. The authors conclude that a much more detailed understanding of the interactions that govern the distribution of such hydrophobic anions between aqueous and nonaqueous phases is necessary to arrive at a quantitative description of the sorption of chlorinated phenols and other hydrophobic ionizable organic compounds (HIOC's) by natural sorbents. It is the purpose of this paper to examine the theoretical framework on which the distribution of HIOC's between aqueous and nonaqueous phases is to be viewed and to test the suitability of this theory in the octanol-water system with two HIOC's of environmental concern, pentachlorophenol and 2,3,4,5-tetrachlorophenol.

Although only two HIOC's are considered in this paper, several of the 129 priority pollutants discussed by Callahan et al. (3) belong to this class of compounds, as is shown in Table I. The K_{ow} referred to in the table is the partition constant for the neutral species. As is seen for the chlorophenols, an increase in the number of chloro substituents

Table II. Association of Organic Compound with Nonaqueous Phase^a

- I. solvation of neutral organic compound in bulk nonaqueous phase:

$$AH = \overline{AH}$$
- II. solvation of ion pair or free ions in bulk nonaqueous phase:

$$A^- + K^+ = \overline{A^-K^+} (= \overline{A^-} + \overline{K^+})$$
- III. adsorption of organic ion from aqueous phase onto lipophilic surface with counterion in electric double layer:

$$\Xi + A^- + K^+ = \overline{\Xi-A^-} + K^+$$
- IV. ligand exchange of organic molecule with surface hydroxyl group at inorganic oxide surface:

$$\overline{\Xi XOH} + AH = \overline{\Xi XA} + H_2O$$

^a Symbols: AH represents neutral pentachlorophenol; A⁻ represents pentachlorophenolate ion; XOH represents an oxide surface hydroxyl group, for example, ≡SiOH, ≡AlOH, and ≡FeOH; the overbar indicates species in the nonaqueous phase; ≡ represents surface (nonaqueous phase).

leads to an increase in the acidity and an increase in the hydrophobicity. Thus, the phenols with more chloro substituents are more likely to be ionized at environmental pH values and are intrinsically more hydrophobic. However, the same effect is not seen for the nitrophenols, since the nitro substituent, which causes the increase in acidity of the phenol, causes much less hydrophobicity than the chloro substituents. These examples point out that the class of HIOC's includes many compounds of environmental concern and that there is reason to include the ionic species in studies of the transport and the fate of these compounds.

Theory

Several mechanisms can be considered for the association of the HIOC with the nonaqueous phase. The relative importance of each mechanism depends primarily on the K_a and K_{ow} of the organic molecule, the pH and ionic strength of the aqueous phase, and the nature of the nonaqueous phase. The experimental work presented here indicates that free ions or ion pairs can be the predominant forms of the organic compound in the nonaqueous phase at pH values favoring the ionized form in the aqueous phase.

Four mechanisms by which organic solutes associate with the nonaqueous phase are presented in Table II. Only mechanisms I and II will be considered in interpretation of the experimental data, but mechanisms III and IV are presented for comparison. To facilitate discussion of the mechanisms, a specific system is considered: distribution of pentachlorophenol (PCP represents the compound in general, AH represents specifically the neutral species, and A⁻ represents the anionic species) between a nonaqueous phase and an aqueous phase containing water, a salt (KCl), an acid (HCl), and a base (KOH). A distinction must be made between the partition constant, K_p , which is defined for a particular species:

$$K_p = \frac{[\overline{AH}]}{[AH]} \quad (1)$$

and the distribution ratio, D , which is defined for the total analytical concentration:

$$D = \frac{[\overline{AH}] + [\overline{A^-}]}{[AH] + [A^-]} = \frac{[\overline{PCP}]}{[PCP]} \quad (2)$$

Table III. Possible Species in the System: H₂O, KOH, HCl, AH, and Octanol

aqueous phase	nonaqueous phase	
	ion pairs	ions
H ₂ O	\overline{AH}	$\overline{H^+}$
H ⁺	\overline{AK}	$\overline{A^-}$
OH ⁻	\overline{KCl}	$\overline{K^+}$
K ⁺	$\overline{H_2O}$	$\overline{Cl^-}$
Cl ⁻	\overline{KOH}	$\overline{OH^-}$
AH	\overline{HCl}	
A ⁻		

For many nonpolar organic compounds only one species of the compound exists, and the values of K_p and D are identical. The concentrations of the neutral and ionized species in the aqueous phase are related by the acidity constant, hydrogen ion concentration, and activity coefficients:

$$K_a = \frac{[A^-][H^+]}{[AH]} \gamma_{A^-} \gamma_{H^+} \gamma_{AH} \quad (3)$$

Mechanism I of Table II involves the distribution of a neutral species between the bulk of the aqueous phase and the bulk of the nonaqueous phase, with no side reactions. This mechanism and the linear free energy relationships described by Leo et al. (4) have been used successfully to interpret energetics of sorption for a wide variety of nonpolar organic compounds (5-8). The partition constant K_p^{ij} of an organic compound i between water and any natural sorbent j can be calculated from the octanol-water partition constant of the compound K_{ow}^i and the fraction organic carbon of the sorbent f_{oc}^j :

$$\log K_p^{ij} = \log K_{oc}^i + \log f_{oc}^j = a \log K_{ow}^i + b + \log f_{oc}^j \quad (4)$$

The intermediate quantity K_{oc}^i is the partition constant for a hypothetical sorbent of 100% organic carbon. For a particular compound and sorbent, the partition constant is the ratio of concentration in the aqueous phase to the nonaqueous phase. For compounds that yield both neutral and ionic species in aqueous solutions, the distribution ratio D can be calculated from the value of K_p given from eq 4 and the acidity constant

$$D = \frac{K_p}{1 + K_a/[H^+]} \quad (5)$$

if it is assumed that only the neutral species is present in the nonaqueous phase and activity corrections are neglected. In many systems it is clear that ionic species do enter the nonaqueous phase, and more complete mechanisms have to be considered.

Mechanism II of Table II is simply the mechanism studied in solvent extraction chemistry, only with the emphasis placed on extraction of the organic compound rather than on extraction of the inorganic ion. This mechanism can be illustrated by considering equilibrium in the system composed of H₂O, HCl, KOH, AH, and octanol, i.e., the partition of PCP between an aqueous phase of variable pH and ionic strength and nonaqueous phase of water-saturated octanol. The species present in the aqueous phase are known with certainty (Table III). In the nonaqueous phase, the species H₂O and AH are certain to exist. The experiments reported here give evidence for the presence of organic and inorganic ions or ion pairs in

Table IV. Reactions in System H₂O, HCl, KOH, PCP, and Octanol

reaction	log K ^a (298 K, I → 0)
(1) K ⁺ + Cl ⁻ = $\overline{K^+} + \overline{Cl^-}$	-7.9 ^b
(2) K ⁺ + A ⁻ = $\overline{K^+} + \overline{A^-}$	-7.1 ^c
(3) K ⁺ + OH ⁻ = $\overline{K^+} + \overline{OH^-}$	
(4) H ⁺ + A ⁻ = $\overline{H^+} + \overline{A^-}$	
(5) H ⁺ + Cl ⁻ = $\overline{H^+} + \overline{Cl^-}$	
(6) H ⁺ + OH ⁻ = $\overline{H^+} + \overline{OH^-}$	
(7) K ⁺ + Cl ⁻ = \overline{KCl}	-2.9 ^b
(8) K ⁺ + A ⁻ = \overline{AK}	2.6 ^c
(9) K ⁺ + OH ⁻ = \overline{KOH}	
(10) AH = \overline{AH}	5.24 ^d
(11) HCl = \overline{HCl}	
(12) H ₂ O = $\overline{H_2O}$	
(13) H ₂ O = H ⁺ + OH ⁻	-14.00
(14) AH = H ⁺ + A ⁻	-4.75 ^d

^a For extrapolation of equilibrium constants to I → 0 the Davies equation was used to estimate aqueous phase activity coefficients. Nonaqueous phase activity coefficients were set equal to 1. ^b Determined from data in Figure 2 (lower curve) with a modified form of FITSQL (10), a weighted nonlinear least-squares optimization procedure for determination of constants in chemical equilibrium systems. Residuals in K⁺ concentration in octanol were minimized with respect to constants for reactions 1 and 7, only. Reactions 3 and 9 were found to be less significant under prevailing experimental conditions and, along with reactions 5, 6, and 11, were not included in the model. ^c Determined from data in Figure 1 with a modified form of FITSQL (10). Weighted residuals in total mass of PCP in the system and total concentrations of PCP in octanol and in water were minimized with respect to constants for reactions 2 and 8 and the constraint of material balance of PCP in the system. ^d From ref 1.

the nonaqueous phase. Since the nonaqueous phase in this system contains ≈ 3.2 M H₂O, solvation of free ions and their presence in the nonaqueous phase is not implausible, as will be discussed.

For the sake of completeness, all of the possible ion pairs and free ions in the organic phase are listed in Table III, even for species likely to be present at very low concentrations. The set of reactions that completely describes the formation of these species is given in Table IV, along with values for equilibrium constants estimated from this work. All of the reactions listed in Table IV are electro-neutral; i.e., they involve no net transfer of charge from the aqueous phase to the nonaqueous phase. If transfer of single ions were considered, an extrathermodynamic assumption would have to be made with regard to how the observed energy of transfer for an electroneutral pair should be divided between the anion and the cation.

Mechanism II has been approached as a multicomponent chemical equilibrium problem. The speciation of solutes in the octanol-water system containing HCl, KOH, and AH is uniquely and completely determined by the material balance equations for the solutes, the electroneutrality equation for each phase, and the mass action equations for the reactions in Table IV. This equilibrium problem can be solved by the computer program MICROQL (9), and equilibrium constants can be determined from experimental data with the program FITSQL (10).

Mechanism III involves the removal of the HIOC to a lipophilic organic surface. For ionized organic compounds, the counterion must no longer be transferred to the organic phase but may remain in the electric double layer in the aqueous phase. In this case the HIOC's behave as ionic surfactants. In natural systems there is certainly a continuous transition between mechanism II (transfer to a

three-dimensional organic phase) and mechanism III (transfer to a two-dimensional organic surface). However, it is instructive to examine laboratory results for a purely mechanism III reaction as a limiting case. Cantwell and Puon (11) found the adsorption of diphenylguanidium (DPGH⁺) ion on XAD-2 (a polystyrene-divinylbenzene resin) to be describable in terms of a Gouy-Chapman model of the interface with Cl⁻ ions as counterions in the electric double layer. For constant surface potential and constant bulk concentration of DPGH⁺, the concentration of adsorbed DPGH⁺ was found to vary with the square root of the ionic strength as predicted by the Gouy-Chapman theory.

Mechanism IV involves the specific interaction of the ionogenic functional group of the organic molecule with a functional group of a purely inorganic surface. This mechanism is unique with respect to the other three in that it involves, at least conceptually, interaction of specific functional groups, as opposed to an undefined interaction of organic solvents and organic sorbents. Mechanism IV can be interpreted in terms of the surface complexation model as reviewed recently by James and Parks (13), Schindler (14), Westall and Hohl (15) and Stumm et al. (16). According to this model hydroxyl groups on the surface of hydrous oxides (silica, alumina, iron and manganese oxides, clays, etc.) react similarly to hydroxide groups in homogeneous solution—complexing cations and exchanging for anions. Stumm et al. (16) have studied the surface complexation of the aromatic compounds benzoic acid, salicylic acid, phthalic acid, and catechol on γ-Al₂O₃ and found detectable removal of all four from solution. These results suggest that the removal of certain ionic organic compounds on pristine oxide surfaces should not be overlooked. However, the results of Schellenberg et al. (1) indicate that organic carbon is still the dominant sorbent of chlorophenolate ions in a sediment and a natural aquifer material.

In this report only anionic HIOC's are considered. It is to be expected that the relative importance of the various mechanisms of transfer is different for cationic HIOC's, since most natural sorbents are negatively charged at environmental pH values.

Experimental Section

The distribution ratios of pentachlorophenol, 2,3,4,5-tetrachlorophenol, and 3,4,5-trichlorophenol were determined in an aqueous phase composed of water, KCl (0.2, 0.1, and 0.05 M), KOH (0.01 M), and the nonaqueous phase of octanol saturated with the aqueous solution.

The chlorophenols were analytical grade from Merck, and the octanol was spectroscopic grade from Merck, all used without further purification. All water was doubly distilled in quartz. HCl and KOH solutions were prepared from Merck ampules, and KCl was analytical grade from Merck.

Aqueous solutions with a particular concentration of KOH and KCl were prepared and preequilibrated with a small volume of octanol. Octanol was preequilibrated with a small volume of the aqueous solution. Then volumes of the preequilibrated aqueous and nonaqueous phases were mixed and spiked with a volume of the chlorophenol dissolved in octanol. The solutions were mixed for 24 h at 20 °C on a shaker, the phases were separated, and samples of the aqueous and nonaqueous phases were withdrawn for analysis from the bulk of the solutions with a pipet.

The concentrations of the chlorophenols in the aqueous and nonaqueous phases were determined by ultraviolet spectrophotometry. Absorbances were measured at 11 wavelengths between 280 and 340 nm, and a nonlinear

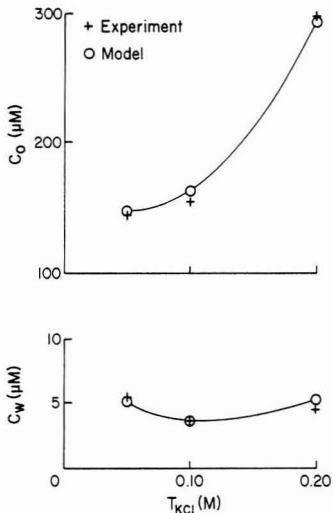


Figure 1. Concentration of PCP distributed between octanol and water. Composition of aqueous phase 0.01 M KOH and KCl. Constants for equilibrium model in Table IV.

least-squares calibration and data reduction technique was used to allow determination of concentrations of both neutral and anionic species. Mass balance between material added and material found agreed to within 1% in most cases and was no worse than 5% in any case. Volumes of solutions were chosen such that the amount of the chlorophenol in either phase was always at least one-fifth of the total amount added.

The concentration of K^+ in the nonaqueous phase was determined by standard addition technique with flame atomic absorption spectrophotometry. Samples were diluted to 2 times their original volume with methanol to decrease viscosity of the solution in order to increase the precision of the analysis.

The pH of the aqueous solutions was determined with a glass electrode and a Ag/AgCl/KCl reference electrode fitted with a Wilhelm salt bridge. The concentration of KCl in the reference electrode and salt bridge was the same as that in the aqueous solution. The glass electrode was calibrated to H^+ concentration by addition of standard HCl and KOH solutions to solutions of the same concentration of KCl as the particular sample of which the pH was to be determined.

The acidity constants of the chlorophenols were determined by the method described by Schellenberg et al. (1).

Results and Discussion

The concentration of PCP in octanol and water as a function of aqueous KCl concentration is shown in Figure 1. The nonaqueous phase concentration of PCP is seen to be a strong function of KCl concentration. The concentration of PCP in the aqueous phase remained approximately constant over the range of KCl concentration, since the volumes of aqueous and nonaqueous phases and amount of PCP added were selected with that goal in mind. The multicomponent chemical equilibrium model (to be discussed) has been used for interpretation of the experimental data; good agreement between the model and the experimental data is seen.

In Figure 2 is shown the concentration of K^+ in the nonaqueous phase as a function of concentration of KCl in the aqueous phase. It is seen that PCP has a dramatic

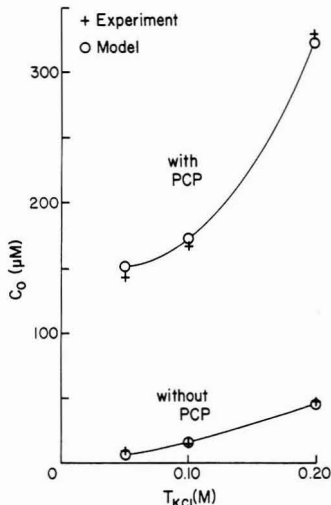


Figure 2. Concentration of K^+ in octanol with PCP (at concentrations shown in Figure 1) and without PCP. Composition of aqueous phase: 0.01 M KOH, KCl, and PCP.

effect on the extraction of K^+ from the aqueous phase. Through comparison with Figure 1 it is seen that the concentration of K^+ in the nonaqueous phase follows very closely the concentration of PCP in the nonaqueous phase.

It is obvious from the data that there is transfer of inorganic ions (K^+) into the nonaqueous phase along with the organic phenolate ion. Also the transfer of salts KCl or KOH must occur. Whether these inorganic ions exist in the organic phase as ion pairs or free ions is not resolved. The experimental data and calculations based on Bjerrum's model (17) of ion association in a continuous dielectric medium suggest that both free ions and ion pairs could contribute significantly to the total amount of PCP in the nonaqueous phase.

Chemical Equilibrium Model. The chemical equilibrium model used to describe the experimental results is completely defined by the material balance equations for PCP, KOH, and KCl, the electroneutrality equation for both phases, and the mass action laws for the reactions given in Table IV. The reactions in the table are written for the transfer of neutral salts from the aqueous phase to the nonaqueous phase. No experiments were carried out to allow estimation of single ion partition constants.

Values of the constants for the reactions representing transfer of $\overline{K^+}$, $\overline{Cl^-}$, and \overline{KCl} (reactions 1 and 7 in Table IV) were found from the data in the lower curve of Figure 2. Other experiments showed that the concentration of K^+ in the nonaqueous phase did not vary strongly with pH for constant KCl concentration in the aqueous phase. On this basis it was decided to omit reactions 3 and 9 from the equilibrium model, although these reactions probably become significant under other experimental conditions.

For a simple salt solution such as KCl the predominance of free ions vs. the predominance of ion pairs in the nonaqueous phase can be assessed from the dependence of nonaqueous phase salt concentration on aqueous phase salt concentration: a predominance of free ions results in a linear dependence, and a predominance of ion pairs results in a quadratic dependence. The formation of ion pairs is favored at higher salt concentrations. From the linear-quadratic form of the lower curve in Figure 2, both the free ion and the ion pair are expected to be significant species. On account of the limited domain over which experimental

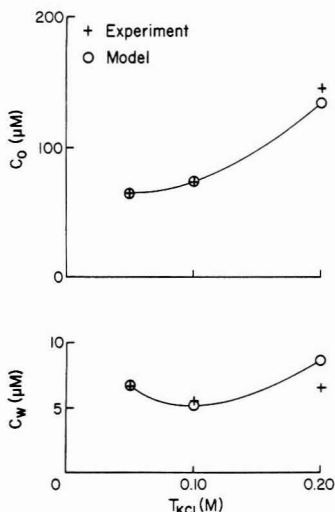


Figure 3. Concentration of TeCP distributed between octanol and water. Composition of aqueous phase: 0.01 M KOH and KCl. Equilibrium model defined in Table IV, except with constants for TeCP (18).

data were obtained, the values found for the constants are subject to considerable covariability. However, it is worth noting that the values obtained for the equilibrium constant for ion association in the organic phase

$$\overline{M^+} + \overline{X^-} = \overline{MX} \quad K_{ip} \quad (6)$$

are in the range predicted by Bjerrum's theory for ion association in a continuous dielectric medium such as octanol or water-saturated octanol. The constants for the other major reactions, the extraction of $\overline{K^+}$, $\overline{A^-}$ and \overline{AK} , were determined from the data in Figure 1 and the previously determined values for $\overline{K^+}$, $\overline{Cl^-}$ and \overline{AH} . Again, both the associated and dissociated forms of $\overline{K^+}$, $\overline{A^-}$ appear to be of importance.

Experiments similar to those described for distribution of pentachlorophenol were carried out with 2,3,4,5-tetrachlorophenol (TeCP). The aqueous phase concentrations are shown in Figure 3. It is seen that transfer to the nonaqueous phase is favored at higher ionic strengths but that tetrachlorophenol is less favored in the nonaqueous phase than is pentachlorophenol. Thus, the order of hydrophobicity of the neutral phenols is maintained for the ionic phenolates. An equilibrium model defined by reactions similar to those of Table IV but with equilibrium constants for TeCP (18) can be used to interpret the experimental data for the partition experiments with TeCP, as seen in Figure 3.

The equilibrium model that was developed for PCP (reactions in Table IV, mass balance, and electroneutrality) has been applied to estimate the concentration distribution ratio of PCP at any ionic strength over a range of pH values. The results of such computations are shown in Figure 4. At pH values less than pH 7 the distribution is dominated by the transfer of the neutral species AH and is independent of salt concentration. (The salting out effect which occurs at higher ionic strengths is not considered in this model.) At pH values greater than pH 10, the predominate PCP species in the nonaqueous phase is the phenolate anion, and the distribution ratio is strongly related to salt concentration. Note that the relationship between $\log D$ and $\log C_{KCl}$ is not linear, reflecting the

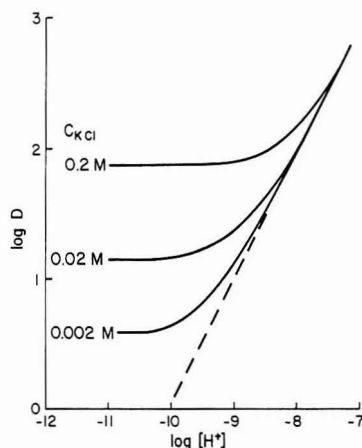


Figure 4. Distribution ratio of PCP between octanol and water as a function of pH for several ionic strengths. Computed for equilibrium among reactions listed in Table IV. Aqueous phase activity coefficients were estimated from the Davies equation. If phenolate ion were not present in the octanol phase (corresponding to $C_{KO} \approx 0$), the observed $\log D$ vs. $\log H^+$ relationship would follow the broken line.

presence of both free phenolate ions and phenolate ions associated with K^+ in the nonaqueous phase.

Summary

A first step toward resolving the influence of aqueous phase pH and ionic strength on the aqueous/nonaqueous distribution of hydrophobic ionizable compounds has been taken. Evidence has been presented that both free organic ions as well as organic-inorganic ion pairs are significant species in the nonaqueous phase. Thus, aqueous phase composition must be considered in calculating the distribution of these compounds. Further experiments are in progress to elucidate the effects of transfer to a three-dimensional nonaqueous phase or transfer to a two-dimensional (surface) nonaqueous phase.

Registry No. 2,3,4,5-Tetrachlorophenol, 4901-51-3; pentachlorophenol, 87-86-5; octanol, 111-87-5.

Literature Cited

- Schellenberg, K.; Leuenberger, C.; Schwarzenbach, R. P. *Environ. Sci. Technol.* **1984**, *18*, 652-657.
- Kaiser, K. L. E.; Valdmanis, I. *Can. J. Chem.* **1982**, *60*, 2104-2106.
- Callahan, M. A.; Slimak, M. W.; Gabel, N. W.; May, I. P.; Fowler, C.; Freed, J. R.; Jennings, P.; Durfee, R. L.; Whitmore, F. C.; Maestri, B.; Mabey, W. R.; Holt, B. R.; Gould, C. "Water-Related Environmental Fate of 129 Priority Pollutants"; U. S. Environmental Protection Agency: Washington, DC, 1979; Vol. I and II, EPA-440/4-79-029a and EPA-440/4-79-029b.
- Leo, A.; Hansch, C.; Elkins, D. *Chem. Rev.* **1971**, *71*, 525-553.
- Kenaga, E. E.; Goring, C. A. I. *ASTM Spec. Tech. Publ.* **1980**, No. 707.
- Schwarzenbach, R. P.; Westall, J. *Environ. Sci. Technol.* **1981**, *15*, 1360-1367.
- Karickhoff, S. W. *Chemosphere* **1981**, *10*, 833-846.
- Brown, D. S.; Flagg, E. W. *J. Environ. Qual.* **1981**, *10*, 382-386.
- Westall, J. "MICROQL: I. A Chemical Equilibrium Program in BASIC"; EAAG: Duebendorf, Switzerland, 1979.
- Westall, J. "FITEQL: A Computer Program for Determination of Chemical Equilibrium Constants from Experimental Data". Department of Chemistry, Oregon State

University, Covallis, OR, 1982, Report 82-01.

- (11) Cantwell, F.; Poon, S. *Anal. Chem.* 1979, 51, 623-632.
- (12) Horvath, C.; Melander, W.; Molnar, I. *Anal. Chem.* 1977, 49, 142-154.
- (13) James, R. O.; Parks, G. *Surf. Colloid Sci.*, 1982, 12, 119-216.
- (14) Schindler, P. W. In "Adsorption of Inorganics at Solid-Liquid Interfaces"; Anderson, M.; Rubin, A., Ed.; Ann Arbor, Science Publishers: Ann Arbor, MI, 1981.
- (15) Westall, J.; Hohl, H. *Adv. Colloid Interface Sci.* 1980, 12, 265-294.

- (16) Stumm, W.; Kummert, R.; Sigg, L. *Croat. Chem. Acta* 1980, 53, 291-312.
- (17) Harned, H. S.; Owen, B. B. "The Physical Chemistry of Electrolytic Solutions"; American Chemical Society: Washington, DC, 1958.
- (18) Westall, J., Oregon State University, Corvallis, OR, unpublished data, 1983.

Received for review January 16, 1984. Revised manuscript received May 15, 1984. Accepted September 4, 1984.

CORRESPONDENCE

Comment on "Fish/Sediment Concentration Ratios for Organic Compounds"

SIR: The examination of fish/sediment concentration ratios by Connor (1) provides an instructive comparison of the environmental behavior and fate of chlorinated aromatic hydrocarbons (CAHs) and polynuclear aromatic hydrocarbons (PAHs). However, errors in his eq 3 led him to erroneously conclude that "fish/sediment ratios greater than about 0.01 are higher than could be predicted" and that each of the fish liver/sediment ratios in his Figure 3 "is 3-5 orders of magnitude higher than predicted by assuming an organic content of 1% carbon." In fact, ratios much higher than 0.01 can be predicted, and the ratios in his Figure 3 are very close to the values predicted by the corrected equation. Thus, fish/sediment ratios predicted by using Connor's approach are much closer to observed field ratios and therefore even more useful than Connor suggested.

Two errors are present in Connor's eq 3. First, in converting the organic-carbon-normalized partition coefficient (K_{oc}) to the mass-normalized, or sediment, partition coefficient (K_{sed}), one should multiply K_{oc} by f_{oc} , the fraction of the sediment, by weight, composed of organic carbon; Connor expressed f_{oc} as a percent, thereby introducing an error of 2 orders of magnitude into his calculations. The relationship shown in his Figure 1 thus represents ratios for sediments containing 100% organic carbon as stated in the text, not 1% as stated in the figure legend. Second, because K_{oc} and f_{oc} are in the denominator of the ratio, the $\log(f_{oc})$ term [or, alternatively, $\log(\% \text{ organic carbon}/100)$] should be subtracted from the right side of eq 3 and not added. This error led Connor to conclude that sediments with less than 100% organic carbon should have a lower fish/sediment concentration ratio, when in fact they are expected to have a higher ratio. The corrected equation for predicting the fish/sediment concentration ratio from Kenaga and Goring's (2) relationships is

$$\log(\text{BCF}/K_{sed}) = -2.872 + 0.391 \log(K_{ow}) - \log(f_{oc}) \quad (1)$$

where BCF is the fish/water bioconcentration factor and K_{ow} is the octanol/water partition coefficient.

For an organic carbon content of 1% (i.e., $f_{oc} = 0.01$), the $\log(\text{BCF}/K_{sed})$ ratio increases from 0.30 to 1.67 as $\log(K_{ow})$ varies from 3.0 to 6.5. If the contaminant concentration in fish liver is 25 times higher than the whole-body

concentration, as Connor notes, then the $\log(\text{fish liver/sediment})$ ratio is expected to be 2.87 and 2.39 for a $\log(K_{ow})$ of 6 and f_{oc} of 0.01 and 0.03, respectively. These two predicted ratios are near the top and center, respectively, of the cluster of observed values for CAHs shown in Connor's Figure 3.

If the fish/sediment ratios for polychlorinated biphenyls (PCBs) shown in Connor's Figure 2 are examined separately as freshwater, marine, and laboratory values, the correlation with flushing time is much less evident. The four freshwater ratios, the four largest ratios in the figure, do not show a strong correlation with flushing time. However, they appear to be within an order of magnitude of 45, the steady-state ratio predicted by eq 1, assuming that $\log(K_{ow}) = 6.47$, as reported for Aroclor 1254 (3), and that the sediments are 1% organic carbon. A similar steady-state ratio of 21 is predicted by using the same assumptions and eq 2, based on the equations of Oliver and Niimi ("low exposure") (4) and Karickhoff et al. (5), and converting K_{oc} to K_{sed} :

$$\log(\text{BCF}/K_{sed}) = [0.997 \log(K_{ow}) - 0.869] - [\log(K_{ow}) - 0.21] - \log(f_{oc}) \quad (2)$$

Variation about the predicted fish/sediment ratio is certainly to be expected. Kenaga and Goring (2) reported 95% confidence limits of ± 1.35 for the $\log(\text{BCF})$ predicted from $\log(K_{ow})$ and ± 1.37 for the $\log(K_{oc})$ predicted from $\log(K_{ow})$. Also, the slope of the $\log(\text{fish/sediment})$ vs. $\log(K_{ow})$ relationship depends upon which equations are used in predicting the ratio. The slope can be positive (eq 1) (1), zero (5, 6), nearly zero (eq 2) (4, 5), or negative (5, 7). Several factors can contribute to variation about the predicted ratio. For example, for certain chemicals, accumulation through the food chain pathway could make the fish/sediment ratio higher than predicted by this analysis (though perhaps still within the 95% confidence limits).

It is not correct to refer to the laboratory bioconcentration factors from the studies cited by Connor (2, 3, 6, 8, 9) as "96-h" values. Although many chemicals can reach steady-state concentrations in fish in less than 96 h, the more lipophilic chemicals may take several weeks, as Connor notes, and some of the BCFs measured in the cited studies were accordingly made after several weeks of exposure. For example, steady-state BCFs were estimated by Veith et al. (3) from 32-day exposures. Although one technique for rapid estimation of BCFs involves 5-day exposures followed by a depuration period (10), this technique is used to estimate steady-state BCFs, not 96-h

or 5-day concentration ratios, from estimates of uptake and elimination rates. If all the laboratory-derived bioconcentration factors had been 96-h values, it would have helped explain how field ratios, presumably closer to steady state, could be higher than predictions based on those laboratory values.

The field data in Connor's figures and these corrected calculations suggest that equations developed from laboratory measurements may be useful in predicting the accumulation of CAHs by fish relative to sediments under field conditions. Comparable predictions of fish/sediment ratios for PAHs must account for their more rapid biotransformation in fish. Connor's approach to predicting fish/sediment ratios thus appears to be more successful than he suggested.

Literature Cited

- (1) Connor, M. S. *Environ. Sci. Technol.* 1984, 18, 31-35.
- (2) Kenaga, E. E.; Goring, C. A. I. *ASTM Spec. Tech. Publ.* 1980, STP 707, 78-115.
- (3) Veith, G. D.; DeFoe, D. L.; Bergstedt, B. V. *J. Fish. Res. Board Can.* 1979, 36, 1040-1048.
- (4) Oliver, B. G.; Niimi, A. G. *Environ. Sci. Technol.* 1983, 17, 287-291.
- (5) Karickhoff, S. W.; Brown, D. S.; Scott, T. A. *Water Res.* 1979, 13, 241-248.
- (6) Mackay, D. *Environ. Sci. Technol.* 1982, 16, 274-278.
- (7) Veith, G. D.; Macek, K. J.; Petrocelli, S. R.; Carrol, J. *ASTM Spec. Tech. Publ.* 1980, STP 707, 116-129.
- (8) Neely, W. B.; Branson, D. R.; Blau, G. E. *Environ. Sci. Technol.* 1974, 8, 1113-1115.
- (9) Chiou, C. T.; Freed, V. H.; Schmedding, D. W.; Kohnert, R. L. *Environ. Sci. Technol.* 1977, 11, 475-478.
- (10) Branson, D. R.; Blau, G. E.; Alexander, H. C.; Neely, W. B. *Trans. Am. Fish. Soc.* 1975, 104, 785-792.

† Operated by Martin Marietta Energy Systems, Inc., under Contract DE-AC05-84OR21400 with the U.S. Department of Energy. Publication No. 2445, Environmental Sciences Division, ORNL.

James E. Breck

Environmental Sciences Division
Oak Ridge National Laboratory[†]
Oak Ridge, Tennessee 37831

SIR: Breck's correction of my eq 3 (1) has the happy result of bringing the field data into better agreement with the mathematical predictions. As I noted in the paper, the fish/sediment ratio seems to reach a plateau when flushing times are greater than 100 days. These plateau values also agree nicely with the predicted steady-state ratios from the corrected eq 3. I believe this behavior is less associated with the freshwater nature of these environments as Breck suggests than with the coincidence that all the freshwater data available here happened to be from the environments with the longest flushing times. If all environmental pools were at steady state, presumably flushing time would have little importance. However, input loads can be highly variable, and fish/sediment ratios are one way of reducing this environmental variation.

Breck also shows that a variety of equations could be combined to yield quite different slopes of the fish/sediment ratio with respect to the octanol-water partition coefficient (K_{ow}). Mackay has recently argued that the relationship between the bioconcentration factor (BCF) and K_{ow} should be linear (2). Karickhoff et al. have developed a similar relationship for the soil partition coefficient (K_{oc}) (3). Combining these two equations yields a fish/sediment ratio independent of K_{ow} :

$$\frac{BCF}{K_{sed}} = \frac{0.077}{\text{fraction organic carbon}}$$

Of all the various combinations of equations, the simplicity of this relationship makes this equation most appealing. In addition, the variation reported by Mackay and Karickhoff et al. was much smaller than the earlier work of Kenaga and Goring (4). From McKay's and Karickhoff's regression data, I ran Monte Carlo simulations to predict the fish/sediment ratio for a mean log K_{ow} of 4.5 with a variance of 1.0. The resulting fish/sediment ratio had a coefficient of variation of about 14%, a small source of error compared to the other sources of error mentioned in my paper. The predicted fish/sediment ratio (approximately 200) using this equation agrees quite well with the data for the high octanol-water partition coefficient chlorinated hydrocarbons in Figure 3 (1). When the caveats cited in my paper and by Breck are recognized, either version of the corrected eq 3 provides a technique for estimating the maximum concentrations in fish given certain sediment loads.

Breck has nicely summarized the appropriate procedures to determine laboratory bioconcentration factors. Much of the earlier data used to develop the first regression equations for bioconcentration factors and octanol-water partition coefficients was based on tests as short as 96 h (ref 5, Table 5-3). Even today the U.S. Environmental Protection Agency and the U.S. Army Corps of Engineers use only 10-day tests in determining the suitability of dredge spoils for dumping (6).

Literature Cited

- (1) Connor, M. S. *Environ. Sci. Technol.* 1984, 18, 31-35.
- (2) Mackay, D. *Environ. Sci. Technol.* 1982, 16, 274-278.
- (3) Karickhoff, S. W.; Brown, D. S.; Scott, T. A. *Water Res.* 1979, 13, 241-248.
- (4) Kenaga, E. E.; Goring, C. A. I. *ASTM Spec. Tech. Publ.* 1980, STP 707, 78-115.
- (5) Bysshe, S. E. In "Handbook of Chemical Property Estimation Methods: Environmental Behavior of Organic Compounds"; Lyman, W. J., Ed; McGraw-Hill: New York, 1982; p 5-1.
- (6) U.S. Army Corps of Engineers "Evaluation of Proposed Discharge of Dredged Material into Ocean Waters"; Environmental Effects Lab: Vicksburg, MI, 1977; G-1.

Michael Stewart Connor

U.S. Environmental Protection Agency, Region 1
Boston, Massachusetts 02203

ADDITIONS AND CORRECTIONS

1983, Volume 17, Pages 369-371

Gregory W. Traynor,* James R. Allen, Michael G. Apte, John R. Girman, and Craig D. Hollowell: Pollutant Emissions from Portable Kerosene-Fired Space Heaters.

All particulate concentration and emission rate data in this paper should be multiplied by 10.

If ORGANOMETALLICS isn't in your library... then you're missing the research that over 3,500 other chemists are reading!

"The new journal will be a focus for organometallic publication in North America, and it already publishes material which might otherwise have appeared in Journal of the American Chemical Society or Inorganic Chemistry. Consequently, this journal is essential reading for all inorganic and organometallic chemists."

G.J. Leigh, *Nature*, September 1983

In just a few short years, *Organometallics* has been recognized as the leading American journal in the field. Last year, over 400 papers from authors around the world were published. Readers received 2,000 pages of timely peer-reviewed research!

Each issue brings readers original research in all aspects of organometallic chemistry, including synthesis, structure and bonding, chemical reactivity and reaction mechanisms, and applications. Also included are Communications and review columns.

And, *Organometallics* is priced at a fraction of what you'd pay for comparable journals in the field while maintaining the high quality for which American Chemical Society publications are known.

Inorganic chemists, organic chemists, polymer chemists — don't let another year of vital organometallic chemistry pass you by. Make sure *Organometallics* is in your research library.

Dietmar Seyferth, Editor
Massachusetts Institute of Technology
Richard Schrock, Associate Editor
Massachusetts Institute of Technology

EDITORIAL ADVISORY BOARD:

H. Alper • E.C. Ashby • J.E. Bercaw •
R.G. Bergman • A.J. Carty • C.P. Casey •
J.Y. Corey • R.J.P. Corriu • F.A. Cotton
• M. Darensbourg • G.L. Geoffroy •
J. Halpern • H.G. Kuivila • T.J. Marks •
D.S. Matteson • G.W. Parshall •
M. Rosenblum • H. Sakurai • J. Satge
• H. Schmidbaur • M.F. Semmelhack •
A. Streitwieser, Jr. • B.M. Trost
• H. Werner • R.C. West • A. Wojcicki •
A. Yamamoto

Organometallics, published monthly,
one volume per year; Vol. 4 (1985)

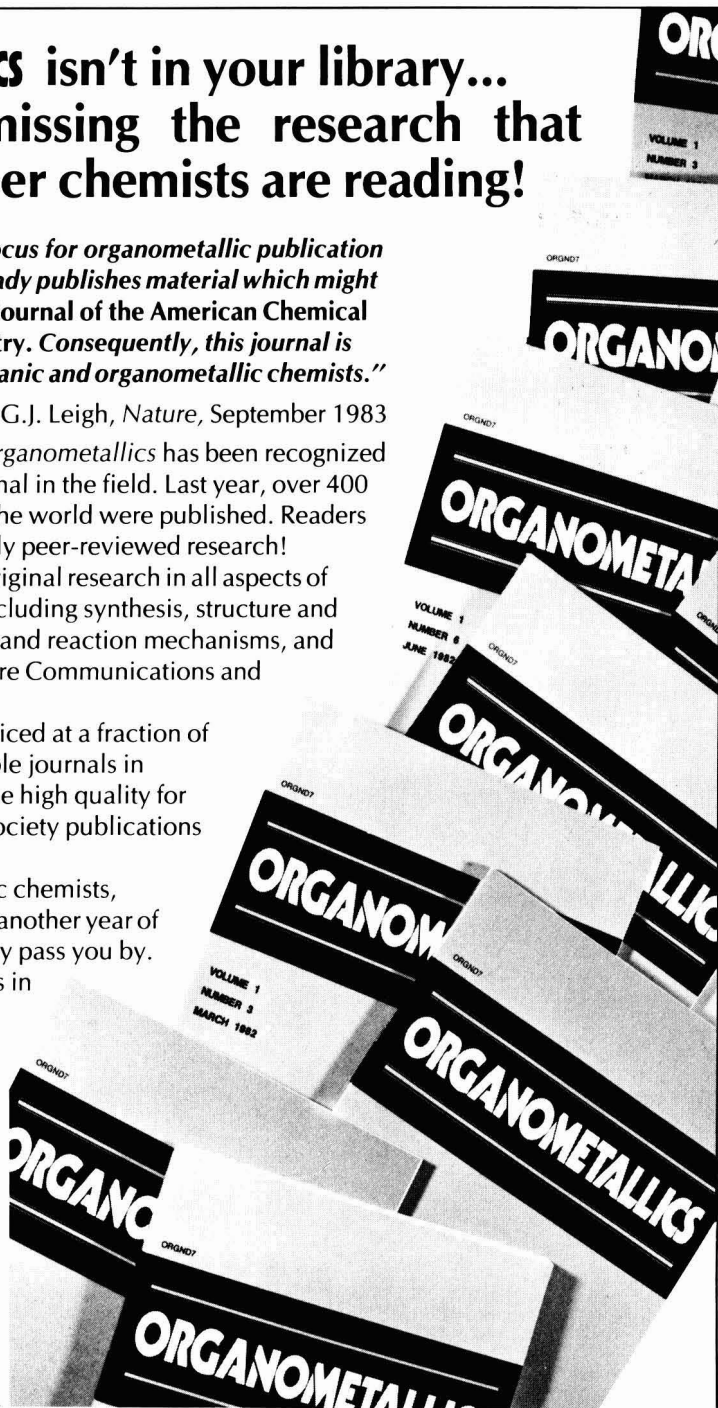
CALL TOLL FREE 800-424-6747

1985 Subscription Rates:

	U.S.	Canada	Europe Air Delivery Included	Other Countries Air Delivery Included
ACS Members	\$ 40	\$ 54	\$ 60	\$ 73
Nonmembers	\$229	\$243	\$249	\$262



American Chemical Society • 1155 Sixteenth St., N.W. • Washington, D.C. 20036



New in 1985!

Accounts of Chemical Research

Joseph F. Bunnett, Editor
University of California, Santa Cruz

Analytical Chemistry

George H. Morrison, Editor
Cornell University

Biochemistry

Hans Neurath, Editor
University of Washington

Chemical & Engineering News

Michael Heylin, Editor
American Chemical Society

Chemical Reviews

Josef Michl, Editor
University of Utah

CHEMTECH

Benjamin J. Luberoff, Editor
American Chemical Society

Environmental Science & Technology

Russell F. Christman, Editor
University of North Carolina, Chapel Hill

**Industrial & Engineering Chemistry—
Fundamentals**

Robert L. Pigford, Editor
University of Delaware

**Industrial & Engineering Chemistry—
Process Design and Development**

Hugh M. Hulburt, Editor
Northwestern University

**Industrial & Engineering Chemistry—
Product Research and Development**

Jerome A. Seiner, Editor
PPG Industries

Inorganic Chemistry

M. Frederick Hawthorne, Editor
University of California, Los Angeles

Journal of Agricultural and Food Chemistry

Irvin E. Liener, Editor
University of Minnesota

Journal of the American Chemical Society

Allen J. Bard, Editor
University of Texas

Journal of Chemical & Engineering Data

Bruno J. Zwolinski, Editor
Texas A&M University

Journal of Chemical Information & Computer Sciences

T. L. Isenhour, Editor
Utah State University

Langmuir

Arthur Adamson, Editor
University of Southern California

Journal of Medicinal Chemistry

Phillip S. Portoghese, Editor
University of Minnesota

The Journal of Organic Chemistry

Frederick D. Greene, Editor
Massachusetts Institute of Technology

The Journal of Physical Chemistry

Mostafa A. El-Sayed, Editor
University of California, Los Angeles

Journal of Physical and Chemical Reference Data

David R. Lide, Jr., Editor
National Bureau of Standards

Macromolecules

Field H. Winslow, Editor
Bell Telephone Laboratories

Organometallics

Dietmar Seyferth, Editor
Massachusetts Institute of Technology

American Chemical Society publications will be delivered via air service to all countries outside the U.S. and Canada!

All prices to foreign destinations now automatically include air service delivery. Readers around the world will now benefit in many ways from faster receipt of their ACS publications.

Delivery time has been dramatically improved! For example, starting in 1985, subscribers in Frankfurt, Germany will be receiving their publications in one week versus waiting eight weeks under our old system.

This of course means that international subscribers will be receiving valuable research published in ACS journals at comparable times to their American counterparts!



American Chemical Society . . .
chemical publishers since 1879.

Cable Address JIECHEM
Telex 440159 ACSPUI or
892582 ACSPUBS

Current subscribers please note . . . air service will begin with the first issue in 1985. Your service will be so much improved that you will receive the first few issues of 1985 before you receive 1984 year end issues being shipped via surface mail!

American Chemical Society • 1155 Sixteenth Street, N.W.
Washington, D.C. 20036